FREIE UNIVERSITÄT BERLIN
INSTITUT FÜR MATHEMATIK

Augmented Generators for Non-autonomous Flows

Dissertation zur Erlangung des Grades
eines Doktors der Naturwissenschaften (Dr. rer. nat.)

am Fachbereich Mathematik und Informatik
der Freien Universität Berlin

vorgelegt von

Martin Stahn (geb. Plonka)

Berlin, Oktober 2022

Erstgutachter:	Prof. Dr. Péter Koltai
Zweitgutachterin:	Prof. Cecilia Gonzáles-Tokman
Tag der Disputation:	04. Mai 2023

Selbstständigkeitserklärung

Name: Stahn
Vorname: Martin

Ich erkläre gegenüber der Freien Universität Berlin, dass ich die vorliegende Dissertation selbstständig und ohne Benutzung anderer als der angegebenen Quellen und Hilfsmittel angefertigt habe. Die vorliegende Arbeit ist frei von Plagiaten. Alle Ausführungen, die wörtlich oder inhaltlich aus anderen Schriften entnommen sind, habe ich als solche kenntlich gemacht. Diese Dissertation wurde ich gleicher oder ähnlicher Form noch in keinem früheren Promotionsverfahren eingereicht.

Mit einer Prüfung meiner Arbeit durch ein Plagiatsprüfungsprogramm erkläre ich mich einverstanden.

Berlin, den

____

Martin Stahn

Zusammenfassung

Diese Dissertation beschäftigt sich mit der Extraktion und der optimalen Manipulation von kohärenten Mengen in nicht-autonomen dynamischen Systemen. Diese kohärenten Mengen können helfen globale Transportmechanismen in komplizierten Systemen zu identifizieren. Anwendungsgebiete dafür sind zum Beispiel Ozeanographie, Meteorologie und Turbulenz. Die relevanten mathematischen Objekte aus den Theorien von dynamischen Systemen, kohärenten Mengen, nicht-autonomen Cauchy Problemen und Lagrangen Multiplikatoren werden rekapituliert. Wir konstruieren einen infinitesimalen Generator für nicht-autonome Probleme, indem wir in der Zeit augmentieren. Für periodische Geschwindigkeitsfelder leiten wir eine Verbindung zwischen dem augmentierten Generator und der zeitasymptotischen Perspektive auf Kohärenz her. Mit der Hilfe einer Reflektion in der Zeit erweitern wir diese Verbindung für den augmentierten Generator auf kohärente Mengen in beschränkten Zeitintervallen und auf aperiodische Probleme. Essentiell für diese Verbindung ist eine spektrale Abbildungseigenschaft des augmentierten Generators, welche wir beweisen. Weiterhin beweisen wir die Fréchet-Differenzierbarkeit dieser Generatoren, zugehöriger Transferoperatoren und ihrer Spektra bezüglich des zugrundeliegenden Geschwindigkeitsfeldes. Diese glatte Abhängigkeit erlaubt es uns, die optimale Störung der Spektra und der kohärenten Mengen mit Hilfe von Lagrangen Multiplikatoren in Banach Räumen zu bestimmen. Für eine quadratische Nebenbedingung in einem Hilbert Raum leiten wir eine explizite Formel für die optimale Störung her. Wir illustrieren den Generator-Ansatz und die optimale Störung numerisch an Standardbeispielen. Schließlich diskutieren wir mögliche Erweiterungen und Verallgemeinerungen der Hauptaussagen dieser Dissertation, die von Interesse für zukünftige Forschung sind.

Abstract

This thesis is concerned with the computation and the optimal manipulation of coherent sets in non-autonomous dynamical systems. These coherent sets can help to unravel global transport dynamics in complicated systems from, for example, oceanography, meteorology and turbulence. The relevant mathematical objects from the theories of dynamical systems, coherent sets, non-autonomous abstract Cauchy problems and Lagrangian multipliers are recapitulated. We construct an infinitesimal generator for non-autonomous problems following the augmentation idea from dynamical systems. In the periodic case we link this augmented generator to an infinite-time perspective on coherent sets. With the help of a reflection trick we extend this relation for the augmented reflected generator to the finite-time perspective on coherent sets even for aperiodic problems. We prove a spectral mapping property for the augmented generator that is essential for the connection to coherence. We establish the Fréchet differentiability of these generators, related transfer operators and their spectra with respect to the underlying velocity field. This regularity enables us to optimally perturb the spectra and the coherent sets with the help of Lagrangian multipliers in Banach spaces. Furthermore, we derive an explicit formula for the optimal perturbation for a quadratic constraint in a Hilbert space. We apply the augmented reflected generator approach and the optimal perturbation method to standard examples. Finally, we outline some generalizations for the main aspects of this thesis that are of interest for future research.

Acknowledgements

The author acknowledges financial support from the DFG SPP 1881 'Turbulent Superstructures' at the Freie Universität Berlin and from the Universität Potsdam for the duration of the research going into and the writing of this thesis.

I want to thank Gary Froyland, Jörg Schumacher, Oliver Junge and Christiane Schneide for fruitful discussions and valuable collaborations.

Furthermore, I would like to thank my family for their support in all aspects of this project.

Special thanks goes to Han Cheng Lie for his expertise and more importantly for keeping me focused and motivated.

My foremost thanks goes to my supervisor Péter Koltai for giving me the chance to contribute to the current state of science with my research and the opportunity to write this thesis. His enthusiasm for mathematical research has always been and still is an inspiration for me and many other students. Furthermore, I would like to thank him for his friendly criticism and his support at all times.

I would also like to thank all those who contributed to the completion of this thesis in other ways and were not named individually.

Disclaimer

The author of this thesis has contributed to four scientific papers that have been published in peer reviewed journals. The results from the two *open access* publications

[KLP19] Koltai, Lie, Plonka 2019: *Fréchet differentiable drift dependence of the Perron–Frobenius and Koopman operators for non-deterministic dynamics*, in **Nonlinearity**, Vol. 32, pp. 4232-4257, DOI: `https://doi.org/10.1088/1361-6544/ab1f2a`

[FKS20] Froyland, Koltai, Stahn 2020: *Computation and Optimal Perturbation of Finite-Time Coherent Sets for Aperiodic Flows without Trajectory integration* in **SIAM Journal on Applied Dynamical Systems**, Vol. 19, No. 3, pp. 1659-1700, DOI: `https://doi.org/10.1137/19M1261791`

form the main content of this thesis. The chapters 3, 4, 5 and 6 and the section 2.5 reproduce parts of and expand on the content of these publications. We indicate the connection between these papers and this thesis throughout the text. All publishers and co-authors have given their permission for the re-use of the content of these publications including any figures for the purpose of this thesis.
Some ideas and comments are inspired and influenced by the authors other publications

[SSP$^+$19] Schneide, Stahn, Pandey, Junge, Koltai, Padberg-Gehle, Schumacher 2019: *Lagrangian coherent sets in turbulent Rayleigh-Bénard convection* in **Physical Review E** Vol. 100, 053103, DOI: `https://doi.org/10.1103/PhysRevE.100.053103`;

[LSS22] Lie, Stahn, Sullivan 2022: *Randomised one-step integration methods for deterministic operator differential equations* in **Calcolo**, Vol 59, pp. 1-33, DOI: `https://doi.org/10.1007/s10092-022-00457-6`.

Contents

1 Introduction

Many processes in nature and civilization can be described mathematically with the help of autonomous or non-autonomous, deterministic or stochastic, ordinary or partial differential equations. The core of these descriptions is that the rate of change and thus the future state of a system depends on the current state of the system and on some rules of evolution specified by the equations. Most of these evolution equations are too complicated to derive explicit solutions, for example in fluid dynamics, meteorology, oceanography and other applications. Even numerical solutions often times do not yield the desired insights into the evolution of the system. Therefore, other methods have been developed to analyze topological, geometric, probabilistic or stability aspects of dynamical systems. Analyzing the transport and mixing behavior of complicated flows has been and still is a highly active research area [MMP84, RKLW90, HP98, Wig05, FSM10, Thi12, KR18, HKK18, BGT20, DFK22].

Let us examine some of the largest and most important eco-systems on earth, the oceans. Analyzing material transport in the ocean is difficult due to the different scales of the temporal dimension and all three spatial dimensions involved. Nevertheless, it is important. Consider a situation where there is a spill in the ocean of some pollutant whose movement is mainly driven by the surface flow of water but could be additionally subject to some small diffusion. Then, in order to coordinate clean-up efforts, it would be useful to know how the pollutant concentration evolves and whether there are areas that keep a high concentration of the pollutant over a significant amount of time. These questions can be tackled with the theory of mixing and coherent sets. The goal of coherent set analysis is to find distinguished material subsets whose evolution is robust with respect to small diffusion. Coherent sets extend the notion of almost invariant [DJ99] or metastable sets [SS13] to non-autonomous problems [KCS16].

With the help of satellite data we can roughly approximate the velocity field of a surface layer of the ocean. A velocity field, a spatial domain, a time span and an initial distribution form a sufficient starting point for many approaches for coherent sets [Fro13, Fro15, HKK20, KK20]. Global long-term properties of dynamical systems, such as their stationary distribution, material transport, coherence or the rate of mixing are strongly related to the Perron–Frobenius operator and the Koopman operator [Pie94, SSA09, FS13]. These transfer operators are infinite-dimensional linear operators describing the evolution of distributions or observables. The eigenpairs and singular pairs of the Perron–Frobenius operator induce coherent sets. Transfer operators and coherent set analysis have been successfully used to study (geophysical) fluid dynamics [FPET07, DFH$^+$09, FLS10, FHRvS15, AM17], molecular dynamics [DDJS99, SFHD99, PWS$^+$11, BPN13, BKK$^+$17], oceanography [BK17, DFK22], meteorology [FSM10, BGT20], turbulent flows [SSP$^+$19, VSPGS21], and plasma physics [Den17]. This thesis investigates a probabilistic approach for coherent set analysis using results from functional analysis.

To compute a discrete Markov approximation of the Perron–Frobenius operator, one usually needs to compute many short or fewer but longer trajectories [KKS16] which can be expensive or even unfeasible. To alleviate the need for trajectory computation [FJK13] introduced the generator approach. The generator is a single time-independent object that can be computed fast by surface integrals and does not need trajectory computations. The eigendata of the infinitesimal generator of a semigroup of Perron–Frobenius operators can be used to obtain coherent sets in the time-asymptotic setting [FJK13]. This approach was extended to coherent sets in the non-autonomous but time-periodic setting in [FK17]. The augmented reflected generator approach from [FKS20] detailed in Chapter 3 extends results from [FJK13] and [FK17] to the aperiodic finite-time setting.

When deriving the surface layer velocity field for the ocean flow from satellite data we may get very rough approximations. However, if the coherent sets depend sufficiently regular on the velocity field, then small errors in the velocity field only lead to small errors for the computed coherent sets. This means that the sensitivity of the transfer operators and the coherent sets with respect to the velocity field is important. In addition, a regular dependence on the data allows for the efficient optimization of fluid mixing processes [FGTW16]. The continuous Fréchet differentiability of expected path functionals, of the stochastic transfer operators, and of their spectra with respect to the velocity field from [KLP19] detailed in Chapter 5 is a result that can be a starting point for linear response, stability analysis, control theory, and optimization.

To contain the spill in the ocean, we could think about deploying turbines to steer the water flow or rerouting ships to influence the surface flow. Then, the question becomes how can we do this to optimally contain or disperse the spill. Optimally perturbing the spectrum of transfer operators and coherent sets using advective forces directly is difficult, because it involves the variation of the non-linear implicit dependence on the velocity field. However, a linearized optimization of the eigenvalue of the generator leads to a well-structured optimization problem. Building on the generator approach and the Fréchet differentiability Chapter 6 presents an optimal perturbation theory from [FKS20] for the spectrum of transfer operators, their generators and related objects such as coherent sets. We provide a technique to find a small perturbation of the underlying aperiodic vector field in a bounded, closed and strictly convex neighborhood of zero in a space or subspace of vector fields, which optimally enhances or destroys the existing finite-time coherent sets. Thereby we extend the optimization results from [FS17], which considered the time-periodic setup of [FK17], to aperiodic dynamics and to infinite-dimensional velocity field space.

Remark 1:

- The references above are just a small selection that is supposed to give the interested reader a starting point for the different aspects and developments. We strongly encourage the reader to look into the sources of the references given here for many more important contributions that have been omitted here.

- We note that a numerical approach to extract coherent sets from the Perron–Frobenius operator by solving the Fokker–Planck equation has been described in [DJM16]. In contrast to [DJM16] we do not require time-integration over the whole time span, which is especially advantageous once we consider the optimization of coherence and mixing.

- We mention that by a similar construction, spatio-temporal dynamical patterns were extracted in [GD20] by considering the generator of the Koopman operator associated with the augmented-space dynamics.

- The stability of transport and mixing properties has also been investigated in [FGTW16, AFJ21]. Many approaches for the optimization of mixing search for switching protocols between some fixed velocity fields to optimize some mixing measure [BAS00, MMG$^+$07, CAG08, OBPG15]. Other strategies that have been explored include optimizing the diffusion component [FGTW16], optimizing the distribution of sources [TP08] and techniques from geometric dynamical systems [Bal15]. If there are no restrictions on the velocity field, one can choose the one that is optimally mixing the actual concentration at every time instance [LTD11]. An interesting general theoretical result from [CKRZ08] shows that arbitrary mixedness under advection-diffusion can be achieved in finite time solely by sufficiently increasing the strength of the advective flow.

$\triangle$

Outline

This thesis briefly introduces the basic notions of coherent set analysis and transfer operators. We devote a larger part of Chapter 3 to introduce some abstract results that the reader might be less familiar with.

Chapter 2 gives a brief introduction to the objects and concepts from ordinary differential equations and stochastic differential equations. We introduce the transfer operators, the Perron–Frobenius operator and the Koopman operator, and their kernel for the case of non-autonomous dynamics. Furthermore, we discuss an infinite-time and a finite-time perspective on coherent sets and introduce the corresponding quantifiers for coherence. The last section of Chapter 2 presents a reflection trick that allows us to extend the generator approach to the finite-time setting in Chapter 3.

Chapter 3 first introduces the theories of C_0 semigroups and non-autonomous abstract Cauchy problems. After establishing important properties for two-parameter solution families of transfer operators, we discuss the construction of evolution semigroups and an augmented infinitesimal generators for non-autonomous flows. Finally, Section 3.4 introduces and Section 3.5 extends the generator approach for coherent sets to the non-autonomous finite-time possibly aperiodic setting using a spectral mapping result.

Chapter 4 gives an outline of how to obtain a suitable discretization for the augmented generator following Ulam's method. Furthermore, we use the results from Chapter 3 to extract coherent sets numerically for the examples of two counter rotating gyres and an idealized zonal jet.

Chapter 5 introduces Girsanov's theorem to prove the Fréchet differentiability of expected path functionals with respect to the velocity field. We extend this differentiability with uniformity and duality arguments to transfer operators associated to non-autonomous stochastic differential equations. We transfer our results to the context of dynamical systems and operator theory, by proving continuous differentiability of the simple and isolated eigenvalues, singular values, and the corresponding eigen- and singular functions of the stochastic Perron–Frobenius and Koopman operators with respect to the velocity field.

Chapter 6 combines the results from the previous chapters with the theory of Lagrangian multipliers in Banach spaces. We obtain a linear objective functional for the local change of eigenvalues of the augmented reflected generator with respect to the velocity field. Assuming a quadratic constraint and a Hilbert space setting, we derive an explicit formula for the optimal perturbation. We apply the optimization procedure to two numerical examples. Finally, we introduce a heuristic to manipulate non-eigenfeatures.

Chapter 7 reviews the related work [FK21] that uses an augmented space-time manifold in a very different way for the analysis of coherent sets. We outline how the augmented generator approach could be extended to find coherent families in systems with an ergodic driving. Furthermore, we discuss some open questions and improvements for the numerical aspects of the augmented reflected generator approach. Finally, we consider alternative constraints and other generalizations for the optimal perturbation approach.

2 Non-Autonomous Flows

This chapter introduces the objects and concepts regarding ordinary or stochastic differential equations and coherent sets that are important for the rest of this thesis. Due to the size and significance of these mathematical fields, this introduction cannot be complete. We start with the perspective on one particle or a passive tracer that is acted upon by a velocity field v and is possibly subject to some noise. Then, we expand our considerations to densities of particles. This leads to partial differential equations. The corresponding solution operators are called transfer operators and are a central object for this thesis.

2.1 Deterministic Flows

In general, we focus on non-deterministic non-autonomous flows. To illustrate some basic principles with more clarity, we briefly introduce some concepts in the deterministic setting. Furthermore, we use this opportunity to introduce objects and give intuition for concepts that are used later. The trajectories of moving particles can often be described by ordinary differential equations. The corresponding evolution of densities of particles is given by a transport equation. The solution operators are transfer operators, namely the deterministic Perron–Frobenius and the deterministic Koopman operator.

Ordinary Differential Equations

The evolution of a particle x in a separable Banach space $(V, \|\cdot\|_V)$ over a time span $[0,T]$ starting in a position $x_0 \in \mathbb{X} \subseteq V$ at $t_0 \in [0,T]$ under the action of a time-dependent vector field, also called velocity field or drift, $v : [0,T] \times V \to V$ can be described by the non-autonomous differential equation

$$\frac{d}{dt}x(t) = x'(t) = v(t, x(t)) \tag{2.1}$$

with the initial condition $x(t_0) = x_0 \in \mathbb{X}$, $t_0 \in [0,T]$. The immediate questions that arise are: Are there conditions such that this is a well-posed problem? For which $x_0 \in \mathbb{X}$ does (2.1) have a unique solution and how does this solution depend on the data, namely, the initial condition x_0 and the velocity field v? These questions are the focus of the theory of differential equations.

Definition 2.1:
A function $x \in C^1([0,T]; V)$ is called classical solution to the initial value problem (2.1) *on* $[0,T]$ *if it satisfies the initial condition and satisfies the equation pointwise for every* $t \in [0,T]$.

Remark 2:

- The name initial condition is chosen here for convenience. More correctly, we should refer to $t_0 = 0$ as initial condition, to $t_0 = T$ as terminal or final condition and to every other $t_0 \in (0,T)$ as intermediate condition.

- The space $C^k([0,T];V)$, for $k \in \mathbb{N} \cup \{0\}$, denotes the separable Banach space of continuous functions $f : [0,T] \to V$ that are k-times continuously differentiable on $[0,T]$. This space is endowed with the canonical norm

$$\|f\|_{k,\infty} := \sum_{\ell=0}^{k} \left\| \frac{d^\ell}{dt^\ell} f \right\|_\infty = \sum_{\ell=0}^{k} \sup_{t\in[0,T]} \left\| \frac{d^\ell}{dt^\ell} f(t) \right\|_V .$$

- For a general introduction to differential equation in finite dimensions we refer to [Hal80, Arn92]. An introduction to equations in infinite dimensions can be found in [Emm13].

△

There are different ways to look at a solution x. We can think of x as a function mapping from a time interval into a vector space. Alternatively, we can look at the trajectory $(x_t)_{t\in[0,T]}$ which consists of an uncountable number of points $x_t \in V$ that are ordered by their time index and which are anchored by the initial condition $x(t_0) = x_0 \in \mathbb{X}$. This duality of a function x and the points of V that constitute its trajectory is an important idea that is used throughout this thesis.

Theorem 2.2:
Let $v : [0,T] \times V \to V$ be continuous and satisfy a Lipschitz condition in the second argument

$$\exists\, L > 0 \;\; \textit{such that} \;\; \|v(t,x) - v(t,y)\|_V \le L\|x-y\|_V .$$

Then, for every initial value x_0 the initial value problem (2.1) *has a unique classical solution x with $x \in C^1([0,T];V)$ that depends Lipschitz continuously on the data. Let x_i be the unique solution to the problem* (2.1) *with v_i and $x_{i,0}$, for $i = 1,2$, then it holds that*

$$\exists\, K > 0 : \|x_1 - x_2\|_{C^1([0,T],V)} \le K\Big(\sup_{\substack{t\in[0,T]\\ x\in V}} \|v_1(t,x) - v_2(t,x)\|_V + \|x_{1,0} - x_{2,0}\|_V \Big) .$$

Furthermore, if the right hand side v is more regular, namely, $v \in C^{(k,k)}([0,T] \times V; V)$, then the solution is also more regular $x \in C^{k+1}([0,T];V)$.

Proof. The existence of a unique solution for $k = 1$ follows from the Picard–Lindelöf theorem [Emm13, Satz 7.2.6]. This gives the *forward* solution, $x \in C^1([t_0,T];V)$, for the initial value problem on $[t_0,T]$. The transformation $t_0 - t$ turns the final value problem on $[0,t_0]$ into an initial value problem that also satisfies the conditions of the Picard–Lindelöf theorem. This gives the *backward* solution $x \in C^1([0,t_0];V)$. The Lipschitz dependence on the data has been shown in [Emm13, Sec. 7.3]. The higher regularity follows from a chain rule argument and the formula $x(t) = x_0 + \int_{t_0}^t v(s,x(s))\,ds$. □

Remark 3:

- The space $C^{(k,\ell)}([0,T] \times \mathbb{X}; V)$ denotes the separable Banach space of bounded V-valued functions $f : [0,T] \times \mathbb{X} \to V$, $(t,x) \mapsto f(t,x)$ that are k-times continuously differentiable in t and ℓ-times continuously differentiable in x.

- There are more general results that give the existence of unique solutions under different, only local or generally weaker assumptions, for example, solutions in the sense of Carathéodory [Hal80, Sec. I.5].
- Extending the question of dependence of the solution on the data or an additional parameter, one could also ask for k-times differential dependence. We also partially investigate this important question in the non-deterministic setting in Chapter 5. Some results for the deterministic case can be found in [Hal80, Sec. I.3] for the finite-dimensional case.

$\triangle$

The existences of a unique solution for a given initial condition $x(t_0) = x_0$ induces a family of possibly non-linear solution operators $(\Phi_{s,t})_{s\leq t}$. The solution operators $\Phi_{s,t} : V \to V$, also called flow maps, evolve a particle x from time s to time t according to the dynamics (2.1)

$$x(t_0 + t) = \Phi_{t_0,t_0+t}(x(t_0)) \quad \text{for } t \geq 0\,.$$

Theorem 2.2 further implies that the flow maps $\Phi_{s,t}$ are reversible. The two-parameter solution family $(\Phi_{s,t})_{s\leq t}$ shares some properties with evolution families introduced in Definition 3.8. In the context of dynamical systems the family $(\Phi_{s,t})_{s\leq t}$ is also called a two-parameter flow. The first parameter is the initial time, and the second parameter is the final time. If the maps $x_s \mapsto \Phi_{s,t}x_s = x(t)$ are additionally k-times continuously differentiable, or equivalently, if the solution of (2.1) is k-times continuously differentiable with respect to the initial condition, then $(\Phi_{s,t})_{s\leq t}$ is a family of C^k-diffeomorphisms, see [Arn92, §. 32] for $V = \mathbb{R}^d$, $d \in \mathbb{N}$.

Building on these results and focusing on other questions, the theory of dynamical systems is interested in properties of trajectories $(x(t))_{t\in[0,T]}$ with a focus on the time-asymptotic behavior and the qualitative behavior of the evolution [Mei07].

Transfer Operators

Let $\mathcal{A}$ be a σ-algebra on $\mathbb{X}$ with a measure μ such that $(\mathbb{X}, \mathcal{A}, \mu)$ is a measure space. A measurable map $T : \mathbb{X} \to \mathbb{X}$ is called non-singular with respect to $(\mathbb{X}, \mathcal{A}, \mu)$ if

$$\mu(T^{-1}(A)) = 0 \quad \text{for each } A \in \mathcal{A} \text{ such that } \mu(A) = 0\,.$$

The map $\Phi_{s,t}$ is continuous and invertible and under sufficient regularity assumptions a C^k-diffeomorphism. For a family $(\Phi_{s,t})_{s\leq t}$ of measurable and non-singular maps with respect to a measure space $(\mathbb{X}, \mathcal{A}, \mu)$, the Perron–Frobenius operator $P_{s,t} : L^1(\mathbb{X}, \mu; \mathbb{R}) \to L^1(\mathbb{X}, \mu; \mathbb{R})$ is defined by the relation

$$\int_A (P_{s,t}f)(x)\, d\mu(x) = \int_{\Phi_{s,t}^{-1}(A)} f(x)\, d\mu(x) \quad \text{for all } A \in \mathcal{A}\,. \tag{2.2}$$

The family $(P_{s,t})_{s\leq t}$ describes the evolution of densities f. The space $L^p(\mathbb{X}, \mu; \mathbb{R}^d)$, for $p \in [1, \infty)$, is the space of equivalence classes of μ-almost everywhere identical $\mathbb{R}^d$-valued functions that are μ-measurable and have the finite norm

$$\|f\|_{L^p(\mathbb{X},\mu)} := \left(\int_{\mathbb{X}} |f(x)|^p\, d\mu(x)\right)^{\frac{1}{p}} < \infty\,.$$

We use $|\cdot|$ for an arbitrary but fixed norm on $\mathbb{R}^d$. Elementary calculations [LM94, Chap. 3] using (2.2) show that for every fixed pair (s,t) the Perron–Frobenius operator $P_{s,t}$ is a Markov operator.

Definition 2.3:
For a measure space $(\mathbb{X},\mathcal{A},\mu)$ a linear and bounded operator $P : L^1(\mathbb{X},\mu;\mathbb{R}) \to L^1(\mathbb{X},\mu;\mathbb{R})$ is called Markov operator, if for all $0 \le f \in L^1(\mathbb{X},\mu;\mathbb{R})$ follows $Pf \ge 0$ and $\|Pf\|_{L^1} = \|f\|_{L^1}$.

Instead of considering the evolution of densities, we can also look at the evolution of observables. This leads to the Koopman operator $K_{s,t} : L^\infty(\mathbb{X},\mu;\mathbb{R}) \to L^\infty(\mathbb{X},\mu;\mathbb{R})$ given by

$$(K_{s,t}g)(x) := g(\Phi_{s,t}(x)) = (g \circ \Phi_{s,t})(x)\,. \tag{2.3}$$

The space $L^\infty(\mathbb{X},\mu;\mathbb{R}^d)$ denotes the space of equivalence classes of μ-almost everywhere identical $\mathbb{R}^d$-valued functions that are essentially bounded with respect to μ.

$$\|f\|_{L^\infty(\mathbb{X},\mu)} := \operatorname*{ess\,sup}_{x\in\mathbb{X}} |f(x)| = \inf\left\{C>0 \,\middle|\, |f(x)| < C \text{ for } \mu\text{-almost every } x \in \mathbb{X}\right\}\,.$$

If there is no risk of confusion, we abbreviate $L^p(\mathbb{X},\mu;\mathbb{R}^d)$ for $p \in [1,\infty]$ by $L^p(\mathbb{X})$ or $L^p(\mu)$ and the corresponding norms by $\|\cdot\|_{L^p}$. The Koopman operator is the dual operator to the Perron–Frobenius operator in the following sense

$$\langle P_{s,t}f, g\rangle_{L^2(\mu)} := \int_{\mathbb{X}} (P_{s,t}f)(x)g(x)\,d\mu(x) = \int_{\mathbb{X}} f(x)(K_{s,t}g)(x)\,d\mu(x) = \langle f, K_{s,t}g\rangle_{L^2(\mu)}$$

for all $f \in L^1(\mathbb{X},\mu;\mathbb{R})$, $g \in L^\infty(\mathbb{X},\mu;\mathbb{R})$ and $s \le t$ fixed, [LM94, Sec. 7.4].

Remark 4:

- If not stated otherwise, we can equip $\mathbb{X}$ with the Borel σ-algebra, specifically, the smallest σ-algebra that contains all open sets. In the case $\mathbb{X} = \mathbb{R}^d$ the properties of $\Phi_{s,t}$ imply that $\Phi_{s,t}$ is measurable and non-singular with respect to $(\mathbb{R}^d,\mathcal{A},\Lambda)$, where Λ denotes the Lebesgue measure for $\mathbb{R}^d$. Except for a small detour in Chapter 5 we are mostly concerned with L^p spaces with regard to the Lebesgue measure Λ.

- The evolution of densities can be characterized by a partial differential equation that is related to (2.1). In the case $\mathbb{X} = \mathbb{R}^d$ the evolution of a density f_0 corresponding to the dynamics (2.1) is given by the first-order hyperbolic linear transport problem [LM94, Sec. 7.6]
$$\partial_t f(t,x) = -\operatorname{div}_x(v(t,x)f(t,x)) = -\sum_{i=1}^d \frac{\partial}{\partial x_i}\left(v_i(t,x)f(t,x)\right) \tag{2.4}$$
with $f(0,\cdot) = f_0(\cdot)$ on $[0,T]\times\mathbb{R}^d$. We use ∂_t as an abbreviation for $\frac{\partial}{\partial t}$.

- Let μ be a $\Phi_{s,t}$-invariant measure with $\mu(\mathbb{X}) < \infty$. The Perron–Frobenius operator $P_{s,t}$ can be considered on $L^p(\mathbb{X},\mu;\mathbb{R})$ for $p \in [1,\infty]$ with its dual, the Koopman operator acting on $L^q(\mathbb{X},\mu;\mathbb{R})$ for $\frac{1}{p}+\frac{1}{q} = 1$ and $q = \infty$ for $p = 1$. Furthermore, $P_{s,t}$ is non-expansive on $L^p(\mathbb{X},\mu;\mathbb{R})$ for $t > s$ [Den17, Chap. 2].

△

An introduction to the deterministic evolution of particles and densities can be found in [LM94, Chap. 7]. The book [LM94] covers time-discrete, time-continuous, deterministic and stochastic problems for time-independent velocity fields $v(t, x) = v(x)$.

The deterministic setting is highly important and very interesting. Nevertheless, it is not the focus of this thesis. Therefore, we end this brief introduction here.

2.2 Stochastic Dynamics

In mathematical models and applications, there can be many reasons that suggest or even necessitate the presence of noise. To incorporate this uncertainty mathematically, we introduce Wiener processes and consider non-autonomous stochastic differential equations.

A rigorous and detailed introduction to the theory of probability spaces, stochastic processes, Wiener processes, conditional expectations, stochastic integration and stochastic differential equations is outside the scope of this thesis. The interested reader can find detailed introductions in [Fri75, Bog98, LS01, Kun19]. We use many concepts, like filtrations, adapted processes, non-anticipative processes, independence of σ-algebras, independence of stochastic processes, conditional probabilities, local martingales, and semi-martingales, which can also be found in the references above. Especially, Chapter 5 requires some stochastic calculus. For the rest of this thesis we are concerned with the following objects.

We fix a time horizon $T > 0$ and choose $\Omega := C([0, T]; \mathbb{R}^d)$. Furthermore, let $\mathcal{F}$ be a σ-algebra on Ω, and $\mathbb{P}$ be a probability measure on $(\Omega, \mathcal{F})$. For a filtration $(\mathcal{F}_t)_{t\in[0,T]}$ with $\mathcal{F}_t \subseteq \mathcal{F}$ for every $t \in [0, T]$, let $W = (W_t, \mathcal{F}_t)_{t\in[0,T]}$ be the d-dimensional Wiener process with respect to $\mathbb{P}$. We use the notation $W = (W_t, \mathcal{F}_t)_{t\in[0,T]}$ to emphasize that $W_t = W(t, \cdot) : \Omega \to \mathbb{R}^d$ is $\mathcal{F}_t$-measurable for every $t \in [0, T]$. A measurable functional h acting on $[0, T] \times \Omega$ is adapted to the filtration $(\mathcal{F}_t)_{t\in[0,T]}$ if $h(t, \cdot)$ is $\mathcal{F}_t$-measurable for every $t \in [0, T]$. We omit the Ω input in the following.

Remark 5: Wiener Processes

- There are different equivalent ways to define and prove the existence of Wiener processes [KS91, Chap. 2].

- A one-dimensional Wiener process $(W_t, \mathcal{F}_t)_{t\in[0,T]}$ on a probability space $(\Omega, \mathcal{F}, \mathbb{P})$ with mean μt and variance $\sigma^2 t$ with respect to a filtration $(\mathcal{F}_t)_{t\in[0,T]}$ is a real-valued $\mathbb{P}$-almost surely continuous stochastic process that is adapted to $(\mathcal{F}_t)_{t\in[0,T]}$. For $t > s$ the increments $W(t) - W(s)$ are independent of $\mathcal{F}_s$. Furthermore, $W(0) = 0$ holds $\mathbb{P}$-almost surely and for every $0 \le s < t \le T$ the random variable $W(t) - W(s)$ is normally distributed with mean $(t - s)\mu$ and variance $(t - s)\sigma^2$.

- A one-dimensional Wiener process $(W(t))_{t\in[0,T]}$ with $\mu = 0$ and $\sigma = 1$ is called normalized one-dimensional Wiener process. From a normalized one-dimensional Wiener process we can construct a Wiener process $X_t = \mu t + \sigma W_t$ that has mean μt and variance $\sigma^2 t$.

- A d-dimensional vector valued process $(W_t)_{t\in[0,T]} = (W_1(t), \dots, W_d(t))_{t\in[0,T]}$ is a d-dimensional Wiener process, if its components $(W_i(t))_{t\in[0,T]}$, $i = 1, \dots, d$, are one-dimensional independent Wiener processes.

- If the filtration $(\mathcal{F}_t)_{t\in[0,T]}$ is not specified, then we can always consider the filtration generated by the Wiener process.
- The concept of Wiener processes can also be extended to separable Banach spaces [Bog98, Sec. 7.2]. In infinite-dimensional Hilbert spaces there are also cylindrical Wiener processes and Q-Wiener processes [LR15, Chap. 2].

$\triangle$

Wiener processes are continuous martingales [LS01, Sec. 4.1.1]. A continuous semi-martingale or a continuous local martingale can be used as a starting point to construct a concept of stochastic integration [Kun97, Chap. 2]. Similar to the deterministic setting, stochastic integration is a foundation for the analysis of stochastic differential equations.

Stochastic Differential Equations

Formally, adding the time-derivative of a normalized d-dimensional Wiener process $(W_t)_{t\in[0,T]}$ with the noise intensity $\sigma : [0,T]\times\mathbb{R}^d \to \mathbb{R}^{d\times d}$ to an ordinary differential equation with the velocity field $v : [0,T]\times\mathbb{R}^d \to \mathbb{R}^d$ leads to a stochastic differential equation (SDE) in Itô form

$$dX_t = v(t, X_t)dt + \sigma(t, X_t)dW_t\,. \tag{2.5}$$

Equation (2.5) is not rigorously defined in this differential form, because a Wiener process is only α-Hölder continuous for $\alpha \in (0, \frac{1}{2})$ and is $\mathbb{P}$-almost surely nowhere β-Hölder continuous for $\beta \in (\frac{1}{2}, 1)$ [Fri75, Chap. 3]. Equation (2.5) is an abbreviation for the integral equation

$$X_t = X_0 + \int_0^t v(s, X_s)\,ds + \int_0^t \sigma(s, X_s)\,dW_s\,. \tag{2.6}$$

Here the initial state X_0 is $\mathbb{P}$-almost surely given by a deterministic point or distributed according to some law given by a density f_0. Equation (2.6) is defined rigorously, under some mild assumptions: The drift $v : [0,T]\times\mathbb{R}^d \to \mathbb{R}^d$ and the diffusion $\sigma : [0,T]\times\mathbb{R}^d \to \mathrm{GL}(\mathbb{R}, d)$, where $\mathrm{GL}(\mathbb{R}, d)$ denotes the space of real invertible $d\times d$ matrices, are functions that are non-anticipative with respect to the filtration corresponding to $(W_t)_{t\in[0,T]}$ and satisfy

$$\mathbb{P}\left(\int_0^T |v(t, X_t)|\,dt < \infty\right) = 1 \quad \text{and} \quad \mathbb{P}\left(\int_0^T |\sigma(t, X_t)|^2\,dt < \infty\right) = 1\,. \tag{2.7}$$

To study the well-posedness of stochastic differential equations, we assume that v and σ satisfy Assumption 1. For simplicity, we assume that v and σ satisfy the global conditions (A1) and (A2), namely, the Lipschitz continuity (2.8) and the growth condition (2.9).

Assumption 1:
There exist constants $0 < L, \lambda_\sigma < \infty$ that do not depend on y, z, or t, such that

(A1) The functions v and σ satisfy the Lipschitz condition

$$|v_i(t, y) - v_i(t, z)| \le L\,|y - z|\,, \quad |\sigma_{ij}(t, y) - \sigma_{ij}(t, z)| \le L\,|y - z| \tag{2.8}$$

for all $(t, y, z) \in [0,T]\times\mathbb{R}^d\times\mathbb{R}^d$ and $1 \le i, j \le d$.

(A2) The functions v *and* σ *satisfy the growth condition*

$$|v_i(t,y)| \leq L(1+|y|), \quad |\sigma_{ij}(t,y)| \leq L(1+|y|) \tag{2.9}$$

for all $(t,y) \in [0,T] \times \mathbb{R}^d$ *and* $1 \leq i,j \leq d$.

(A3) The function σ *satisfies*

$$\lambda_\sigma^{-2}\,|\xi|^2 \leq \xi^\top \sigma(t,y)\sigma^\top(t,y)\xi, \tag{2.10}$$

for all $(t,y,\xi) \in [0,T] \times \mathbb{R}^d \times (\mathbb{R}^d \setminus \{0\})$, *where* $\xi^\top$ *denotes the transpose of* ξ.

The next result, that has been adapted from [LS01, Sec. 4.4.2, Corollary], gives the existence of a unique solution; see also [Fri75, Chap. 5].

Theorem 2.4:
Consider the stochastic differential equation

$$dX_t = v(t,X_t)dt + \sigma(t,X_t)dW_t, \tag{2.11}$$

where the functions $v : [0,T] \times \mathbb{R}^d \to \mathbb{R}^d$, $\sigma : [0,T] \times \mathbb{R}^d \to \mathbb{R}^{d\times d}$ *satisfy the assumptions (A1) and (A2). If* $\mathbb{P}(|\nu_i| < \infty) = 1$ *for all* $1 \leq i \leq d$, *then* (2.11) *with the initial condition* $X_0 = \nu$ *has a unique strong solution [LS01, Sec. 4.4, Def. 8 & 11]. In particular,* (2.7) *is satisfied.*

Remark 6:

- There are more general results that guarantee the existence of a unique strong solution under weaker assumptions, for example local Lipschitz, one-sided Lipschitz or weak monotonicity conditions and local growth or weak coercivity conditions; [LR15, Thm. 3.1.1].
- Stochastic differential equations are not time-reversible in the same sense as ordinary differential equations. Due to the measurability requirements with respect to the filtration a backward stochastic differential equation poses a structurally different problem. See [HP86] for the time-reversal of diffusion processes and see [PR14] for backwards stochastic differential equations. The book [Kun19] investigates stochastic flows of diffeomorphisms and establishes many related results and arguments that are similar to the deterministic case.

$\triangle$

The solution $(X_t)_{t\in[0,T]}$ is a time-inhomogeneous Markov diffusion process and admits a transition probability function

$$p(s,t,x,A) := \mathbb{P}(X_t \in A \,|\, X_s = x)$$

for Borel measurable sets A. The function p satisfies the Chapman–Kolmogorov equation [Fri75, Thm. 5.3.1 & 5.3.2]

$$p(s,t,x,A) = \int_{\mathbb{R}^d} p(r,t,y,A)p(s,r,x,d\Lambda(y)) = \int_{\mathbb{R}^d} p(r,t,y,A)p(s,r,x,dy)\,.$$

for $s \leq r \leq t$. In Theorem 2.7, this fact enables an important connection between stochastic differential equations and the theory of solution operators of parabolic partial differential equations. Note the similarity to the concatenation property $\Phi_{r,t}\Phi_{s,r} = \Phi_{s,t}$ of flows $(\Phi_{s,t})_{s\leq t}$ and to the property $U(t,r)U(r,s) = U(t,s)$ of evolution families, Definition 3.8.

Kolmogorov Backward and Forward Problems

Instead of investigating a single solution $(X_t)_{t\in[0,T]}$ of the SDE or an ensemble of particles, we consider the evolution of densities and observables. For $\alpha, \beta \in (0,1]$ and $k, l \in \mathbb{N} \cup \{0\}$ the space $C^{(k+\alpha,\ell+\beta)}([0,T] \times \mathbb{X}; \mathbb{R}^d)$ denotes the space of functions $f : [0,T] \times \mathbb{X} \to \mathbb{R}^d$ that are k-times continuously differentiable in t and ℓ-times continuously differentiable in x and whose k-th time derivative is α-Hölder continuous and ℓ-th spatial derivatives are β-Hölder continuous. The canonical norm for these spaces is the sum of the $C^{(k,\ell)}$ norm and the corresponding Hölder norm for the highest derivatives. See [Alt16, Sec. 3.7], [Cia13, Chap. 1] or [AF03, Chap. 1] for details on Hölder spaces.

Theorem 2.5:
Suppose that $\sigma \in C^{(\alpha,2+\alpha)}([0,T]\times\mathbb{R}^d; \mathbb{R}^{d\times d})$ and $v \in C^{(\alpha,1+\alpha)}([0,T]\times\mathbb{R}^d; \mathbb{R}^d)$, for some $\alpha \in (0,1]$, satisfy the assumptions from this section and $f_0 \in C(\mathbb{R}^d)$ and $g \in C(\mathbb{R}^d)$ are bounded, then the following statements hold.

(1) The evolution of an observable g given the dynamics (2.5) can be described by the Kolmogorov backward equation

$$-\partial_t f(t,x) = \langle v(t,x), \nabla_x f(t,x)\rangle_{\mathbb{R}^d} + \frac{1}{2}\sum_{i=1}^{d}\sum_{j=1}^{d}(\sigma(t,x)\sigma^\top(t,x))_{ij}\frac{\partial^2 f}{\partial x_i \partial x_j}(t,x) \tag{2.12}$$

on $[0,T] \times \mathbb{R}^d$ with the final condition $f(T) = g$.

(2) The evolution of a density f_0 under the dynamics (2.5) can be described by the Kolmogorov forward equation

$$\partial_t f(t,x) = -\mathrm{div}_x\left(v(t,x)f(t,x)\right) + \frac{1}{2}\sum_{i=1}^{d}\sum_{j=1}^{d}\frac{\partial^2}{\partial x_i \partial x_j}\Big((\sigma(t,x)\sigma^\top(t,x))_{ij}f(t,x)\Big) \tag{2.13}$$

on $[0,T] \times \mathbb{R}^d$ with initial condition $f(0) = f_0$.

Sketch of proof. There are several sources for the time-homogeneous case, $v(t,x) = v(x)$ and $\sigma(t,x) = \sigma(x)$, that derive (2.12) or (2.13) independently or derive one from the other; see for example [LM94, Chap. 11], [Oks13, Chap. 8] or [KS91, Chap. 5].

(1) The Kolmogorov backward equation can be derived by applying Itô's formula to the conditional expectation

$$f(t,x) = \mathbb{E}[g(X_T) \mid X_t = x]$$

under the assumption $f \in C^{(1,2)}([0,T] \times \mathbb{R}^d)$. We refer to [Fri75, Sec. 5.4 & 5.6, Thm. 6.1] for an execution of this argument. Standard results for parabolic evolution equations [Fri75, Chap. 6], [Lun95, Chap. 6] or [Tan97, Chap. 6] imply that our assumptions on v and σ are sufficient to guarantee $f \in C^{(1,2)}([0,T] \times \mathbb{R}^d)$.

(2) The Kolmogorov forward equation can be derived by obtaining the adjoint problem to the Kolmogorov backward equation. See [Fri75, Sec. 6.4 & 6.5] for an execution of this argument. For a general procedure to obtain adjoint problems for parabolic equations we refer to [Fri08, Chap. 1] and to [Tan97, Chap. 5 & 6] for adjoint boundary conditions and higher-order problems.

In [Pav14, Sec. 2.5] both equations are derived from the probability transition function of the Markov diffusion process $(X_t)_{[t\in[0,T]}$ corresponding to (2.5). □

Before we investigate these partial differential equations, their solution properties and their solution operators, we want to address boundary conditions.

Boundary Conditions
In this thesis we assume that $\mathbb{X} \subset \mathbb{R}^d$, $d \in \mathbb{N}$, is an open, bounded, non-empty, connected domain with a piecewise C^4 boundary. Let us refer to this assumption as (A0).

(A0) $\mathbb{X} \subset \mathbb{R}^d$ is an open, bounded, non-empty, connected domain with a piecewise C^4 boundary.

Since a Wiener process is supported on all of $\mathbb{R}^d$, the question arises as to what happens on $\partial\mathbb{X}$, the boundary of $\mathbb{X}$. Possible choices are reflecting, absorbing or mixed boundary conditions. To analyze material transport with regards to coherent sets, we consider evolutions that stay in a bounded set. Therefore, we want to use SDEs with reflecting boundary conditions. From the theory of SDEs this necessitates an additional correcting process, also called Skorokhod correction process. This process ensures that the particle modeled by $(X_t)_{t\in[0,T]}$ does not leave $\mathbb{X}$. Therefore, a solution of an SDEs with reflecting boundary condition necessitates two processes X_t and the Skorokhod correction process. These differences simplify, when we are looking at the evolution of densities. The works [And09] and [Pil14, Thm. 3.1.1] show that the evolution of densities for SDEs with reflecting boundary conditions is given by the Kolmogorov forward equation on $\mathbb{X}$ with homogeneous Neumann boundary conditions

$$\frac{\partial f}{\partial n}(t,\cdot) = 0 \qquad \text{on } \partial\mathbb{X}\,.$$

Here, n is the outer normal unit vector on $\partial\mathbb{X}$.

Remark 7:
We note that the regularity assumptions in Theorem 2.5 are chosen to be sufficient. We expect similar or slightly weaker results to hold on $\mathbb{X}$ for slightly weaker assumptions such as $g \in L^q(\mathbb{X})$, with $q \in [1,\infty)$, $\sigma_{ij} \in C^{(\alpha,\alpha)}([0,T] \times \overline{\mathbb{X}})$, $v \in C^{(\alpha,\alpha)}([0,T] \times \overline{\mathbb{X}}; \mathbb{R}^d)$ for the backward equation and $f_0 \in L^p(\mathbb{X})$, $p \in [1,\infty)$, $\sigma_{ij} \in C^{(\alpha,2+\alpha)}([0,T] \times \overline{\mathbb{X}})$, $v \in C^{(\alpha,1+\alpha)}([0,T] \times \overline{\mathbb{X}}; \mathbb{R}^d)$ for the forward equation, where $\overline{\mathbb{X}}$ denotes the closure of $\mathbb{X}$. △

2.3 Transfer Operators

The goal of this section is to introduce the stochastic Perron–Frobenius operators $\mathcal{P}_{s,t}$ and stochastic Koopman operators $\mathcal{K}_{s,t}$ as solution operators to Kolmogorov forward and backward problems with homogeneous Neumann boundary conditions. Furthermore, we discuss some of their properties such as the operators being adjoint, their common kernel k, and some spectral properties. A reader, that is already familiar with these ideas or who is more interested in the other parts of this thesis, may read this sometimes technical section after reading the next sections up to and including Section 3.3. This section uses concepts such as compact operators, the spectrum of an operator (Def. 3.3), evolution families (Def. 3.8), non-autonomous parabolic partial differential equations, and classical solutions (Def. 3.7) that are rigorously introduced in Chapter 3. Furthermore, we refer to arguments and results from Section 3.2 and Section 3.3 that are independent of Chapter 2.

To a reader, that might not be familiar with these topics and who would benefit more from a linear presentation, we suggest to read Section 3.1, Section 3.2 and Section 3.3 now, before proceeding. We present the following results here to motivate the ideas presented in Section 2.4 and Section 2.5. Section 3.1, Section 3.2 and Section 3.3 are located in Chapter 3, because they have a strong connection to and are necessary for Section 3.4 and Section 3.5, which in turn also rely on Section 2.4 and Section 2.5.

This section and other parts of this thesis investigate the evolution of densities and observables with tools from stochastic differential equations, Markov processes, parabolic partial differential equations and operator theory. Throughout this thesis, we utilize these different perspectives on common questions to gain synergistic insights into the evolution.

Perron–Frobenius Operators and Koopman Operators

We consider the problem (2.5) on $\mathbb{X} \subset \mathbb{R}^d$, satisfying (A0), with reflecting boundary condition. This leads for $s \in [0, T)$ to the initial-boundary value problem

$$\partial_t f(t,x) = -\mathrm{div}_x\big(v(t,x) f(t,x)\big) + \frac{1}{2}\sum_{i=1}^{d}\sum_{j=1}^{d} \frac{\partial^2}{\partial x_i \partial x_j}\Big((\sigma(t,x)\sigma^\top(t,x))_{ij} f(t,x)\Big) \tag{2.14}$$
$$f(s,x) = f_s(x)\,, \qquad \frac{\partial f(t,\cdot)}{\partial n} = 0 \text{ on } \partial\mathbb{X}.$$

Theorem 2.6:
Suppose that $\sigma_{ij} \in C^{(\alpha,2+\alpha)}([0,T]\times\overline{\mathbb{X}})$ and $v \in C^{(\alpha,1+\alpha)}([0,T]\times\overline{\mathbb{X}};\mathbb{R}^d)$, for some $\alpha \in (0,1]$, satisfy Assumption 1, then the following statements hold. We use the convention $f(t,\cdot) = f(t)$.

(1) For every initial condition $f_s \in L^p(\mathbb{X})$, for $p \in [1,\infty)$, the parabolic initial-boundary value problem (2.14) has a unique classical solution $f \in C([s,T];L^p(\mathbb{X})) \cap C^1((s,T];L^p(\mathbb{X}))$. Furthermore, the solution operators $\mathcal{P}_{s,t} : f_s \mapsto f(t) = \mathcal{P}_{s,t} f_s$ form a two-parameter evolution family of linear operators on $L^p(\mathbb{X})$. For $t > s$, the operator $\mathcal{P}_{s,t}$ maps into the Sobolev space $W^{2,p}(\mathbb{X})$, specifically $\mathcal{P}_{s,t} f_s \in W^{2,p}(\mathbb{X})$, and $\mathcal{P}_{s,t} : L^p(\mathbb{X}) \to L^p(\mathbb{X})$ is a compact operator for $t > s$.

(2) The Kolmogorov backward equation on $\mathbb{X}$ equipped with homogeneous Neumann boundary conditions and a final condition $f_t \in L^q(\mathbb{X})$, for $q \in [1,\infty)$, has a unique classical solution $f \in C([0,t];L^q(\mathbb{X})) \cap C^1([0,t);L^q(\mathbb{X}))$. The solution operators $\mathcal{K}_{s,t} : f_t \mapsto f(s) = \mathcal{K}_{s,t} f_t$ form a two-parameter family of linear operators on $L^q(\mathbb{X})$. For $s < t$, the operator $\mathcal{K}_{s,t}$ maps into the Sobolev space $W^{2,q}(\mathbb{X})$, specifically $\mathcal{K}_{s,t} f_t \in W^{2,q}(\mathbb{X})$, and $\mathcal{K}_{s,t} : L^q(\mathbb{X}) \to L^q(\mathbb{X})$ is a compact operator for $s < t$.

(3) For every fixed pair $s < t$, the compact linear operators $\mathcal{P}_{s,t}$ and $\mathcal{K}_{s,t}$ have discrete spectrum. In particular, the spectrum without $\{0\}$ consists of at most countably many non-zero eigenvalues with finite multiplicity, that can only accumulate at 0.

We refer to [AF03] for details and results on the Sobolev spaces $W^{k,p}$, $k \in \mathbb{N} \cup \{0\}$, $p \in [1,\infty]$.

Sketch of proof. We omit a detailed proof here. We refer to the more elaborate arguments from [Tan97], [Fri75], and [Fri08]. The statements (1) and (2) essentially follow from [Tan97, Chap. 6].

(1) In Section 3.2 and Section 3.3, we present results from [Tan97, Chap. 6] that can be used to prove Theorem 2.6 (1) and (2). In Theorem 3.12, we provide a more detailed proof for the case $\sigma(t,x) = \varepsilon I_{d\times d}$, for $\varepsilon > 0$, using the results from [Tan97, Chap. 6]. The arguments from Theorem 3.12 can be adapted to the case $\sigma(t,x)$ considered here, because σ is sufficiently regular and the assumption (A3) guarantees uniform ellipticity (3.16). The compactness of the operators $\mathcal{P}_{s,t}$ and $\mathcal{K}_{s,t}$ for $s < t$ follows from the compact embedding $W^{2,p}(\mathbb{X}) \overset{c}{\hookrightarrow} L^p(\mathbb{X})$ in [AF03, Thm. 6.3].

(2) The arguments from [Tan97, Chap. 6] and from Section 3.3 can be applied to the Kolmogorov backward problem as well. This can be seen by using the time reversal $t \mapsto T-t$ to transform the backward problem into a forward problem.

(3) See Lemma 3.4 (1) for this spectral property of compact operators.

□

If not stated otherwise, we assume in the following that σ, v satisfy Assumption 1 and that $\sigma_{ij} \in C^{(\alpha,2+\alpha)}([0,T] \times \overline{\mathbb{X}})$ and $v \in C^{(\alpha,1+\alpha)}([0,T] \times \overline{\mathbb{X}}; \mathbb{R}^d)$, for some $\alpha \in (0,1]$.

The stochastic Perron–Frobenius operator $\mathcal{P}_{s,t}$ is the solution operator to the Kolmogorov forward equation and is mapping an initial density f_s to a final density $f(t) = \mathcal{P}_{s,t} f_s$. The mapping $t \mapsto \mathcal{P}_{s,s+t} f$ is continuous as a mapping from $[0, T-s]$ to $L^p(\mathbb{X})$ for any fixed $f \in L^p(\mathbb{X})$.

The stochastic Koopman operator $\mathcal{K}_{s,t}$ is the solution operator of the Kolmogorov backward equation and can be characterized equivalently [Pil14, Thm. 3.1.1] by

$$(\mathcal{K}_{s,t} g)(x) = \mathbb{E}[g(X_t) | X_s = x] \,.$$

Fundamental Solution and Transition Kernel Families

Let us further investigate the connections between time-inhomogeneous Markov processes and non-autonomous parabolic differential equations. The Markov process $(X_t)_{t\in[0,T]}$ has a transition probability function p satisfying for all $t > s$

$$\mathbb{P}(X_t \in A \,|\, X_s = x) = p(s,t,x,A)$$

almost surely for all $A \in \mathcal{B}(\mathbb{R}^d)$ [Fri75, Chap. 5, Thm. 3.1].

If the process $(X_t)_{t\geq s}$ at time t, namely X_t, has a distribution that is absolutely continuous with respect to the Lebesgue measure Λ on $\mathbb{X}$, then it has a respective density $k(s,t)$

$$k(s,t) \,:\, \mathbb{X} \times \mathbb{X} \to \mathbb{R} \,,\ (x,y) \mapsto k(s,t,x,y) \,, \tag{2.15}$$

such that $\mathbb{P}(X_t \in A \,|\, X_s = x) = \int_A k(s,t,x,y)\, dy$.

Following [Fri08, Chap. 1], the non-autonomous parabolic initial and final value problems (2.13) and (2.12) have a fundamental solution Γ satisfying

$$f(t,y) = \int_{\mathbb{R}^d} \Gamma(s,t,x,y) f_s(x)\, dx \quad \text{and} \quad g(s,x) = \int_{\mathbb{R}^d} \Gamma(s,t,x,y) g_t(y)\, dy \,,$$

where f and g are solutions to the initial and final value problems with initial condition f_s and final condition g_t for (2.13) and (2.12).

The results in [KS91, Sec. 5.7] give for the whole space case, $\mathbb{X} = \mathbb{R}^d$, that the fundamental solution of the forward and backward problem corresponds to the transition kernel of the Markov process.

In the setting of Theorem 2.6, this follows from adapting and extending the arguments of [KS91, Sec. 5.7] and [Fri08] to the bounded domain $\mathbb{X}$ with homogeneous Neumann boundary conditions and from the proof of [KLP19, Lem. 4.1] given in [KLP19, App. B]. We summarize some results in Theorem 2.7.

Theorem 2.7:
The operator families $(\mathcal{P}_{s,t})_{s\leq t}$ and $(\mathcal{K}_{s,t})_{s\leq t}$ have a common family of kernels $(k(s,t,\cdot,\cdot))_{s\leq t}$ with

$$\mathcal{P}_{s,t}f(y) = \int_{\mathbb{X}} k(s,t,x,y)f(x)\,dx \quad \text{and} \quad \mathcal{K}_{s,t}g(x) = \int_{\mathbb{X}} k(s,t,x,y)g(y)\,dy \tag{2.16}$$

for all $f \in L^p(\mathbb{X})$ and $g \in L^q(\mathbb{X})$. The family of kernels is given by the fundamental solution of (2.14). Furthermore, we have $k(s,t,\cdot,\cdot) \in L^2(\mathbb{X}\times\mathbb{X})$, there exist a constant $M > 0$ such that $k(s,t,x,y) \leq M$ for all $x, y \in \overline{\mathbb{X}}$ and $k(s,t,x,\cdot)$ is stochastic.

Sketch of proof. Note that the assumptions made in this Chapter and thesis imply those in the references used. In [KLP19, App. B] the arguments of [Fri75] have been adapted to a bounded domain $\mathbb{X}$ with reflecting boundary conditions to show that the fundamental solution of the parabolic equation (2.13) is the density of the probability transition function (2.15) for the stochastic process and that it is a stochastic kernel.

- The arguments in [KLP19, App. B] establish that the fundamental solution Γ_N of the non-autonomous parabolic problem (2.14) exists and is equal to the probability transition kernel k of the corresponding time-inhomogeneous Markov process $(X_t)_{t\in[0,T]}$, more specifically $\Gamma_N(s,t,x,y) = k(s,t,x,y)$. For the existence and a construction of $\Gamma_N(s,t,x,y)$ see also [Itô57, Sec. I.3].
- The kernel representations (2.16) follow from theory of Markov processes [Fri75, Chap. 5] or alternatively from the properties of fundamental solutions [Fri08, Chap. 1].
- The square integrability $k(s,t,\cdot,\cdot) \in L^2(\mathbb{X}\times\mathbb{X})$ and the bound $k(s,t,x,y) \leq M$ for all $x, y \in \overline{\mathbb{X}}$ follow from [KLP19, Lem. 4.1].
- The kernel $k(s,t,x,\cdot)$ is stochastic, namely $\int_{\mathbb{X}} k(s,t,x,y)\,dy = 1$, because the characteristic function $\mathbb{1}_{\mathbb{X}}$ of the whole domain $\mathbb{X}$ is a constant solution to the Kolmogorov backward equation with homogeneous Neumann boundary conditions.

□

Theorem 2.7 indirectly contains the result that the operators $\mathcal{P}_{s,t}$ and $\mathcal{K}_{s,t}$ are adjoint in the following sense. With Fubini's theorem [Cia13, Thm. 1.15-5], we obtain

$$\begin{aligned}\langle \mathcal{P}_{s,t}f, g\rangle_{L^2} &= \int_{\mathbb{X}} \mathcal{P}_{s,t}f(x)g(x)\,dx = \int_{\mathbb{X}}\int_{\mathbb{X}} k(s,t,x,y)f(x)\,dx\,g(y)\,dy \\ &= \int_{\mathbb{X}}\int_{\mathbb{X}} k(s,t,x,y)g(y)\,dy\,f(x)\,dx = \int_{\mathbb{X}} f(x)\mathcal{K}_{s,t}g(x)\,dx = \langle f, \mathcal{K}_{s,t}g\rangle_{L^2}\,.\end{aligned} \tag{2.17}$$

for all $f \in L^p(\mathbb{X})$ and $g \in L^q(\mathbb{X})$ with $\frac{1}{p} + \frac{1}{q} = 1$. From the perspective of fundamental solutions to adjoint parabolic problems this also follows from [Fri08, Sec. 1.8, Thm. 15].

Properties of the Transfer Operators

For most parts of this thesis we use $\sigma(t,x) = \varepsilon I_{d\times d}$, for $\varepsilon > 0$. Here $I_{d\times d}$ denotes the identity in $\mathbb{R}^{d\times d}$. This uniform isotropic diffusion is the most appropriate choice in the context of the phenomenon of coherence in real world systems. However, many results presented in this thesis hold for general $\sigma \in C^{(\alpha,2+\alpha)}([0,T]\times\overline{\mathbb{X}};\mathbb{R}^{d\times d})$, satisfying (A1), (A2), and (A3), as well.

Theorem 2.8:

We assume $\mathrm{div}_x(v) = 0$ *and* $\sigma(t,x) = \varepsilon I_{d\times d}$, *for* $\varepsilon > 0$. *This corresponds to the volume-preserving setting with uniform and spatially isotropic diffusion. Then the following statements hold for* $0 \le s < t \le T$.

(1) The operators $\mathcal{P}_{s,t} : L^p(\mathbb{X}) \to L^p(\mathbb{X})$, $p \in [1,\infty)$, *and* $\mathcal{K}_{s,t} : L^q(\mathbb{X}) \to L^q(\mathbb{X})$, $q \in [1,\infty)$ *are integral preserving and non-negativity preserving, hence they are Markov operators. In particular, the kernel* $k(s,t)$ *is strictly positive. Furthermore,* $\mathcal{P}_{s,t}$ *is non-expansive on* $L^p(\mathbb{X})$ *for* $p \in [1,\infty)$ *and* $\mathcal{K}_{s,t}$ *is non-expansive on* $L^q(\mathbb{X})$ *for* $q \in [1,\infty)$.

(2) The spectra of $\mathcal{P}_{s,t}$ *and* $\mathcal{K}_{s,t}$ *are independent of* $p \in [1,\infty)$ *and* $q \in [1,\infty)$, *coincide for* $p,q \in (1,\infty)$ *with* $\frac{1}{p}+\frac{1}{q} = 1$, *are contained in the unit disk of* $\mathbb{C}$, *and contain the eigenvalue* 1 *with multiplicity one.*

Non-expansive linear operators are sometimes called contractions or contractive operators. Non-negative preserving operators are sometimes called positive operators.

Proof.

(a) Looking at the Kolmogorov backward equation (2.12), we see that $g = \mathbb{1}_{\mathbb{X}}$ is a constant solution satisfying the homogeneous Neumann boundary conditions on $\partial\mathbb{X}$. Thus, $\mathbb{1}_{\mathbb{X}}$ is an eigenfunction of $\mathcal{K}_{s,t}$ corresponding to the eigenvalue 1. For $\sigma(t,x) = \varepsilon I_{d\times d}$ and $\mathrm{div}_x(v) = 0$, we see that $f = \mathbb{1}_{\mathbb{X}}$ is a constant solution of (2.14). Therefore, $\mathbb{1}_{\mathbb{X}}$ is an eigenfunction of $\mathcal{P}_{s,t}$ corresponding to the eigenvalue 1. This implies that the kernel $k(s,t,\cdot,\cdot)$ is doubly stochastic if the flow is volume-preserving and if $\sigma(t,x) = \varepsilon I_{d\times d}$ holds.

(b) We use $\mathcal{K}_{s,t}\mathbb{1}_{\mathbb{X}} = \mathbb{1}_{\mathbb{X}}$ to show that $\mathcal{P}_{s,t}$ preserves the integral. For $f \in L^1(\mathbb{X})$ we obtain

$$\int_{\mathbb{X}} f\,dx = \langle \mathbb{1}_{\mathbb{X}}, f\rangle_{L^2} = \langle \mathcal{K}_{s,t}\mathbb{1}_{\mathbb{X}}, f\rangle_{L^2} = \langle \mathbb{1}_{\mathbb{X}}, \mathcal{P}_{s,t}f\rangle_{L^2} = \int_{\mathbb{X}} \mathcal{P}_{s,t}f\,dx\,.$$

For $\sigma(t,x) = \varepsilon I_{d\times d}$ and $\mathrm{div}_x(v) = 0$, it follows analogously that $\mathcal{K}_{s,t}$ preserves integrals.

(c) The result [Fri08, Sec. 2.4, Thm. 11] gives the strict positivity for the fundamental solution Γ_N. The general arguments and [Fri08, Chap. 2, Thm. 5] used in the proof of [Fri08, Sec. 2.4, Thm. 11] hold in the case of a bounded domain with homogeneous Neumann boundary condition. Note that, in the arguments of [Fri08, Sec. 2.4, Thm. 11], we can replace [Fri08, Chap. 2, Lem.5] for preserving non-negativity with the result [Itô57, Thm. 1] which gives that the fundamental solution is non-negative $\Gamma_N \ge 0$. This immediately implies that for an initial condition $f_s \in L^p(\mathbb{X})$ which is non-negative Λ-almost everywhere on $\overline{\mathbb{X}}$ that the function $\mathcal{P}_{s,t}f_s$ is also non-negative. The non-negative preserving property for $\mathcal{K}_{s,t}$ follows analogously.

(d) The properties (b) and (c) imply that $\mathcal{P}_{s,t}$ and $\mathcal{K}_{s,t}$ are Markov operators on $L^1(\mathbb{X})$ with $\|\mathcal{P}_{s,t}\|_{L(L^1,L^1)} \le 1$ and $\|\mathcal{K}_{s,t}\|_{L(L^1,L^1)} \le 1$.

(e) For a non-negative $0 \leq f \in L^q(\mathbb{X})$ follows with the non-negativity and the stochasticity of the kernel k and the Hölder inequality

$$\begin{aligned}
(\mathcal{K}_{s,t} f)^q(x) &= \left(\int_{\mathbb{X}} \left(k(s,t,x,y)^{\frac{1}{q}} f(y) \right) \left(k(s,t,x,y)^{1-\frac{1}{q}} \mathbb{1}_{\mathbb{X}}(y) \right) dy \right)^q \\
&\leq \int_{\mathbb{X}} k(s,t,x,y)(f(y))^q \, dy \cdot \left(\int_{\mathbb{X}} k(s,t,x,y)^{(1-\frac{1}{q})\cdot\frac{q}{q-1}} \, dy \right)^{q\cdot(1-\frac{1}{q})} \\
&= \mathcal{K}_{s,t}(f)^q(x) \cdot 1 \,.
\end{aligned}$$

Using this estimate for $f^+ := \max\{f, 0\}$ and $f^- := -\min\{f, 0\}$ implies that $\mathcal{K}_{s,t}$ is non-expansive on $L^q(\mathbb{X})$, specifically

$$\|\mathcal{K}_{s,t} f\|_{L^q} \leq \|\mathcal{K}_{s,t}|f|^q\|_{L^1} \leq \|\mathcal{K}_{s,t}\|_{L(L^1,L^1)} \cdot \|f\|_{L^q} \,.$$

For $\sigma(t,x) = \varepsilon I_{d\times d}$ and $\operatorname{div}_x(v) = 0$, it follows analogously that $\mathcal{P}_{s,t}$ is non-expansive on $L^p(\mathbb{X})$ for $p \in [1, \infty)$.

(f) Lemma 3.4 (3) gives that the spectra $\sigma(\mathcal{P}_{s,t})$ and $\sigma(\mathcal{K}_{s,t})$ coincide, if $\mathcal{K}_{s,t}$ and $\mathcal{P}_{s,t}$ are adjoint. For $s < t$, the corresponding eigenvalues have the same multiplicity, because the operators are compact; Lemma 3.4 (3).

(g) The arguments from [Dav07, Thm. 4.2.15 & p. 49] show that the spectrum of the compact operators $\mathcal{P}_{s,t} : L^p(\mathbb{X}) \to L^p(\mathbb{X})$, for $t > s$, is independent of $p \in [1, \infty)$ and that the eigenspaces coincide. This holds analogously for $\mathcal{K}_{s,t} : L^q(\mathbb{X}) \to L^q(\mathbb{X})$ with $s < t$ and $q \in [1, \infty)$. Note that this does not hold for only bounded operators [Dav07, Ex. 2.2.11].

(h) With the strict positivity of the kernel (c), the integral representation (2.16), and [Dav07, Thm. 13.3.1] follows that $\mathcal{P}_{s,t}$ and $\mathcal{K}_{s,t}$ are irreducible. Furthermore, the result [Dav07, Thm. 13.3.6] implies that the eigenvalue 1 is simple.

□

Theorem 2.8 summarizes some properties of $\mathcal{P}_{s,t}$ and $\mathcal{K}_{s,t}$ for fixed $s < t$. However, the analysis of the families $(\mathcal{P}_{s,t})_{s\leq t}$ and $(\mathcal{K}_{s,t})_{s\leq t}$ is more complicated, because it is not immediately clear how the spectra, the eigenspaces, and other properties evolve in time.

Remark 8:

- For some results in the whole space case $\mathbb{R}^d$ we refer to [Fri08] and [Kun19, Sec. 6.3]. Absorbing boundary conditions for stochastic differential equations can be treated with killing times or exit times and lead to homogeneous Dirichlet conditions for the Kolmogorov equations [Fri75, Sec. 6.5]. We refer to [Kun19, Sec. 6.10] and [Fri08] for the case of homogeneous Dirichlet conditions.

- From the deterministic setting, we would expect to consider the Perron–Frobenius operator on the space of densities $L^1(\mathbb{X})$ and the Koopman operator on $L^\infty(\mathbb{X})$. However, the function space $L^\infty(\mathbb{X})$ requires a different treatment in the context of parabolic equations [Lun95, Chap. 3].

△

A rigorous and detailed analysis of the spectrum of the transfer operators is beyond the scope of this thesis. We refer to the Kolmogorov forward equation (2.14) with $\sigma(t,x) = \varepsilon I_{d\times d}$ as the Fokker–Planck equation and consider homogeneous Neumann boundary conditions.

2.4 Measures of Coherence

An important and interesting topic in the context of dynamical systems is the transportation of mass within a given system. We analyze this transport from the perspective of coherent sets.

The General Idea of Coherent Sets

There is no single agreed upon mathematical definition of coherence. Nevertheless, there seem to be some generally accepted intuitive notions for coherent sets in different settings. Let us collect some intuitive notions that can but do not have to be considered simultaneously. Coherent sets should

- extend the notion of almost invariant sets to the non-autonomous setting.
- be distinguished subsets of the domain $\mathbb{X} \subset \mathbb{R}^d$ that significantly resist mixing with their surroundings for some time.
- be regions that are enclosed by material barriers that inhibit transport.
- be regions in state space that keep their geometric integrity under advective dynamics.
- be material subsets that are robust under advection with respect to some small diffusion.
- be robust under perturbed or noisy forward-backward evolutions.

The references [FSM10, FLS10, Fro13, Fro15, Den17, KK20, HKK20] are just some examples that give and investigate mathematical descriptions of these intuitive notions. Some of these geometric and probabilistic approaches can be related to each other in the context of the dynamic Laplacian [Fro15, KK20]. There are also data-driven methods that are well-suited for sparse, noisy or incomplete data; see [SSP$^+$19] and the references therein.

Figure 2.1 illustrates some of the intuitive notions of coherence. We consider a red liquid and a yellow liquid spilled in a rectangular spatial domain filled with otherwise blue liquid; Figure 2.1 (a). This configuration is then evolved for some time $T = 4$ using advective dynamics, Figure 2.1 (b), or advective-diffusive dynamics with $\sigma(t,x) = \varepsilon I_{d\times d}$ and noise strength $\varepsilon = 0.01$, Figure 2.1 (c). For this specific visualization we used a standard fourth-order Runge–Kutta or Runge–Kutta–Maruyama scheme for the periodically driven double gyre, which is introduced in Section 4.2.

Escape Rates and the Time-Asymptotic Perspective

When we consider evolution problems and the general idea of coherence, we distinguish between finite-time and time-asymptotic properties. Pursuing the idea that coherent subsets of $\mathbb{X}$ should leak the least to their surroundings, and should not mix with their complement in $\mathbb{X}$, we can look at rate of escape from those sets for a time-asymptotic quantifier of coherence.

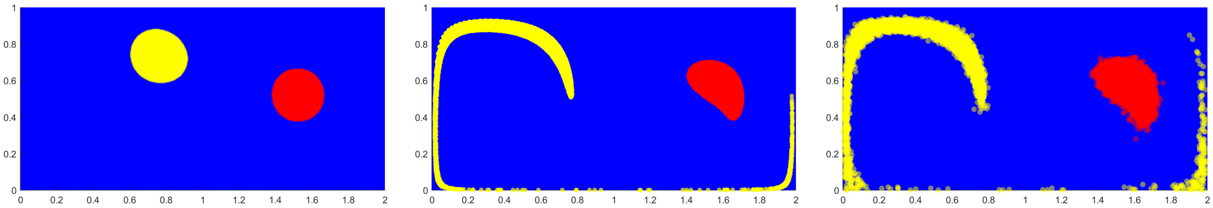

(a) Initial distribution of a red spill and a yellow spill.

(b) Final distribution of the spills under advection.

(c) Final distribution of the spills under advection and diffusion.

Figure 2.1: Illustrations of sets that we would intuitively call coherent, the red sets, or not coherent, the yellow sets.

To track and to quantify whether a stochastic trajectory $(X_t)_{t\geq s}$ stays within a given family of sets $(A_t)_{t\geq s}$, $A_t \subset \mathbb{X}$, we expect the probability $\mathbb{P}_{\Lambda_u}(X_r \in A_r\,,\,\forall r \in [s,t])$ to be well-defined. We denote the law of the process $(X_t)_{t\in[0,T]}$ generated by the SDE (2.5), initialized with the uniform distribution $X_0 \sim \Lambda_u$ on $\mathbb{X}$, by $\mathbb{P}_{\Lambda_u}$. Furthermore, Λ_u denotes the normalized Lebesgue measure on the bounded domain $\mathbb{X}$. This probability is well defined under some regularity assumptions on the family $(A_t)_{t\geq s}$, in particular on its boundaries. Sufficient properties are summarized in [FK17, Def. 4 & 17] under the names *nice* and *sufficiently nice*. In Theorem 3.21, we show that for the family of sets, that we construct from eigenfunctions of an unbounded linear operator, this probability is well-defined.

Definition 2.9:
For a set $A \subset \mathbb{X}$, a time-independent velocity field $v(t,x) = v(x)$, and the one-parameter family $(\mathcal{P}_s)_{s\geq 0}$ of stochastic Perron–Frobenius operators, we define the (upper) escape rate as

$$\begin{aligned} E(A) &:= -\liminf_{k\to\infty} \frac{1}{k} \log \int_A (\mathcal{P}_{t,A})^k (\mathbb{1}_{\mathbb{X}})\, d\Lambda_u \\ &= -\liminf_{k\to\infty} \frac{1}{k} \log \mathbb{P}_{\Lambda_u}(X_0 \in A, X_t \in A, \dots, X_{kt} \in A) \end{aligned} \tag{2.18}$$

with $\mathcal{P}_{t,A}(f) := \mathcal{P}_t(f\mathbb{1}_A)$.
For a family of (sufficiently nice) sets $(A_t)_{t\geq s}$ in the non-autonomous case, we define the (lower) escape rate as

$$E((A_t)_{t\geq s}) := -\limsup_{t\to\infty} \frac{1}{t-s} \log \mathbb{P}_{\Lambda_u}(X_r \in A_r\,,\,\forall\, r \in [s,t])\,. \tag{2.19}$$

The escape rate describes the asymptotic rate of the probability of a particle X_t leaving a set or a family of sets.

Remark 9:

- Comparing (2.18) to

$$-\liminf_{t\to\infty} \frac{1}{t} \log \mathbb{P}_{\Lambda_u}(X_s \in A\,,\,\forall\, s \in [0,t)) \tag{2.20}$$

  we can interpret (2.18) as a time-sampled version. We could use (2.20) instead of (2.18). However, we use (2.18) here for historical and consistency reasons. The sampled version (2.18) was used in [FJK13] for the generator approach to escape rates. In [FK17] the authors used (2.19) for the augmented generator approach.

- The escape rate approach from [FJK13] and [FK17] extends the results from discrete time and discrete space from [FS10].

△

Another notion that is strongly related to escape rates are Lyapunov exponents; see Theorem 3.16 from [FK17, Thm. 19].

Definition 2.10:
For $f \in L^1(\mathbb{X})$ the Lyapunov exponent of f with respect to the initial time s is given by

$$\operatorname{Lyap}_s(f) := \limsup_{t\to\infty} \frac{1}{t-s} \log \|\mathcal{P}_{s,t} f\|_{L^1} .$$

The reader might be tempted to assume that for an autonomous problem an almost invariant set [DFH+09, p. 48] gives a set with low escape rate, but that is not necessarily the case. In [FS10, Ex. 3.5 & 3.6] the authors show that, in the discrete-time and deterministic setting, there are almost invariant sets that have arbitrarily high escape rate and there are sets with low almost invariance and arbitrarily low escape rate.

Mixing

Recall that intuitively coherent sets are the structures that inhibit mixing the most. Thus, mixing can be seen as the opposite of coherence. Therefore, let us briefly introduce the concept of mixing. There are several different ways to measure mixing and mixedness for advection-diffusion processes, such as considering dispersion statistics or the change of variation in a concentration field [Pro99, LH04, TDG04, Thi08]. Multiscale norms of mixing measure how oscillatory a concentration field is [MMP05]; see [Thi12] for a review.

In the purely advective setting, $\sigma = 0$, we can look at mixing in the ergodic sense. For a normalized measure space $(\mathbb{X}, \mathcal{A}, \mu)$, a family of measure-preserving flow maps $\Phi_{s,t}$ is called mixing in the ergodic sense if

$$\lim_{t\to\infty} \mu(A \cap (\Phi_{s,t})^{-1}(B)) = \mu(A)\mu(B) .$$

In the stochastic and volume preserving setting, we can measure mixing for a concentration field $f \in C([0,\infty); L^2(\mathbb{X}))$ with zero mean, $\langle f(t,\cdot), \mathbb{1}_{\mathbb{X}}\rangle_{L^2} = 0$ by the rate of decay $\lambda < 0$ of the L^2 norm [FS17]

$$\|f(s+t,\cdot)\|_{L^2} \le Ce^{\lambda t} .$$

As it turns out, we can derive the rate λ independent of f from the spectrum of an infinitesimal generator. Theorem 3.16 relates this rate to the maximum Lyapunov exponent on the subspace of zero-mean functions. This is also consistent with the characterization of mixing as the opposite of coherence.

Although escape rates are asymptotic properties and thus are not appropriate for a finite-time perspective on coherence, a finite-time concept for Lyapunov exponents has been developed and served as a starting point for the analysis of material transport, see [HS11] and the references therein. We take a different approach to finite-time coherent sets.

Coherent Families and the Finite-time Perspective

Finite-time coherent sets on the time interval $[0, T]$, as introduced in [FSM10, Fro13, FPG14], can be extracted from singular functions of the Perron–Frobenius operator $\mathcal{P}_{0,T}$. Recall that $\mathcal{P}_{0,T}$ is the linear transfer operator describing the evolution of densities under the advection-diffusion dynamics. The singular modes of $\mathcal{P}_{0,T}$ are eigenmodes of $\mathcal{P}_{0,T}^*\mathcal{P}_{0,T}$, where $\mathcal{P}_{0,T}^*$ denotes the adjoint of $\mathcal{P}_{0,T}$. For volume-preserving dynamics, $\operatorname{div}_x(v) = 0$, $\mathcal{P}_{0,T}^*$ is the transfer operator of the time-reversed dynamics, namely, the stochastically perturbed evolution governed by the time-reflected velocity field $(t, x) \mapsto -v(T - t, x)$, see also [HP86] and [FKS20]. An intuitive notion behind this operator-based characterization is that finite-time coherent sets are those subsets that are to a large extent mapped back to themselves by the noisy forward-backward evolution $\mathcal{P}_{0,T}^*\mathcal{P}_{0,T}$. This operator-based approach gives a qualitative framework for coherence. Furthermore, the singular values of $\mathcal{P}_{0,T}$ provide quantitative bounds for coherence [Fro13, FPG14]. The closer the singular value is to one, the less mixing occurs between the coherent set, induced by the singular function, and its exterior under the noisy dynamics. A measure for coherence used in the references above is the coherence ratio of a coherent pair (A_0, A_T). We extend this concept here to the coherence ratio of a time-parameterized family of sets.

We consider the probability $\mathbb{P}_{\Lambda_u}(X_r \in A_r\,, \forall r \in [s, t])$. The following definition from [FKS20, Def. 4.4] is repeated in Definition 3.18 for convenience.

Definition 2.11:
Let $(A_t)_{t\in[0,T]}$ be a family of measurable sets. We denote the law of the process $(X_t)_{t\in[0,T]}$ generated by the SDE (2.5), initialized with the uniform distribution $X_0 \sim \Lambda_u$ on $\mathbb{X}$, by $\mathbb{P}_{\Lambda_u}$. Here Λ_u denotes the normalized Lebesgue measure on the bounded domain $\mathbb{X}$. For $\Lambda_u(A_0) > 0$ we define the coherence ratio of the family $(A_t)_{t\in[0,T]}$ as

$$\rho_{\Lambda_u}((A_t)_{t\in[0,T]}) := \frac{\mathbb{P}_{\Lambda_u}\left(\bigcap_{t\in[0,T]}\{X_t \in A_t\}\right)}{\Lambda_u(A_0)}\,.$$

Recalling Figure 2.1 we would expect that the red fluid corresponds to a family of sets with higher coherent ratio than the yellow fluid. In Section 4.2, we see that this is indeed the case.

Remark 10:

- Two real examples of finite-time coherent sets are the Agulhas Rings [FHRvS15] and the polar vortex [FSM10, BGT20].
- Instead of considering the stochastic Perron–Frobenius operator $\mathcal{P}_{s,t}$ that includes time-continuous diffusion, some approaches consider the deterministic Perron–Frobenius operator $P_{s,t}$ with time-discrete diffusion D_ε at initial and final time $D_\varepsilon P_{s,t} D_\varepsilon$ [Fro13, DJM16]. Intuitively we expect that these approaches are close depending on ε and $t - s$. Furthermore, we expect that the coherent sets extracted from level sets of the eigenfunctions become more material as ε decreases [Fro15, Sec. 5].
- Another approach to coherent sets in the stochastic setting utilizing stochastic flows [Kun19] can be found in [Den17, Chap. 4].

△

There are many different approaches and quantifiers to characterize coherence in dynamical systems. Chapter 3 introduces the generator approach to coherence that has first been used for the time-asymptotic perspective and has been adapted to the finite-time setting with the help of the reflection trick from Section 2.5. The connection between transfer operators and the coherence ratio of a family of sets is investigated further in Section 3.5.

2.5 Reflection

The general content of Section 2.5, except the figures, has been published in [FKS20, Sec. 2 & 4] and is re-used with the permission of the publisher and the authors.

Let us summarize our setting. We consider a spatial domain $\mathbb{X} \subset \mathbb{R}^d$ that satisfies (A0); page 13. For $v \in C^{(\alpha,1+\alpha)}([0,T] \times \overline{\mathbb{X}}; \mathbb{R}^d)$ with $\operatorname{div}_x(v) = 0$, we consider

$$dX_t = v(t, X_t)dt + \varepsilon\, dW_t$$

with reflecting boundary conditions on the time interval $[0,T]$. The initial condition X_0 is distributed according to some initial density $f_0 \in L^2(\mathbb{X})$. The evolution of the density is given by the Fokker–Planck equation, or Kolmogorov forward equation,

$$\begin{aligned} \partial_t f(t,x) &= -\operatorname{div}_x\big(v(t,x)f(t,x)\big) + \frac{\varepsilon^2}{2}\Delta_x f(t,x) \\ f(0,x) &= f_0(x)\,, \quad \frac{\partial f(t,\cdot)}{\partial n} = 0 \text{ on } \partial\mathbb{X}, \end{aligned} \tag{2.21}$$

where $\frac{\partial}{\partial n}$ is the normal derivative on the boundary. Associated to (2.21), there is a two-parameter family of Perron–Frobenius operators $\mathcal{P}_{s,t} : L^2(\mathbb{X}) \mapsto L^2(\mathbb{X})$ that transport a density $f \in L^2(\mathbb{X})$ at time s to the solution density of (2.21) at time t.

Following [Fro13, Den17] in the volume-preserving setting, coherent sets over the time interval $[0,T]$ can be extracted from the eigenfunctions of $\mathcal{P}_{0,T}^*\mathcal{P}_{0,T}$ corresponding to large eigenvalues, where $\mathcal{P}_{s,t}^*$ is the L^2-adjoint of $\mathcal{P}_{s,t}$, defined to be the unique linear operator satisfying

$$\langle \mathcal{P}_{s,t} f, g\rangle_{L^2} = \langle f, \mathcal{P}_{s,t}^* g\rangle_{L^2}$$

for all $f, g \in L^2(\mathbb{X})$. A useful intuition for the operator $\mathcal{P}_{0,T}^*\mathcal{P}_{0,T}$ is that $\mathcal{P}_{0,T}$ describes evolution in forward time and that $\mathcal{P}_{0,T}^*$ describes evolution under the time-reversed dynamics. Finite-time coherent sets can be characterized exactly by the property that they are robust under a noisy forward-backward evolution.

This work is focused on a generator based approach. The generator is in general an unbounded operator whose singular values are less accessible than its eigenvalues. Therefore, we introduce a reflection trick that behaves well with respect to the information that we are interested in. This reflection allows us to derive finite-time information from eigendata of the resulting evolution.

Construction of a Forward-Backward Process

According to Section 2.3, the adjoint operator $\mathcal{P}^*_{t,T}$ is the solution operator to the Kolmogorov backward problem (2.12)

$$\begin{aligned}-\partial_t g(t,x) &= \langle v(t,x), \nabla_x g(t,x)\rangle_{\mathbb{R}^d} + \frac{\varepsilon^2}{2}\Delta_x g(t,x) \\ g(T,x) &= g_T(x)\,, \quad \frac{\partial g(t,\cdot)}{\partial n} = 0 \text{ on } \partial\mathbb{X}.\end{aligned} \tag{2.22}$$

The operator $\mathcal{P}^*_{t,T}$ maps a final density g_T at time $t = T$ backward in time according to (2.22)

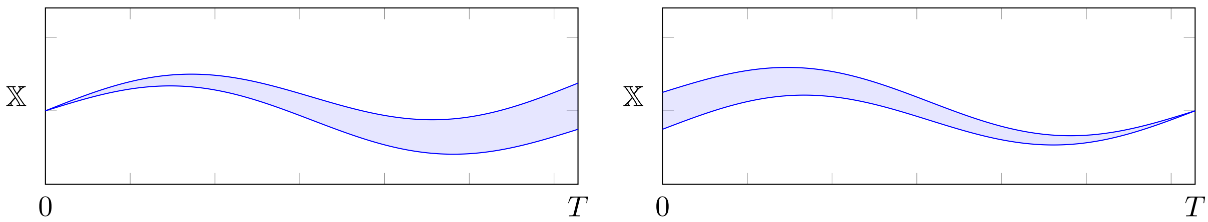

(a) Kolmogorov forward problem.

(b) Kolmogorov backward problem.

Figure 2.2: A pictographic representation of the forward and the backward problem.

to the corresponding density g_t at time $t < T$. The forward problem and the corresponding backward problem are illustrated in Figure 2.2. We rewrite (2.22) using $\mathrm{div}_x(v) = 0$ as follows

$$\begin{aligned}\langle v(t,x), \nabla_x g(t,x)\rangle_{\mathbb{R}^d} &= \mathrm{div}_x(v(t,x)g(t,x)) - \mathrm{div}_x(v(t,x))g(t,x) \\ &= \mathrm{div}_x(v(t,x)g(t,x))\,.\end{aligned}$$

Thus, equation (2.22) takes the form

$$-\partial_t g(t,x) = \mathrm{div}_x(v(t,x)g(t,x)) + \frac{\varepsilon^2}{2}\Delta_x g(t,x)\,.$$

By reversing time $t \mapsto T - t$ in (2.22), we obtain an initial value problem

$$\begin{aligned}\partial_t f(t,x) &= -\mathrm{div}_x(\bar{v}(t,x)f(t,x)) + \frac{\varepsilon^2}{2}\Delta_x f(t,x) \\ f(0,x) &= \bar{f}_0(x)\,, \quad \frac{\partial f(t,\cdot)}{\partial n} = 0 \text{ on } \partial\mathbb{X}\end{aligned} \tag{2.23}$$

using $f(t,x) = g(T-t,x)$, $\bar{f}_0(x) = g_T(x)$ and the velocity field $\bar{v}(t,x) := -v(T-t,x)$. The forward version of Figure 2.2 (b) is visualized in Figure 2.3 (a).

Comparing (2.21) and (2.23), we see that the evolution of the adjoint problem, the Kolmogorov backward equation, corresponds to a forward problem, a Kolmogorov forward equation, using the time-reversed dynamics.

We want to concatenate the forward velocity field v on $[0,T]$ and the shifted and reversed backward velocity field $\tilde{v}$ on $[T,\tau]$, to construct a process on $[0,\tau]\times\mathbb{X}$ with $\tau = 2T$ that mimics the forward-backward evolution. Therefore, the evolution on $[T,\tau]$ should correspond to the action of the operator $\mathcal{P}^*_{0,T}$. To achieve this, we shift (2.23) by T time units and define

$$\tilde{v}(t,x) := \bar{v}(t-T,x) = -v(\tau - t,x) = -v(2T-t,x)\,.$$

We obtain a forward problem on $[T, \tau]$

$$\begin{aligned} \partial_t f(t,x) &= -\mathrm{div}_x(\tilde{v}(t,x) f(t,x)) + \frac{\varepsilon^2}{2}\Delta_x f(t,x) \\ f(T,x) &= \tilde{f}_T(x) = \bar{f}_0(x)\,, \quad \frac{\partial f(t,\cdot)}{\partial n} = 0 \text{ on } \partial\mathbb{X}. \end{aligned} \tag{2.24}$$

We denote the solution operator of this problem by $\tilde{\mathcal{P}}_{T,t}$ which corresponds to $\mathcal{P}^*_{\tau-t,T}$.

Now, we concatenate the two forward problems (2.21) and (2.24) to construct the desired evolution on $[0, \tau]$. We mark objects that live on this extended interval $[0, \tau]$ with a hat $\hat{\ }$.

We define the reflected velocity field

$$\hat{v}(t,\cdot) := \zeta'(t) v(\zeta(t),\cdot) = \begin{cases} v(t,\cdot), & t \in [0,T]; \\ -v(\tau - t,\cdot), & t \in (T,\tau], \end{cases} \tag{2.25}$$

using the reflection map

$$\zeta(t) := \begin{cases} t, & t \in [0,T]; \\ \tau - t, & t \in (T,\tau]. \end{cases} \tag{2.26}$$

The resulting reflected velocity field $\hat{v}$ exhibits a discontinuity in T, whenever it does not vanish there. However, the one-sided derivatives exist. This leads to the Fokker–Planck problem

$$\begin{aligned} \partial_t \hat{f}(t,x) &= -\mathrm{div}_x(\hat{v}(t,x)\hat{f}(t,x)) + \frac{\varepsilon^2}{2}\Delta_x \hat{f}(t,x) \\ \hat{f}(0,x) &= f_0(x)\,, \quad \frac{\partial \hat{f}(t,\cdot)}{\partial n} = 0 \text{ on } \partial\mathbb{X}\,, \end{aligned} \tag{2.27}$$

on the interval $[0, \tau]$; more precisely on $(0, T) \cup (T, \tau)$ with L^2-continuous concatenation at $t = T$. Theorem 2.12 and Figure 2.3 (b) summarize the above construction.

Theorem 2.12:
The concatenation $\mathcal{P}^*_{0,T}\mathcal{P}_{0,T} \triangleq \hat{\mathcal{P}}_{0,\tau}$ with $\tilde{f}_T = \mathcal{P}_{0,T} f_0$ comprises initializing (2.21) at time 0, solving forward using the vector field $v(t,\cdot)$ until time T, then continuing to evolve (2.24) for another T time units, but now using the reflected and shifted vector field $-v(\tau - t,\cdot)$ for $t \in [T,\tau]$ corresponding to the reversed dynamics.

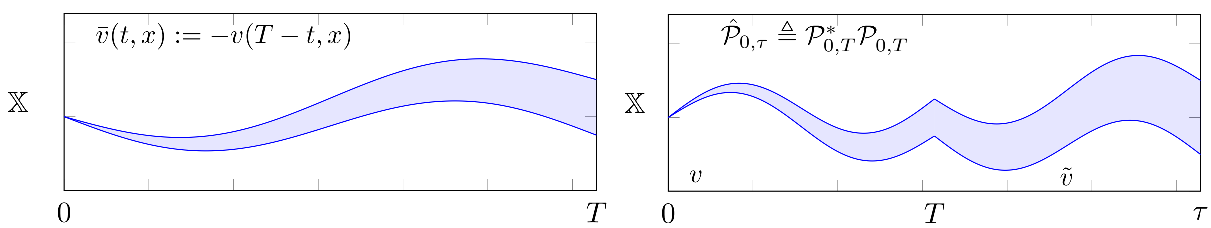

(a) The time-reversed backward problem is a forward problem with time-reversed advection.

(b) The concatenated problem on $[0, \tau]$.

Figure 2.3: Visualization of the new forward process (2.23) on $[0, T]$ leading to the forward-backward dynamics (2.27) on $[0, \tau]$.

Remark 11:

- The following regularity may not be most general, but it is meant to give some intuition. For $v \in C^{(\alpha,1+\alpha)}([0,T]\times\overline{\mathbb{X}};\mathbb{R}^d)$ follows $\hat{v} \in C^{(\alpha,1+\alpha)}(((0,T)\cup(T,\tau))\times\overline{\mathbb{X}};\mathbb{R}^d)$ which further implies $\hat{v} \in L^p((0,\tau)\times\mathbb{X};\mathbb{R}^d)$, for $1 \le p \le \infty$. Theorem 3.19 gives some details for the point $t = T$.

- For non-zero divergence velocity fields, we could investigate normalized versions of the operators $\mathcal{P}_{0,T}$ and $\mathcal{P}^*_{0,T}$. For more details on normalized transfer operators see also [Fro13, Den17].

$\triangle$

The Two-Parameter Solution Family for the Reflected Periodically Extended Process

Following [Fro13], the second largest eigenvalue $\lambda_2(\hat{\mathcal{P}}_{0,\tau})$ and singular value $\sigma_2(\mathcal{P}_{0,T})$ satisfy

$$\sqrt{\lambda_2(\hat{\mathcal{P}}_{0,\tau})} = \sigma_2(\mathcal{P}_{0,T}) = \max_{\substack{f_0\in L^2(\mathbb{X},\mu_0)\\ g_T\in L^2(\mathbb{X},\mu_T)\\ \langle f_0,\mathbb{1}_{\mathbb{X}}\rangle_{\mu_0}=0\\ \langle g_T,\mathbb{1}_{\mathbb{X}}\rangle_{\mu_T}=0}} \left\{ \frac{\langle \mathcal{P}_{0,T} f_0, g_T\rangle_{\mu_T}}{\|f_0\|_{L^2(\mathbb{X},\mu_0)}\|g_T\|_{L^2(\mathbb{X},\mu_T)}} \right\} < 1, \tag{2.28}$$

where in the volume-preserving setting μ_0 and μ_T are both the Lebesgue measure $\Lambda = \mu_0 = \mu_T$. In the non-zero divergence case, μ_0 is a reference measure describing the initial mass distribution of the possibly compressible fluid being evolved, and μ_T is the forward evolution of μ_0 under a normalized Perron–Frobenius operator [Fro13, Den17].

In this thesis, we consider the problem (2.27) as a time-periodic problem on $\tau S^1 \times \mathbb{X}$. In particular, we extend the velocity field $\hat{v}$ in time τ-periodically which introduces another discontinuity in $0, \tau$. To describe the evolution family, we assume $s \in [0,\tau]$ without loss of generality. The evolution operator $\hat{\mathcal{P}}_{s,s+t}$ starting from time s and flowing for time $t \ge 0$ to $s+t = kT + r$, $k = \lfloor \frac{s+t}{T} \rfloor \in \mathbb{N}\cup\{0\}$ and $(s+t) \mod T = r \in [0,T)$, is given by

$$\hat{\mathcal{P}}_{s,s+t} = \begin{cases} \mathcal{P}_{s,s+t} & s\in[0,T], t\in[0,T-s],\ k=0,\\ \mathcal{P}^*_{\tau-r,T}(\mathcal{P}_{0,T}\mathcal{P}^*_{0,T})^{\frac{k-1}{2}}\mathcal{P}_{s,T}, & s\in[0,T], t > T-s, k \text{ odd},\\ \mathcal{P}_{0,r}\mathcal{P}^*_{0,T}(\mathcal{P}_{0,T}\mathcal{P}^*_{0,T})^{\frac{k-2}{2}}\mathcal{P}_{s,T}, & s\in[0,T], t>T-s, 2\le k \text{ even},\\ \mathcal{P}^*_{\tau-(s+t),\tau-s}, & s\in[T,\tau], t\in[0,\tau-s],\ k=1,\\ \mathcal{P}_{0,r}(\mathcal{P}^*_{0,T}\mathcal{P}_{0,T})^{\frac{k-2}{2}}\mathcal{P}^*_{0,\tau-s}, & s\in[T,\tau], t>\tau-s, 2\le k\text{ even},\\ \mathcal{P}^*_{T-r,T}\mathcal{P}_{0,T}(\mathcal{P}^*_{0,T}\mathcal{P}_{0,T})^{\frac{k-3}{2}}\mathcal{P}^*_{0,\tau-s}, & s\in[T,\tau], t>\tau-s, 3\le k \text{ odd}.\end{cases} \tag{2.29}$$

The situation when t is exactly the period τ is of particular importance:

$$\hat{\mathcal{P}}_{s,s+\tau} = \begin{cases} \mathcal{P}_{0,s}\mathcal{P}^*_{0,T}\mathcal{P}_{s,T}, & s\in[0,T],\\ \mathcal{P}^*_{\tau-s,T}\mathcal{P}_{0,T}\mathcal{P}^*_{0,\tau-s}, & s\in[T,\tau].\end{cases} \tag{2.30}$$

The operator $\hat{\mathcal{P}}_{s,s+\tau}$ is self-adjoint for $s = kT$, $k\in\mathbb{N}\cup\{0\}$. The eigenvalues of $\mathcal{P}^*_{0,T}\mathcal{P}_{0,T}$, which are the singular values of $\mathcal{P}_{0,T}$, are contained in the interval $[0,1]$. This follows from Theorem 2.8 and the fact that the compact and self-adjoint operator $\mathcal{P}^*_{0,T}\mathcal{P}_{0,T}$ on the Hilbert space $L^2(\mathbb{X})$ has real spectrum [Alt16, 12.13].

In Chapter 2 we introduced the noisy evolution of particles and densities, the concept of coherent sets and the reflection trick. In the next chapter, we introduce non-autonomous abstract evolution problems and extend the concept of the infinitesimal generator to non-autonomous problems from which we obtain coherent families.

3 A Space-Time Generator Approach

After introducing stochastic differential equations and coherent families in Chapter 2, this chapter connects semigroup theory for partial differential equations to coherence. This chapter gives an abstract but powerful approach to analyze autonomous and non-autonomous evolutions involving linear unbounded operators in infinite dimensions.

Section 3.1 introduces some basic concepts of semigroup theory for abstract Cauchy problems (ACPs). Then Section 3.2 and Section 3.3 are concerned with non-autonomous abstract Cauchy problems (NACPs). Using the results from [Kol11], [FJK13], [FK17] and [FKS20], Section 3.4 and Section 3.5 investigate one of the main objects of semigroup theory, the infinitesimal generator (Def. 3.1), in order to extract coherent families.

3.1 Semigroup Theory

The theory of strongly continuous semigroups is one of the main tools to deal with autonomous ordinary and partial as well as operator differential equations. This theory gives an abstract framework to investigate the autonomous problems from Section 2.1 and Section 2.2. There are many recommendable introductions to semigroup theory and its applications, for example, [EN00] and [Paz83].

This section on semigroup theory roughly follows [Paz83]. We consider semigroups acting on an arbitrary Banach space $(V, \|\cdot\|_V)$. Let us define two main objects: the semigroup and its infinitesimal generator.

Definition 3.1:
A one-parameter family $(S(t))_{t\in I}$, $I = [0,T]$ or $I = [0,\infty)$, of bounded linear operators $S(t)$ mapping from V into V, $S(t) \in L(V,V)$, is called an operator semigroup on V if

1. $S(0) = Id_V$ *(the identity on V)*
2. $S(t+s) = S(t)S(s)$ *for every $s, t \in I$, with $s+t \in I$ (semigroup property)*

The operator $G : \mathcal{D}(G) \to V$ defined by

$$\mathcal{D}(G) := \left\{ x \in V \,\middle|\, \lim_{t\downarrow 0} \frac{S(t)x - x}{t} \text{ exists} \right\} \quad \text{and} \quad Gx := \lim_{t\downarrow 0} \frac{S(t)x - x}{t} \quad \text{for } x \in \mathcal{D}(G) \tag{3.1}$$

is called the infinitesimal generator of the semigroup $(S(t))_{t\in I}$ with the domain $\mathcal{D}(G)$.
The semigroup is called strongly continuous or a C_0 semigroup if

$$\lim_{t\downarrow 0} S(t)x = x$$

holds for all $x \in V$.

Remark 12:

- For a C_0 semigroup there are constants $M \geq 1$ and $\omega \geq 0$ such that $\|S(t)\|_{L(V,V)} \leq Me^{\omega t}$ [Paz83, Thm. 1.2.2].
- Every C_0 semigroup $(S_t)_{t\in I}$ has a unique infinitesimal generator G and every C_0 semigroup is uniquely defined by its infinitesimal generator [Paz83, Thm. 1.2.6]. The infinitesimal generator G of a C_0 semigroup $(S(t))_{t\in I}$ has dense domain $\mathcal{D}(G) \subset V$ and is a closed operator [Paz83, Cor. 1.2.5].
- The domain $\mathcal{D}(G)$ defined in (3.1) is the maximal domain. In many cases it is possible and useful to consider G on smaller domains, in particular appropriate subsets of $\mathcal{D}(G)$.
- A semigroup $(S(t))_{t\in I}$ is called uniformly continuous if $\lim\limits_{t\downarrow 0} \|S(t) - Id_V\|_{L(V,V)} = 0$. A linear operator G is the infinitesimal generator of a uniformly continuous semigroup if and only if G is bounded [Paz83, Thm. 1.1.2].

△

The definition in (3.1) suggests the formal relationship $S(t) = e^{tG}$. The expression e^{tG} is in general not well-defined for unbounded operators G. Nevertheless, it can serve as an intuition for the properties that can be derived from this relation. Theorem 3.2 is concerned with some properties of the generator and the semigroup. Furthermore, it gives a more precise characterization of the idea $S(t) = e^{tG}$.

Theorem 3.2:
Let $S(t)_{t\in I}$ be a C_0 semigroup with infinitesimal generator G. Then the following holds.

1. *For $x \in V$ it holds that* $\lim\limits_{h\to 0} \frac{1}{h}\int_t^{t+h} S(s)x\,ds = x$.
2. *For $x \in V$ it follows that* $\int_0^t S(s)x\,ds \in \mathcal{D}(G)$ *and*
$$G\left(\int_0^t S(s)x\,ds\right) = S(t)x - S(0)x = S(t)x - x\,. \tag{3.2}$$
3. *For $x \in \mathcal{D}(G)$ we obtain $S(t)x \in \mathcal{D}(G)$ and* $\frac{d}{dt}S(t)x = GS(t)x = S(t)Gx$.
4. *For $x \in \mathcal{D}(G)$ it holds that* $S(t)x - S(s)x = \int_s^t GS(\tau)x\,d\tau = \int_s^t S(\tau)Gx\,d\tau$.

Proof. Theorem 3.2 and a proof can be found in [Paz83, Thm. 1.2.4]. □

Remark 13:

- The relation $S(t) = e^{tG}$ can be made more rigorous using the results [Paz83, Sec. 1.8] and [EN00, Sec. II.3.3] or the Borel functional calculus [RS80, Chap. VII].
- Semigroups or more precise the mappings $t \mapsto S_t := S(t)$ and $t \mapsto S_t x = S(t)x$ for $x \in V$ with specific topologies, can have higher regularity. They can be differentiable or analytic [Paz83, Def. 2.4.1 & 2.5.1]. There are other interesting properties such as for all $t \in I$ the operator $S(t)$ being a compact operator or even a contraction [Paz83, Sec. 2.3]. These additional properties lead to stronger results.

△

We prefer the notation $S(t)$ for general abstract semigroup operators, but we may use S_t instead to improve the readability.

The question which operators G are generators of C_0 semigroups and what properties these semigroups possess has been important for the theory of partial differential equations. This question has lead to multiple theorems concerned with sufficient conditions. There are several theorems mostly motivated from partial differential problems that give necessary and sufficient conditions, like the Hille–Yosida theorem [Paz83, Thm. 1.3.1], the Lumer–Phillips theorem [Paz83, Thm. 1.4.3], the Crandall–Liggett theorem [CL71] and many others.

Some of these conditions involve the spectrum of the generator [Paz83, Sec. 2.4 & 2.5].

The Spectrum

Bounded and unbounded operators can be characterized by their spectrum.

Definition 3.3:
For a linear possibly unbounded operator A on a Banach space V, the set $\rho(A)$ of complex numbers $z \in \mathbb{C}$ for which $(zId_V - A)$ is invertible is called the resolvent set of A. Furthermore, $R(z, A) := (zId_V - A)^{-1}$ for $z \in \rho(A)$ is called the resolvent and $\sigma(A) := \mathbb{C}\backslash\rho(A)$ is called the spectrum of A.
The spectrum can be partitioned with respect to the properties of $(zId_V - A)$. The point spectrum $\sigma_p(A)$, the continuous spectrum $\sigma_c(A)$, and the residual spectrum $\sigma_r(A)$ are defined as follows

1. *$\lambda \in \sigma_p(A)$ if $(\lambda Id_V - A)$ is not injective.*
2. *$\lambda \in \sigma_c(A)$ if $(\lambda Id_V - A)$ is injective, but it is not surjective and its range is dense in V.*
3. *$\lambda \in \sigma_r(A)$ if $(\lambda Id_V - A)$ is injective, it is not surjective, and its range is not dense in V.*

The spectrum of a linear unbounded operator can be more complicated than the set of eigenvalues of a matrix. In general, the point spectrum of an operator behaves similar to the spectrum of a matrix. Lemma 3.4 summarizes some properties of the the spectrum for compact linear operators.

Lemma 3.4:

(1) *Consider the spectrum $\sigma(A)$ of a compact linear operator $A : V \to V$. For $\dim V = \infty$, the set $\sigma(A)\backslash\{0\}$ consists of at most countably many eigenvalues $0 \neq \lambda_i \in \sigma_p(A)$ with finite multiplicity that can only accumulate at 0.*

(2) *The infinitesimal generator of a C_0 semigroup of compact operators has pure point spectrum.*

(3) *For a bounded linear operator $A \in L(V, V)$ and its adjoint A^* acting on V^*, the dual space of V, $A^* \in L(V^*, V^*)$, holds $\sigma(A) = \sigma(A^*)$. Furthermore, A is compact if and only if A^* is compact and the non-zero eigenvalues of A and A^* have the same multiplicity.*

Proof.

(1) See [Alt16, Sec. 11.9 & 11.14].

(2) See [Paz83, Cor. 2.3.7]. This also follows from (1) and the spectral mapping property (3.3).

(3) See [DS88, VII.3.7] for $\sigma(A) = \sigma(A^*)$. See [Rud91, Thm. 4.19] for the compactness and [Rud91, Thm. 4.25] for the multiplicities of the non-zero eigenvalues.

□

Remark 14:

- There are examples for either $\sigma(A) = \emptyset$ or $\rho(A) = \emptyset$ [EN00, Chap. IV].
- The resolvent set $\rho(G)$ of the infinitesimal generator G of a C_0 semigroup contains the ray $\{z \in \mathbb{C} \,|\, \mathrm{Im}(z) = 0 \text{ and } z > \omega\}$ for some $\omega \geq 0$ [Paz83, Cor. 1.3.8].
- The continuous and residual spectrum, if it is non-empty $(\sigma_c \cup \sigma_r) \neq \emptyset$, may require additional attention. The theory of spectral measures can give insights into the continuous and residual spectrum of an operator [RS80, Chap. VII].

△

While the *shape* and the *boundaries* of the spectrum as a subset of $\mathbb{C}$ are important for many results [EN00, Sec. II.4], sometimes the actual position of the spectrum in $\mathbb{C}$ is not necessarily important as the next paragraph shows.

Rescaling

Given a generator G with the domain $\mathcal{D}(G)$, the resolvent set $\rho(G)$ and the spectrum $\sigma(G)$ that induces a semigroup $(S(t))_{t\in I}$, we can rescale [EN00, Sec. II.2.2] this semigroup for some $\beta \in \mathbb{C}$ and $\alpha > 0$ and obtain the rescaled semigroup

$$T(t) := e^{\beta t} S(\alpha t)\,,$$

which has the generator H with

$$\mathcal{D}(H) = \mathcal{D}(G) \qquad H = \alpha G + \beta Id_V \qquad \sigma(H) = \alpha\sigma(G) + \beta\,.$$

This rescaling trick is often used to simplify notation, without being specifically mentioned by authors in the field of semigroup theory. If a generator satisfies $0 \in \sigma(G)$, but a theorem imposes the condition $0 \in \rho(G)$, then we may consider a rescaled semigroup for which $0 \in \rho(H)$ holds. After applying the theorem, we can often transfer the result back using the same rescaling trick.

Spectral Mapping Property

The following spectral mapping property relates the point spectrum of the generator to the spectrum of an operator from the semigroup.

Theorem 3.5:
Let $(S(t))_{t\in I}$ be a C_0 semigroup and let G be its infinitesimal generator. Then for the point spectrum holds

$$e^{t\sigma_p(G)} \subset \sigma_p(S(t)) \subset e^{t\sigma_p(G)} \cup \{0\}\,. \tag{3.3}$$

More precisely, if $\lambda \in \sigma_p(G)$, then $e^{\lambda t} \in \sigma_p(S(t))$, and if $e^{\lambda t} \in \sigma_p(S(t))$, then there exists a $k \in \mathbb{N}$ such that $\lambda_k = \lambda + \frac{2\pi k i}{t} \in \sigma_p(G)$.
For the general spectrum holds

$$e^{t\sigma(G)} \subset \sigma(S(t))\,.$$

Proof. See [Paz83, Thm. 2.2.4] for the point spectrum and [Paz83, Thm. 2.2.3] or [EN00, Thm. IV.3.6] for the general spectral inclusion result. □

In Section 3.4 and Section 3.5 we encounter more spectral mapping theorems and use them to relate eigenvalues of an infinitesimal generator to coherence.

Abstract Cauchy Problems

The most prominent application of semigroup theory is the analysis of linear autonomous operator differential equations arising from ordinary and partial differential equations [Paz83, Chap. 4 & 7]. These initial value and initial-boundary value problems can be rephrased more general as autonomous abstract Cauchy problems (ACPs)

$$\text{(ACP)} \begin{cases} \dfrac{df(t)}{dt} = Gf(t) + g(t) \\ f(0) = f_0 \end{cases} \tag{3.4}$$

with $g : I \to V$ in a Banach space V. Section 3.3 gives further details on how to rephrase partial differential equations as abstract Cauchy problems.

Let us now define different types of solutions to the ACP. We denote the Bochner-Lebesgue spaces by $L^p(0,T;V)$, $p \in [1,\infty]$. For a short introduction to Bochner-Lebesgue spaces we refer to [Zei90a, Chap. 23].

Definition 3.6:

1. *A function $f : [0,T] \to V$ is called a classical solution if f is continuous on $[0,T)$, f is continuously differentiable on $(0,T)$, $f(t) \in \mathcal{D}(G)$, and f satisfies* (3.4) *for every $t \in [0,T)$.*
2. *Let G be the generator of a semigroup $(S(t))_{t\in[0,T]}$, $u_0 \in V$ and $g \in L^1(0,T;V)$. The function $f \in C([0,T];V)$ given by*

$$f(t) = S(t)f_0 + \int_0^t S(t-s)g(s)\,ds \tag{3.5}$$

   is called mild solution of (3.4)*.*
3. *A function f that is differentiable almost everywhere on $[0,T]$ with $f' \in L^1(0,T;V)$ is called a strong solution of* (3.4) *if $f(0) = f_0$ and $f'(t) = Gf(t) + g(t)$ almost everywhere on $[0,T]$.*

There are sufficient conditions to guarantee the existence of a unique classical [Tan97, Chap. 6], strong [Paz83, Thm. 4.2.9] or mild [Paz83, Def. 4.2.3, Sec.4.2] solution which require G to generate a C_0 semigroup. As expected, under suitable assumptions on g, f_0 and G a mild solution is a classical solution [Paz83, Thm. 4.3.6].

The formula (3.5) shows that we can compute the unique solution to an abstract Cauchy problem if G generates a C_0 semigroup on V. Recalling the problems from Chapter 2 for time-independent velocity fields $v(t,x) = v(x)$, we could investigate whether the partial differential equations from Section 2.1 and Section 2.2 induce abstract Cauchy problems with suitable operators G. The sources [Paz83, Chap. 5] and [LM94, Chap. 7 & 11] investigate these types of problems also from the semigroup perspective.

Section 3.2 and Section 3.3 discuss the non-autonomous problem from Section 2.3. The concept of one-parameter semigroups is not appropriate for non-autonomous problems, because in the non-autonomous case not only the time passed but also the initial time has to be considered a relevant parameter for the evolution. This leads to a similar approach using two-parameter evolution families. Section 3.2 introduces the main objects for the solution theory of non-autonomous abstract Cauchy problems and evolution families.

3.2 Non-Autonomous Abstract Cauchy Problems

To deal with time-dependent dynamics, we introduce evolution families (Def. 3.8), families of two-parameter solution operators, for non-autonomous evolution equations. In this section, we consider possibly inhomogeneous, non-autonomous abstract Cauchy problems (NACPs) of the form:

$$\text{(NACP)} \begin{cases} \dfrac{df(t)}{dt} = G(t)f(t) + g(t) \\ f(s) = f_s, \end{cases} \tag{3.6}$$

over some finite time interval $[s,T] \subset [0,T]$ on a Banach space $(V, \|\cdot\|_V)$. We state the results from the theory of NACPs that we need in Section 3.3. This section follows [Tan97] instead of [Paz83, Chap. 7], because the former allows us to consider $V = L^p(\mathbb{X})$ for $p \in [1,\infty)$, whereas the latter does not deal with the case $p = 1$.

In general, for NACPs induced by partial differential equations the operators $G(t)$ are unbounded operators on V and need to be equipped with suitable domains $\mathcal{D}(G(t))$ for the evolution problem to make sense.

Remark 15:

- The results here and in [Tan97] are formulated for the time interval $[0,T]$. However, they also hold for arbitrary time intervals $[a,b]$. The important part is that the evolution depends also on the initial time and not just at the duration. To emphasize this dependence, we sometimes consider the initial time $s \in [0,T)$.
- In this work, we focus on the non-autonomous problem introduced in Section 2.3. The transport problem (2.4) from Section 2.1 might be investigated with [Tan97, Chap. 7].

△

Theorem 3.9 is concerned with the existence of unique solutions to (3.6) and some regularity properties of the solution. Theorem 3.14 states further regularity results.

The following definition introduces two notions of solutions from [Tan97, Def. 6.1 & 6.2] for NACPs that differ in the regularity of the solution at the initial time.

Definition 3.7:

1. *A function $f \in C([0,T];V) \cap C^1((0,T];V)$ is a classical solution of (3.6), if for every $t \in (0,T]$*

$$\frac{df(t)}{dt} = G(t)f(t) + g(t) \qquad f(0) = f_0$$

and $f(t) \in \mathcal{D}(G(t))$ holds.

2. *A function $f \in C^1([0,T];V)$ is a strict solution of* (3.6)*, if for every $t \in [0,T]$*

$$\frac{df(t)}{dt} = G(t)f(t) + g(t) \qquad f(0) = f_0$$

and $f(t) \in \mathcal{D}(G(t))$ holds.

Next, we introduce evolution families which have a parameter for the initial time and a second parameter for the final time of the evolution.

Definition 3.8:
A family of operators $(U(t,s))_{\substack{s \le t \\ s,t \in [0,T]}} \subset L(V,V)$ is called family of evolution operators for the problem (3.6) *if*

1. *$U(s,s) = Id_V$ and $U(t,r)U(r,s) = U(t,s)$, for all $v \in V$ the mapping $(t,s) \mapsto U(t,s)v$ is continuous.*
2. *For all $t,s \in [0,T]$, with $s < t$, holds $U(t,s) \in L(V, \mathcal{D}(G(t)))$, specifically, for all $x \in V$ follows $U(t,s)x \in \mathcal{D}(G(t))$.*
3. *The mapping $t \mapsto U(t,s)$ is differentiable in $(s,T]$ with values in $L(V,V)$ and*

$$\frac{\partial}{\partial t} U(t,s) = G(t)U(t,s)\,. \tag{3.7}$$

4. *The family $(U(t,s))_{s \le t}$ is called exponentially bounded if there are $M \ge 1$ and $\omega > 0$ such that*

$$\|U(t,s)\|_{L(V,V)} \le M e^{\omega(t-s)} \qquad \text{for } s \le t\,. \tag{3.8}$$

Note the similarities between (3.2) and (3.7) and between the bound from Remark 12 and (3.8).

Let us now state the assumptions on the operators $G(t)$ that we use to establish well-posedness of the NACP. These assumptions might look enigmatic at first, but Lemma 3.11 shows that these assumptions are satisfied in the setting introduced in Section 2.3.

Assumption 2:

(P1) The condition [Tan97, (P1), p. 221]: There exists an angle $\theta_0 \in (\frac{\pi}{2}, \pi]$ such that

1. *For each $t \in [0,T]$ for the resolvent set $\rho(G(t))$ (Def. 3.3) of $G(t)$ holds*

$$\rho(G(t)) \supset \Sigma := \left\{ z \in \mathbb{C} \,\middle|\, |\arg(z)| < \theta_0 \right\} \cup \{0\}\,.$$

2. *There exists $M > 0$ such that the following bound for the resolvent*

$$\|R(z, G(t))\|_{L(V,V)} \le \frac{M}{|z|} \quad \text{for}\, z \in \Sigma$$

holds uniformly in $t \in [0,T]$ on the sector Σ contained in the resolvent set.

(P2) The condition [Tan97, (P2), p. 222]: For every $z \in \Sigma$ the mapping $t \mapsto R(z, G(t))$ is continuously differentiable on $[0,T]$ in the uniform operator topology and there exists a $K_1 > 0$ and $\varrho \in (0,1]$ such that

$$\|\frac{\partial}{\partial t} R(z, G(t))\|_{L(V,V)} \le \frac{K_1}{|z|^{\varrho}}\,.$$

(P4) The condition [Tan97, (P4), p. 256]: There exist a $K_2 > 0$, $n \in \mathbb{N}$, and real numbers $\alpha_1, \dots \alpha_n, \beta_1, \dots, \beta_n \in [0, 2]$ with $\beta_i < \alpha_i$ such that

$$\|G(t)R(z, G(t))(G(t)^{-1} - G(s)^{-1})\|_{L(V,V)} \leq K_2 \sum_{i=1}^{n} (t-s)^{\alpha_i} |z|^{\beta_i - 1}$$

for $z \in \Sigma \backslash \{0\}$ and $0 \leq s < t \leq T$. We set $\delta := \min\{\min_{i=1,\dots,n}\{\alpha_i - \beta_i\}, 1\}$.

Remark 16:

- The first part of (P1) states that the resolvent sets $\rho(G(t))$ contain a sector Σ. The second part describes the behavior of the resolvents on that sector. The property (P1) can be rephrased as: The operator family $(G(t))_{t\in[0,T]}$ is uniformly (in t) sectorial [Lun95, Def. 2.0.1].
- The assumption $0 \in \rho(G(t))$ is chosen in [Tan97] for notational purposes and can be achieved by rescaling, if the semigroups $(S_\theta(t))_{t\in I}$ induced by $G(\theta)$, for θ arbitrary but fixed, can be rescaled uniformly in t. This can be done due to the regularity of v in t; also see Lemma 3.11 and [Lun95, Lem. 6.1.1]. Other books that work in similar settings such as [Lun95] do not make this mostly aesthetic assumption.
- In (P4) the object $G(t)^{-1} = R(0, G(t))$ is well-defined, if we have $0 \in \rho(G(t))$ in (P1). Otherwise $R(0, G(t))$ has to be replaced by an appropriate shift.
- The parameter δ from (P4) appears in several bounds and regularity results in [Tan97, Chap. 6]. However, it is not explicitly used here.

△

Lemma 3.11 shows that these assumptions are fulfilled in the setting for the transportation of density problem introduced in Section 2.3.

Theorem 3.9:

1. *If Assumption 2, $f(0) \in \overline{\mathcal{D}(G(0))}$, and $g \in C^\alpha(0, T; V)$ hold, then the NACP (3.6) has a unique classical solution f.*
2. *If in addition $f(0) \in \mathcal{D}(G(0))$ and $G(0)f(0) + g(0) \in \overline{\mathcal{D}(G(0))}$ hold, then the classical solution is a strict solution.*
3. *There exists a two-parameter family of solution operators $(U(t,s))_{s\leq t}$ such that the solution (classical or strict) can be represented with the help of the evolution family $(U(t,s))_{s\leq t}$*

$$f(t) = U(t,0)f_0 + \int_0^t U(t,s)g(s)\,ds\,. \tag{3.9}$$

Proof. The statements of Theorem 3.9 are the content of [Tan97, Thm. 6.6]. □

Remark 17:

- As expected, in order to obtain strict solutions which have higher regularity at the initial time, we need some compatibility conditions for the objects at initial time.

- There are more results in [Tan97, Chap. 6] that have stronger assumptions and stronger conclusions; see [Tan97, Thm. 6.1] for classical and [Tan97, Thm. 6.2] for strict solutions. There are also other notions of solutions, such as strong solutions [Tan97, Rem. 6.1].

$\triangle$

Theorem 3.9 already guarantees some regularity for the solution. We make the following additional assumptions to derive results for higher regularity of solutions.

Assumption 3:

(L1) There exists a Banach space $\mathcal{D}$, a common domain of $(G(t))_{t\in[0,T]}$, with $\mathcal{D} \subseteq \mathcal{D}(G(t))$ for all $t \in [0,T]$, and $\mathcal{D}$ is continuously embedded in V, $\mathcal{D} \hookrightarrow V$.

(L2) For all $t \in [0,T]$ the operator $G(t)$ is sectorial. There exists $\omega \in \mathbb{R}$, $M > 0$ and $\theta \in (\frac{\pi}{2}, \pi)$ such that the resolvent set $\rho(G(t))$ contains a sector $\Sigma_{\omega,\theta}$, specifically

$$\rho(G(t)) \supset \Sigma_{\omega,\theta} = \{z \in \mathbb{C} \,|\, z \neq \omega \,\wedge\, |\arg(z-\omega)| < \theta\} \tag{3.10}$$

and for all $z \in \Sigma_{\omega,\theta}$ holds $\|R(z, G(t))\|_{L(V,V)} \leq \dfrac{M}{|z-\omega|}$.

(L3) The family $(G(t))_{t\in[0,T]}$ satisfies $t \mapsto G(t) \in C^{\alpha}([0,T]; L(\mathcal{D}, V))$ for some $\alpha \in (0,1)$.

Assumption 3 implies that the family $(G(t))_{t\in[0,T]}$ is uniformly sectorial [Lun95, Lem. 6.1.1]. Furthermore, the ω shift in (3.10) has the same functionality as rescaling. The definition of $\Sigma_{\omega,\theta}$ emphasizes that being sectorial is related to the shape and not the position of the spectrum of the operator [EN00]. Assumptions (P1) and (L1) imply (L2). The assumption (L3) is strongly related to the Hölder regularity of the coefficients that is required in [Tan97, Chap. 6].

The next result from [Lun95, Cor. 6.1.9 (iv)] allows us to derive a higher regularity for solutions that we use in Theorem 3.14.

Theorem 3.10:
Under Assumption 2 and Assumption 3 the following equivalence holds for $0 \leq s < T$

$$U(\cdot, s)f \in C([s,T]; \mathcal{D}) \cap C^1([s,T]; V) \quad \Leftrightarrow \quad f \in \mathcal{D} \text{ and } G(s)f \in \overline{\mathcal{D}}\,.$$

Proof. A proof can be found in [Lun95, Cor. 6.1.9 (iv)]. $\square$

These type of compatibility conditions for higher regularity of the solution of an evolution problem can be found in Theorem 3.9 and in other approaches to evolution equations such as the variational approach [Emm13, Satz 8.5.1].

To get some intuition for the objects and results introduced in Section 3.1 and Section 3.2, we look at the following important example of advection-diffusion problems.

3.3 Non-Autonomous Parabolic Evolution Problems

Non-autonomous parabolic evolution problems include many important applications including the Fokker–Planck equations from Section 2.3. We approach these problems from the perspective of NACPs. Some content of this section has been published in [FKS20] and is re-used with the permission of the publisher and the authors.

Let us recall and specify some properties from Chapter 2.

- The domain $\mathbb{X} \subset \mathbb{R}^d$ is a bounded and open set with piecewise C^4 boundary satisfying the assumption (A0); page 13.
- The velocity field v satisfies $v \in C^{(\alpha,1+\alpha)}([0,T] \times \overline{\mathbb{X}}; \mathbb{R}^d)$. For $\alpha, \beta \in (0,1]$ and $k, l \in \mathbb{N} \cup \{0\}$ the space $C^{(k+\alpha,\ell+\beta)}([0,T] \times \overline{\mathbb{X}}; \mathbb{R}^d)$ denotes the space of functions $f : [0,T] \times \overline{\mathbb{X}} \to \mathbb{R}^d$ that are k-times continuously differentiable in t and ℓ-times continuously differentiable in x and whose k-th time derivative is α-Hölder continuous and ℓ-th spatial derivative is β-Hölder continuous.
- We use the Sobolev spaces $W^{k,p}(\mathbb{X})$ of functions $f \in L^p(\mathbb{X})$, $p \in [1, \infty]$, that have weak derivatives up to order $k \in \mathbb{N} \cup \{0\}$ such that the weak derivatives are L^p functions. For an overview on Sobolev spaces we refer to [AF03].

Referring to the objects in the general setting of the previous sections, we choose the Banach space $V = L^p(\mathbb{X})$ and an operator domain $\mathcal{D}_p \subset W^{2,p}(\mathbb{X}) \subset L^p(\mathbb{X})$.

A general inhomogeneous parabolic partial differential equation (PDE) is given by

$$\partial_t f(t,x) = (L(t)f(t))(x) + g(t,x) \,, \tag{3.11}$$

where $L(t)$ is an elliptic differential operator, see (3.16), for every $t \in [0,T]$. In particular, a general form for L is

$$\begin{aligned} (L(t)f)(x) :&= \sum_{|\boldsymbol{\alpha}| \le 2} a_{\boldsymbol{\alpha}}(t,x) \frac{\partial^{|\boldsymbol{\alpha}|}}{\partial x^{\boldsymbol{\alpha}}} f(x) \\ &= \sum_{i=1}^d \sum_{j=1}^d a_{ij}(t,x) \frac{\partial^2}{\partial x_i \partial x_j} f(x) + \sum_{j=1}^d b_j(t,x) \frac{\partial}{\partial x_j} f(x) + c(t,x) f(x) \,, \end{aligned} \tag{3.12}$$

for multi-indices $\boldsymbol{\alpha} \in (\mathbb{N} \cup \{0\})^d$ and sufficient coefficient functions $a_{\boldsymbol{\alpha}}$ or a_{ij}, b_j, c.

Remark 18:

- There are elliptic operators of higher order
$$(L(t)f)(x) := \sum_{|\boldsymbol{\alpha}| \le m} a_{\boldsymbol{\alpha}}(t,x) \frac{\partial^{|\boldsymbol{\alpha}|}}{\partial x^{\boldsymbol{\alpha}}} f(x) \,,$$
that can be treated similarly. Furthermore, these higher-order operators require higher-order boundary conditions and a more regular spatial domain $\mathbb{X}$. We refer to [Tan97, Chap. 6], [Paz83, Chap. 7] and [Zei90a] for introductions to higher-order elliptic operators.
- The regularity required of the coefficient functions $a_{\boldsymbol{\alpha}}$ and the domain $\mathbb{X}$ depends on the desired results, the notion of solution and the literature consulted. We choose the stronger assumptions from [Tan97], because they simplify the presentation especially in the non-autonomous and L^1-setting significantly.

$\triangle$

The Kolmogorov forward equation with the objects v, or $\hat{v}$, and σ from Section 2.3

$$\partial_t f = -\sum_{i=1}^d \frac{\partial}{\partial x_i}(v_i f) + \frac{1}{2} \sum_{j=1}^d \sum_{k=1}^d \frac{\partial^2}{\partial x_j \partial x_k} ((\sigma \sigma^\top)_{jk} f) \,, \tag{3.13}$$

is a homogeneous ($g = 0$) non-autonomous, parabolic equation. This equation is complemented by an initial condition $f(s,\cdot) = f_s(\cdot)$ on $\mathbb{X}$ and boundary conditions. Motivated by Chapter 2, we choose homogeneous Neumann boundary conditions

$$\frac{\partial f}{\partial n}(t,\cdot) = 0 \quad \text{on } \partial\mathbb{X}\,,$$

where n is the outer normal unit vector on $\partial\mathbb{X}$.

The following analysis can be done for inhomogeneous problems, $g \neq 0$, and for different or possibly inhomogeneous boundary conditions as well; see for example [Tan97], [Lun95] and the references therein. In the notation of [Tan97], the homogeneous Neumann boundary conditions correspond to the formal boundary operator

$$B(t,x)(\xi) := \langle n(x), \xi\rangle_{\mathbb{R}^d} \quad \text{and} \quad B(t,x)(\nabla_x)f = \langle n(x), \nabla_x f(t,x)\rangle_{\mathbb{R}^d} = \frac{\partial f}{\partial n}(t,x) = 0 \tag{3.14}$$

for $x \in \partial\mathbb{X}$ with $n(x)$ being the outer normal unit vector at $x \in \partial\mathbb{X}$ and $\xi \in \mathbb{R}^d$.

To see that the Fokker–Planck equations (2.21), (2.27) or (3.13) with $\sigma = \varepsilon I_{d\times d}$ fit in the setting of non-autonomous abstract Cauchy problems, we use of the following relation for $p \in [1,\infty)$, see also [Emm13, Sec. 7.1],

$$f \in L^p((s,T); L^p(\mathbb{X})) \text{ with } f(t) := f(t,\cdot) \in L^p(\mathbb{X}) \quad \Leftrightarrow \quad (t,x) \mapsto f(t,x) \in L^p((s,T)\times\mathbb{X})\,.$$

Analogously, $C([s,T]; L^p(\mathbb{X}))$ denotes the space of functions mapping $[s,T]$ continuously to $L^p(\mathbb{X})$. Instead of considering the PDE pointwise in every (t,x), the NACP considers f as a mapping from $[s,T]$ into the Banach space $L^p(\mathbb{X})$. This leads to the operator differential equation (3.6) in $V = L^p(\mathbb{X})$.

Existence and Uniqueness of Solutions

Lemma 3.11 establishes that the family of operators $(G(t))_{t\in[0,T]}$ defined by

$$G(t)f := -\mathrm{div}_x(v(t,\cdot)f) + \frac{\varepsilon^2}{2}\Delta_x f \quad \text{ in } L^p(\mathbb{X}) \text{ for } f \in W^{2,p}(\mathbb{X}), \tag{3.15}$$

for $\varepsilon > 0$ considered on $L^p(\mathbb{X})$, $1 \leq p < \infty$, satisfies the assumptions made in the references [Tan97, Lun95] using the domain $\mathcal{D}(G(t)) = \mathcal{D}_p := \left\{ f \in W^{2,p}(\mathbb{X}) \,\middle|\, \frac{\partial f}{\partial n} = 0 \text{ on } \partial\mathbb{X} \right\}$ for all $t \in [0,T]$ to encode the boundary condition (3.14).

Lemma 3.11 and its proof due to the author have been published in [FKS20, Lem. A.2].

Lemma 3.11:
The family $(G(t))_{t\in[0,T]}$ of unbounded linear operators on $L^p(\mathbb{X})$ defined by (3.15) with the domain $\mathcal{D}(G(t)) = \mathcal{D}_p$ fulfills the following conditions.

(C1) The spatial domain $\mathbb{X}$ is a bounded open subset of $\mathbb{R}^d$ of class C^4 (locally) [Tan97, Def. 5.5].

(C2) The coefficients $a_{\boldsymbol{\alpha}}$ of the differential operator $G(\cdot)$ and the coefficients of the boundary operator B are Hölder continuous in t [Tan97, Sec. 6.13].

(C3) The coefficients of $G(\cdot)$ are bounded and uniformly continuous in x on $\overline{\mathbb{X}}$ [Tan97, Sec. 6.13].

(C4) The differential operator $G(\cdot)$ and the boundary operator B, satisfy the complementing condition [Tan97, p. 131] for all $t \in [0,T]$.

(C5) *The family* $(G(t))_{t\in[0,T]}$ *is uniformly strongly elliptic [Tan97, Def. 5.4]. In particular, there exists a* $c > 0$ *such that for all* $(t,x) \in [0,T] \times \overline{\mathbb{X}}$ *and all* $\xi \in \mathbb{R}^d$ *holds*

$$\sum_{|\boldsymbol{\alpha}|=2} a_{\boldsymbol{\alpha}}(t,x)\xi^{\boldsymbol{\alpha}} \geq c|\xi|^2 \,. \tag{3.16}$$

Furthermore, $G(t)$ *satisfies the root condition [Tan97, p. 130] for all* $t \in [0,T]$.

(C6) *The conditions [Tan97, (P1), p. 221], [Tan97, (P2), p. 222] and [Tan97, (P4), p. 256], that have been stated in Assumption 2 and used in Theorem 3.9, are fulfilled.*

Before we continue with the proof of Lemma 3.11, let us remark, that parts of the proof have already been done in [Tan97]. Some conditions, namely, (C3),(C4) and (C5), are easy to check in our case, because the highest order part of $G(t)$, called principal part in [Tan97], is the time-independent spatial Laplace operator Δ_x.

Proof. Most of the statements of Lemma 3.11 are proven at some point in [Tan97].

(C1) The regularity required of the spatial domain $\mathbb{X}$ is guaranteed by the assumption (A0), page 13, on $\mathbb{X}$ made in Chapter 2. In [Tan97], the author also mentions the assumption that the domain $\mathbb{X}$ should be globally uniformly regular of class C^2 [Tan97, Def. 3.2 & Sec. 5.2] for the case of unbounded domains [Tan97, Sec. 3.6]. This condition is irrelevant for our setting.

(C2) The boundary operator $B(t,x)$ (3.14) is constant in t, and consequently it is Hölder continuous in t. The assumption $v \in C^{(\alpha,1+\alpha)}([0,T]\times\overline{\mathbb{X}})$ guarantees that v and $\frac{\partial v_i}{\partial x_i}$ are Hölder continuous in t.

(C3) The coefficients $a_{\boldsymbol{\alpha}}$ are either constant, $\frac{\varepsilon^2}{2}$, or induced by $v \in C^{(\alpha,1+\alpha)}([0,T]\times\overline{\mathbb{X}})$, namely, v_i or $\frac{\partial v_i}{\partial x_i}$. Thus, all the coefficient functions of $G(t)$ are bounded and uniformly continuous on $\overline{\mathbb{X}}$.

(C4) The complementing condition can be verified by straightforward calculations. The important thing to note is that the principal part $\frac{\varepsilon^2}{2}\Delta_x$, denoted by L^0 in [Tan97], of $G(t)$ is independent of t. This implies that the roots of $L^0(x,\xi + rn(x))$ for ξ perpendicular to $n(x)$ with unit norm are given by $r_1 = i, r_2 = -i$. Furthermore, for ξ being perpendicular to $n(x)$ follows $B(t,x)(\xi + rn(x)) = r$. The polynomials r and $(r-i)(r+i)$ are linearly independent. Therefore, the complementing condition is fulfilled.

(C5) It is well known that the operator family $(G(t))_{t\in[0,T]}$, defined by (3.15), is uniformly strongly elliptic in our setting with $m = 2$ and

$$\sum_{|\boldsymbol{\alpha}|=m} a_{\boldsymbol{\alpha}}(t,x)\xi^{\boldsymbol{\alpha}} = \frac{\varepsilon^2}{2}|\xi|^2 \,.$$

Now [Tan97, Thm. 5.4] shows that every uniformly strongly elliptic operator satisfies the root condition.

(C6) Assuming $0 \in \rho(G(t))$ for simplicity, [Tan97, Sec. 6.13] shows that (P1), (P2) and (P4) are satisfied for $(G(t))_{t\in[0,T]}$. We can ensure that zero is in the resolvent set using the rescaling trick. The main arguments that enable the analysis in [Tan97, Sec. 6.13] is the uniformity and Hölder continuity in t. Note that [Tan97, Sec. 6.13] considers a general uniformly strongly elliptic operator (3.12). Therefore, (C6) holds for general $\sigma \in C^{(\alpha,2+\alpha)}([0,T]\times\overline{\mathbb{X}})$ satisfying (A3) (2.10) as well.

□

Remark 19:

- One important aspect of Lemma 3.11 is to establish that the choice $\mathcal{D}_p$ for the domain $\mathcal{D}(G(t))$ is appropriate. The domain $\mathcal{D}_p$ is used in (C2), (C4), and (C6).

- Lemma 3.11 can also be proven for $\operatorname{div}_x(v) \neq 0$ and suitable $\sigma(t,x) \neq \varepsilon I_{d\times d}$. Some conditions are straightforward for the general case, for example (A3) (2.10) implies (C5) (3.16) for general σ. However, other conditions like (C4) might be more involved.

- In the literature, the evolution equation (3.11) is often stated as

$$\partial_t f(t) + H(t)f(t) = g(t)$$

  with $H(t) = -L(t)$, which leads to a sign modification in the definition of ellipticity [Tan97, p. 279] and other minor notational changes.

△

With these properties ensured, we prove the existence of a unique solution and a corresponding two-parameter evolution family.

Theorem 3.12:
The NACP (3.6)*, with the operators defined by* (3.15) *with* $\mathcal{D}_p$*, for* $p \in (1,\infty)$ *, the initial condition* $f(s,\cdot) = f_s$*, and the conditions ensured by Lemma 3.11, has a unique classical solution*

$$f \in C([s,T];L^p(\mathbb{X})) \cap\ C^1((s,T];L^p(\mathbb{X}))$$

given by $f(t) = \mathcal{P}_{s,t}f_s$*. Furthermore,* $f(t) \in \mathcal{D}(G(t))$ *holds for all* $t \in (s,T]$*, and* $(\mathcal{P}_{s,t})_{s\le t}$ *is a two-parameter evolution family of linear, bounded, and for* $t > s$ *compact, operators on* $L^p(\mathbb{X})$*.*

Theorem 3.12 and its proof due to the author have been published in [FKS20, Thm. A.3].

Proof. Lemma 3.11 ensures that we can apply the results from [Tan97] that we use in the following. The results from [Tan97, Chap. 6] that use more abstract results from Acquistapace and Terreni [AT86, AT87] give the existence of a unique solution f to (3.6) [Tan97, Thm. 6.6] and a corresponding two-parameter family of solution operators $(\mathcal{P}_{s,t})_{s\le t}$.

- The fact that the function f is a classical solution [Tan97, Def. 6.1]

$$f \in C([s,T];L^p(\mathbb{X})) \cap C^1((s,T];L^p(\mathbb{X}))$$

  and that $f(t) \in \mathcal{D}(G(t)) = \mathcal{D}_p$ for $t \in (s,T]$ follows directly from [Tan97, Thm. 6.6].

- From [Tan97, Thm. 6.5] follows that for all $t > s$ the solution is given by $f(t) = \mathcal{P}_{s,t} f(s)$ with the two-parameter solution family $(\mathcal{P}_{s,t})_{s \le t}$.
- For $t > s$ the operator $\mathcal{P}_{s,t}$ is compact on $L^p(\mathbb{X})$. The result [Tan97, Thm. 6.6], specifically, the property $\mathcal{P}_{s,t} f \in \mathcal{D}_p$ for $f \in L^p(\mathbb{X})$, gives that the operator $\mathcal{P}_{s,t} : L^p(\mathbb{X}) \to \mathcal{D}_p$ with $\mathcal{D}_p \subset W^{2,p}(\mathbb{X})$ is a bounded linear operator from $L^p(\mathbb{X})$ to $W^{2,p}(\mathbb{X})$. The Rellich–Kondrachov embedding theorem [AF03, Thm. 6.3] states that $W^{2,p}(\mathbb{X})$ is compactly embedded in $L^p(\mathbb{X})$. Thus, $\mathcal{P}_{s,t}$ is a compact operator on $L^p(\mathbb{X})$, because it maps bounded sets in $L^p(\mathbb{X})$ to bounded sets in $W^{2,p}(\mathbb{X})$ which are relatively compact in $L^p(\mathbb{X})$.

□

Theorem 3.13 also uses results from [Tan97] and deals with the case $p = 1$.

Theorem 3.13:

(a) For $t > s$ the non-autonomous abstract Cauchy problem (3.6) *with the operators defined by* (3.15) *has a unique solution $f \in C([s,T], L^1(\mathbb{X})) \cap C^1((s,T]; L^1(\mathbb{X}))$ that is given on $L^1(\mathbb{X})$ by $\mathcal{P}_{s,t} f_s = f(t) \in \mathcal{D}(G(t))$. Furthermore, the transfer operators $\mathcal{P}_{s,t}$ satisfy*

$$\mathcal{P}_{r,t}\mathcal{P}_{s,r} = \mathcal{P}_{s,t} \quad \text{for } s \le r \le t\,,$$

and there is a constant $C > 0$ such that

$$\|\partial_t \mathcal{P}_{s,t}\|_{L(L^1,L^1)} = \|G(t)\mathcal{P}_{s,t}\|_{L(L^1,L^1)} \le \frac{C}{t-s} \quad \text{for } t > s\,.$$

(b) The operators $\mathcal{P}_{s,t} : L^1(\mathbb{X}) \to L^1(\mathbb{X})$ are compact for every $t > s$.

Proof. A proof can be found in [FK17, Lem. 30]. □

Additional Regularity

Due to the common and time-independent domain $\mathcal{D}_p$ of all $G(t)$, we can derive a higher regularity for the the solution f, if the initial condition is more regular than simply $L^p(\mathbb{X})$.

Theorem 3.14 and its proof due to the author have been published in [FKS20, Thm. A.4].

Theorem 3.14:

Consider the same assumptions as in Theorem 3.12.

(a) It holds that $t \mapsto f(t) = \mathcal{P}_{s,t} f_s \in C([s,T]; \mathcal{D}_p)) \cap C^1([s,T]; \mathbb{X})$ if and only if it holds that $f_s \in \mathcal{D}_p$ and $G(s) f_s \in L^p(\mathbb{X})$.

(b) The regularity $f \in C([s,T]; W^{m,p}(\mathbb{X}))$ implies Hölder continuity in space for every time-slice, specifically, $f(t,\cdot) \in C^\alpha(\overline{\mathbb{X}})$ for all α such that $0 < \alpha \le m - \frac{d}{p}$, with uniformly (in t) bounded Hölder norm.

(c) Furthermore, $f \in C([s,T]; W^{2,p}(\mathbb{X}))$ for $0 < 2 - \frac{d}{p}$ implies $f \in C([s,T] \times \overline{\mathbb{X}})$.

Note that, Lemma 3.11 shows that (L1) is satisfied. We have seen above that (P1) and (L1) imply (L2). Finally, (L1) and (C2) imply (L3).

Proof.

(a) This equivalence follows from Theorem 3.10, [Lun95, Cor. 6.1.9 (iv)], with the common domain $\mathcal{D}_p = \mathcal{D}(G(t)) \subset W^{2,p}(\mathbb{X})$ of the family of unbounded operators $(G(t))_{t\in[0,T]}$ in the Banach space $L^p(\mathbb{X})$. The domain $\mathcal{D}_p$ is dense in $L^p(\mathbb{X})$, and the resulting two-parameter evolution family is $(\mathcal{P}_{s,t})_{s\leq t}$.

(b) For every $t \in [s,T]$ we have $f(t,\cdot) \in W^{m,p}(\mathbb{X})$. From the Sobolev embedding theorem [AF03, Thm. 4.12] (Morrey's inequality) follows that the space $W^{m,p}(\mathbb{X})$ is continuously embedded in $C^{r+\alpha}(\overline{\mathbb{X}})$ with $0 < \alpha \leq m - \frac{d}{p} - r$ for locally Lipschitz domains $\mathbb{X} \subset \mathbb{R}^d$, [AF03, 4.10 & 4.11]. Here $C^{r+\alpha}(\overline{\mathbb{X}})$ denotes the space of r-times continuously differentiable functions whose r-th derivative is $\alpha \in (0,1)$ Hölder continuous. We only need $r = 0$. Thus, there exists a $K > 0$ such that

$$\|u\|_{C^\alpha} \leq K\|u\|_{W^{m,p}}$$

for all $u \in W^{m,p}(\mathbb{X})$. This estimate together with the regularity $f \in C([s,T];W^{m,p}(\mathbb{X}))$ implies that there is a constant independent of t for the continuous embedding for $(f(t))_{t\in[s,T]}$ into $C^\alpha(\overline{\mathbb{X}})$.

(c) We consider a function $f \in C([s,T];W^{2,p}(\mathbb{X}))$. Part (b) gives $f(t,\cdot) \in C^\alpha(\overline{\mathbb{X}})$ for all $t \in [s,T]$ with $0 < \alpha \leq 2 - \frac{d}{p}$. Together with part (a), this implies

$$\sup_{t\in[s,T]} \|f(t,\cdot)\|_{C^\alpha} \leq K \sup_{t\in[s,T]} \|f(t,\cdot)\|_{W^{2,p}} \leq M < \infty \,.$$

This immediately implies $f \in C([s,T];C(\overline{\mathbb{X}}))$ which is equivalent to $f \in C([s,T] \times \overline{\mathbb{X}})$; see [GGZ74, Lem. IV.2.1]. Let us briefly show the direction of the last statement that we need. For $f \in C([s,T];C(\overline{\mathbb{X}}))$ we have

$$|f(t_n,x_n) - f(t,x)| \leq \|f(t_n,\cdot) - f(t,\cdot)\|_\infty + |f(t,x_n) - f(t,x)| \xrightarrow{n\to\infty} 0 \,.$$

□

Theorem 3.14 is used in the proof of Theorem 3.21 which is concerned with the regularity of eigenfunctions of the augmented generator $\boldsymbol{G}$; see (3.21).

Remark 20:

- The general theory of semigroups and mild solutions to PDEs has produced some approaches for non-linear problems as well; see [Paz83, Chap. 6 & 8] and [CL71].
- There is an alternative solution theory for PDEs leading to variational solutions that deals with linear, autonomous and non-linear, non-autonomous systems equally well; see for example [Zei90a] and [Zei90b]. One disadvantage of the variational theory is that there are usually no explicit formulas like (3.9) for the solution, because the solutions are often obtained by limits of (Galerkin or Petrov–Galerkin) discretization schemes.

△

3.4 The Generator Approach and Augmentation

Autonomous Flows

In Chapter 2 and Section 3.1 we have seen that the evolution of densities for autonomous systems is given by a semigroup of transfer operators $(\mathcal{P}_t)_{t\geq 0}$ and that the semigroup can be characterized equivalently by its infinitesimal generator G. The advantage is that the generator is a single time-independent object while the corresponding semigroup depends on the time span of the evolution. Therefore, we want to use the infinitesimal generator G of $(\mathcal{P}_t)_{t\geq 0}$ and related objects, its eigendata, namely pairs of eigenvalues and eigenfunctions, to analyze transport in the original dynamical system. In [FJK13] and [Kol11] the authors used the relation between a C_0 semigroup and its infinitesimal generator to develop the generator approach for escape rates; Definition 2.9.

Let us recall the main objects for the non-deterministic autonomous setting. Starting from a stochastic differential equation

$$dX_t = v(X_t)dt + \varepsilon dW_t \qquad X_0 \sim f_0$$

with reflecting boundary conditions, the evolution of the initial density f_0 is given by the Fokker–Planck equation

$$\partial_t f(t,x) = -\mathrm{div}_x(v(x)f(t,x)) + \frac{\varepsilon^2}{2}\Delta_x f(t,x) =: (Gf(t,\cdot))(x)$$

with homogeneous Neumann boundary condition

$$\frac{\partial f}{\partial n}(t,x) = 0 \quad x \in \partial\mathbb{X}\,.$$

The solution operators for this problem, $(\mathcal{P}_t)_{t\geq 0}$, form a C_0 semigroup of bounded operators on $L^p(\mathbb{X})$ for $p \in [1,\infty)$. Analogously to Section 3.2, this induces an abstract Cauchy problem

$$\frac{df(t)}{dt} = Gf(t) \qquad f(0) = f_0$$

with the operator $G : \mathcal{D}(G) \to L^p(\mathbb{X})$. The unbounded operator G also corresponds to the infinitesimal generator of the semigroup, intuitively $\mathcal{P}_t = e^{tG}$. The spectrum of the generator and the spectrum of a transfer operator $\mathcal{P}_t$ are related by a spectral mapping property (Thm. 3.5).

Theorem 3.15 from [FJK13, Thm. 3.5] connects the escape rate (Def. 2.9) of the support of an eigenfunction to the corresponding eigenvalue.

Theorem 3.15:
Suppose that $Gf = \mu f$ for some real $\mu < 0$ and $f \in L^\infty(\mathbb{X})$, then

$$-\liminf_{k\to\infty} \frac{1}{k} \log \mathbb{P}_{\Lambda_u}(X_0 \in A^\pm, X_t \in A^\pm, \ldots, X_{kt} \in A^\pm) = E(A^\pm) \leq -t\mu$$

with $A^\pm = \{x \in \mathbb{X} \,|\, \pm f(x) \geq 0\}$ being the positive respectively negative support of f.

Proof. A proof has been published in [FJK13, Thm. 3.5]. □

Remark 21:

- The condition $f \in L^\infty(\mathbb{X})$ is satisfied, because eigenfunctions of G have enough regularity, specifically, $f \in \mathcal{D}(G) = \mathcal{D}_p = W^{2,p}(\mathbb{X}) \hookrightarrow L^\infty(\mathbb{X})$ for $p > \frac{d}{2}$ [AF03, Chap. 4].
- Discrete approximations of the generator and other related topics are discussed in [Kol11, Chap. 5], [FJK13, Sec. 4], and Section 4.1.

△

The spectral mapping property in Theorem 3.5 suggests that the generator or its spectrum contains all necessary information for the whole evolution. The solution family $(\mathcal{P}_{s,t})_{s\leq t}$ for the non-autonomous problem is a two-parameter evolution family and not a semigroup. The evolution family does not have an infinitesimal generator on $L^p(\mathbb{X})$. Non-autonomous dynamical systems in $\mathbb{R}^d$ can be augmented in time to obtain an autonomous system in $\mathbb{R}^{d+1}$ where the additional dimension corresponds to the evolution of time. Applying this idea to non-autonomous abstract Cauchy problems and evolution families leads to *evolution semigroups*. These evolution semigroups have an infinitesimal generator. This approach is useful, but it also introduces additional complexity. We proceed by briefly discussing the concept of evolution semigroups, before introducing augmentation and focusing on the augmented generator.

Evolution Semigroups in the Autonomous Case

We can consider autonomous problems as special cases of non-autonomous ones with $G(t) = G$ constant. If the evolution family $(U(t,s))_{s\leq t}$ does not depend on the initial time s and only depends on the time span $t-s$, then the definition $S(t) := U(s_1+t, s_1) = U(s_2+t, s_2)$ makes sense, and $(S(t))_{t\geq 0}$ is a semigroup due to the properties of the evolution family (Def. 3.8). Furthermore, G is the infinitesimal generator of this semigroup. Analogously $U(t,s) := S(t-s)$ gives an evolution family due to the properties of the semigroup $(S(t))_{t\geq 0}$.

There is another way of constructing a semigroup from an evolution family. Let us first consider the autonomous setting. Following [CL99, Sec. 2.2] and starting with a C_0 semigroup $(S(t))_{t\geq 0}$ acting on a separable Banach space V, there are three different ways to augment the abstract Cauchy problem that lead to an evolution semigroup. We can augment on the whole line $\mathbb{R}$ [CL99, Sec. 2.2.2] by

$$(E^0(t)f)(s) := S(t)f(s-t) \quad f \in L^p(\mathbb{R}; V)\,,$$

on the half-line $\mathbb{R}_{\geq 0}$ [CL99, Sec. 2.2.3] by

$$(E^+(t)f)(s) := \begin{cases} S(t)f(s-t) & \text{if}\, s \geq t \\ 0 & \text{if}\, t \geq s \geq 0 \end{cases} \qquad f \in L^p(\mathbb{R}_{\geq 0}; V)\,,$$

and periodically on τS^1 [CL99, Sec. 2.2.1], for a chosen period $\tau \in \mathbb{R}_{>0}$, by

$$(E^\tau(t)f)(s) := S(t)f(s-t \bmod \tau) \quad f \in L^p(\tau S^1; V)\,.$$

Now $(E^\blacklozenge(t))_t$, for $\blacklozenge \in \{0,+,\tau\}$, is a semigroup acting on $L^p(\mathbb{R}, V)$, $L^p(\mathbb{R}_{\geq 0}, V)$ or $L^p(\tau S^1, V)$, respectively.

Remark 22:
These evolution semigroups can be considered as a product of two commuting semigroups. Let $(T_r^{\blacklozenge}(t))_t$ denote the right translation semigroup, with the generator $-\frac{d}{dt}$ on $\mathcal{D}_{\blacklozenge}\big(-\frac{d}{dt}\big)$, and let $(\mathcal{S}(t))_t$ denote the multiplication semigroup

$$(\mathcal{S}(t)f)(s) = S(t)f(s)\,,$$

with the generator $\mathcal{G}$, such that $(\mathcal{G}f)(s) = Gf(s)$. Then the evolution semigroup $(E^{\blacklozenge}(t))_t$, for $\blacklozenge \in \{0, +, \tau\}$ can be represented as

$$E^{\blacklozenge}(t) = T_r^{\blacklozenge}(t)\mathcal{S}(t)\,.$$

This perspective can be useful and has been investigated in [EN00, Sec. VI.9] and [Sch99]. In particular, [AGG$^+$86, Chap. A-I.3.7] investigates the generators of product semigroups. △

The infinitesimal generator of $(E^{\blacklozenge}(t))_t$, for $\blacklozenge \in \{0, +, \tau\}$, is given by the closure of

$$(G^0 f)(s)\,,\ (G^+ f)(s)\,,\ (G^\tau f)(s) := -\frac{d}{ds}f(s) + Gf(s)\,,$$

with its corresponding domain

$$\mathcal{D}(G^0) = \mathcal{D}\Big(-\frac{d}{ds}\Big) \cap \mathcal{D}(\mathcal{G})\,,\quad \mathcal{D}(G^+) = \mathcal{D}_+\Big(-\frac{d}{ds}\Big) \cap \mathcal{D}(\mathcal{G})\,,\quad \mathcal{D}(G^\tau) = \mathcal{D}_\tau\Big(-\frac{d}{ds}\Big) \cap \mathcal{D}(\mathcal{G})\,.$$

For details we refer the reader to [CL99, pp. 38,42,48] and [AGG$^+$86, Sec. A-I.3.7]. We note that the involved semigroups can exhibit different properties on different spaces and domains [EN00]. For most intents and purposes, we can consider $-\frac{d}{ds} + G$ to be the generator of the evolution semigroup. Even in the autonomous setting, the identification of the generator of the evolution semigroup and its domain is harder than in the C_0 semigroup setting. In [CL99, Sec. 2.2] the authors investigate the spectral properties of G^0, G^+ and G^τ and provide spectral mapping results. These spectral mapping properties are useful to relate eigendata of the generator to the eigendata of the evolution semigroup $(E^{\blacklozenge}(t))_t$, for $\blacklozenge \in \{0, +, \tau\}$, and the original semigroup $(S(t))_{t\geq 0}$.

Evolution Semigroups in the Non-Autonomous Case

Let us now look at the non-autonomous setting. Starting with a two-parameter evolution family $(U(t,s))_{s\leq t}$ acting on a separable Banach space V, we can again define evolution semigroups $(E^{\blacklozenge}(t))_t$, for $\blacklozenge \in \{0, +, \tau\}$, for the three cases following [CL99, Chap. 3].

$$\begin{aligned}
(E^0(t)f)(s) &:= U(s, s-t)f(s-t)\,,\\
(E^+(t)f)(s) &:= \begin{cases} U(s, s-t)f(s-t) & \text{if}\, s \geq t\,,\\ 0 & \text{if}\, t \geq s \geq 0\,,\end{cases}\\
(E^\tau(t)f)(s) &:= U(s, s-t)f(s-t \bmod \tau)\,.
\end{aligned}\tag{3.17}$$

In the non-autonomous setting, [CL99] only considers E^0 and E^+. The families $(E^0(t))_t$ and $(E^+(t))_t$ are C_0 semigroups [CL99, Prop. 3.11] whose generators G^0 and G^+ with their domains are characterized in [CL99, Thm. 3.12]. Furthermore, the spectra of G^0 and G^+ are characterized and spectral mapping properties are proven in [CL99, Thm. 3.13 & Thm. 3.22, Prop. 3.21]. However, we are interested in the periodic augmentation in the non-autonomous setting. Therefore, the brief digression into evolution semigroups ends here. Section 3.4 provides a sufficient characterization of the generator and a spectral mapping property. We refer to [CL99] for a more detailed investigation of E^0 and E^+.

Remark 23:

- In the non-autonomous setting, the translation $T_r^{\blacklozenge}(t)$ generated by $-\frac{d}{ds}$ and the action of the evolution family do not commute. Therefore, $E^{\blacklozenge}(t)$ should be viewed as a multiplicative perturbation of the translation $T_r^{\blacklozenge}(t)$.
- We focused on the L^p spaces for $p \in [1, \infty)$ here. In [CL99] the authors also simultaneously provide analogue results for the case when the semigroups are considered on the C spaces of continuous functions.

△

In Section 3.5.2 we provide a spectral mapping property for the periodically augmented non-autonomous case.

Augmentation

A non-autonomous dynamical system can be transformed into an augmented autonomous system by introducing an additional variable θ that plays the role of time. The velocity field is also augmented to accommodate the evolution of θ which evolves with constant velocity 1. This increases the overall dimension of the system by one.

$$x'(t) = v(t, x(t)) \xrightarrow{\text{Augmentation}} \boldsymbol{x}'(t) = \begin{pmatrix} \theta'(t) \\ x'(t) \end{pmatrix} = \boldsymbol{v}(\boldsymbol{x}(t)) = \begin{pmatrix} 1 \\ v(\theta(t), x(t)) \end{pmatrix}.$$

We denote objects from the augmented setting with bold symbols. Recall that applying this augmentation idea to the stochastic differential equation with the reflected velocity field $\hat{v}$, see (2.25) in Section 2.5, and reflecting boundary conditions leads to

$$\begin{cases} d\hat{\theta}_t = 1dt \\ d\hat{X}_t = \hat{v}(\hat{\theta}_t, \hat{X}_t)dt + \varepsilon d\hat{W}_t \end{cases} \tag{3.18}$$

on the reflected space-time domain $\hat{\boldsymbol{X}} := \tau S^1 \times \mathbb{X}$, with $\tau := 2T$. Note that $(\hat{W}_t)_{t \geq 0}$ is a standard Wiener process in $\mathbb{R}^d$ that is not constructed by reflection in time. Furthermore, we define augmented versions of $\hat{X}_t, \hat{v}$, ε, and $\hat{W}_t$

$$\hat{\boldsymbol{X}}_t := (\hat{\theta}_t, \hat{X}_t), \quad \hat{\boldsymbol{v}}(\boldsymbol{x}) := (1, \hat{v}(\theta, x)) \text{ for } \boldsymbol{x} = (\theta, x) \in \hat{\boldsymbol{X}}, \quad \boldsymbol{\varepsilon} := \begin{pmatrix} 0_{1\times 1} & 0_{1\times d} \\ 0_{d\times 1} & \varepsilon I_{d\times d} \end{pmatrix}.$$

Here, $\hat{\boldsymbol{W}}_t$ is a $d+1$ dimensional standard Wiener process. The augmented versions are again denoted by bold symbols. This results in the augmented stochastic differential equation

$$d\hat{\boldsymbol{X}}_t = \hat{\boldsymbol{v}}(\hat{\boldsymbol{X}}_t)dt + \boldsymbol{\varepsilon} d\hat{\boldsymbol{W}}_t\,. \tag{3.19}$$

This problem lives on the space-time cylinder $\hat{\boldsymbol{X}}$ that is visualized for $d = 1$ in Figure 3.1.

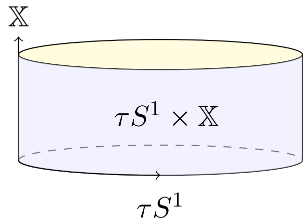

Figure 3.1: Space-time manifold for the periodic augmentation.

Remark 24:

- This augmentation turns linear systems into non-linear systems that are still affine-linear. The extra dimension may increase the numerical effort significantly. The results and insights gained from the augmented system often require non-trivial work to be transferred back to the original system.

- From the space-time perspective the SDE (3.19) is degenerate, because there is by definition of $\boldsymbol{\varepsilon}$ effectively no noise in the time dimension.

$\triangle$

The augmentation is independent of the reflection done in Section 2.5. We focus on the augmented reflected setting, but the naturally periodic or autonomous setting can be treated analogously by skipping the reflection step and using v instead of $\hat{v}$.

The Augmented Reflected Generator

The first paragraph of this section was concerned with autonomous problems and the time-asymptotic perspective on coherence. To extend the generator approach to non-autonomous systems, we use augmentation. We focus on the reflected problem here because the naturally periodic problem can be treated analogously. To access finite-time properties with the arguments of the generator approach, we use the reflection in time introduced in Section 2.5.

Considering the time-periodic version of problem (2.27) with $\hat{v}$ on $\tau S^1 \times \mathbb{X}$, we can state a Fokker–Planck equation on the space-time domain $\hat{\boldsymbol{X}}$. To avoid confusion with the (new) state variable θ that is simulating the time from the non-autonomous setting, we denote the time-dependence of the evolution of the augmented objects with a subscript t, namely, $\boldsymbol{f}_t : \hat{\boldsymbol{X}} \to \mathbb{R}$ for all $t \geq 0$. The augmented Fokker–Planck equation is

$$\partial_t \boldsymbol{f}_t(\boldsymbol{x}) = -\mathrm{div}_{\boldsymbol{x}}\big(\hat{\boldsymbol{v}}(\boldsymbol{x})\boldsymbol{f}_t(\boldsymbol{x})\big) + \Delta_{\boldsymbol{x}} \left(\frac{\boldsymbol{\varepsilon}^2}{2}\boldsymbol{f}_t(\boldsymbol{x})\right) . \tag{3.20}$$

By definition of $\boldsymbol{\varepsilon}$, there is no diffusion in the θ direction. Therefore, the right hand side does not induce an elliptic or even a hypo-elliptic differential operator. Nevertheless, we can consider this Fokker–Planck equation as a linear operator differential equation on the space $L^p(\hat{\boldsymbol{X}})$. The right-hand side is given by (3.21), the augmented generator $\hat{\boldsymbol{G}} : \mathcal{D}(\hat{\boldsymbol{G}}) \subset L^p(\hat{\boldsymbol{X}}) \to L^p(\hat{\boldsymbol{X}})$.

The connection of $\hat{\boldsymbol{G}}$ and (3.20) in terms of the original non-autonomous dynamics is given by

$$\begin{aligned}\big(\hat{\boldsymbol{G}}\boldsymbol{f}\big)(\boldsymbol{x}) &= -\partial_\theta \boldsymbol{f}(\theta,x) + \big(\hat{G}(\theta)\boldsymbol{f}(\theta,\cdot)\big)(x) \\ &= -\partial_\theta \boldsymbol{f}(\theta,x) - \operatorname{div}_x\big(\hat{v}(\theta,x)\boldsymbol{f}(\theta,x)\big) + \frac{\varepsilon^2}{2}\Delta_x \boldsymbol{f}(\theta,x)\,.\end{aligned} \tag{3.21}$$

Here $\hat{G}(\theta)$ is the time-θ differential operator of the Fokker–Planck equation on $[0,\tau]$, specifically, it is the right-hand side operator of (2.27) at time $\theta \in \tau S^1$. The augmented Fokker–Planck equation (3.20) on the augmented space-time manifold is given by

$$\begin{aligned}\partial_t \boldsymbol{f}_t &= \hat{\boldsymbol{G}}\boldsymbol{f}_t \text{ on } \big((0,T)\cup(T,\tau)\big)\times X, \\ \frac{\partial \boldsymbol{f}_t}{\partial \boldsymbol{n}} &= 0 \text{ on } \big((0,T)\cup(T,\tau)\big)\times \partial X\,.\end{aligned} \tag{3.22}$$

The second equation is the augmented adaptation of the homogeneous Neumann boundary conditions.

Remark 25:

- Additional conditions such as the periodicity in θ and the boundary conditions from (3.22) are integrated into the domain of $\hat{\boldsymbol{G}}$, as is common in semigroup theory. The domain $\mathcal{D}(\hat{\boldsymbol{G}})$ can be used to impose continuity conditions in θ at $0, T, \tau$.

- Similarly to the paragraph on evolution equations and non-autonomous abstract Cauchy problems the choice for the domain $\mathcal{D}(\hat{\boldsymbol{G}})$ is important and not trivial. An exact characterization of this domain is rather difficult. However, it is non-empty since

  $$\{\boldsymbol{f} \in L^p(\hat{\boldsymbol{X}}) \,|\, \theta \mapsto \boldsymbol{f}(\theta,\cdot) \in C^1(\tau S^1; L^p(\mathbb{X}))\,,\ \boldsymbol{f}(\theta,\cdot) \in \mathcal{D}(G(\theta)) \text{ for all } \theta \in \tau S^1\} \subset \mathcal{D}(\hat{\boldsymbol{G}})\,.$$

  Furthermore, the results discussed in the paragraph about evolution semigroups suggest that, with $\mathcal{D}(\hat{G}(t)) = \mathcal{D}_p$ constant in time, the domain can be thought of as

  $$\mathcal{D}(\hat{\boldsymbol{G}}) \cong \left(\mathcal{D}_\tau\left(-\frac{d}{d\theta}\right) \cap \mathcal{D}_p\right) \subset L^p(\tau S^1 \times \mathbb{X})\,.$$

  This is not completely correct, because we would have to consider the domain of the induced multiplication semigroup. For details we refer to [EN00, Sec. VI.9.b, Par III.4.13].

- For the results presented in this thesis, we do not require a well-posed augmented Fokker–Planck initial-boundary value problem. We use the operator $\hat{\boldsymbol{G}}$ and its relation to the transfer operator family $\hat{\mathcal{P}}_{s,t}$, $s < t$, of the non-autonomous dynamics. The next paragraph addresses the augmented evolution problem and gives references for more detailed investigations and additional results.

- Any non-constant solution $\boldsymbol{f} : (t,\theta,x) \mapsto \boldsymbol{f}_t(\theta,x)$ to (3.22) has the input variables t, θ and x. However, $\boldsymbol{f}$ may have different regularity properties with respect to each variable. In Section 3.5 we focus on eigenfunctions of $\hat{\boldsymbol{G}}$ that are by nature constant in t, but not necessarily constant in θ. The regularity in different variables is important for the derivation of coherent families.

$\triangle$

The Augmented Evolution Problem

From [CL99] we know that the augmented generator $\boldsymbol{G}$ and the augmented reflected generator $\hat{\boldsymbol{G}}$ with suitable domains generate C_0 semigroups. Recalling Section 3.1 we may expect that there is a well-posed abstract Cauchy problem, or more specifically a partial differential initial-boundary problem, that corresponds to the evolution semigroup. Identifying an underlying PDE problem can be difficult regardless whether we consider augmentation on $\mathbb{R}$, $\mathbb{R}_{\geq 0}$ or periodically on τS^1. The augmentation introduces the new boundaries and a different larger space for initial conditions. Ideally, we would like to take any initial condition $\boldsymbol{f}$ from $\mathcal{D}(\boldsymbol{G})$ or $L^p(\boldsymbol{X})$, or from $\mathcal{D}(\hat{\boldsymbol{G}})$ or $L^p(\hat{\boldsymbol{X}})$, respectively, and evolve it with the evolution semigroup. However, the desired connection to the original non-autonomous abstract Cauchy problem raises the question if an initial condition $\boldsymbol{f}$ should correspond to a full time evolution $\boldsymbol{f}(\theta,\cdot) = (U(\theta,0)f)_{\theta\in[0,\tau]}$ for some $f \in L^p(\mathbb{X})$. Note that the augmented stochastic differential equation (3.18) relates to evolving the non-autonomous SDE (2.5) from any initial time s by setting $\theta_0 = s$. In an analogous manner, the augmented Fokker–Planck equation (3.22) with initial condition $\boldsymbol{f}_0$ evolves every initial condition $\boldsymbol{f}_0(s,\cdot)$, $s \in [0,\tau)$, by the non-autonomous reflected Fokker–Planck equation (2.27). Here $(\boldsymbol{f}_0(s,\cdot))_s$ can be thought of as a configuration of initial conditions. More precisely, with Theorem 3.12 and (3.17) follows:

$$\boldsymbol{f}_t(\theta + t \bmod \tau, x) = \left(e^{t\hat{\boldsymbol{G}}}\boldsymbol{f}_0\right)(\theta + t, x) = \hat{\mathcal{P}}_{\theta,\theta+t}\big(\boldsymbol{f}_0(\theta,x)\big). \tag{3.23}$$

for the evolution of (3.22).

Remark 26:

At this point the reader might ask about the different structure in the variables, namely, the representation in (3.23) differs from (3.17). Following (3.17) directly, it would be

$$\boldsymbol{f}_t(\theta,x) = \left(e^{t\hat{\boldsymbol{G}}}\boldsymbol{f}_0\right)(\theta,x) = \hat{\mathcal{P}}_{\theta-t,\theta}\big(\boldsymbol{f}_0(\theta - t \bmod \tau, x)\big)\,.$$

Evaluating the evolution semigroup action at $\theta + t$ instead of θ gives our notation (3.23). We consider the same action, but our point of evaluation and our perspective are different. △

We do not need to formulate or solve a well-posed abstract Cauchy problem in the augmented setting. We only need the augmented reflected generator $\hat{\boldsymbol{G}}$ and its relation to $(\mathcal{P}_{s,t})_{s\leq t}$.

In the terminology of semigroup theory [CL99, EN00], the solution operators of (3.22), here formally denoted by $(e^{t\hat{\boldsymbol{G}}})_{t\geq 0}$, form an evolution semigroup, also called Howland semigroup, and it is given by (3.23). Informally, the action of $e^{t\hat{\boldsymbol{G}}}$, in the context of $\hat{\mathcal{P}}_{\theta,\theta+t}$, can be described as follows. On the left-hand side of (3.23), $e^{t\hat{\boldsymbol{G}}}$ takes the initial configuration $\boldsymbol{f}_0$ on all of $\hat{\boldsymbol{X}}$ and evolves the entire configuration for the time duration t, to obtain $\boldsymbol{f}_t$. The result is then evaluated at the $(\theta + t \mod \tau)$ fiber. The $(\theta + t \mod \tau)$ fiber of $\boldsymbol{f}_t$ corresponds to the θ fiber of $\boldsymbol{f}_0$ evolved for time t due to the constant drift in the θ variable, $-\partial_\theta$; see (3.21). The fact that equation (3.23) indeed gives the solutions to (3.22), is a consequence of [CL99, Thm. 6.20] adapted to the concatenation of the forward and backward evolutions described by the reflected system (2.27). As we do not require a result of this generality, we omit the details. For our purposes it is sufficient to consider the special case, where $\boldsymbol{f}_0 = \boldsymbol{f}$ is an eigenfunction of $\hat{\boldsymbol{G}}$.

Section 3.5 establishes a connections between the spectrum of the augmented reflected generator $\hat{\boldsymbol{G}}$ and the singular values of the transfer operators, $(\mathcal{P}_{s,t})_{s\leq t}$.

3.5 Coherent Families from the Augmented Generator

In this section we connect the augmented and reflected objects introduced above to the original dynamics (2.21) and to our measures for coherence (Sec. 2.4). Therefore, we prove a spectral mapping theorem for the augmented reflected process (Thm. 3.19), and we prove a bound for the finite-time coherence of a family of sets $(A_t)_{t\in[0,\tau]}$. The family and its bound are induced by the eigenpairs of the augmented generator corresponding to a reflected non-autonomous advection-diffusion process (Thm. 3.21). To achieve this we build on the discrete-time theory from [Fro13] and the periodic continuous-time theory from [FK17], and extend the idea from [FJK13] to finite-time coherence for aperiodic flows.

3.5.1 The Periodic Case

Let us first summarize some results from [FK17] regarding the infinite-time perspective on coherence. We recall the augmented Fokker–Planck equation for a T-periodic vector field v and obtain

$$\partial_t \boldsymbol{f}(t,\boldsymbol{x}) = -\mathrm{div}_{\boldsymbol{x}}(\boldsymbol{v}(\boldsymbol{x})\boldsymbol{f}(t,\boldsymbol{x})) + \frac{1}{2}\Delta_{\boldsymbol{x}}\boldsymbol{\varepsilon}^2\boldsymbol{f}(t,\boldsymbol{x}) = \boldsymbol{G}\boldsymbol{f}(t,\boldsymbol{x})$$

and the augmented generator $\boldsymbol{G}$. The original non-autonomous version (2.21)

$$\partial_t f(t,x) = -\mathrm{div}_x(v(t,x)f(t,x)) + \frac{1}{2}\Delta_x\varepsilon^2 f(t,x)$$

has a solution family $(\mathcal{P}_{s,t})_{s\le t}$ of Perron–Frobenius operators. Theorem 3.16 connect the Lyapunov exponent with the spectrum of $\mathcal{P}_{s,t}$ and with the escape rate (Def. 2.9) of a family of sets.

Theorem 3.16:

1. *Assume that $f\in L^1(\mathbb{X})\cap L^\infty(\mathbb{X})$ with $\int_{\mathbb{X}} f\,d\Lambda = 0$, and that the families $(A_t^\pm)_{t\ge s}$, given by $A_t^\pm := \{\pm\mathcal{P}_{s,t}f \ge 0\}$ are sufficiently nice [FK17, Def. 17], then*

$$E((A_t^\pm)_{t\ge s}) \le -\mathrm{Lyap}_s(f) := -\limsup_{t\to\infty}\frac{1}{t-s}\log\|\mathcal{P}_{s,t}f\|_{L^1}.$$

2. *For every $s,t\in TS^1$ we have*

$$\max_{f:\int_{\mathbb{X}} f\,d\Lambda=0}\mathrm{Lyap}_s(f) = \frac{1}{T}\log|\lambda_2(\mathcal{P}_{s,s+T})| = \frac{1}{T}\log|\lambda_2(\mathcal{P}_{t,t+T})|,$$

where $\lambda_2(\cdot)$ denotes the second largest eigenvalue of the argument. The maximizer of the left hand side is the eigenfunction f_2 of $\mathcal{P}_{s,s+T}$ corresponding to the eigenvalue λ_2.

Proof. The first part can be found in [FK17, Thm. 19] and the second part can be found in [FK17, Prop. 20]. □

The second part shows that the Lyapunov exponent is independent of the starting time.

The Augmented Generator and Coherence

For a time-periodic velocity field v with period T, it was shown in [FK17] that the families of sets

$$A_\theta^+ := \{\boldsymbol{f}(\theta,\cdot) \geq 0\} \quad \text{and} \quad A_\theta^- := \{\boldsymbol{f}(\theta,\cdot) \leq 0\}$$

have an escape rate of at most $\mathrm{Re}(\mu_2)$. Here μ_2 is the first non-trivial eigenvalue of $\boldsymbol{G}$ and the sets $A_\theta^\pm$ are induced by the corresponding eigenfunction $\boldsymbol{f}$, $\boldsymbol{G}\boldsymbol{f} = \mu_2\boldsymbol{f}$, of the augmented generator.

Recall that, for the time-asymptotic perspective, we measure coherence using escape rates. In order to relate the augmented generator and its eigendata to escape rates, we use the following spectral mapping property [FK17, Lem. 22]

$$\boldsymbol{f}(s+t \bmod T,\cdot) = e^{-\mu t}\mathcal{P}_{s,s+t}\boldsymbol{f}(s,\cdot)\,. \tag{3.24}$$

This result also follows from the more general result for the aperiodic setting (Thm. 3.19). The following result from [FK17, Thm. 23] gives the desired relation.

Theorem 3.17:
For every $s \in TS^1$ we have

$$\max_{f\,:\,\int_{\mathbb{X}} f\,d\Lambda=0} \mathrm{Lyap}_s(f) = \mathrm{Re}(\mu_2(\boldsymbol{G}))$$

with $\mu_2(\boldsymbol{G})$ being the first subdominant eigenvalue of $\boldsymbol{G}$. The s-dependent maximizer of the left-hand side is $f = \boldsymbol{f}(s,\cdot)$ where $\boldsymbol{f}$ is the corresponding eigenfunction of $\boldsymbol{G}$.

Proof. The proof can be found in [FK17, Thm. 23]. □

Next, we investigate the general spectral structure of $\boldsymbol{G}$.

Complex Eigenvalues

This paragraph follows [FK17, Rem. 24]. The augmented generator has two different types of complex eigenvalues that have different origins and meanings. One type that contains relevant information about the dynamics is discussed in this paragraph. The discussion of the other type, the companion eigenvalues, is postponed to Section 4.1, because it is more important for numerical approximations.

If there is $\mu_2(\boldsymbol{G}) = \mu \in \mathbb{C}\backslash\mathbb{R}$, then there exists a $\delta > 0$ such that $e^{\delta\mu} \in \mathbb{R}$. For $t = s+k\delta$, $k \in \mathbb{N}$, we obtain

$$\mathcal{P}_{s,t}f_s = e^{\mu(t-s)}f_t = e^{k\delta\mu}f_t\,, \tag{3.25}$$

using the spectral mapping property (3.24). Since $\mathcal{P}_{s,t}$ is a Markov operator, it maps real-valued functions to real-valued functions. Hence (3.25) holds for the real part $\mathrm{Re}(f)$ and the imaginary part $\mathrm{Im}(f)$ of f_s and f_t respectively. The mapping $t \mapsto \|\mathcal{P}_{s,t}g\|_{L^1}$ is monotonically decreasing, because $\mathcal{P}_{s,t}$ is non-expansive. Together with (3.25) follows $\mu = \mathrm{Lyap}_s(\mathrm{Re}(f)) = \mathrm{Lyap}_s(\mathrm{Im}(f))$. For $\mu = \alpha + \beta i$, with $\alpha, \beta \in \mathbb{R}$, follows

$$\mathcal{P}_{s,t}\mathrm{Re}(f_s) = \mathrm{Re}(e^{\mu(t-s)}f_t) = e^{\alpha(t-s)}(\cos(\beta(t-s))\mathrm{Re}(f_t) - \sin(\beta(t-s))\mathrm{Im}(f_t)\,. \tag{3.26}$$

To obtain a coherent family in the sense of Theorem 3.17, we may consider the positive or negative support of the real or imaginary parts. In particular, the real part of f_s returns to a real function f_t at some later time $t = \frac{2\pi}{\beta}$, where β is independent of the driving period T. The induced coherent family is periodic if and only if T and $\frac{2\pi}{\mathrm{Im}(\mu)}$ are rationally dependent, otherwise the family is quasi-periodic. Next, we show that the choice $\mathrm{Re}(f)$ represents one phase from a cycle of period $\frac{2\pi}{\beta}$. Since $\mathrm{Re}(f_s)$ and $\mathrm{Im}(f_s)$ have the Lyapunov exponent μ, any complex linear combination of these functions also has the Lyapunov exponent μ. Thus, for every $\vartheta \in [0, 2\pi)$ the function $(s, x) \mapsto \mathrm{Re}(e^{i\vartheta} f_s(x))$ yields a coherent family and ϑ acts as a phase for the family. With the same evolution rule as in (3.26) we obtain

$$\mathcal{P}_{s,t} f_s^{\vartheta} = \mathrm{Re}(e^{i\vartheta + \mu(t-s)} f_t)\,.$$

Remark 27:

- A similar analysis for complex eigenvalues and phases has been done for the discrete case in [FGTQ14].
- This type of complex eigenvalue has been investigated numerically in [FK17, Sec. 7].

△

Another type of complex eigenvalue of $\boldsymbol{G}$, the *companion eigenvalues*, where the complex eigenvalue does not contain any additional information about the underlying dynamics is investigated in Chapter 4.

3.5.2 The Aperiodic Case

In the context of non-autonomous, finite-time, stochastic dynamics and coherence, the notion of escape rate is not adequate. Thus, we consider the coherence ratio (Def. 3.18) of a family of sets. For an aperiodic velocity field v we quantify the coherence of families $(A_t^{\pm})_{t\in[0,T]}$ using Definition 3.18 and construct coherent families with an associated coherence bound using Theorem 3.21.

Definition 3.18: Coherence Ratio
Let $(A_t)_{t\in[0,T]}$ be a family of measurable sets. We denote the law of the process $(X_t)_{t\in[0,T]}$ generated by the SDE (2.5) initialized with the uniform distribution $X_0 \sim \Lambda_u$ on $\mathbb{X}$, where Λ_u denotes the normalized Lebesgue measure on the bounded domain $\mathbb{X}$, by $\mathbb{P}_{\Lambda_u}$. For $\Lambda_u(A_0) > 0$ we define the coherence ratio of the family $(A_t)_{t\in[0,T]}$ as

$$\rho_{\Lambda_u}((A_t)_{t\in[0,T]}) := \frac{\mathbb{P}_{\Lambda_u}\left(\cap_{t\in[0,T]}\{X_t \in A_t\}\right)}{\Lambda_u(A_0)}\,. \tag{3.27}$$

In [FK17, App. A.6] the authors showed that the quantity (3.27) is well-defined for a family of sets, if this family has sufficient regularity. This regularity property is called *sufficiently nice* in [FK17, Def. 17]. In [FKS20] an alternative approach was used to discard this requirement. Lemma 3.20 shows that the eigenfunctions inherently possess additional regularity in our setting. Theorem 3.21 below shows that this additional regularity is sufficient to prove the desired results.

A Spectral Mapping Property

The following theorem can be obtained from (3.23) by observing that an eigenpair $(\mu, \boldsymbol{f})$ of $\hat{\boldsymbol{G}}$ induces a solution to (3.22) by $\boldsymbol{f}_t = e^{\mu t}\boldsymbol{f}$. To emphasize the connection between the augmented reflected generator $\hat{\boldsymbol{G}}$ and the non-autonomous dynamical system, we take a different approach for the proof. Remember that for the aperiodic setting on $[0, T]$ the reflected dynamics on $[0, 2T]$ are extended and augmented τ-periodically, with $\tau = 2T$.

Theorem 3.19:

(1) Consider the family $(\mathcal{P}_{s,t})_{s\leq t}$ on $L^p(\mathbb{X})$ for $p \in (1, \infty)$. Let $\boldsymbol{f}$ be an eigenfunction of $\hat{\boldsymbol{G}}$ corresponding to the eigenvalue $\mu \in \mathbb{C}$, namely, $\hat{\boldsymbol{G}}\boldsymbol{f} = \mu\boldsymbol{f}$. Then

$$\hat{\mathcal{P}}_{s,s+t}\boldsymbol{f}(s, \cdot) = e^{\mu t}\boldsymbol{f}(s + t \bmod \tau, \cdot) \tag{3.28}$$

holds for all $s \in \tau S^1$ and $t \geq 0$.

(2) The result from (1) also holds for $p = 1$. Furthermore, if v is naturally T-periodic, then the results hold analogously without the reflection for $\boldsymbol{G}$ on TS^1 instead of $\hat{\boldsymbol{G}}$ on τS^1.

Theorem 3.19 and its proof due to the author have been published in [FKS20, Prop. 4.2].

Proof. The proof of (3.28) uses ideas from [FK17]. First, we ensure the existence of a unique solution with a certain regularity on $[0, T]$ and $[T, \tau]$ using Theorem 3.12. We consider the original problem (2.21) on $[0, T]$ and the reflected, shifted, time-reversed problem (2.27) on $[T, 2T]$. By construction of $\hat{\mathcal{P}}_{0,\tau}$ in Section 2.5, Theorem 3.12 guarantees that for any initial condition $f_0 \in L^p(\mathbb{X})$ with $p \in (1, \infty)$ there exists a unique function f with the regularity

$$f \in C\big([0, \tau]; L^p(\mathbb{X})\big), \quad f|_{[0,T]} \in C^1\big((0, T]; L^p(\mathbb{X})\big), \quad f|_{[T,\tau]} \in C^1\big((T, \tau]; L^p(\mathbb{X})\big)$$

and the properties

$$f|_{[0,T]} \text{ solves (2.21)}, \quad f|_{[T,\tau]} \text{ solves (2.27)}, \quad f(t) = \hat{\mathcal{P}}_{s,t}f(s)\ ,\ s, t \in [0, \tau] \text{ with } s < t\ .$$

Furthermore, $f(t) \in \mathcal{D}(\hat{G}(t))$ holds for all $t \in (0, \tau]$.

(1) We can proceed similar to [FK17, Lem. 22]. Let $\mu \in \mathbb{C}$ and $\boldsymbol{f} \in \mathcal{D}(\hat{\boldsymbol{G}})$ with $\hat{\boldsymbol{G}}\boldsymbol{f} = \mu\boldsymbol{f}$. According to the construction above (3.21) we know

$$\mu\boldsymbol{f}(\theta, \cdot) = (\hat{\boldsymbol{G}}\boldsymbol{f})(\theta, \cdot) = -\partial_\theta\boldsymbol{f}(\theta, \cdot) + \hat{G}(\theta)\boldsymbol{f}(\theta, \cdot)$$

and this implies, using (3.22), for all $\theta \in \tau S^1\backslash\{0, T\}$

$$\partial_\theta\boldsymbol{f}(\theta, \cdot) = (\hat{G}(\theta) - \mu)\boldsymbol{f}(\theta, \cdot). \tag{3.29}$$

Now $\hat{\mathcal{P}}_{\theta,\theta+t}$ is the evolution operator to the evolution equation

$$\partial_\theta u(\theta) = \hat{G}(\theta)u(\theta)\,.$$

Thus, the function $e^{-\mu t}\hat{\mathcal{P}}_{\theta,\theta+t}\boldsymbol{f}(\theta, \cdot)$ solves (3.29) uniquely and Theorem 3.12 guarantees continuity in θ. Therefore, we can connect the eigenfunctions of the augmented reflected generator $\hat{\boldsymbol{G}}$ with the evolution given by $\hat{\mathcal{P}}_{s,s,+t}$ for all s, t as stated in the claim.

(2) As stated in Theorem 3.13 the case $p = 1$ can also be treated with results from [Tan97]. Using Theorem 3.13 instead of Theorem 3.12 in the arguments above gives the claim of part (1) for $p = 1$. Furthermore, if v is already T-periodic we consider $\mathcal{P}_{0,T}$ and the augmented generator $\boldsymbol{G}$ instead of $\hat{\boldsymbol{G}}$. The general arguments used above do not require reflection and thus hold analogously in the naturally periodic setting as well. See [FK17] for a detailed proof for the periodic setting with $p = 1$.

□

Remark 28:

- The arguments and results of Theorem 3.19 hold in the periodic case as well. However, the chosen measure of coherence, to which we can relate the eigendata, is different, see Section 3.5.1 and [FK17, Sec. 6].
- Note that Theorem 3.9 ensures that for every initial condition $f_s \in \mathcal{D}(G(s))$ the solution $\hat{\mathcal{P}}_{s,s+t} f_s = f(t)$ is a continuous mapping in t to the domain of the operator $G(s+t)$, namely $\mathcal{D}(G(s+t)) = \mathcal{D}_p := \left\{ f \in W^{2,p}(\mathbb{X}) \,\middle|\, \frac{\partial f}{\partial n} = 0 \text{ on } \partial\mathbb{X} \right\}$. Theorem 3.14 further gives for each eigenfunction $\boldsymbol{f}$ that $\boldsymbol{f} : \theta \mapsto \boldsymbol{f}(\theta, \cdot) \in C(\tau S^1; \mathcal{D}_p)$ and that $\boldsymbol{f} \in C(\hat{\boldsymbol{X}})$. This regularity is utilized in the proof of Theorem 3.21 below.

△

Lemma 3.20:
Let $\boldsymbol{f}$ be an eigenfunction of $\hat{\boldsymbol{G}}$ considered on $L^p(\hat{\boldsymbol{X}})$ for $p > \frac{d}{2}$. Then $\boldsymbol{f} \in C([0,\tau] \times \mathbb{X})$.

Lemma 3.20 and its proof due to the author have been published in [FKS20, Cor. A.5].

Proof. From the spectral mapping result Theorem 3.19, it follows for an eigenfunction $\boldsymbol{f}$ of $\hat{\boldsymbol{G}}$ that

$$\hat{\mathcal{P}}_{0,t} \boldsymbol{f}(0,\cdot) = e^{\mu t} \boldsymbol{f}(t \bmod \tau, \cdot)\,.$$

Additionally, Theorem 3.12 implies the regularity $e^{-\mu\tau} \hat{\mathcal{P}}_{0,\tau} \boldsymbol{f}(0,\cdot) = \boldsymbol{f}(0,\cdot) \in \mathcal{D}(\hat{G}(\tau))$. Now the claimed regularity follows from Theorem 3.14 (a) and (c) with $\mathcal{D}(\hat{G}(\tau)) = \mathcal{D}_p$. □

Let μ be an eigenvalue of $\hat{\boldsymbol{G}}$ corresponding to an eigenfunction $\boldsymbol{f}$, meaning $\hat{\boldsymbol{G}} \boldsymbol{f} = \mu \boldsymbol{f}$. Now Theorem 3.19 gives for $s = 0$ and $t = \tau = 2T$ the spectral mapping type result:

$$\hat{\mathcal{P}}_{0,\tau} \boldsymbol{f}(0,\cdot) = e^{\mu\tau} \boldsymbol{f}(\tau,\cdot). \tag{3.30}$$

Equation (3.30) connects the eigenvalues and eigenfunctions of the evolution operator $\hat{\mathcal{P}}_{s,s+\tau}$ to the eigenvalues and eigenfunctions of the augmented reflected generator $\hat{\boldsymbol{G}}$. For every μ there must be a $0 < \sigma \in \mathbb{R}$ such that $e^{\mu\tau} = \sigma^2$, because $\hat{\mathcal{P}}_{0,\tau} = \hat{\mathcal{P}}_{0,2T} = \mathcal{P}^*_{0,T} \mathcal{P}_{0,T}$ is a compact, self-adjoint, and positive operator. This implies the equality

$$0 < \sigma = \left(e^{\mu\tau}\right)^{\frac{1}{2}} = \left(\left(e^{\mu T}\right)^2\right)^{\frac{1}{2}} = e^{\mathrm{Re}(\mu)T} \left(\left(\cos(\mathrm{Im}(\mu)T) + i \sin(\mathrm{Im}(\mu)T)\right)^2\right)^{\frac{1}{2}}\,. \tag{3.31}$$

Equation 3.31 further implies that $\mathrm{Im}(\mu) = \frac{2k\pi}{\tau} = \frac{k\pi}{T}$ for some $k \in \mathbb{Z}$.

The argument above shows that the type of complex eigenvalues discussed at the end of Section 3.5.1 cannot appear in the augmented reflected setting.

Figure 3.2 visualizes a family of sets $\bigcup_{\theta\in[0,\tau]}\{\theta\}\times A_\theta$ on the space-time cylinder $\hat{\boldsymbol{X}} = \tau S^1 \times \mathbb{X}$. Furthermore, it shows how the augmented reflected dynamic is related to the original dynamic on $[0,T]$.

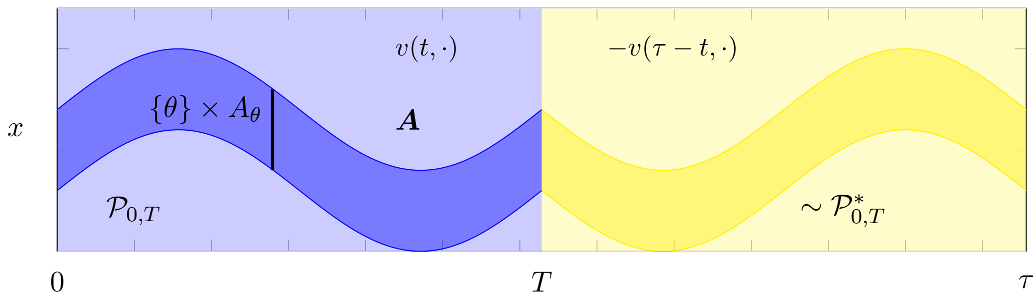

Figure 3.2: Augmented set $\boldsymbol{A} = \bigcup_{\theta\in[0,\tau]}\{\theta\}\times A_\theta$, space-time cylinder $\hat{\boldsymbol{X}} = \tau S^1 \times \mathbb{X}$.

Main Results

Theorem 3.21 connects the coherence ratio ρ_{Λ_u} in (3.27) of the family of sets $(A_t)_{t\in[0,T]}$ defined by the positive or the negative support of an eigenfunction $\boldsymbol{f}$ of $\hat{\boldsymbol{G}}$ to the corresponding eigenvalue $\mu < 0$. The probability of a trajectory remaining in a family of sets constructed from the positive or negative spatial support of $\boldsymbol{f}$ decays no faster than the rate given by the corresponding eigenvalue μ. This result extends similar results for autonomous systems in discrete time [FS10] and continuous time [FJK13], and periodically driven dynamics in continuous time [FK17] to general non-autonomous flows.

Theorem 3.21:
Let $\hat{\boldsymbol{G}}\boldsymbol{f} = \mu\boldsymbol{f}$ with $\mu < 0$ and $\|\boldsymbol{f}(T,\cdot)\|_{L^1} = 2$. Then for the family of sets $(A_t^\pm)_{t\in[0,T]}$ given by $A_t^\pm := \{\pm\boldsymbol{f}(t,\cdot)\geq 0\}$ it holds that

$$\frac{e^{\mu T}}{\|\boldsymbol{f}(0,\cdot)\|_{L^\infty}\Lambda(A_0^\pm)} \leq \rho_{\Lambda_u}\left((A_t^\pm)_{t\in[0,T]}\right), \tag{3.32}$$

where $\Lambda(A)$ denotes the non-normalized Lebesgue measure of the set A. In particular, eigenfunctions for eigenvalues $\mu\approx 0$ yield families of sets with high coherence ratio.

Proof. A proof can be found in [FKS20, Thm. 4.5]. Note that by Lemma 3.20 the eigenfunction $\boldsymbol{f}$ is continuous on $\hat{\boldsymbol{X}}$. This regularity of $\boldsymbol{f}$ is used in the proof. $\square$

The estimate in (3.32) compares two spectral aspects of the dynamics. The right hand side

$$\frac{\mathbb{P}_{\Lambda_u}\left(\cap_{t\in[0,T]}\{X_t\in A_t\}\right)}{\Lambda_u(A_0)}$$

quantifies the probability of the process $(X_t)_{t\geq 0}$ leaving from the family of sets $(A_t)_{t\geq 0}$, and the left hand side is a scaled measure of mixing, Section 2.4. The estimate (3.32) states that the probability of escape is less than the mixing incurred over the same time duration.

The bound (3.32) is not intended to be sharp. In [FP09], the authors show that we could optimize the level set cutoff to improve the coherence ratio ρ_{Λ_u}.

Theorem 3.22 generalizes Theorem 3.21 to give an estimate for functions that are finite linear combinations of eigenfunctions.

Theorem 3.22:
For multiple eigenpairs $\hat{\boldsymbol{G}}\boldsymbol{f}_i = \mu_i \boldsymbol{f}_i$, $i = 1, \dots, k \in \mathbb{N}$, with $\mu_k \leq \dots \leq \mu_1 \leq 0$, Theorem 3.21 holds for the finite linear combinations $\boldsymbol{f} = \sum_{i=1}^k \alpha_i \boldsymbol{f}_i$ with $\alpha_i \in \mathbb{R}$ and $\mu = \mu_k$ if

$$\alpha_i \int_{A_T^+} \boldsymbol{f}_i(T, \cdot)\, d\Lambda \geq 0 \quad \textit{for } i = 1, \dots, k. \tag{3.33}$$

Proof. A proof of Theorem 3.22 has been published in [FKS20, Prop. 4.6]. □

Theorem 3.22 is useful for the numerical example in Section 4.3. There, a sparse eigenbasis approximation is computed for the six dominant eigenvectors of $\hat{\boldsymbol{G}}$ to separate individual coherent subdomains. This approximation includes a rotation which results in linear combinations of eigenvectors. The algorithm used is also briefly introduced in Section 4.3.

4 Numerical Aspects and Examples

In this chapter, we use Theorem 3.21 and Theorem 3.22 in two examples. Therefore, we need to consider how to obtain a discrete approximation of the augmented reflected generator to solve the discrete versions of the eigenproblem for the augmented reflected generator. First, we provide a discretization for the Perron–Frobenius operator in the autonomous setting. Following the defining relation for the infinitesimal generator (3.1), we then derive a discretization for the infinitesimal generator. This approach is extended to the augmented generator on the space-time manifold. We analyze some implications of the augmentation and its discretization. Finally, we include the reflection and obtain a discretization method for the augmented reflected generator. We illustrate the efficacy of the trajectory-free approach and its properties on two standard examples. The numerical examples in Section 4.2 and Section 4.3 have been published in [FKS20, Sec. 5.2 & 5.3] and are re-used and expanded upon here with permission of the publisher and the authors. We may use the same symbol for the operators $\mathcal{P}_{s,t}$ or generators and their discretizations, if there is no risk of confusion.

4.1 Numerical Analysis for the Augmented Generator

As with many operators acting on or between infinite-dimensional spaces, there are different ways to approximate an operator and related equations or eigenproblems. Generally, there are interior and exterior approximation schemes [Zei90b, Chap. 34 & 35]. Since there are many schemes with general convergence results for the operators or the associated eigendata derived in different settings, the question arises as to whether some schemes are better suited for our problems than others. In order to maintain the interpretability of the eigendata, we would like to preserve certain properties of the transfer operators and their generators, like the Markov property. Therefore, we discuss the so-called Ulam's approach [Ula60] that uses piecewise constant test and ansatz functions. Section 4.1.2 briefly discusses higher-order Markov approximations and spectral approaches. This section is kept brief on purpose, because the numerical treatment of the augmented reflected generator requires only the reflection in addition to the ideas from [FJK13, FK17].

4.1.1 Ulam's Approach

The basic idea of Ulam's approach for the discretization $P_{s,t}^{\mathrm{Ulam}}$ of the transfer operator $\mathcal{P}_{s,t}$ for fixed $s, t \in [0, T]$ with $s < t$, can be phrased as a generalized Petrov–Galerkin scheme

$$c_\psi^\top P_{s,t}^{\mathrm{Ulam}} c_\varphi = \langle \psi, \mathcal{P}_{s,t}\varphi \rangle_{V^* \times V} \quad \text{for} \quad \psi = \sum_{i=1}^m c_i \psi_i \quad \text{and} \quad \varphi = \sum_{j=1}^n c_j \varphi_j \,.$$

We use the convention $\langle \psi_j, f\rangle_{V^*\times V} = \int_{\mathbb{X}} \psi_j f \, d\Lambda$ for $f \in V = L^p(\mathbb{X})$ and $\psi_j \in V^* = (L^p(\mathbb{X}))^*$ with Λ being the Lebesgue measure on $\mathbb{R}^d$. For Ulam's approach let us consider a partition $(B_i)_{i=1}^n$, $m = n \in \mathbb{N}$, of the state space $\mathbb{X}$ into measurable sets B_i and choose the test and ansatz functions as (normalized) indicator functions of that partition: $\psi_i := \frac{1}{\Lambda(B_i)} \mathbb{1}_{B_i} =: \varphi_i$. Note that $\mathrm{unif}(B_j)$ denotes the uniform distribution over the measurable set B_j. This leads to the entries

$$(P_{s,t}^{\mathrm{Ulam}})_{i,j} := \frac{1}{\Lambda(B_j)} \int_{B_j} \mathcal{P}_{s,t}\varphi_i \, d\Lambda = \mathbb{P}_{X_s\sim\mathrm{unif}(B_j)}(X_t \in B_i)\,,$$

and $P_{s,t}^{\mathrm{Ulam}} : V_n \to V_n$ with $V \supset V_n := \mathrm{span}(\varphi_i)_{i=1}^n$ and $V^* \supset W_n := \mathrm{span}(\psi_j)_{j=1}^n$. For the choice of spaces $V = L^p$ and $V^* = (L^p)^*$ and fixed n, the mapping π_n is the L^2-orthogonal projection onto the subspace V_n. This can be seen as a zeroth order discontinuous finite element method, and it can also be considered a finite volume method.

Remark 29:

- Generalized (Petrov–) Galerkin schemes are used if an operator A maps from a Banach space V to itself, $A : V \to V$ or to its dual, $A : V \to V^*$ and there is second space W that allows for a bilinear pairing $\langle\cdot,\cdot\rangle_{W\times V}$ or $\langle\cdot,\cdot\rangle_{W\times V^*}$. The cases $W = V^*$ and $W = V$ are the most common. For for recent advances in the field of discontinuous Petrov–Galerkin schemes, we refer to [Hel19], and for an extended treatment of discontinuous Petrov–Galerkin schemes, we refer the works [DG10, DG11, DGN12].

- A more detailed discussion, generalizations, like $m \neq n$, and applications of Ulam's method for transfer operators to extract coherent sets can be found in [FSM10], [Kol11, Chap. 2.3 & 3] and [Den17, Chap. 2 & 3]. Ulam's approach for the deterministic transfer operator $P_{s,t}$ is very similar to the approach given here for $\mathcal{P}_{s,t}$. The deterministic case is also covered in the references above.

- Generally, the partition elements B_i of $(B_i)_{i=1}^n$ are assumed to be closed and bounded with non-empty interior and to have piecewise smooth boundary. We choose the B_i to be cubes or boxes that are close to cubes so that the numerical diffusion is compatible with isotropic diffusion.

$\triangle$

Next we focus on the adaptation of this approach to the generator based on [Kol11, Chap. 5] and [FJK13], the augmented generator for periodic problems based on [FK17] and the augmented reflected generator for aperiodic flows based on [FKS20].

Ulam's Approach for the Generator

The starting point for the adaptation in the case $v(t,x) = v(x)$ is the relation between the semigroup $(\mathcal{P}_t)_{t\geq 0}$ and its infinitesimal generator G

$$\mathcal{P}_t = e^{tG} \quad \text{and} \quad Gf = \lim_{t\downarrow 0} \frac{\mathcal{P}_t f - f}{t} \quad \text{for } f \in \mathcal{D}(G)\,.$$

The problem arises that indicator functions for a given partition $(B_i)_{i=1}^n$ do not belong to the domain of the generator $\mathcal{D}(G)$. In [Kol11, Chap. 5], the author circumvents this problem by exchanging the discretization and the limit process for the generator. In the autonomous and deterministic setting this leads to

$$G_n^{\text{det}} := \frac{d}{dt} P_t^{\text{Ulam}}|_{t=0} \,. \tag{4.1}$$

There is no guarantee that discretization and limit processes are exchangeable. The semigroup property $\mathcal{P}_{s+t} = \mathcal{P}_t \, \mathcal{P}_s$ does not need to hold for the discretizations $P_{s+t}^{\text{Ulam}} \neq P_t^{\text{Ulam}} \, P_s^{\text{Ulam}}$. This problem is not unique to Ulam's approach. The derivation in [FK17, Sec. 7.2] describes the entries of the matrix G_n^{det} as

$$(G_n^{\text{det}})_{i,j} = \begin{cases} \frac{1}{\Lambda(B_j)} \int_{\partial B_i \cap \partial B_j} \langle v(x), n_j(x) \rangle_{\mathbb{R}^d}^+ \, d\Lambda^{d-1}(x) & i \neq j \,, \\ -\frac{1}{\Lambda(B_i)} \int_{\partial B_i} \langle v(x), n_i(x) \rangle_{\mathbb{R}^d}^+ \, d\Lambda^{d-1}(x) & i = j \,. \end{cases} \tag{4.2}$$

Here $(\ )^+$ denotes the non-negative part, $(f)^+ := \max\{f, 0\}$, Λ^{d-1} denotes the surface measure, and $n_j(x)$ denotes the outer normal unit vector on the boundary ∂B_j of the box B_j.

(a) The Ulam discretization of $\mathcal{P}_{s,t}$ can be computed using Monte–Carlo methods, that is, uniformly seeding an ensemble of points per box, evolving the points using the dynamics, and analyzing the resulting distribution for each ensemble.

(b) The boxes B_i and B_j share the blue surface. The outward unit normal vector pointing from B_i to B_j is denoted by $n_{i\to j}$. The entry $(G_n^{\text{det}})_{i,j}$ denotes the instantaneous (outflow) flux across the blue surface in the direction $n_{i\to j}$; see also [FK17, Sec. 2].

Figure 4.1

The Monte–Carlo computation for trajectories initialized in each set B_i in the discretization of $\mathcal{P}_t$ is replaced by surface integrals over the boundaries of each B_i to discretize the generator. Figure 4.1 (b) and (4.2) show that only neighboring boxes are relevant. This leads to a sparse matrix G_n^{det}.

This approach includes numerical diffusion [FJK13, Rem. 4.6] and is the spatial part of a finite volume upwind scheme [L$^+$02]. In the non-deterministic case with explicit diffusion, the limit on the right hand side of (4.1) diverges, because Wiener processes lack (Lipschitz) regularity [Fri75, Chap. 3]. The discretization (4.2) from the deterministic setting corresponds the advective part $-\text{div}_x(vf)$ in the non-deterministic setting. The second component of the Ulam discretization of the generator corresponds to diffusion, specifically to the term $\frac{\varepsilon^2}{2}\Delta_x f$ in the Fokker–Planck equation (3.13). We consider

$$G_n := G_n^{\text{det}} + \frac{\varepsilon^2}{2}\Delta_n = G_n^{\text{det}} + G_n^{\text{diff}}$$

for the non-deterministic case for a suitable and compatible discretization Δ_n of the Laplace operator. A compatible discretization is given by the finite difference approximation of the

Laplace operator using the centroids of the boxes B_i with $\pi_n f = \sum_{i=1}^{n} f_i \mathbb{1}_{B_i}$

$$\Delta_n f = \sum_{i=1}^{n} \left(\sum_{\substack{j \neq i \\ \Lambda^{d-1}(B_i \cap B_j) \neq 0}} h(B_i \cap B_j)^{-2} (f_j - f_i) \right) \mathbb{1}_{B_i} \,, \tag{4.3}$$

where $h(B_i \cap B_j)$ is the edge length in the direction along which B_i and B_j are adjacent. This approach may be modified to account for boundary conditions [Kol11, Sec. 5.4]. The matrix G_n can also be interpreted as a rate matrix for a finite-state Markov chain. It has an eigenvalue 0 and its spectrum is confined to the left half of the complex plane. Furthermore, $\exp(tG_n)$ is similar, in the matrix sense [Fis11, p. 160], to a column stochastic matrix. For details on the handling of explicit diffusion and boundary conditions for the discretization of the generator see [Kol11, Sec. 5.4 & 5.5]. In particular, [Kol11, Sec. 5.4 & 5.5] provide the relevant convergence results.

To adapt this approach to the non-autonomous setting we use the idea introduced in Chapter 3 of augmenting the system in time. Now we have to discretize the time-dimension and track the relation to the original non-autonomous dynamics carefully.

Ulam for the Augmented Generator

As we have seen in Section 3.4, in particular (3.21), the time-component θ differs in the augmented generator $\boldsymbol{G}$ compared to the spatial components. Therefore, we carefully monitor the θ-dimension, and if necessary, treat it differently, when applying Ulam's approach to the augmented generator. This helps us to obtain the coherent families in the state space $\mathbb{X}$. The derivative in the augmented dimension $\frac{\partial}{\partial \theta}$ reduces to a simple backward difference [FJK13, Cor. 4.5]. The θ evolution is a rigid rotation of constant velocity 1. The entries which correspond to rates between boxes that are adjacent in the temporal coordinate are given by $1/h$, where the periodic time-domain τS^1 is discretized into intervals of length $h > 0$. As before, we split the parts $G_n(\theta) := G_n^{\mathrm{det}}(\theta) + G_n^{\mathrm{diff}}$. The entries in the d spatial dimensions of the deterministic part are computed as in (4.2) from the rate of flux out of the hypercube faces by numerical integration ($d-1$ dimensional Gauss quadrature) of the component of the velocity field normal to the face; see the expression for G_n^{det} in (4.2) and [FK17, Sec. 7.2]. Analogously to the autonomous case, the diffusive part needs to be treated differently. There is only diffusion in the d spatial dimensions, there is no diffusion in the θ coordinate. The entries of the matrix corresponding to diffusive dynamics are again computed from a finite difference approximation of the Laplace operator. As we have seen earlier in Chapter 3 the periodic augmentation leads to some special spectral structure. This leads to companion eigenvalues and is also reflected in the numerics.

Companion Eigenvalues

Companion eigenmodes denote eigenmodes that are in some sense *higher-order harmonics* of existing eigenmodes. These only differ in temporal modulation and more importantly encode the same information as the original eigenmode. Let us first consider the analytical case before discretization. After augmentation, the augmented generator in the periodic case has the time-drift component $\frac{\partial}{\partial \theta}$ acting on τ-periodic functions which has the eigenfunction

$$\psi_k(\theta, x) = \psi_k(\theta) = \exp\left(2\pi i \frac{k\theta}{\tau}\right)$$

for the eigenvalue $2\pi i \frac{k}{\tau}$. Now if $\boldsymbol{f}$ is an eigenfunction of $\boldsymbol{G}$ for an eigenvalue μ, then $\boldsymbol{f}\psi_k$ is an eigenfunction for the eigenvalue $\mu - 2\pi i \frac{k}{\tau}$. The fact that ψ_k is constant with respect to x and the product rule imply

$$\begin{aligned}(\boldsymbol{G}(\boldsymbol{f})\psi_k)(\theta, \cdot) &= (G(\theta)\boldsymbol{f}(\theta, \cdot) - \partial_\theta \boldsymbol{f}(\theta, \cdot))\psi_k(\theta) + \boldsymbol{f}(\theta, \cdot)(G(\theta)\psi_k(\theta) - \partial_\theta \psi_k(\theta)) \\ &= \mu \boldsymbol{f}(\theta, \cdot)\psi_k(\theta) - 2\pi i \frac{k}{\tau} \boldsymbol{f}(\theta, \cdot)\psi_k(\theta)\,. \end{aligned} \tag{4.4}$$

To investigate how this behaves with the chosen discretization scheme, let δ_h denote the backward difference operator $(\delta_h \boldsymbol{w})(t) = \frac{w_t - w_{t-h}}{h}$. We denote the time-slice for $t = 0, h, \dots \tau - h$ by w_t. For the Ulam discretization $\boldsymbol{G}$ of the augmented generator, consider an eigenvector $\boldsymbol{w}$, $\boldsymbol{G}\boldsymbol{w} = \mu\boldsymbol{w}$, that lives in discretized augmented space. Under the assumption that the eigenvector $\boldsymbol{w}$ is sufficiently smooth in time and that time is sufficiently resolved, $w_t \approx w_{t-h}$, each eigenpair $(\mu, \boldsymbol{w})$ of the discretized generator $\boldsymbol{G}$ has approximate companion pairs $(\mu - \mu^{(k)}, \psi_k \boldsymbol{w})$ for $k \in \mathbb{Z}$, where $\boldsymbol{v} = \boldsymbol{w}\psi_k$ is understood as pointwise multiplication and $\psi_k(t) = \omega^{kt}$, which only varies in time but not in space. For $\omega = \exp(2\pi i \frac{h}{\tau})$ and $\mu^{(k)} = \frac{1 - \omega^{-k}}{h}$ follows $\mu^{(k)} \to 2\pi i \frac{k}{\tau}$ for $h \to 0$ and the discrete analogue to (4.4)

$$(\boldsymbol{G}\boldsymbol{v})(t) = (G(t) - \delta_h)v_t = \mu v_t - \frac{1 - \omega^{-k}}{h} w_{t-h}\psi_k(t) \tag{4.5}$$

holds. If h is small and w_t is sufficiently smooth in t, then $\boldsymbol{v}$ is close to being an eigenvector for $\mu - \mu^{(k)}$, because $w_t \approx w_{t-h}$ holds. For more details on the companion eigenvalues for the Ulam-discretization, we refer to [FK17, Sec. 7.3] and [FKS20, Sec. 5.3].

Ulam for the Augmented Reflected Generator

For the augmented reflected generator $\hat{\boldsymbol{G}}$ we can use Ulam's approach for the generator as well [FKS20, Sec. 5]. The reflected velocity field $\hat{v}$ from (2.25) is substituted for the velocity field v used in [FK17] and the methodology for the augmented generator of [FK17] is applied to the augmented reflected generator. This is the approach taken in the numerical experiments below. We note that for the augmented reflected generator all non-real eigenvalues have to be companion eigenvalues (3.31).

Algorithm 1 summarizes the ideas introduced here to compute a discretization of the augmented reflected generator. There are some short-cuts we can take when implementing this algorithm. We can parallelize many computations (each box, each surface). Furthermore, we can include the diffusion in the surface integral iteration if we keep rigorously track of the dimensions and can distinguish purely in-time-slice spatial normal computations from others. We can skip the steps 2,3 and 4 if we take $\hat{\boldsymbol{v}}$ and $(C_i)_{i=1}^M$ as the input for Algorithm 1 and if we can distinguish the different dimensions sufficiently. If v is time-independent, then we can set $N_t = 1$, skip the steps 2,3,4, and use (4.2) for v and $(B_i)_{i=1}^n$ to get the discretization G_n of the generator G. The approach and the algorithm are idealized to some degree, because in reality we need to properly account for boundary conditions and the periodicity in time and possibly other dimensions.

Algorithm 1 Ulam Type Discretization of the Augmented Reflected Generator

function $\textsc{DiscARGen}((B_i)_{i=1}^n, [0,T], N_t, v, \varepsilon)$
  Construct the reflected velocity field $\hat{v}$ according to (2.25).
  Construct the augmented reflected velocity field $\hat{\boldsymbol{v}}$ according to (3.18).
  Construct a space-time partition $(C_i)_{i=1}^M$, $C_i \subset 2TS^1 \times \mathbb{X}$ using the spatial partition $(B_i)_{i=1}^n$, $B_i \subset \mathbb{X}$ and the temporal granularity $h = \frac{1}{N_t}$, $M = N_t \cdot n$.
  Compute the entries $(\hat{\boldsymbol{G}}_M^{\mathrm{det}})_{ij}$ according to (4.2) in the augmented setting using the augmented reflected velocity field $\hat{\boldsymbol{v}}$ and the space-time partition $(C_i)_{i=1}^M$.
  Compute the diffusion Δ_n for the spatial components using the spatial boxes $(B_i)_{i=1}^n$ according to (4.3)
  Assuming a specific ordering for the boxes, we can expand Δ_n appropriately to $\hat{\boldsymbol{G}}_M^{\mathrm{diff}}$. We combine $\hat{\boldsymbol{G}}_M := \hat{\boldsymbol{G}}_M^{\mathrm{det}} + \hat{\boldsymbol{G}}_M^{\mathrm{diff}}$ to add the appropriate diffusion to the correct entries corresponding to purely spatial, in-time-slice surfaces.
  return $\hat{\boldsymbol{G}}_M$.

To summarize, the Ulam discretization for the augmented reflected generator yields a matrix that can be considered a rate matrix of a discrete, continuous-time Markov chain, with the states corresponding to a partition of $2TS^1 \times \mathbb{X}$ into boxes (hypercubes or hyperrectangles) in $\mathbb{R}^{d+1}$.

Remark 30:
The computation of $G_n^{\mathrm{det}}(\theta)$, the discretization of the deterministic spatial parts, uses only the outward-pointing velocity field values on the faces of the partition elements. For a slightly more efficient implementation we could store the evaluations of the velocity field normal to hypercube faces in both directions (not only in the outward-pointing direction), because of the reflected structure of $\hat{v}$. The outward-pointing components would be used on the time-slice $\theta \in [0,T]$, while the inward-pointing components would be used on the time-slice $\theta_1 = 2T - \theta \in (T, 2T)$, where they are outward-pointing because of the changing sign in (2.25). This would halve the computational effort in evaluating the velocity field components normal to the hypercube faces. However, the assembly of the generator matrices is relatively fast, and we have not tried to optimize our implementation of Ulam's method for the generator in this reflected setting. The main contribution for the run-time comes from solving the eigenvalue problem for the sparse but large and non-symmetric matrices G, $\boldsymbol{G}$ or $\hat{\boldsymbol{G}}$. △

In the computations performed in the next sections we approximate $\hat{\boldsymbol{G}}$ numerically, compute its dominant spectrum and associated eigenfunctions, and plot superlevel or sublevel sets of the eigenfunctions.

4.1.2 Other Approaches

Higher-Order Approaches

As with many discretization methods, it is reasonable to ask whether there are appropriate higher-order schemes that give better approximations. The transfer operator and its generator can be discretized by higher-order test and ansatz functions $\psi_i = \phi_i$ but the resulting operators are no longer Markov operators [Kol11, Thm. 3.7]. If we want to preserve some properties for interpretation, then we cannot simply apply higher-order finite element methods. In [DL91] the authors use piecewise constant test functions but higher-order ansatz functions to preserve the Markov property when discretizing the Perron–Frobenius operator for a fixed map in the deterministic setting. In [Thi20] the idea from [DL91] was combined with the ideas from [Kol11] to investigate higher-order Markov approximations of the generator in the time-continuous, autonomous setting, for both deterministic and stochastic dynamics.

The question of how this can be adapted to the augmented or the augmented reflected generator is still open.

Spectral Approaches

Instead of slowly increasing the regularity of the test or ansatz functions supported on small disjoint or slightly overlapping areas of the state space, there is also the idea of spectral discretization using infinitely smooth functions that are supported on the whole state space. For periodic problems this leads to the use of Fourier modes. For an introduction to spectral methods we refer to [Boy01] and [Tre00]. This approach has been explored for the time-periodic setting, which leads to an Ulam-spectral hybrid approach in [FK17, Sec. 7.4]. While working on [FKS20] the authors also experimented with a Chebyshev approach for the time-dimension. However, the non-smoothness in the reflection point posed challenges for the Chebyshev approach and further investigations were postponed in favor of other contributions. For spatially periodic autonomous problems a purely spectral approach that leads to a smaller but dense matrix is discussed in [FJK13, Sec. 4.3 & 4.4].

4.2 Example: The Forced Double Gyre Flow

Our first example is the periodically driven double gyre system [SLM05]. This system has been a standard example of transport in non-autonomous flows and has been investigated with respect to finite-time coherent set in for example [FPG14]. We consider

$$x'(t) = -\pi A \sin(\pi f(t,x)) \cos(\pi y) \qquad y'(t) = \pi A \cos(\pi f(t,x)) \sin(\pi y) \frac{df}{dx}(t,x) \tag{4.6}$$

on the time interval $[0,T] = [0,4]$ and on the spatial domain $\mathbb{X} = [0,2] \times [0,1]$ with reflecting boundary. The force $f(t,x) = \gamma \sin(2\pi\Omega t)x^2 + (1 - 2\gamma \sin(2\pi t))x$ and the choice of parameters $A = 0.25$, $\Omega = 2\pi$, and $\gamma = 0.25$ imply that the forcing period is 1. This system preserves the Lebesgue measure.

The goal of this example is to show that the Ulam method for the augmented reflected generator $\hat{\boldsymbol{G}}$ reliably computes the singular functions and values of the transfer operator $\mathcal{P}_{0,T}$.

The discretization of the augmented reflected generator $\hat{\boldsymbol{G}}$ with a resolution of $40 \times (100 \times 50)$, namely, 40, 100 and 50 for t, x and y, respectively, and noise intensity $\varepsilon = 0.1$ gives the non-trivial dominant eigenvectors of $\hat{\boldsymbol{G}}$ at time $t = 0$ shown in Figure 4.2. In Table 4.1 the third,

μ_1	0	μ_4	−0.35061	σ_1	1	σ_4	0.24599
μ_2	−0.09033	μ_5	−0.44766	σ_2	0.69674	σ_5	0.16685
μ_3	−0.34938	μ_6	−0.45702	σ_3	0.24720	σ_6	0.16072

Table 4.1: Eigenvalues μ_k of $\hat{\boldsymbol{G}}$ ordered in ascending magnitude and corresponding approximate singular values σ_k of $\mathcal{P}_{0,T}$ according to (3.31).

fourth and sixth eigenvalues ordered in ascending magnitude and their eigenvectors (not shown) correspond to features that are similar to features that have also been detected in the time-asymptotic setting in [FK17, Sec. 7.6]. In [FK17] these eigenfeatures are connected to complex non-companion eigenvalues. We investigate the numerical aspects of companion eigenvalues further in the context of the next example. These features become less coherent, specifically, the real parts of their corresponding eigenvalues decrease compared to the other eigenvalues, as the length T of the time interval increases. We revisit and expand this example in the context

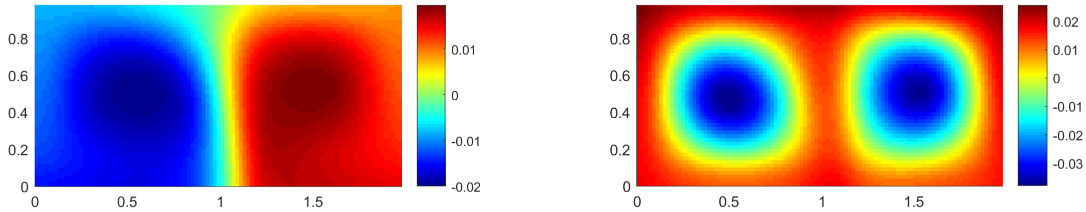

(a) Second eigenvector. (b) Fifth eigenvector.

Figure 4.2: Time-slice $t = 0$ of the second and fifth eigenvector of $\hat{\boldsymbol{G}}$ for the double gyre flow. This figure has been published in [FKS20, Fig. 2].

of optimal manipulation of these coherent families in Section 6.4.1. There we choose to target the second eigenvalue to increase the left right separation and we choose to target the fifth eigenvalue to decrease the coherence of the gyres.

4.3 Example: The Bickley Jet

In this second example we discretize the augmented reflected generator for a perturbed Bickley Jet [RBBV+07]. The Bickley Jet is an idealized model of an atmospheric flow that has been investigated with several approaches for coherence. The following model describes an idealized zonal jet in a band around a fixed latitude, assuming incompressibility, on which two traveling Rossby waves are superimposed. The stream function

$$\Psi(t, x, y) = -U_0 L \tanh\left(\frac{y}{L}\right) + U_0 L \operatorname{sech}^2\left(\frac{y}{L}\right) \sum_{n=2}^{3} A_n \cos\left(k_n(x - c_n t)\right) \tag{4.7}$$

induces the velocity field $v = (-\frac{\partial\Psi}{\partial y}, \frac{\partial\Psi}{\partial x})$. The parameters are chosen according to [RBBV+07]. The time unit is days and the length unit is Mm ($1\,Mm = 10^6 m$). We choose

$$c_2 = 0.205U_0, \qquad c_3 = 0.461U_0, \qquad A_2 = 0.1, \qquad A_3 = 0.3, \qquad r_e = 6.371,$$

for the speeds c_n and the amplitudes A_n of the Rossby waves with r_e being the Earth's radius. For the remaining parameters we choose

$$U_0 = 5.4138, \qquad L = 1.77, \qquad k_n = \frac{2n}{r_e}.$$

The state space is chosen to be $\mathbb{X} = \pi r_e S^1 \times [-3, 3]$ which is periodic in the x direction, and the time interval under consideration is $[0, T] = [0, 9]$. For good numerical tractability, we resolve the reflected space-time manifold with a $108 \times (120 \times 36)$ grid that is spatially somewhat coarse. This grid is uniform in space (120×36) which leads to square boxes needed for isotropic diffusion. As in Section 4.2, we choose the noise strength $\varepsilon = 0.1$.

The system induced by Ψ is equipped with homogeneous Dirichlet boundary conditions on $\partial\mathbb{X}$ instead of homogeneous Neumann boundary conditions. As is known from operator theory for partial differential equations, different boundary conditions lead to different spectral structures. For this example, the generator now generates a semigroup of sub-Markovian operators and its leading eigenvalue is strictly less than zero. We expect Theorem 3.21 to hold in the case of Dirichlet boundary conditions, because empirically the spectrum of our operators only changes slightly with the boundary conditions. There are more rigorous arguments. One possible theoretical justification would require us to close the open system by introducing an artificial external state, then apply the Neumann theory to that system. Alternatively we could establish all the relevant results leading up to Theorem 3.21 in the setting of homogeneous Dirichlet boundary conditions. This is beyond the scope of this thesis and will be tackled in future work.

Remark 31:
Since the Bickley Jet was also investigated in [FK17], we want to emphasize that the computations in this section are different to those performed in [FK17, Sec. 7.6].

- Firstly, the Bickley Jet under investigation here is aperiodically driven, whereas the Bickley Jet in [FK17, Sec. 7.6] is periodically driven.
- Secondly, we are interested in the finite-time evolution and properties. In contrast, in [FK17] the authors are looking for time-asymptotic behaviour, specifically, functions that decay at the slowest time-asymptotic ($t \to \infty$) rate under periodic driving.
- Despite considering the time span $[0, 9]$ as in [FK17], the finite-time investigation here is different to the infinite-time question addressed in [FK17], even if we would consider a periodically driven Bickley Jet.

$\triangle$

Computational Results

We use and verify the relations for companion eigenvalues derived in Section 4.1.1. To accommodate for the appearance of non-real companion eigenvalues, we compute the N eigenvalues and vectors of $\hat{\boldsymbol{G}}$ with the smallest magnitude instead of largest real part using `eigs(G,N,'SM')` in Matlab. In Table 4.2, we find a gap after the first and after the sixth eigenvalue. Figure 4.3 shows

μ_1	-0.02523	μ_6	-0.29908	σ_1	0.79690	σ_6	0.06776
μ_2	-0.21086	μ_7	$-0.03534 - 0.35003i$	σ_2	0.14990	σ_7	$-0.72750 + 0.00634i$
μ_3	-0.25710	μ_8	$-0.03534 + 0.35003i$	σ_3	0.09887	σ_8	$-0.72750 - 0.00634i$
μ_4	-0.25836	μ_9	-0.39208	σ_4	0.09776	σ_9	0.02934
μ_5	-0.29905	μ_{10}	$-0.21995 - 0.33451i$	σ_5	0.06778	σ_{10}	$-0.13695 + 0.01805i$

Table 4.2: Eigenvalues μ_k of $\hat{\boldsymbol{G}}$ ordered in ascending magnitude and the corresponding approximate singular values σ_k of $\mathcal{P}_{0,T}$ according to (3.31). The eigenvalues μ_7, μ_8, μ_{10} correspond to companion modes. They do not induce real singular values $\sigma_7, \sigma_8, \sigma_{10}$, because the numerically computed companions (4.8) contain a bias induced by discretization; see (4.5) and [FK17, Sec. 7.3] for further details.

the eigenvectors corresponding to the dominant, specifically, smallest real part, six eigenvalues. The first eigenvector that represents the quasistationary or conditionally invariant distribution, highlights parts of the domain that get pushed out of the region $\mathbb{X}$. These parts are colored in blue in Figure 4.3 (a). The parts of phase space that remain longest in $\mathbb{X}$ under the dynamics (4.7) with some additional diffusion are colored in red. This leakage effect is caused by the outflow conditions. As mentioned above, this example is explorative, because the theory introduced in Chapter 2 and 3 only considers reflecting and not outflow boundary conditions.

The second eigenvector indicates a separation of the upper and the lower part by the zonal jet. The next four (the third to the sixth) eigenvectors show combinations of coherent vortices. To investigate which elements of the spectrum of $\hat{\boldsymbol{G}}$ contain genuinely new information about

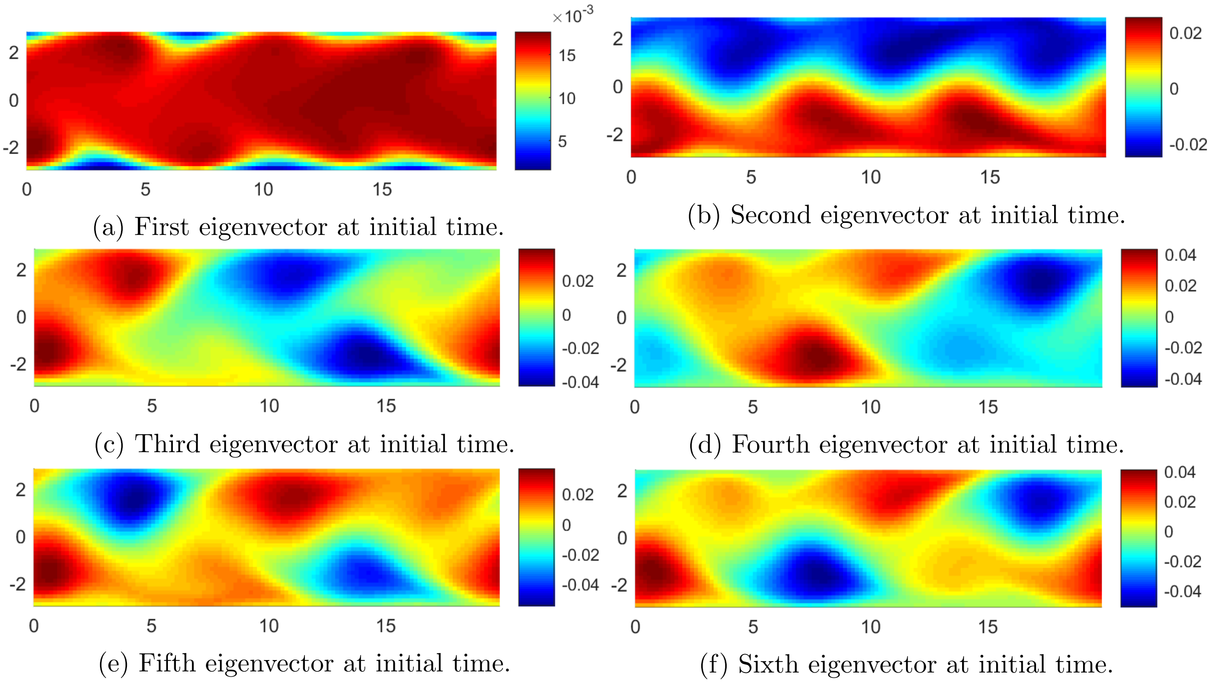

(a) First eigenvector at initial time.

(b) Second eigenvector at initial time.

(c) Third eigenvector at initial time.

(d) Fourth eigenvector at initial time.

(e) Fifth eigenvector at initial time.

(f) Sixth eigenvector at initial time.

Figure 4.3: Approximate leading eigenvectors of $\hat{\boldsymbol{G}}$ computed from the Ulam discretization of the reflected augmented generator with a $108 \times (120 \times 36)$ time-space resolution. Recalling (3.30) we see that these are singular vectors of $\mathcal{P}_{0,T}$. This figure has been published in [FKS20, Fig. 3].

the dynamics, we checked that the non-real eigenvalues of $\hat{\boldsymbol{G}}$ from μ_7 to μ_{50} are all companion eigenvalues equal to

$$\mu - \mu^{(k)} \quad \text{with} \quad \mu^{(k)} = \frac{1-\omega^{-k}}{h}, \quad \omega = \exp\left(2\pi i \frac{h}{\tau}\right), \; \psi_k(t) = \omega^{kt} \tag{4.8}$$

for an eigenvalue μ of $\hat{\boldsymbol{G}}$ and a $k \in \mathbb{Z}$, as derived in (4.5) with the temporal grid spacing $h > 0$. For the eigenpair $(\mu, \boldsymbol{w})$, we expect companion eigenpairs of the form $(\mu - \mu^{(k)}, \boldsymbol{w}\psi_k)$. To verify this we computed the correlation of the companion eigenvectors

$$c_n^m(k) := \frac{\langle \psi_k \boldsymbol{w}_m, \boldsymbol{w}_n \rangle}{\|\psi_k \boldsymbol{w}_m\|_2 \|\boldsymbol{w}_n\|_2} \tag{4.9}$$

as in [FK17, Sec. 7.5]. For instance, noting that $\mu^{(\pm 1)} = 0.01015 \pm 0.34887i$ $(h = 18/108)$ for μ_1 in Table 4.2, the eigenvalues $\mu_7, \mu_8 \approx \mu_1 - \mu^{(\pm 1)}$ present themselves as potential companion eigenvalues for μ_1. The small difference in the numerical values of $\mu_1 - \mu_7$ or $\mu_1 - \mu_8$ and the shift $\mu^{(\pm 1)}$, which is approximately $2.3 \cdot 10^{-3}$ in magnitude, is due to the fact that the first eigenvector is not constant in time. It merely holds that $w_t \approx w_{t-h}$. Nonetheless, the non-real eigenvalues μ_7 and μ_8 are companion eigenvalues to μ_1. This is supported by the correlation for the corresponding eigenvectors

$$c^1_{7,8}(\pm 1) = \frac{\langle \psi_{\pm 1}\boldsymbol{w}_1, \boldsymbol{w}_{7,8}\rangle_{\mathbb{R}^{120\cdot 36\cdot 108}}}{\|\psi_{\pm 1}\boldsymbol{w}_1\|_2 \|\boldsymbol{w}_{7,8}\|_2} = 0.84597 \pm 0.53312i, \qquad \left|c^1_{7,8}(\pm 1)\right| = 0.9999\,.$$

The correlation with other eigenfunctions $n \in \{2,\dots,10\}\backslash\{7,8\}$ satisfies $|c^1_n(\pm 1)| \leq 0.00323$. The arguments around (3.31) imply that every singular value of $\mathcal{P}_{0,T}$ must be real. Our numerical computations strongly suggest that every complex eigenvalue within the first 50 eigenvalues is a companion eigenvalue to a real eigenvalue with smaller magnitude. We do not show the results here, because the correlations using (4.9) yield results similar to those stated in the special case above and offer no additional insight beyond the example $n = 7, 8$ above.

The space-time signatures of six coherent vortices in the Bickley flow are captured in the leading six singular vectors shown in Figure 4.3. Note that only the initial time-slice is displayed. To isolate these six vortices in the space-time manifold, we look for a sparse orthogonal basis approximating a basis of the six-dimensional subspace of $\mathbb{R}^{108\times(120\times 36)}$ spanned by the leading six (space-time) eigenvectors shown in Figure 4.3. To find such a sparse approximating basis, we applied the sparse eigenbasis approximation algorithm [FRS19, Alg. 3.1]. Theorem 3.22 gives in principle a bound for the results obtained by linear combinations.

Sparse Eigenbasis Approximation

The sparse eigenbasis approximation (SEBA) from [FRS19] offers an alternative approach to disentangling features from eigendata in the sense of spectral clustering. It aims to avoid typical pitfalls of clustering and to take more of the original dynamics into account than other approaches such as *k-means*. It performs a rotation R and imposes a sparsity condition (4.10). The rotation is done such that an approximating basis of the space spanned by the input eigenvectors $(f_i)_{i=k_1}^{k_2}$ is constructed.

$$\begin{aligned} (f_i)_{i=k_1}^{k_2} \xrightarrow{SEBA} (\varphi_i)_{i=k_1}^{k_2}\,, \text{ such that } &\operatorname{span}(f_i)_{i=k_1}^{k_2} \approx \operatorname{span}(\varphi_i)_{i=k_1}^{k_2}\,, \\ &R[f_{k_1}, \dots f_{k_2}] \approx [\varphi_{k_1}, \dots, \varphi_{k_2}] \\ \text{and } &\sum_{i=k_1}^{k_2}\sum_{j=1}^{d} |(\varphi_i)_j| \text{ is minimal.} \end{aligned} \tag{4.10}$$

Furthermore, SEBA offers some naturally motivated qualitative and quantitative criteria for the extracted features that are well-suited to the case of coherent families derived from transfer operators and its generators [FRS19, Sec. 2 & 4]. The Bickley Jet has also been investigated in [FRS19, Sec. 5.1] combining the FEM discretization for the dynamic Laplacian from [FJ18] with SEBA. The SEBA algorithm helps to clarify the structures obtained from the eigendata also for the augmented reflected generator approach.

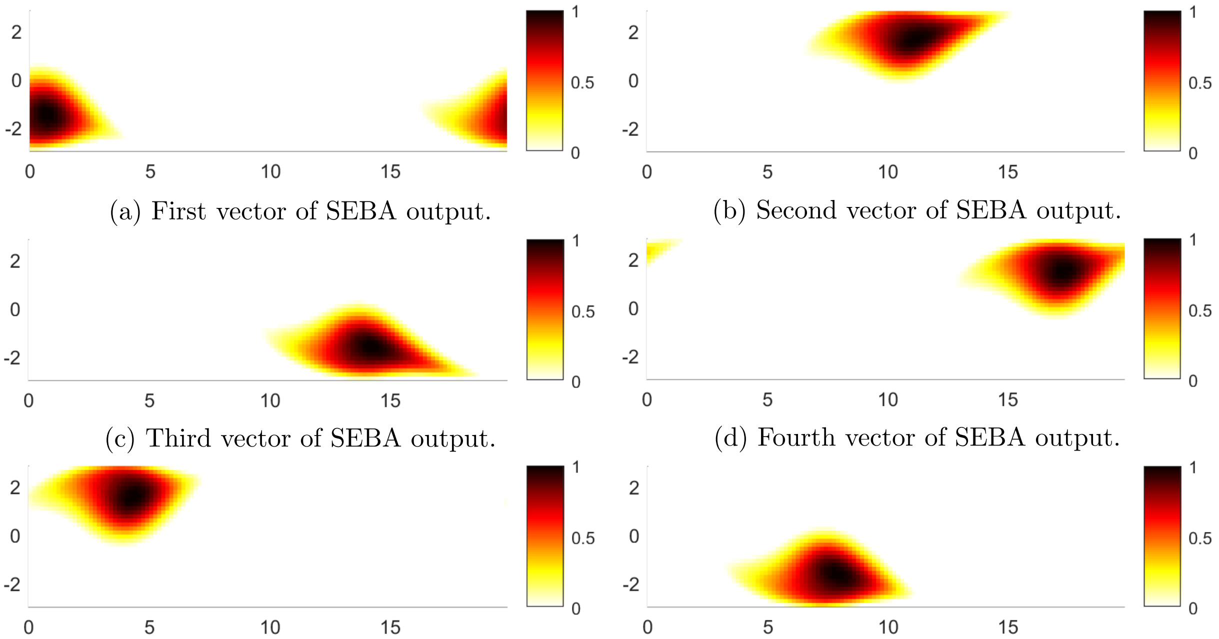

(a) First vector of SEBA output.
(b) Second vector of SEBA output.
(c) Third vector of SEBA output.
(d) Fourth vector of SEBA output.
(e) Fifth vector of SEBA output.
(f) Sixth vector of SEBA output.

Figure 4.4: Initial time-slices of space-time estimates of coherent sets extracted from the leading six eigenvectors using SEBA. This figure has been published in [FKS20, Fig. 4].

Vortex Isolation

The six sparse basis vectors φ_k, $k = 1, \ldots, 6$, shown in Figure 4.4 are obtained by applying the SEBA algorithm to the leading six eigenvectors of $\hat{\boldsymbol{G}}$. Each of these SEBA vectors strongly isolates and encodes a single vortex. Let us emphasize that the full space-time vectors are used for the SEBA algorithm, but Figure 4.4 displays only the initial time-slice. In Figure 4.5 (a) particles have been seeded inside the computed vortical feature of the sixth SEBA vector; see Figure 4.4 (f). In particular, the particles have been seeded in the super-level set $\{\varphi_k(0, \cdot) > 0.4\}$ after φ_k has been scaled to have maximum-norm 1. These particles are evolved forward in time to visualize the coherence of the computed vortical feature. In addition to the deterministic evolution shown in Figure 4.5 (b), we also visualize a stochastic evolution using the noise intensity $\varepsilon = 0.1$ in Figure 4.5 (c). The simulations use a fourth-order Runge–Kutta scheme in the deterministic case and a fourth-order Runge–Kutta–Maruyama scheme in the stochastic case with step size $\frac{9}{4 \cdot 108} = \frac{1}{48}$. Thus, Figure 4.5, (b) and (c), illustrates the coherence of the single vortex in Figure 4.5 (a). Proposition 3.22 does not apply directly to the positive parts of the $\varphi_k(0, \cdot)$, the vortical features extracted by the SEBA algorithm, because the $\varphi_k(0, \cdot)$, for $k = 1, \ldots, 6$, do not exactly span the same subspace as the leading six eigenvectors of $\hat{\boldsymbol{G}}$. Recall that the rotation R encodes linear combinations of the input eigenfunctions $\boldsymbol{f}_i$ that result in the SEBA features $\varphi_k(0, \cdot)$. It turns out that the hypotheses of Proposition 3.22 were satisfied by these linear combinations with a slight modification: wherever the contributions (3.33) were negative, the corresponding α_i in (3.33) were set to zero. Any α_i that was set to zero, was very close to zero. The resulting linear combinations then satisfy the requirements of Proposition 3.22, and thus yield coherent families. We do not show these slightly modified linear combinations, because they are very close to the SEBA features in Figure 4.4.

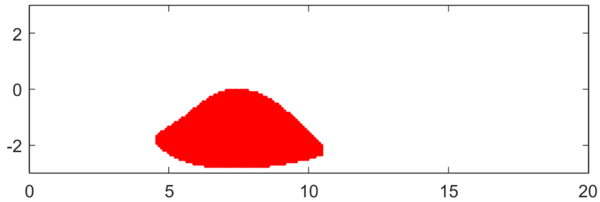

(a) Initial particles seeded in the gyre induced by the sixth SEBA vector.

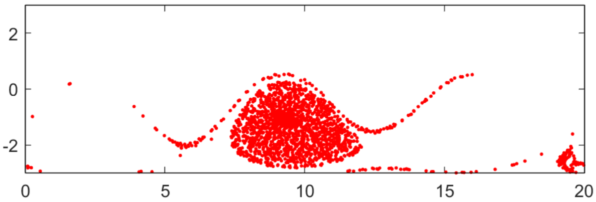

(b) Final time configuration of the seeded particles evolved by the Bickley Jet flow.

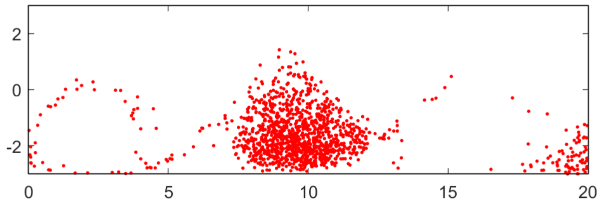

(c) Final time configuration of the particles evolved by the Bickley Jet flow with noise $\varepsilon = 0.1$.

Figure 4.5: Illustration of a coherent set provided by SEBA applied to the leading numerical eigenvectors. This figure has been published in [FKS20, Fig. 5].

Remark 32:
The augmented reflected generator approach can be used for experimental velocity data as well. We applied the augmented reflected generator approach to velocity field data described in [SSP$^+$19]. The results are not shown, because they are qualitatively very similar to the periodically driven double gyre. The Rayleigh-Bénard convection flow in [SSP$^+$19] behaves similar to a periodically driven double gyre with some noisy perturbation of the periodic forcing $f(t, x)$. Therefore, any experimental realization is a non-autonomous aperiodic system. It might be worthwhile to explore this type of stochastic driving more intensively instead of simply analyzing a realization as an aperiodic flow. △

5 Regularity

In Chapter 3, we introduced the augmented reflected generator approach to extract coherent families. We investigated numerical aspects and examples in Chapter 4. Another topic of this thesis is the optimal manipulation of coherent sets discussed in Chapter 6. For the optimization, the regularity of the spectrum of the augmented reflected generator with respect to the velocity field v will be crucial. Therefore, this chapter is concerned with the regularity of the Perron–Frobenius operators $\mathcal{P}_{s,t}$ and the Koopman operators $\mathcal{K}_{s,t}$, introduced in Chapter 2, with respect to the velocity field v. The results of this chapter together with the spectral mapping result Theorem 3.19 are used in Chapter 6 to linearize the dependence of eigenvalues of the augmented reflected generator $\hat{\boldsymbol{G}}$ on the velocity field v. Nevertheless, the continuous Fréchet differentiability proven in Theorem 5.13 may be of interest for other applications and other areas of mathematics as well.

There exists a general theory for the approximation of semigroups and the perturbation of generators by bounded or closed operators originating from [Tro58] and [Kat13], also see [Paz83, Chap. 3]. These powerful results are not applicable in our case, because we consider unbounded perturbations of the non-elliptic operator $\hat{\boldsymbol{G}}$ and the two-parameter evolution family $\mathcal{P}_{s,t}$. Therefore, we prove the continuous Fréchet differentiability by other means, and thereby combine the three areas of mathematics stochastic calculus, semigroup theory, and dynamical systems. In contrast to the other chapters of this thesis that are concerned to some degree with coherent sets, we allow for a space- and time-dependent diffusion coefficient $\sigma(t,x)$ in this chapter, because the differentiability results may be of broader interest in this more general setting.

The results, examples, figures and the general content presented in this chapter have been published in [KLP19] and are re-used and expanded upon here with permission of the authors and the publisher.

Remark 33:

- The smooth dependence of invariant measures has been investigated in specific cases. For instance, Butterley and Liverani show in [BL07] the differentiability of Sinai–Ruelle–Bowen measures corresponding to Anosov flows with respect to one-dimensional parameters. The publication [BL07] gives a report on the work that has been done previously on this field.

- We refer to [Bal14] for a survey on linear response results for deterministic stationary systems. Results for non-deterministic systems arise in the context of random compositions of maps [BRS20], or for stochastic ordinary and partial differential equations in the weak topology [HM10]. The latter reference shows Gateaux type pointwise differentiability of the transfer operators acting on smooth functions with respect to a real parameter, where also the constant-in-space diffusion matrix can vary with the parameter. It belongs to the class of approaches where functional-analytic tools are used to derive quantitative perturbation results for transfer operators and their dominant eigenmodes [KL99, GG19].

$\triangle$

One important aspect of differential equations is the sensitivity of the solution with respect to changes in the data. For the deterministic case, there exist classical results, for example [Hal80], that deal with dependence on the initial data and the right hand side v. Some of these dependencies have been investigated for non-deterministic systems, see for example [FGP10, AJKW17] for Fréchet type dependencies on the initial data and [FLL$^+$99, GM05, Mon13, DG14] for the dependence of path functionals or their expectations with respect to changes in the velocity field v. The paper [KLP19] and this chapter follow the ideas of [FLL$^+$99], which provides a Gateaux type dependence on the data. This is achieved in [FLL$^+$99] by establishing the existence of directional derivatives with respect to the velocity field v. Before we prove Fréchet type dependence of the transfer operators with respect to an additive change of velocity field v, we are concerned with the path functional (5.1). In Theorem 5.5, we establish for a suitable observable g the Fréchet derivative at $u = 0$ of the non-linear functional

$$\varphi_g^x(u) := \mathbb{E}\left[g(X^u) \,\middle|\, X_0^u = x\right] \tag{5.1}$$

with respect to additive perturbations in u. In equation (5.1), X^u denotes the solution of the perturbed stochastic differential equation (5.3) below.

For convenience we recall from Chapter 2: We consider the probability space given by the base set $\Omega := C([0,T];\mathbb{R}^d) := \{f : [0,T] \to \mathbb{R}^d \mid f \text{ continuous}\}$, a σ-algebra $\mathcal{F}$ on Ω, and a probability measure $\mathbb{P}$ on $(\Omega, \mathcal{F})$. We use a d-dimensional Wiener process $W = (W_t, \mathcal{F}_t)_{t\in[0,T]}$ with respect to $\mathbb{P}$ for a filtration $(\mathcal{F}_t)_{t\in[0,T]}$, with $\mathcal{F}_t \subseteq \mathcal{F}$ for every $t \in [0,T]$, where W_t is $\mathcal{F}_t$-measurable for every $t \in [0,T]$. A measurable functional h acting on $[0,T] \times \Omega$ is called adapted to the filtration $(\mathcal{F}_t)_{t\in[0,T]}$ if $h(t,\cdot)$ is $\mathcal{F}_t$-measurable, for every $t \in [0,T]$. The drift $b : [0,T] \times \mathbb{R}^d \to \mathbb{R}^d$ and the diffusion matrix $\sigma : [0,T] \times \mathbb{R}^d \to GL(\mathbb{R}, d)$, the real invertible $d \times d$ matrices, are adapted functions that satisfy Assumption 1 from Section 2.2. Assumption 1 states that σ is uniformly elliptic (A3), that b and σ are uniformly Lipschitz continuous in x (A1), and that b and σ satisfy a growth condition (A2). With these assumptions, Theorem 2.4 shows that the stochastic differential equation (SDE) with initial condition

$$dX_t = b(t, X_t)dt + \sigma(t, X_t)dW_t, \quad X_0 = x \tag{5.2}$$

admits a unique strong solution. We choose b for the velocity field here instead of v to better distinguish it from the perturbation u and the space V introduced below.

For a fixed deterministic initial condition $x \in \mathbb{R}^d$, the probability measure $\mathbb{P}^x$ denotes the conditioning of $\mathbb{P}$ to the subset of paths $\{f : [0,T] \to \mathbb{R}^d \mid f(0) = x\}$ of Ω.

5.1 Stochastic Calculus

First we construct a Banach space V of admissible perturbations $u \in V$. In this context *admissible* means that the perturbed drift $b + u$ satisfies the conditions of Theorem 2.4 such that the perturbed SDE (5.3) has a unique solution and such that we can apply Girsanov's theorem (Thm. 5.2).

Let us start with the following vector spaces of Borel measurable functions

$$\mathcal{C} := \Big\{ f : [0,T] \times \mathbb{R}^d \to \mathbb{R}^n \,\Big|\, \exists\, 0 < L < \infty \text{ such that } |f_i(t,y) - f_i(t,z)| \le L\,|y-z| \\ \text{and } |f_i(t,y)| \le L(1+|y|),\ \forall\,(t,y),(t,z) \in [0,T]\times\mathbb{R}^d,\ 1 \le i \le n \Big\}$$

and

$$\mathcal{D} := \Big\{ f : [0,T] \times \mathbb{R}^d \to \mathbb{R}^{n\times k} \,\Big|\, \exists\, 0 < L < \infty \text{ such that } |f_{ij}(t,y) - f_{ij}(t,z)| \le L\,|y-z| \\ \text{and } |f_{ij}(t,y)| \le L(1+|y|),\ \forall(t,y),(t,z) \in [0,T]\times\mathbb{R}^d,\ 1 \le i \le n\,,\, 1 \le j \le k \Big\}\,.$$

The sets $\mathcal{C}$ and $\mathcal{D}$ contain the vector- and matrix-valued Borel measurable functions whose entries satisfy a uniform Lipschitz condition (A1) and grow at most linearly (A2). In particular, the drift b and diffusion σ introduced earlier belong to $\mathcal{C}$ and $\mathcal{D}$.

If the perturbation u belongs to $\mathcal{C}$, then

$$dX^u_t = [b(t,X^u_t) + u(t,X^u_t)]dt + \sigma(t,X^u_t)dW_t, \quad X^u_0 = x, \tag{5.3}$$

admits a unique strong solution X^u according to Theorem 2.4. We denote the unique strong solution of the unperturbed SDE (5.2) by X^0.

Let $\mathbb{E}^x$ denote the expectation operator with respect to $\mathbb{P}^x$, and let $\mu^{u,x} := \mathbb{P}^x \circ (X^u)^{-1}$ denote the law of the solution to (5.3). We use $\mathbb{E}^{u,x}$ to denote the expectation with respect to $\mu^{u,x}$. Using this notation, it follows that $\mu^{0,x}$ is the law of the solution of the unperturbed SDE (5.2).

A function $f : [0,T]\times\mathbb{R}^d \to \mathbb{R}^d$ is $\mu^{0,x}$-almost surely bounded if there exists some $0 < C < \infty$ such that

$$\mathbb{P}^x\left(\left|f(s,X^0_s)\right| \le C,\ \forall s \in [0,T]\right) = 1 \tag{5.4}$$

holds. Utilizing this notion we define the space

$$L^\infty(\mu^{0,x}) := \{ f : [0,T]\times\mathbb{R}^d \to \mathbb{R}^d \,|\, f \text{ satisfies (5.4) for some } 0 < C < \infty \}$$

and the norm

$$\|f\|_{L^\infty(\mu^{0,x})} := \inf\{ C > 0 \,|\, (5.4) \text{ holds} \}$$

for every $f \in L^\infty(\mu^{0,x})$. In the following, we omit the dependence on the parameter $\mu^{0,x}$ in the notation for the norm and write $\|f\|_{L^\infty}$. The space $(L^\infty(\mu^{0,x}), \|\cdot\|_{L^\infty})$ is a Banach space, specifically, it is the space of essentially bounded measurable functions with respect to the measure $\mu^{0,x}$.

The function space $V := \mathcal{C} \cap L^\infty(\mu^{0,x})$ is equipped with the following norm:

$$\|f\|_V := \inf\Big\{ C > 0 \,\Big|\, |f_i(t,y)| \le C,\ |f_i(t,y) - f_i(t,z)| \le C\,|y-z|\,, \\ \text{for all } 1 \le i \le n,\ \text{for all } (t,y,z) \in [0,T]\times\mathbb{R}^d\times\mathbb{R}^d \Big\}. \tag{5.5}$$

Lemma 5.1 below proves that $(V, \|\cdot\|_V)$ is a Banach space.

Lemma 5.1:
The linear space $V := \mathcal{C} \cap L^\infty(\mu^{0,x})$ is closed and complete with respect to $\|\cdot\|_V$, (5.5). Therefore, $(V, \|\cdot\|_V)$ is a Banach space.

Lemma 5.1 and the parts (1) and (2) of the proof have been published in [KLP19, Lem. A.5]. The parts (3) and (4) have been added here.

Proof. We note that V consists of all Borel measurable functions whose $\|\cdot\|_V$-norm is finite.

(1) First, we show that $\|\cdot\|_V$ is a norm on $V := \mathcal{C} \cap L^\infty(\mu^{0,x})$. The linear growth condition (A2), equation (2.9), is a weaker condition than the boundedness condition (5.4). The Lipschitz continuity together with (5.4) ensures that any $f \in \mathcal{C} \cap L^\infty(\mu^{0,x})$ is bounded everywhere. Thus, the Lipschitz continuity and boundedness conditions imply that $\|f\|_V = 0$ if and only if f is constant and equal to zero. Straightforward computations give that if $f, g \in V$ then $\|f+g\|_V \le \|f\|_V + \|g\|_V$, and also that $\|\alpha f\|_V = |\alpha|\,\|f\|_V$ for all $\alpha \in \mathbb{R}$.

(2) The space V is closed with respect to $\|\cdot\|_V$. Take a sequence $(f_n)_{n\in\mathbb{N}} \subset V$ that converges with respect to $\|\cdot\|_V$ to some function $f : [0,T]\times\mathbb{R}^d \to \mathbb{R}^d$. Since $f_n \in V$ and since $(\|f_n - f\|_V)_{n\in\mathbb{N}}$ by definition converges to zero, we have

$$\|f\|_V \le \|f_n - f\|_V + \|f_n\|_V, \quad \text{for all } n \in \mathbb{N}\,.$$

Both quantities on the right-hand side are finite for any $n \in \mathbb{N}$, so $f \in V$ and hence f is Lipschitz continuous. Since $L^\infty(\mu^{0,x})$ contains discontinuous functions, it follows that V is a normed vector space and a proper subset of $L^\infty(\mu^{0,x})$.

(3) As an intermediate step we prove the completeness of $(\mathcal{C}, \|\cdot\|_{\mathcal{C}})$ using adaptations of the arguments in (2) above. For brevity we neglect the measurable uniform dependence on t. We equip the space

$$\mathcal{C} = \{f : \mathbb{R}^d \to \mathbb{R}^d \,|\, \exists L > 0 : |f(x) - f(y)| \le L|x-y| \text{ and } |f(x)| \le L(1+|x|)\,, \forall\, x, y \in \mathbb{R}^d\}$$

of Lipschitz continuous functions that grow at most linearly with the norm

$$\|f\|_{\mathcal{C}} := \inf\left\{L > 0 \,\middle|\, |f(x) - f(y)| \le L|x-y| \text{ and } |f(x)| \le L(1+|x|)\,, \forall\, x, y \in \mathbb{R}^d\right\}\,.$$

Note that $\|\cdot\|_{\mathcal{C}}$ is equivalent to the Lipschitz-norm

$$\|f\|_{\mathcal{C}} \le \|f\|_{\text{Lip}} := |f(0)| + \sup_{x\neq y} \frac{|f(x) - f(y)|}{|x-y|} \le 2\|f\|_{\mathcal{C}}\,.$$

Consider a Cauchy sequence $(f_n)_{n\in\mathbb{N}} \subset \mathcal{C}$ with respect to $\|\cdot\|_{\mathcal{C}}$. It is well-known that a Cauchy sequence with respect to $\|\cdot\|_{\text{Lip}}$ of Lipschitz continuous functions $(f_n)_n$ converges uniformly to a Lipschitz continuous limit f. It remains to show that f grows at most linearly. The uniform convergence implies that there exists $N_1 \in \mathbb{N}$ such that

$$|f(x)| \le |f(x) - f_n(x)| + |f_n(x)| \le 1 + |f_{N_1}(x)| \le 1 + L_{N_1}(1+|x|)$$

for all $n \ge N_1$. Therefore, f grows at most linearly and the space $(\mathcal{C}, \|\cdot\|_{\mathcal{C}})$ with the norm $\|f\|_{\mathcal{C}}$ is a Banach space.

(4) We use a general abstract argument. The intersection $Z := X \cap Y$ of the two Banach spaces $(X, \|\cdot\|_X)$ and $(Y, \|\cdot\|_Y)$, which can be embedded in a common locally convex space E, is a Banach space with the canonical norm $\|\cdot\|_Z := \max\{\|\cdot\|_X, \|\cdot\|_Y\}$; [Zei90a, Prob. 23.14] or [GGZ74, Bem. 5.12]. We can embed $\mathcal{C}$ and $L^\infty(\mu^{0,x})$ into a common locally convex space E, for example a suitable space of distributions [Hör15] or $L^1_{\mathrm{loc}}(\mu^{0,x})$. Therefore, the vector space $V := L^\infty(\mu^{0,x}) \cap \mathcal{C}$ with the equivalent norms

$$\|f\|_V = \max\{\|f\|_{L^\infty}, \|f\|_{\mathcal{C}}\} \text{ and } \|f\|_{V2} := \|f\|_{L^\infty} + \|f\|_{\mathcal{C}} \text{ with } \|f\|_V \leq \|f\|_{V2} \leq 2\|f\|_V\,,$$

is a Banach space.

□

Before we proceed with other results, we formulate an assumption that expands Assumption 1.

Assumption 4:
Consider the velocity field b and the diffusion σ according to Assumption 1 and $u \in V$.

(A4) It holds that

$$\mathbb{P}^x \left(\int_0^T \left(\left|\sigma_s^{-1}(b_s + u_s)\right|^2 + \left|\sigma_s^{-1} b_s\right|^2 \right) \left(X_s^0\right) ds < \infty \right) = 1\,. \tag{5.6}$$

The condition (A4) can be derived from the assumptions (A1), (A2), and (A3), even under the more general condition of locally Lipschitz drift and diffusion matrix. However, in [KLP19, Lem. A.4] a proof is given for globally Lipschitz drift b, change of drift u, and diffusion σ for the sake of simplicity.

From now on, we only consider perturbations $u \in V$.

Auxiliary Results

For an arbitrary but fixed starting position $x \in \mathbb{R}^d$ and a suitable observable g, we define the non-linear functional $\varphi_g^x : V \to \mathbb{R}$ by

$$\varphi_g^x(u) := \mathbb{E}^x\left[g(X^u)\right] = \mathbb{E}\left[g(X^u) | X_0^u = x\right]\,. \tag{5.7}$$

The set of suitable observables g is specified below in Theorem 5.5 (C2). Furthermore, Theorem 5.5 establishes that φ_g^x is a Fréchet differentiable map from $(V, \|\cdot\|_V)$ to $(\mathbb{R}, |\cdot|)$. Note that g considers the whole path X^u.

Theorem 5.2 below allows us to rephrase probabilistic objects involving the process X^u in terms of the law of the unperturbed process X^0. Theorem 5.2 is adapted from [LS01, Sec. 7.6.4] and is crucial for the steps leading to the differentiability of (5.7) with respect to u. In the adaptation of Girsanov's theorem from [KLP19, Thm. 2.4] stated below, the Wiener process W is allowed to be of different dimension than the two diffusion processes ξ and η. An introduction to Girsanov's theorem and related concepts is given in [LS01].

Theorem 5.2:
Let $\mathbb{X} \subset \mathbb{R}^d$, and let $\xi = (\xi_t, \mathcal{F}_t)_{t\in[0,T]}$ and $\eta = (\eta_t, \mathcal{F}_t)_{t\in[0,T]}$ be $\mathbb{X}$-valued processes that satisfy

$$d\xi_t = \tilde{b}_t(\xi)dt + \sigma_t(\xi)dW_t, \quad \xi_0 = \eta_0, \tag{5.8}$$

$$d\eta_t = b_t(\eta)dt + \sigma_t(\eta)dW_t, \tag{5.9}$$

where $W = (W_t, \mathcal{F}_t)_{t\in[0,T]}$ is a k-dimensional Wiener process, η_0 is a $\mathcal{F}_0$-measurable random variable with $\mathbb{P}(\sum_{i=1}^d |(\eta_0)_i| < \infty) = 1$, b and $\tilde{b}$ are measurable functions from $[0,T]\times\mathbb{X}$ to $\mathbb{R}^d$, and σ is a measurable function from $[0,T]\times\mathbb{X}$ to $\mathbb{R}^{d\times k}$, such that the following assumptions are fulfilled:

(B1) The system of algebraic equations

$$\sigma_t(y)\alpha_t(y) = \tilde{b}_t(y) - b_t(y)$$

has a solution α_t for all $(t,y)\in[0,T]\times\mathbb{X}$.

(B2) The components of the functions $(b_t(\cdot))_{t\in[0,T]}$, $(\tilde{b}_t(\cdot))_{t\in[0,T]}$, and $(\sigma_t(\cdot))_{t\in[0,T]}$ are adapted to the filtration $(\mathcal{F}_t)_{t\in[0,T]}$ and satisfy (A1) and (A2), so that both (5.8) *and* (5.9) *have unique strong solutions ξ and η respectively.*

(B3) It holds that

$$\mathbb{P}\left(\int_0^T \left(\tilde{b}_t^\top(\sigma_t\sigma_t^\top)^\#\tilde{b}_t + b_t^\top(\sigma_t\sigma_t^\top)^\# b_t\right)(\xi)dt < \infty\right) = 1,$$

where $(\sigma_t\sigma_t^\top)^\#$ denotes the pseudoinverse of the $d\times d$ matrix $\sigma_t\sigma_t^\top$.

Then, the law μ_ξ of ξ is absolutely continuous with respect to the law μ_η of η, and

$$\left.\frac{d\mu_\xi}{d\mu_\eta}\right|_{\mathcal{F}_t}(\eta) = \exp\left(\int_0^t (\tilde{b}_s - b_s)^\top(\sigma_s\sigma_s^\top)^\#(\eta)d\eta_s - \frac{1}{2}\int_0^t (\tilde{b}_s - b_s)^\top(\sigma_s\sigma_s^\top)^\#(\tilde{b}_s - b_s)(\eta)ds\right). \tag{5.10}$$

Proof. A proof of Girsanov's theorem can be found in [LS01, Sec. 7.6.4]. □

Remark 34:

- Similar to the steps in [KLP19, Lem. A.4], the condition (B3) can be derived from (B2) and (A3). Furthermore, with $b_t(X) = b(t, X_t)$ follows that $(b_t)_{t\in[0,T]}$ is adapted to $(\mathcal{F}_t)_{t\in[0,T]}$. Thus Assumption 1 implies (B2). The same arguments hold for the perturbed drift $\tilde{b}_t := b_t + u_t$ and the noise σ. Finally, (B1) is satisfied as well, because we assume $\sigma(t,x)$ to be invertible for all (t,x); see Assumption 1 (A3).

- The conditions (B1) and (B2) are symmetrical in b and $\bar{b}$. The condition (B3) is not. The other direction of (B3) is

$$\mathbb{P}\left(\int_0^T \left(\tilde{b}_t^\top(\sigma_t\sigma_t^\top)^\#\tilde{b}_t + b_t^\top(\sigma_t\sigma_t^\top)^\# b_t\right)(\eta)dt < \infty\right) = 1\,. \tag{5.11}$$

  Replacing condition (B3) in Theorem 5.2 with (5.11) leads to the result that μ_η is absolutely continuous with respect to μ_ξ and gives a formula for $\frac{d\mu_\eta}{d\mu_\xi}|_{\mathcal{F}_t}(\xi)$.

△

In [KLP19] the authors prove the Fréchet differentiability of φ_g^x on the infinite-dimensional space of velocity fields driving the stochastic differential equations and the Fréchet differentiability of the associated transfer operators in the strong norm topology, and consequently obtain Fréchet differentiability of all simple and isolated eigenvalues.

A question that the paper [KLP19] does not investigate in detail is the dependence of the transfer operators with respect to the diffusion matrix. The strategy in [KLP19] relies on Girsanov's formula (Thm. 5.2) to obtain an expression for the Radon–Nikodym derivative between two path measures. This expression leads to sufficient estimates for computing the Fréchet derivative. Girsanov's formula is a fundamental result in the field of stochastic differential equations and applies in the case where the drift term is changed. To the best of our knowledge, no analogous formula for changes of the diffusion term exists. This is, because the set of possible changes that one can apply to the diffusion matrix while still obtaining a mutually absolutely continuous path measure is severely constrained; see Example 1 below.

Example 1: Dependence on the Noise
Consider the simple case of a constant zero drift term $b = 0$ and the constant diffusion matrix

$$dX_t = 1 \cdot I_{d\times d} dW_t \, .$$

In this case, the path measure is the Wiener measure on path space, which is a Gaussian measure. If one scales the identity diffusion matrix by a constant whose absolute value is not 1, then the resulting path measure is not mutually absolutely continuous with respect to Wiener measure; see for example [Bog98, Ex. 2.7.4]. More specifically, the path measure for $(Y_t^\varepsilon)_{t\in[0,T]}$ given by

$$dY_t^\varepsilon = (1+\varepsilon) \cdot I_{d\times d} dW_t$$

with $\varepsilon > 0$ has to be mutually singular to the path measure for $(X_t)_{t\in[0,T]}$. Two non-negative measures μ_1, μ_2 on a measurable space $(\Omega, \mathcal{F})$ are called mutually singular if there is a set $A \in \mathcal{F}$ such that $\mu_1(A) = \mu_2(\Omega\backslash A) = 0$ [Sul15, Def. 2.23]. This singularity result is known as the Feldman–Hájek theorem; see for example [Bog98, Thm. 2.7.2] or [Sul15, Thm. 2.51]. Thus, there cannot exist a Radon–Nikodym derivative, and the approach we follow for changes of the drift cannot be applied for such changes of the diffusion. Furthermore, the mutual singularity implies that there are observables g such that the respective path functional does not change continuously. $\diamondsuit$

We can re-write (5.10) from Girsanov's formula with $\tilde{b} = b + u$ using the continuous semimartingale

$$M_t^u\left(X^0\right) := \int_0^t u^\top (\sigma\sigma^\top)^{-1}(s, X_s^0) dX_s^0, \tag{5.12}$$

and the associated quadratic variation process

$$\langle M^u \rangle_t \left(X^0\right) := \int_0^t \left|\sigma^{-1} u(s, X_s^0)\right|^2 ds \tag{5.13}$$

to arrive at (5.14) in Lemma 5.3 below.

Before we tackle our main result, we state two rather technical results [KLP19, Lem. 2.6 & 2.8]. The interested reader may find the proofs in [KLP19, App. A.2].

Lemma 5.3:
The exponential martingale $(Z_t^u(X^0))_{t\in[0,T]}$ *defined by*

$$Z_t^u\left(X^0\right) := \left.\frac{d\mu^{u,x}}{d\mu^{0,x}}\right|_{\mathcal{F}_t}\left(X^0\right) = \exp\left(M_t^u(X^0) - \frac{1}{2}\langle M^u\rangle_t(X^0)\right)$$
$$= \exp\left(\int_0^t u^\top(\sigma\sigma^\top)^{-1}(s,X_s^0)dX_s^0 - \frac{1}{2}\int_0^t \left|\sigma^{-1}u(s,X_s^0)\right|^2 ds\right) \tag{5.14}$$

is square integrable with respect to $\mathbb{P}^x$.

Proof. Lemma 5.3 and its proof have been published in [KLP19, App. A.2]. □

We choose (5.2) to correspond to (5.9) and (5.3) to correspond to (5.8), this gives that u, $\mu^{0,x}$, and $\mu^{u,x}$ in (5.14) correspond to $\tilde{b}-b$, μ_η, and μ_ξ in (5.10), respectively.

The following result provides a sufficient bound for the series expansion of Z_t^u from above in order to pass to the limit $u \to 0$ for the differentiability result Theorem 5.5.

Lemma 5.4:
Under Assumption 1 and 4 with the definitions (5.12) *and* (5.13)*, the following estimate holds:*

$$\mathbb{E}^{0,x}\left[\left(\sum_{n=2}^\infty \frac{1}{n!}\left(|M_t^u| + \frac{1}{2}\langle M^u\rangle_t\right)^n\right)^2\right] \le 2C\Big(\exp\left(\lambda_\sigma\sqrt{t}\|u\|_{L^\infty}\right) - 1 - 2\lambda_\sigma\sqrt{t}\|u\|_{L^\infty}\Big)^2$$

for $0 \le t \le T$. *Recall that* λ_σ^{-1} *is the ellipticity constant from (A3)* (2.10).

Proof. Lemma 5.4 and its proof have been published in [KLP19, App. A.2]. □

5.2 Fréchet Differentiability of the Path Functional

To prove the Fréchet differentiability of the non-linear functional φ_g^x with respect to u, we propose a linear operator (5.15) and show the required convergence which establishes the proposed operator as the unique Fréchet derivative. To achieve this, we first shift all the u-dependence to a new stochastic process Z^u using Theorem 5.2, then we employ Lemma 5.3, and finally we use the bound derived in Lemma 5.4 to pass to the limit. Theorem 5.5 and its proof have been published in [KLP19, Thm. 3.1] and are presented here with the permission of the authors and the publisher.

Theorem 5.5:
Let $x \in \mathbb{R}^d$. *Suppose that Assumption 1, (A1), (A2), and (A3), from Section 2.2 and therefore Assumption 4, (A4), hold true. Furthermore, we assume that the following assumptions hold true:*

(C1) $b : [0,T]\times\mathbb{R}^d \to \mathbb{R}^d$ *and* $\sigma : [0,T]\times\mathbb{R}^d \to GL(\mathbb{R},d)$ *are elements of* $\mathcal{C}$ *and* $\mathcal{D}$*, respectively.*

(C2) $g : \Omega \to \mathbb{R}$ *satisfies* $g \in L^2(\mu^{0,x}) \cap L^1(\mu^{u,x})$*, for all* $u \in V$.

Then the Fréchet derivative of $\varphi_g^x : V \to \mathbb{R}$ *at* 0 *applied to direction* u *exists, and is given by*

$$D_\beta\varphi_g^x\big|_{\beta=0}(u) := \mathbb{E}^x\left[g(X^0)\int_0^T u^\top(\sigma\sigma^\top)^{-1}(s,X_s^0)dX_s^0\right] = \mathbb{E}^{0,x}\left[gM_T^u\right]. \tag{5.15}$$

Before giving the proof, let us make two remarks. Firstly, we examine which observables g satisfy condition (C2) above, and secondly, we introduce a special type of observable that is important for the applications in Section 5.3 and Chapter 6.

Remark 35:

(a) From the definition of V in (5.5) follows that every $u \in V$ is continuous and almost surely bounded on $[0,T] \times \mathbb{R}^d$. Therefore, u is bounded everywhere. By reversing the roles of $\tilde{b}$ and b in Theorem 5.2, we obtain that $\mu^{0,x}$ and $\mu^{u,x}$ are mutually locally equivalent; see Remark 34. Thus, any $g \in L^\infty(\mu^{0,x})$ satisfies (C2), because $\mu^{0,x}$ and $\mu^{u,x}$ are probability measures, in particular they are finite.

(b) For the differentiability of the transfer operators in Section 5.3 and the optimization in Chapter 6, we use special observables of the kind $g = \tilde{g} \circ \pi_t$. Here $\tilde{g} : \mathbb{R}^d \to \mathbb{R}$ holds, and $\pi_t : \Omega \to \mathbb{R}^d$ is the coordinate projection for some $t \in [0,T]$ given by $\pi_t(X) = X_t$. We use these *snapshot* observables, because we are interested in specific time horizons and not the whole path. This leads to

$$\|g\|^2_{L^2(\mu^{0,x})} = \int_\Omega \tilde{g}\left(\pi_t\left(X\right)\right)^2 \, d\mu^{0,x} = \int_{\mathbb{R}^d} \tilde{g}(y) \, d\left(\pi_t^{\#}\mu^{0,x}\right)(y)\,, \tag{5.16}$$

where $\pi_t^{\#}$ denotes the push-forward by π_t, more precisely $\pi_t^{\#}\mu^{0,x} = \mu^{0,x} \circ \pi_t^{-1}$. The push-forward of the path-measure $\mu^{0,x}$ is the distribution of the process X^0 at time t. With the transition kernel $k_{0,t}$ introduced in Section 2.3 and recalled in (5.26) below, we have $\pi_t^{\#}\mu^{0,x}(dy) = k_{0,t}(x,y,0)dy$. Following part (i) of this remark, the function g satisfies the condition (C2) for any $\tilde{g} \in L^\infty(\mathbb{R}^d, \Lambda)$, with Λ being the Lebesgue measure.

△

Proof of Theorem 5.5. Applying Theorem 5.2 yields the formula (5.14) for the Radon–Nikodym derivative of $\mu^{u,x}$ with respect to $\mu^{0,x}$. The definition (5.7) of the map φ_g^x implies

$$\varphi_g^x(u) - \varphi_g^x(0) = \mathbb{E}^x\left[g\left(X^0\right)\left(Z_T^u\left(X^0\right) - 1\right)\right] = \mathbb{E}^{0,x}\left[(Z_T^u - 1)g\right]\,. \tag{5.17}$$

In the last equality, we used the notation $\mathbb{E}^{0,x}$ to denote the expectation of functionals of X^0, or equivalently the expectation with respect to $\mu^{0,x}$. Lemma 5.3 implies the square integrability of Z_t^u with respect to $\mu^{0,x}$.

Next we prove that $\mathbb{E}^{0,x}\left[\,|Z_T^u - 1 - M_T^u|^2\,\right]$ converges to zero for $\|u\|_{L^\infty} \to 0$. Using the definition of Z_T^u, the series expansion of the exponential, the triangle inequality, and the estimate $(a+b)^2 \leq 2(a^2+b^2)$, we get

$$|Z_T^u - 1 - M_T^u|^2 \leq \left(\frac{1}{2}\langle M^u\rangle_T^2 + 2\left[\sum_{n=2}^{\infty}\frac{1}{n!}\left(M_T^u - \frac{1}{2}\langle M^u\rangle_T\right)^n\right]^2\right) \tag{5.18}$$

uniformly in $\omega \in \Omega$.

Lemma 5.4 implies the following estimate

$$\mathbb{E}^{0,x}\left[\left(\sum_{n=2}^{\infty}\frac{1}{n!}\left(|M_T^u|+\frac{1}{2}\langle M^u\rangle_T\right)^n\right)^2\right]\leq 2C(\exp(\lambda_\sigma\sqrt{T}\|u\|_{L^\infty})-1-2\lambda_\sigma\sqrt{T}\|u\|_{L^\infty})^2$$

$$=2C\sum_{\ell=4}^{\infty}\sum_{\substack{j,k\geq 2\\ j+k=\ell}}\frac{1}{k!j!}(2\lambda_\sigma\sqrt{T})^l\|u\|_{L^\infty}^l\,. \tag{5.19}$$

By the definition of $\langle M^u\rangle_t(X^0)$ and the ellipticity (2.10) of σ (A3) follows the bound

$$\big(\langle M^u\rangle_t(X^0)\big)^r\leq\left(\lambda_\sigma^2\,\|u\|_{L^\infty}^2\,t\right)^r\leq\left(\lambda_\sigma\sqrt{t}\,\|u\|_{L^\infty}\right)^{2r}\quad\text{for all } r\geq 1\,. \tag{5.20}$$

With this bound we obtain

$$\frac{\mathbb{E}^{0,x}\left[|Z_T^u-1-M_T^u|^2\right]}{\|u\|_{L^\infty}^2}\leq\frac{1}{2}(\lambda_\sigma\sqrt{T})^4\|u\|_{L^\infty}^2+2C\sum_{\ell=4}^{\infty}\sum_{\substack{j,k\geq 2\\ j+k=\ell}}\frac{1}{j!k!}\left(2\lambda_\sigma\sqrt{T}\right)^\ell\|u\|_{L^\infty}^{\ell-2}, \tag{5.21}$$

where the right-hand side behaves like $\mathcal{O}(\|u\|_{L^\infty}^2)$, and hence decreases to zero as $\|u\|_{L^\infty}$ decreases to zero. Note that the parameter $\lambda_\sigma\sqrt{T}$ determines the convergence rate. Subtracting (5.15) from (5.17) gives

$$\varphi_g^x(u)-\varphi_g^x(0)-\mathbb{E}^{0,x}\left[gM_T^u\right]=\mathbb{E}^{0,x}\left[(Z_T^u-1-M_T^u)\,g\right]\,. \tag{5.22}$$

Applying the Cauchy–Schwarz inequality to (5.22) gives

$$\frac{\left|\varphi_g^x(u)-\varphi_g^x(0)-\mathbb{E}^{0,x}\left[gM_T^u\right]\right|}{\|u\|_{L^\infty}}\leq\mathbb{E}^{0,x}\left[|g|^2\right]^{1/2}\left(\frac{\mathbb{E}^{0,x}\left[|Z_T^u-1-M_T^u|^2\right]}{\|u\|_{L^\infty}^2}\right)^{1/2}. \tag{5.23}$$

Finally, the bound (5.21) implies

$$\lim_{\|u\|_{L^\infty}\to 0}\frac{\mathbb{E}^{0,x}\left[|Z_T^u-1-M_T^u|^2\right]}{\|u\|_{L^\infty}^2}=0, \tag{5.24}$$

which shows that the Fréchet derivative of φ_g^x at zero applied to u exists and is given by $\mathbb{E}^{0,x}[gM_T^u]$.

The definition (5.5) of $\|\cdot\|_V$ implies $\|u\|_{L^\infty}\leq\|u\|_V$ for $u\in V$. Thus, the estimate (5.19) gives

$$\lim_{\|u\|_V\to 0}\frac{\mathbb{E}^{0,x}\left[|Z_T^u-1-M_T^u|^2\right]}{\|u\|_V^2}=0\,,$$

as desired. □

Remark 36: Differentiability everywhere

By a simple change of notation we could call the above "differentiation in $\beta=b$" instead of "differentiation in $\beta=0$" and denote X^0 by X^b instead. We chose 0 here for simplicity and for the interpretation of being unperturbed having our application in Chapter 6 in mind.

The different notation would lead to the following representation of the Fréchet derivative

$$D_\beta \varphi_g^x\big|_{\beta=b}(u) := \mathbb{E}^x\left[g(X^b)\int_0^T u^\top(\sigma\sigma^\top)^{-1}(s,X_s^b)dX_s^b\right] = \mathbb{E}^{b,x}\left[gM_T^u\right]. \tag{5.25}$$

$\triangle$

The following proposition shows that we have continuous Fréchet differentiability everywhere.

Proposition 5.6:
Suppose the assumptions of Theorem 5.5 hold for X^0 replaced by X^b, then gM_T^u belongs to $L^2(\mu^{b,x})$ and the map $b \mapsto D_\beta\varphi_g^x|_{\beta=b}(\cdot)$ is continuous in b.

The publication [KLP19, Prop. 3.4] gives a sketch for this proof that is expanded here.

Proof. Under the stated hypotheses, we use the same strategy as for the proof of Theorem 5.5 to show continuous Fréchet differentiability everywhere. Consider h such that $b+h$ satisfies the assumptions of Theorem 5.5. As for equation (5.17), we replace the dependence on the process X^{b+h} with a new process Z^h. The assumptions (C1) and (C2) from Theorem 5.5 imply that gM_T^u belongs to $L^2(\mu^{b,x})$. Formally, equation (5.17) can be summarized as

$$\mathbb{E}^{u,x}[g] - \mathbb{E}^{0,x}[g] = \mathbb{E}^{0,x}[(Z_T^u - 1)g].$$

With (5.25) and the arguments for (5.17), especially Girsanov's theorem and the Radon–Nikodym derivative therein, we compute

$$\begin{aligned}
&D_\beta\varphi_g^x\big|_{\beta=b+h}(u) - D_\beta\varphi_g^x\big|_{\beta=b}(u) = \mathbb{E}^{b+h,x}[gM_T^u] - \mathbb{E}^{b,x}[gM_T^u] \\
&= \mathbb{E}^x\left[g(X^{b+h})\int_0^T u^\top(\sigma\sigma^\top)^{-1}(s,X_s^{b+h})\,dX_s^{b+h}\right] - \mathbb{E}^x\left[g(X^b)\int_0^T u^\top(\sigma\sigma^\top)^{-1}(s,X_s^b)\,dX_s^b\right] \\
&= \mathbb{E}^x\left[g(X^b)\int_0^T u^\top(\sigma\sigma^\top)^{-1}(s,X_s^b)dX_s^b\left(\frac{d\mu^{b+h,x}}{d\mu^{b,x}} - 1\right)(X^b)\right] \\
&= \mathbb{E}^x\left[g(X^b)\int_0^T u^\top(\sigma\sigma^\top)^{-1}(s,X_s^b)dX_s^b\left(Z_T^h(X^b) - 1\right)\right] = \mathbb{E}^{b,x}\left[(Z_T^h - 1)gM_T^u\right].
\end{aligned}$$

Analogously to the proof of Theorem 5.5 using Lemma 5.4 we get the bound

$$\begin{aligned}
\mathbb{E}^{b,x}\left[|Z_T^h - 1|^2\right] &\le \mathbb{E}^{b,x}\left[\left(\sum_{n=1}^\infty \frac{1}{n!}\left(M_T^h - \frac{1}{2}\langle M^h\rangle_T\right)^n\right)^2\right] \\
&\le C(\exp(\lambda_\sigma\sqrt{T}\|h\|_{L^\infty}) - 1)^2 \\
&= C\sum_{\ell=2}^\infty \sum_{\substack{j,k\ge 1\\ j+k=\ell}} \frac{1}{j!k!}(2\lambda_\sigma\sqrt{T})^\ell \|h\|_{L^\infty}^\ell .
\end{aligned}$$

This bound implies $\mathbb{E}^{b,x}\left[|Z_T^h(X^b) - 1|^2\right] \to 0$ for $\|h\|_V \to 0$. Using Cauchy–Schwarz we get

$$\mathbb{E}^{b,x}\left[(Z_T^h - 1)gM_T^u\right] \le \mathbb{E}^{b,x}\left[|Z_T^h - 1|^2\right]^{\frac{1}{2}}\mathbb{E}^{b,x}\left[|gM_T^u|^2\right]^{\frac{1}{2}}$$

For fixed g, the term $\mathbb{E}^{b,x}\left[|gM_T^u|^2\right]^{\frac{1}{2}}$ can be bounded by a constant for all u with $\|u\|_{L^\infty} \le 1$. This uniformity gives the claim. $\square$

Remark 37: Time-t-observables
For a fixed but arbitrary $t \in [0,T]$, we investigate the structure of the derivative (5.15) for the *snapshot* observables $\tilde{g} \circ \pi_t$ introduced in Remark 35 (b). The $\mathcal{F}_t$-measurability of π_t implies that $g = \tilde{g} \circ \pi_t$ is also $\mathcal{F}_t$-measurable. Analogously to the proof of Theorem 5.5 we derive

$$\begin{aligned}
\varphi_g^x(u) = \mathbb{E}^x\left[g\left(X^u\right)\right] = \int_\Omega g\, d\mu^{u,x} \quad &= \quad \int_\Omega g\, d\mu^{u,x}\big|_{\mathcal{F}_t} \\
&\overset{(5.10),(5.14)}{=} \quad \int_\Omega g Z_t^u\, d\mu^{0,x}\big|_{\mathcal{F}_t} \\
&= \quad \int_\Omega g Z_t^u\, d\mu^{0,x} \\
&= \quad \mathbb{E}^x\left[g\left(X^0\right) Z_t^u\left(X^0\right)\right] = \mathbb{E}^x\left[\tilde{g}\left(X_t^0\right) Z_t^u\left(X^0\right)\right] .
\end{aligned}$$

In the third equality and in the fifth equality we used that $\int g\, d\mu = \int g\, d\mu|_{\mathcal{F}_t}$ for any $\mathcal{F}_t$-measurable function g. This explicit time-dependence introduced by the projection gives the following formula for the derivative

$$D_\beta \varphi_g^x\big|_{\beta=0}(u) = \mathbb{E}^x\left[\tilde{g}\left(X_t^0\right) \int_0^t u^\top (\sigma\sigma^\top)^{-1}(s, X_s^0) dX_s^0\right] = \mathbb{E}^{0,x}\left[(\tilde{g} \circ \pi_t) M_t^u\right].$$

The difference in the equation above with respect to (5.15) is that the observable $\tilde{g}$ does not depend on the entire path X^0 but only on its value at time t, and the Itô integral goes up to t instead of up to T. △

The results of Section 5.1 and Section 5.2 extend to the case where the SDE (5.2) is equipped with normal reflecting boundary conditions for a sufficiently smooth and bounded domain $\mathbb{X}$. The reflecting boundary conditions are encoded by the local time process associated to the boundary. We refer the interested reader to [RY99, Chapter IX, §2, Exercise 2.14] for a one-dimensional example and to [Pil14, Thm. 2.4.1] for the general case. Girsanov's formula describes the Radon–Nikodym derivative of two mutually equivalent probability measures. The preceding analysis transfers to the case of diffusion with reflection, because the boundary conditions are invariant under changes between mutually equivalent probability measures.

For an interesting extension of this approach to the Fréchet differentiability of path functionals we refer to [Lie21].

5.3 Fréchet Differentiability of Transfer Operators

In this section, we use the differentiability of the map $u \mapsto \varphi_g^x(u)$ to prove continuous Fréchet differentiability of the Perron–Frobenius operator $\mathcal{P}_{0,t}$ and the Koopman operator $\mathcal{K}_{0,t}$ with respect to perturbations in the velocity field v. In the following, we take the perspective of v being the unperturbed velocity and $v+u$ being a perturbed velocity field and investigate the behavior with respect to the perturbation u. Therefore $\mathcal{P}_{0,t}(u)$ denotes the solution operator according to Theorem 2.6 corresponding to $v+u$.

On a compact set $\mathbb{X} \subset \mathbb{R}^d$ with piecewise C^4 boundary, we consider the processes X^0 and X^u on $\mathbb{X}$, governed by (5.2) and (5.3) with reflecting boundary conditions [Pil14]. In addition to Assumptions 1 and 4, we assume $\sigma \in C^{(\alpha,2+\alpha)}([0,T]\times\overline{\mathbb{X}}; \mathbb{R}^{d\times d})$ and $v, u \in C^{(\alpha,1+\alpha)}([0,T]\times\overline{\mathbb{X}}; \mathbb{R}^d)$ for some $\alpha > 0$, such that we can use the results from [Fri75, Fri08, Tan97] and from Section 2.3.

The choice $u \in C^{(\alpha,1+\alpha)}([0,T]\times\overline{\mathbb{X}};\mathbb{R}^d)$ implies $u \in V$. With $\|u\|_V \le \|u\|_{C^{(\alpha,1+\alpha)}}$ follows that the space $C^{(\alpha,1+\alpha)}([0,T]\times\overline{\mathbb{X}};\mathbb{R}^d)$ can be continuously embedded in V, $C^{(\alpha,1+\alpha)} \hookrightarrow V$. Furthermore, with Lemma 5.1 and the arguments at the end of the proof of Theorem 5.5 around (5.24) follows that $u \mapsto \varphi_g^x(u)$ is continuously Fréchet differentiable from $C^{(\alpha,1+\alpha)}([0,T]\times\overline{\mathbb{X}};\mathbb{R}^d)$ to $\mathbb{R}$. Intuitively, we require u to be in a smaller Banach subspace of V with a smaller and compatible topology, $C^{(\alpha,1+\alpha)}([0,T]\times\overline{\mathbb{X}};\mathbb{R}^d) \hookrightarrow V$. Therefore, we have to consider fewer sequences for the limit process for differentiability. In [KLP19], the authors choose slightly stronger assumptions for convenience.

Following Remark 35 and fixing the initial time to be 0, the process X^u at time t, X_t^u, corresponding to $v+u$, has the distribution $\mu_t^{u,x} := \pi_t^{\#}\mu^{u,x}$, with $\pi_t^{\#}$ being the push-forward operator associated with the coordinate projection map π_t. With the assumption above, the distribution is absolutely continuous with respect to the Lebesgue measure Λ on $\mathbb{X}$. The respective density $k_{0,t}$ is given by

$$\begin{aligned} \pi_t^{\#}\mu^{u,x}(dy) &=: \mu_t^{u,x}(dy) =: \; k_{0,t}(x,y,u)\,dy, \\ k_0 &: (t,x,y,u) \mapsto k_{0,t}(x,y,u)\;,\; [0,T]\times\mathbb{X}\times\mathbb{X}\times V \to \mathbb{R}\,. \end{aligned} \tag{5.26}$$

This follows from adapting the arguments of Theorem 2.7 to account for the dependence on u and from Lemma 5.7. We refer to [KLP19, App. B] for more details. The absolute continuity of the transition kernel k, Section 2.3, is proven in the next result from [KLP19, App. B.1].

Lemma 5.7:
For any sufficiently small $\varepsilon > 0$ there exists a constant $\overline{K} < \infty$ such that for every u that satisfies $\|u\|_V \le \varepsilon$, and for every $x, y \in \mathbb{X}$,

$$k_{0,t}(x,y,u) \le \overline{K}\,. \tag{5.27}$$

In particular, $k_{0,t}(\cdot,\cdot,u) \in L^2(\Lambda\otimes\Lambda)$ holds, and $f \in L^2(\Lambda)$ implies $f \in L^2(\mu_t^{u,x})$.

Proof. Lemma 5.7 has been proven in [KLP19, App. B.1]. □

The Perron–Frobenius operator $\mathcal{P}_{0,t}(u)$ and the Koopman operator $\mathcal{K}_{0,t}(u)$ can be expressed in terms of the common transition kernel

$$\left(\mathcal{P}_{0,t}(u)f\right)(y) = \int_{\mathbb{X}} k_{0,t}(x,y,u)f(x)\,dx \quad \text{and} \quad \left(\mathcal{K}_{0,t}(u)g\right)(x) = \int_{\mathbb{X}} k_{0,t}(x,y,u)g(y)\,dy \tag{5.28}$$

for an initial density $f \in L^2(\Lambda)$ and an observable $g \in L^2(\Lambda)$ at initial time $t = 0$; see (2.16) in Section 2.3. By (5.7), the Koopman operator has the useful representation

$$\left(\mathcal{K}_{0,t}(u)g\right)(x) = \mathbb{E}\left[g(X_t^u)\,|\,X_0^u = x\right] = \varphi_g^x(u)\,,$$

where we abuse the notation $\varphi_g^x(u)$ to denote $\varphi_{g\circ\pi_t}^x(u)$ if $g \in L^2(\Lambda)$. At this point Theorem 5.5 implies pointwise differentiability of the mapping $u \mapsto \left(\mathcal{K}_{0,t}(u)g\right)(x)$ for fixed x and g. The following results lift this property to the operator level. Using the transition kernel, duality arguments, and uniformity in $x \in \mathbb{X}$ of the bounds, the Fréchet differentiability from Theorem 5.5 extends to the Perron–Frobenius operator and the Koopman operator. We prove the Fréchet differentiability in the strong operator topology. Lemma 5.8 shows that the differentiability with respect to u holds uniformly in g and Lemma 5.9 shows that the differentiability with respect to u holds uniformly in x. These intermediate results are combined in Theorem 5.10.

Lemma 5.8:
The operator $u \mapsto (\mathcal{K}_{0,t}(u)(\cdot))(x)$, mapping from V to $(L^2(\Lambda))^*$, is Fréchet differentiable with respect to u.

Lemma 5.8 and its proof due to the author have been published in [KLP19, Lem. 4.2].

Proof. To lift the pointwise result, Theorem 5.5, to the operator level, we use quantitative bounds derived in the proof of Theorem 5.5. By Lemma 5.7, $g \in L^2(\Lambda)$ implies $g \in L^2\big(\mu_t^{0,x}\big)$, and we have

$$D_\beta \varphi_g^x\big|_{\beta=0}(u) = \mathbb{E}^{0,x}\left[(g \circ \pi_t) M_t^u\right] \tag{5.29}$$

for the derivative of φ_g^x at 0 applied to u. The equations (5.23) and (5.24) imply the existence of the residual

$$r_g^x(u) := \varphi_g^x(u) - \varphi_g^x(0) - D_\beta \varphi_g^x\big|_{\beta=0}(u) \tag{5.30}$$

with the property

$$\lim_{\|u\|_\blacklozenge \to 0} \frac{|r_g^x(u)|}{\|u\|_\blacklozenge} = 0\,,$$

where $\blacklozenge = V$ or $\blacklozenge = L^\infty\left(\mu^{0,x}\right)$. The equations (5.29), (5.30), (5.22), (5.19), (5.16), (5.27), and the Cauchy–Schwarz inequality imply the existence of a constant C independent of x, g and u, and a non-negative function $q_\blacklozenge(u)$ independent of x and g such that

$$|r_g^x(u)| \le C\|g\|_{L^2(\mu_t^{0,x})} q_\blacklozenge(u) \le C\overline{K}^{1/2}\, \|g\|_{L^2(\Lambda)} q_\blacklozenge(u)\,. \tag{5.31}$$

The function $q_\blacklozenge$ has the property

$$\lim_{\|u\|_\blacklozenge \to 0} \frac{q_\blacklozenge(u)}{\|u\|_\blacklozenge} = 0\,.$$

If we consider $\varphi_g^x(u)$ and its derivative (5.29) as linear functionals on $g \in L^2(\Lambda)$, that is,

$$\begin{aligned} \varphi_{(\cdot)}^x(u) &: g \mapsto (\mathcal{K}_{0,t}(u)g)(x) = \langle g, k_{0,t}(x,\cdot,u)\rangle_{L^2(\Lambda)}\,, \\ D_\beta \varphi_{(\cdot)}^x\big|_{\beta=0}(u) &: g \mapsto \mathbb{E}^{0,x}\left[(g\circ\pi_t)M_t^u\right]\,, \end{aligned}$$

then we can use the following representation of the norm of the dual space $L^2(\Lambda)^*$

$$\|\ell\|_{L^2(\Lambda)^*} = \sup_{\substack{g\neq 0\\ g\in L^2(\Lambda)}} \frac{\ell(g)}{\|g\|_{L^2(\Lambda)}} = \sup_{\substack{g\neq 0\\ g\in L^2(\Lambda)}} \frac{\langle \ell, g\rangle_{(L^2)^*\times L^2}}{\|g\|_{L^2(\Lambda)}} \quad \text{for } \ell \in L^2(\Lambda)^*\,.$$

Dividing (5.30) by $\|g\|_{L^2(\Lambda)}$, taking the supremum over all $g \neq 0$, and using (5.31), we obtain

$$0 \le \frac{\left\|\varphi_{(\cdot)}^x(u) - \varphi_{(\cdot)}^x(0) - D_\beta\varphi_{(\cdot)}^x|_{\beta=0}(u)\right\|_{L^2(\Lambda)^*}}{\|u\|_\blacklozenge} \le C\overline{K}^{1/2}\,\frac{q_\blacklozenge(u)}{\|u\|_\blacklozenge}. \tag{5.32}$$

With $\frac{|q_\blacklozenge(u)|}{\|u\|_\blacklozenge} \to 0$ for $\|u\|_\blacklozenge \to 0$ follows the claim. $\square$

The equations (5.18) and (5.19) give an explicit choice for q:

$$q_{\blacklozenge}(u)^2 = \frac{1}{2}(\lambda_\sigma\sqrt{T})^4\|u\|_{\blacklozenge}^4 + 2C\sum_{\ell=4}^{\infty}\sum_{\substack{j,k\geq 2\\ j+k=\ell}}\frac{1}{j!k!}(2\lambda_\sigma\sqrt{T})^\ell\|u\|_{\blacklozenge}^\ell \,.$$

The derivative corresponding to the differentiability proven in Lemma 5.8 is given by

$$D_\beta\varphi^x_{(\cdot)}\big|_{\beta=0}(u) = \mathbb{E}^{0,x}\left[\cdot M_t^u\right] .$$

The uniformity of the bounds (5.31) and (5.32) with respect to x enables us to remove the x-dependence of Lemma 5.8 in the following result.

Lemma 5.9:
The kernel k, more specifically, the mapping $u \mapsto k_{0,t}(\cdot,\cdot,u)$ from V to $L^2(\Lambda\otimes\Lambda)$, is Fréchet differentiable with respect to u.

Lemma 5.9 and its proof due to the author have been published in [KLP19, Lem. 4.4].

Proof. Considering Lemma 5.8, we still need to get rid of the evaluation in x. Fortunately, all relevant bounds are uniform in x. First, we use the Riesz isomorphism $\mathcal{R}$ [Cia13, Sec. 4.6] to identify $L^2(\Lambda)^*$ with $L^2(\Lambda)$, which leads to

$$\mathcal{R}\big(\mathcal{K}_{0,t}(u)(\cdot)(x)\big) = \mathcal{R}\big(\varphi^x_{(\cdot)}(u)\big) = k_{0,t}(x,\cdot,u)\,. \tag{5.33}$$

See Remark 38 for some more details. This further guarantees the existence of

$$D_\beta k_{0,t}(x,\cdot,\beta)|_{\beta=0}(u) := \mathcal{R}\big(D_\beta\varphi^x_{(\cdot)}\big|_{\beta=0}(u)\big)\,.$$

The mapping $u\mapsto D_\beta k_{0,t}(x,\cdot,\beta)|_{\beta=0}(u)$, $V\to L^2(\Lambda)$ is a linear and bounded operator. Since $\mathcal{R}$ is a linear isomorphism, Lemma 5.8 and in particular (5.32) provide

$$\big\|k_{0,t}(x,\cdot,u) - k_{0,t}(x,\cdot,0) - D_\beta k_{0,t}(x,\cdot,\beta)\big|_{\beta=0}(u)\big\|_{L^2(\Lambda)} \leq C\overline{K}^{1/2}\, q_{\blacklozenge}(u).$$

Finally, differentiability of $u\mapsto k_{0,t}(\cdot,\cdot,u)$, $V\to L^2(\Lambda\otimes\Lambda)$, follows from

$$\begin{aligned}
&\big\|k_{0,t}(\cdot,\cdot,u) - k_{0,t}(\cdot,\cdot,0) - D_\beta k_{0,t}(\cdot,\cdot,\beta)\big|_{\beta=0}(u)\big\|_{L^2(\Lambda\otimes\Lambda)}\\
&\quad= \left(\int_{\mathbb{X}}\big\|k_{0,t}(x,\cdot,u) - k_{0,t}(x,\cdot,0) - D_\beta k_{0,t}(x,\cdot,\beta)\big|_{\beta=0}(u)\big\|^2_{L^2(\Lambda)}\,dx\right)^{1/2}\\
&\quad\leq \Lambda(\mathbb{X})^{1/2}\,C\overline{K}^{1/2}\,|q_{\blacklozenge}(u)|.
\end{aligned}$$

and the fact that $\frac{|q_{\blacklozenge}(u)|}{\|u\|_{\blacklozenge}}\to 0$ as $\|u\|_{\blacklozenge}\to 0$ for $\blacklozenge = V$ or $\blacklozenge = L^\infty(\mu^{0,x})$. □

Remark 38:
The Riesz representation $\mathcal{R}(\ell)\in H$ of a functional $\ell\in H^*$ on a Hilbert space H is uniquely defined by

$$\langle\mathcal{R}(\ell),u\rangle_{H\times H} = \ell(u) \quad \text{for all } u\in H\,.$$

In particular, $\mathcal{R}$ is an isomorphism, a linear operator with $\|\mathcal{R}(\ell)\|_H = \|\ell\|_{H^*}$. Therefore, equation (5.33) and

$$\mathcal{R}(\mathcal{K}_{0,t}(u)(\cdot)(x)) = k_{0,t}(x,\cdot,u) \quad \text{and} \quad \mathcal{R}(\mathcal{P}_{0,t}(u)(\cdot)(y)) = k_{0,t}(\cdot,y,u)$$

hold true. The fact that the Riesz representation is indeed given by the transition kernel follows from the arguments of Section 2.3. Note that the argument of the functional $(\mathcal{K}_{0,t}(u)(\cdot))\,(x)$ is an L^2 function, and the argument of $k_{0,t}(x,\cdot,u)$ is an element of $\mathbb{R}^d$. The same holds for $(\mathcal{P}_{0,t}(u)(\cdot))\,(y)$ and $k_{0,t}(\cdot,y,u)$. △

The relation between the Perron–Frobenius operator and the kernel is given by (5.28). Now the Fréchet differentiability of $\mathcal{P}_{0,t}(u)$ with respect to the velocity field is an immediate consequence of Lemma 5.9.

Theorem 5.10:
The mapping $\mathcal{P}_{0,t} : V \to \boldsymbol{L}(L^2(\Lambda), L^2(\Lambda))$ that maps $u \in V$ to the Perron–Frobenius operator $\mathcal{P}_{0,t}(u)$ is Fréchet differentiable.

Theorem 5.10 and its proof due to the author have been published in [KLP19, Thm. 4.5].

Proof. The mapping $k_{0,t}(\cdot,\cdot,u) \mapsto \mathcal{P}_{0,t}(u)$, $L^2(\Lambda \otimes \Lambda) \to \boldsymbol{L}(L^2(\Lambda), L^2(\Lambda))$ is linear. If this mapping is bounded, then it is continuously differentiable. We consider $\mathcal{P}_{0,t}(u) \in \boldsymbol{L}(L^2(\Lambda), L^2(\Lambda))$ with the induced norm. By the Cauchy–Schwarz inequality we obtain

$$\begin{aligned}
\sup_{f\neq 0} \frac{\|\mathcal{P}_{0,t}(u)f\|_{L^2(\Lambda)}}{\|f\|_{L^2(\Lambda)}} &= \sup_{f\neq 0} \|f\|^{-1}_{L^2(\Lambda)} \Big\| \int_{\mathbb{X}} k_{0,t}(x,\cdot,u) f(x)\,dx \Big\|_{L^2(\Lambda)} \\
&= \sup_{f\neq 0} \|f\|^{-1}_{L^2(\Lambda)} \left(\int_{\mathbb{X}} \left| \int_{\mathbb{X}} k_{0,t}(x,y,u) f(x)\,dx \right|^2 dy \right)^{\frac{1}{2}} \\
&\leq \sup_{f\neq 0} \|f\|^{-1}_{L^2(\Lambda)} \left(\int_{\mathbb{X}} \|k_{0,t}(\cdot,y,u)\|^2_{L^2(\Lambda)} \|f\|^2_{L^2(\Lambda)}\,dy \right)^{\frac{1}{2}} \\
&= \left(\int_{\mathbb{X}} \int_{\mathbb{X}} |k_{0,t}(x,y,u)|^2\,dy\,dx \right)^{\frac{1}{2}} = \|k_{0,t}(\cdot,\cdot,u)\|_{L^2(\Lambda\otimes\Lambda)}\,.
\end{aligned}$$

This gives the desired boundedness

$$\|\mathcal{P}_{0,t}(u)\|_{\boldsymbol{L}(L^2(\Lambda),L^2(\Lambda))} \leq \|k_{0,t}(\cdot,\cdot,u)\|_{L^2(\Lambda\otimes\Lambda)}\,.$$

Now, Lemma 5.9 and the chain rule for $u \mapsto k_{0,t}(\cdot,\cdot,u) \mapsto \mathcal{P}_{0,t}(u)$ imply the Fréchet differentiability of $\mathcal{P}_{0,t}(u)$ with respect to u. □

The differentiability of the Koopman operator $\mathcal{K}_{0,t}(u)$ can be proven analogously to Theorem 5.10. Lemma 5.11 and Remark 39 below provide an alternative approach to prove the Fréchet differentiability of the Koopman operator with respect to the velocity field.

Lemma 5.11:
Let U, V, W and Z be arbitrary (real or complex) Banach spaces with their respective norms. Consider a family of operators $(A(z))_{z\in Z} \subset \boldsymbol{L}(U,V)$, a linear and bounded operator $j : \boldsymbol{L}(U,V) \to W$ and the mapped family $(j(A(z)))_{z\in Z}$. Now, if $z \mapsto A(z)$ is Fréchet differentiable, then the mapping $z \mapsto j(A(z)) =: B(z)$ is Fréchet differentiable as well. The derivative satisfies

$$D_z B|_{z=z_0} = j \circ (D_z A|_{z=z_0}) \ .$$

Lemma 5.11, its proof and Remark 39 due to the author have been published in [KLP19, App. A.1].

Proof. The claims follow from the chain rule for Fréchet derivatives and the rule for differentiating linear operators. □

Remark 39:
More important than the proof are some special cases that we are interested in. For the linear isometry $j : A \mapsto A^*$ and $W = \boldsymbol{L}(V^*, U^*)$, Lemma 5.11 implies the Fréchet differentiability of the adjoint family $(A(z)^*)_{z\in Z}$. If in this special case the spaces U and V are also reflexive spaces, then the reverse direction of Lemma 5.11 holds as well. △

Example 2 is an expansion of [KLP19, Ex. 1] and shows that a similar result to Theorem 5.10 cannot hold in the deterministic case in the same general setting.

Example 2: Discontinuous drift-dependence for deterministic dynamics

(1) Recall Section 2.1, let us consider the time-t solution map Φ_t of some deterministic differential equation $x'(t) = b(x(t))$, and the time-t solution map Φ_t^ε of a slight perturbation $x'(t) = b_\varepsilon(x(t))$ of the previous differential equation with $\|b - b_\varepsilon\| \le \varepsilon$. Let Φ_t and Φ_t^ε be flows such that the associated Koopman operators (2.3) $K_t : g \mapsto g \circ \Phi_t$ and $K_t^\varepsilon : g \mapsto g \circ \Phi_t^\varepsilon$ are well-defined on $L^2(\Lambda)$, where Λ is the Lebesgue measure; see [LM94, Wal00] for details. For x with $\Phi_t(x) \ne \Phi_t^\varepsilon(x)$, let us consider the function sequence $(f_n)_{n\in\mathbb{N}}$ given by $f_n = \Lambda(A_n)^{-1/2}\mathbb{1}_{A_n}$, where $(A_n)_{n\in\mathbb{N}}$ is a sequence of balls centered around $\Phi_t(x)$ such that $A_{n+1} \subset A_n$, $\lim_{n\to\infty} \bigcap_{i=1}^n A_i = \{\Phi_t(x)\}$ and $\|f_n\|_{L^2} = 1$. As before $\mathbb{1}_A$ denotes the characteristic function of a set A. Now, for some fixed $t > 0$ and any $\varepsilon > 0$ there exists $N_\varepsilon \in \mathbb{N}$ such that $\|K_t f_n - K_t^\varepsilon f_n\|_{L^2(\Lambda)} \ge 1$ for all $n \ge N_\varepsilon \in \mathbb{N}$.

(2) To make the above argument more explicit, we choose $d = 1$ and

$$b(x) := -x \qquad \text{and} \qquad b_\varepsilon(x) := -x + \varepsilon$$

with b_ε converging uniformly to b, $\|b_\varepsilon - b\|_\infty \le \varepsilon$. This implies

$$\Phi_t(x) = e^{-t}x\,, \quad \Phi_t^\varepsilon(x) = (x-\varepsilon)e^{-t}+\varepsilon\,, \quad K_t(g)(x) = g(e^{-t}x)\,, \quad K_t^\varepsilon(g)(x) = g((x-\varepsilon)e^{-t}+\varepsilon)$$

and K_t and K_t^ε are well-defined operators on $L^2(\Lambda)$. Now, we choose $t > 0$ and $x = 1$ such that $\Phi_t(1) \ne \Phi_t^\varepsilon(1)$ and $A_{n,t} := (e^{-t}(1 - \frac{1}{2n}), e^{-t}(1 + \frac{1}{2n}))$ with $\Lambda(A_{n,t}) = \frac{e^{-t}}{n}$. For the functions $f_{n,t}(x) := \Lambda(A_{n,t})^{-\frac{1}{2}}\mathbb{1}_{A_{n,t}}(x)$ and $N_{\varepsilon,t} > \frac{1}{\varepsilon e^t - \varepsilon}$ the functions $K_t f_{n,t}$ and $K_t^\varepsilon f_{n,t}$ have disjoint support.

Now, we can compute

$$\|K_t f_{n,t} - K_t^\varepsilon f_{n,t}\|_{L^2} = 2e^t > 2$$

for all $n > N_{\varepsilon,t}$.

(3) The abstract argument (1) or the explicit example (2) show that K_t cannot depend continuously on the velocity field b in the strong operator norm. For all $\delta > 0$ there exists an $\varepsilon < \delta$ such that

$$\|K_t - K_t^\varepsilon\|_{\boldsymbol{L}(L^2,L^2)} = \sup_{\|f\|_{L^2}=1} \|K_t f - K_t^\varepsilon f\|_{L^2} \geq \|K_t f_{n,t} - K_t^\varepsilon f_{n,t}\|_{L^2(\Lambda)} \geq 1 \,,$$

for $n \in \mathbb{N}$ sufficiently large, for example in (2), $n \geq N_{\varepsilon,t} > \frac{1}{\varepsilon e^t - \varepsilon}$.

♢

Applying the duality arguments from Lemma 5.11 and Remark 39 to Example 2 shows that the deterministic Perron–Frobenius operator P_t cannot be Fréchet differentiable with respect to the drift on $L^2(\Lambda)$. In the deterministic setting, the main reason for the non-continuous drift-dependence is that K_t and P_t, $t > 0$, map functions with highly localized supports to functions with highly localized supports. However, in non-deterministic systems driven by non-degenerate noise the support of the initial conditions is spread everywhere by the noise in an arbitrary small time span $t > 0$. This follows intuitively from the strict positivity of the transition kernel.

Remark 40:
There could be other function spaces where smooth drift-dependence holds in the deterministic setting [Bal18]. However, these function spaces would require norms that penalize increasingly localized densities [GL06, Thi12]. △

5.4 Extension to the Spectrum

The following classical result, Theorem 5.12, derived in [Ros55] compactly presented in, for example, [Klo19, Thm. 1] is based on the implicit function theorem. Theorem 5.12 enables us to extend our results on Fréchet differentiable dependence to the eigenvalues and eigenfunctions of the transfer operators.

Theorem 5.12:
Let V be an arbitrary Banach space. If $A_0 \in \boldsymbol{L}(V,V)$ has a simple and isolated eigenvalue λ^0 with an eigenfunction f^0, then there is an open neighborhood $\mathcal{N}$ of A_0 in $\boldsymbol{L}(V,V)$ such that all $A \in \mathcal{N}$ have a simple and isolated eigenvalue λ^A close to λ^0. The map $\lambda : \mathcal{N} \to \mathbb{R}\,,\ A \mapsto \lambda^A$ is analytic. There exists another analytic map $f : \mathcal{N} \to V\,,\ A \mapsto f^A$ such that f^A is an eigenfunction of A for λ^A.

Proof. See [Ros55]. □

Under some conditions on the data, all non-zero eigenvalues of $\mathcal{P}_{0,t}(u)$ and $\mathcal{K}_{0,t}(u)$ are isolated, because these transfer operators are compact operators; see Theorem 3.12 or Theorem 2.6. The fact that the space V equipped with the norm $\|\cdot\|_V$ defined in (5.5) is indeed a Banach space (Lem. 5.1) is relevant for the next theorem.

Theorem 5.13:
Let us assume that λ^0 *is a simple and isolated eigenvalue with eigenfunction* f^0 *of the unperturbed linear and bounded operator* $\mathcal{P}_{0,t}(0)$ *that belongs to* $\boldsymbol{L}\big(L^2(\Lambda), L^2(\Lambda)\big)$. *There exists a neighborhood* $\mathcal{U}$ *of the constant function* 0 *that is a subset of the Banach space* $(V, \|\cdot\|_V)$ *(Lem. 5.1), such that for all* $u \in \mathcal{U}$ *the operators* $\mathcal{P}_{0,t}(u)$ *have an isolated eigenvalue* λ^u *close to* λ^0. *Furthermore, the mappings* $u \mapsto \lambda^u$ *and* $u \mapsto f^u$ *(corresponding eigenfunction) are continuously Fréchet differentiable. The eigenfunction map* $u \mapsto f^u$ *– which is unique only up to scaling – can be chosen such that it is Fréchet differentiable.*

An analogous result for the Koopman operator can be shown directly using similar arguments or using Lemma 5.11. Theorem 5.13 and its proof due to the author have been published in [KLP19, Thm. 5.1].

Proof. By the Fréchet differentiability of $u \mapsto \mathcal{P}_{0,t}(u)$ from Theorem 5.10, we have

$$\mathcal{P}_{0,t}(u) = \mathcal{P}_{0,t}(0) + \mathcal{Q}_{0,t}(u), \quad \text{with} \quad \mathcal{Q}_{0,t}(u) = \mathcal{O}\left(\|u\|_V\right) .$$

We consider $\mathcal{P}_{0,t}(u)$ as an additive perturbation of $\mathcal{P}_{0,t}(0)$ in the space $\boldsymbol{L} := \boldsymbol{L}(L^2(\Lambda), L^2(\Lambda))$. Using Theorem 5.12, we can deduce the existence of $\boldsymbol{U} \subset \boldsymbol{L}$, a neighborhood of $\mathcal{P}_{0,t}(0)$, and mappings $m_1 : \mathcal{P}_{0,t}(u) \mapsto \lambda^u$ and $m_2 : \mathcal{P}_{0,t}(u) \mapsto f^u$ such that m_1 and m_2 are analytic on $\boldsymbol{U}$. By Theorem 5.10, $h : u \mapsto \mathcal{P}_{0,t}(u)$ is a continuously differentiable mapping. Thus, there exists a neighborhood $\mathcal{U} \subset V$ of 0 such that the mappings $n_1 = m_1 \circ h : \mathcal{U} \to \mathbb{R}\,, u \mapsto \lambda^u$ and $n_2 = m_2 \circ h : \mathcal{U} \to L^2(\Lambda)\,, u \mapsto f^u$ are continuously Fréchet differentiable. □

Remark 41:

- The Fréchet differentiability can be extended to the spectrum of the generator in the autonomous case, the spectrum of the augmented generator in the non-autonomous periodic case, and the spectrum of the augmented reflected generator in the non-autonomous aperiodic case using the corresponding spectral mapping property.

- We have chosen the initial time to be 0 for better readability. A different initial time $s \in \mathbb{R}$, with the time span $[s, s+T]$, would introduce additional and more complicated notation. Nevertheless, the arguments of this chapter respect the time-dependence of v, u, b and σ and hold analogously for a different initial time s with $t > s$. The result have been derived in the non-autonomous setting. Therefore, also the operators $\mathcal{P}_{s,t}(u)$ and $\mathcal{K}_{s,t}(u)$ are Fréchet differentiable of with respect to u.

- The results from Section 5.3 and Section 5.4 can be adapted to hold on the smaller space $C^{(\alpha,1+\alpha)}([0,T] \times \overline{\mathbb{X}}; \mathbb{R}^d)$ instead of V as well using the arguments introduced at the beginning of Section 5.3.

△

To conclude this chapter, we briefly discuss two applications of the differentiability derived in this chapter.

Periodically Forced Systems

For non-autonomous periodically forced systems, where

$$v(t+T,\cdot)=v(t,\cdot),\; u(t+T,\cdot)=u(t,\cdot), \quad \text{and} \quad \sigma(t+T,\cdot)=\sigma(t,\cdot),$$

hold for some $T>0$, Theorem 5.13 shows that the ergodic averages of the type

$$\bar{g}^u(x) := \lim_{t\to\infty}\frac{1}{t}\int_0^t g(s \bmod T, X_s^u)\,ds, \quad X_0^u = x\,,$$

with $g:[0,T)\times\mathbb{X}\to\mathbb{R}$, are continuously Fréchet differentiable with respect to u. Let $\mathcal{P}_{t_0,t_1}(u)$ denote the Perron–Frobenius operator corresponding to the perturbed SDE (5.3) evolving from time t_0 to t_1. Let $(f_t^u)_{t\in[0,T)}$ be the stationary family of densities satisfying $\mathcal{P}_{s,t}(u)f_s^u = f^u_{t \bmod T}$. In particular, $\mathcal{P}_{s,s+T}(u)f_s^u = f_s^u$ holds. Theorem 5.10 and Theorem 5.13 imply that the eigenfunctions are differentiable with respect to u. The process X^u is irreducible due to non-degenerate noise, Theorem 2.8. Therefore, the dominant eigenvalue 1 of $\mathcal{P}_{s,s+T}(u)$ is simple. By Birkhoff's individual ergodic theorem [Kre85]

$$\bar{g}^u(x) = \frac{1}{T}\int_0^T\int_{\mathbb{X}} g(s,y)f^u(y)\,dy\,ds$$

holds $\mathbb{P}^x$-almost surely for Λ-almost every x and $\bar{g}^u(x)$ is continuously differentiable in u.

Adjoint Operators and Singular Values

By Theorem 5.10 and Remark 5.11 both $\mathcal{P}_{0,t}(u)$ and $\mathcal{K}_{0,t}(u)$ are Fréchet differentiable with respect to u. Therefore, also their concatenations $\mathcal{P}_{0,t}(u)\mathcal{K}_{0,t}(u)$ and $\mathcal{K}_{0,t}(u)\mathcal{P}_{0,t}(u)$ are Fréchet differentiable with respect to u. Furthermore, we have the differentiability of $\mathcal{P}_{0,t}(u)^*\mathcal{P}_{0,t}(u)$ and $\mathcal{P}_{0,t}(u)\mathcal{P}_{0,t}(u)^*$. Thus, the simple and isolated singular values and the right and left singular vectors of $\mathcal{P}_{0,t}(u)$ and $\mathcal{K}_{0,t}(u)$ are also Fréchet differentiable with respect to u. As we have seen in Chapter 2 and Chapter 3, the singular values of transfer operators are of particular interest for non-autonomous systems, because they can be connected to finite-time persistent dynamical structures, such as coherent sets.

6 Spectral Optimization

In Chapter 3, we constructed singular pairs of $\mathcal{P}_{0,T}$ as eigenpairs of the augmented reflected generator $\hat{\boldsymbol{G}}$. In this chapter, we want to optimally perturb the velocity field v to manipulate coherent sets and mixing. Chapter 5 was concerned with the continuous Fréchet differentiability of transfer operators and their spectra with respect to the velocity field v. Having established this regularity we can now use it to formulate a locally valid optimization problem for changes in the velocity field v to increase or decrease selected eigenvalues and singular values and thus increase or decrease coherence for the induced coherent sets. This chapter is concerned with [FKS20, Sec. 6 & 7]. Section 6.1 deals with a slightly more general setting, but starting from Section 6.2 we follow the specific setting and examples from [FKS20, Sec. 6 & 7]. The results, the examples, the figures, and the general content of this chapter, with the exception of Section 6.1 and Figure 6.1, have been published in [FKS20] and are re-used and expanded upon here with permission of the authors and the publisher. Section 6.2 constructs an optimization problem designed to manipulate a simple and isolated eigenvalue of the augmented reflected generator and derives an explicit expression for the optimal time-dependent local perturbation of the velocity field. Section 6.3 transfers the results of Section 6.2 from infinite dimensions to the finite-dimensional numerical setting via discretization. Section 6.4 includes examples of the reduction and enhancement of coherence.

6.1 Lagrange Multipliers in Banach Spaces

First, let us to briefly introduce the general theory of Lagrangian multipliers in Banach spaces and apply it to general C_0 semigroups, their generators and their spectra. For introductions and references regarding Lagrangian multipliers in Banach spaces we refer to [Kur76, Lue69, IK08, Don11, Bot13] and [Ste18]. For an extensive general introduction into linear and non-linear optimization in infinite dimensions including Lagrangian multipliers see [Zei85]. The following results are mainly from [Lue69] which partially even deals with normed possibly non-complete vector spaces. The necessary conditions in Theorem 6.3 are considered *local theory* [Lue69, Chap. 9], and, assuming convexity, the sufficient conditions in Theorem 6.4 are considered *global theory* [Lue69, Chap. 8].

The Problem

The main problem under consideration for Lagrangian multipliers is usually concerned with a continuously differentiable objective functional c and constraints of the form

$$\begin{aligned} &\min_{u\in V}\ c(u) \\ &\text{s.t. } h(u) = 0 \text{ or } g(u) \leq_P 0\ . \end{aligned} \tag{6.1}$$

Here $c : V \to \mathbb{R}$ is a real valued functional defined on a Banach space $(V, \|\cdot\|_V)$. Furthermore, $h, g : V \to W$ map from the Banach space V to another Banach space $(W, \|\cdot\|_W)$. The Banach space $(W, \|\cdot\|_W)$ has a positive cone P (Def. 6.1) that induces the relation $\leq_P$. Additionally, we assume that the optimization problem (6.1) admits a local solution u^* and that g and h are Fréchet differentiable at u^*.

Definition 6.1:

(1) A subset M of a Banach space W is called a convex cone if and only if all non-negative linear combinations of elements from M are still contained in M:

$$\forall\, x, y \in M\,,\, \forall\, \alpha, \beta \geq 0\,:\, \alpha x + \beta y \in M\,.$$

(2) Let P be a convex cone in a Banach space W. For $u, v \in W$ the relation $\geq_P$ is given by

$$u \geq_P v \Leftrightarrow u - v \in P\,.$$

The cone P is called a positive cone and $N = -P$ inducing

$$u \leq_P v \Leftrightarrow u - v \in N \Leftrightarrow v \geq_P u$$

is called a negative cone. The strict relations $>_P$ and $<_P$ are defined by asking for the difference to be contained in $\operatorname{int}(P)$, the interior of P, instead of P.

(3) The subset of functionals

$$P^{\oplus} := \{z \in W^* \,|\, z(u) \geq 0 \textit{ for all } u \in P\}$$

is called the positive convex dual cone.

Often we can chose the positive cone P and the relation $\geq_P$, such that P is a consistent generalization of the canonical positive cone $\mathbb{R}_{\geq 0}$ known in $\mathbb{R}$. Nevertheless, there are other possible choices.

At first glance cones might seem a little clumsy to work with, but they will be useful. For many applications it is important that the positive cone has an interior point. However, not every positive cone has an interior point.

Example 3:
Consider the Banach space $L^p(0,1;\mathbb{R})$, $p \in [1,\infty)$, and define the cone

$$P := \{f \in L^p(0,1;\mathbb{R}) \,|\, f(t) \geq 0 \text{ for almost every } t \in (0,1)\}\,.$$

Straightforward computations show that P is a convex cone. However, P does not contain an interior point. For $f \in P$ and $\varepsilon > 0$ we define

$$\tilde{f}_\varepsilon(t) := \begin{cases} -1 & \text{on } (0,\varepsilon)\,, \\ f(t) & \text{else}\,. \end{cases}$$

Now $\tilde{f}_\varepsilon \notin P$ holds and for any $\delta > 0$ follows

$$\|f - \tilde{f}_\varepsilon\|_{L^p} = \left(\int_{(0,\varepsilon)} |f(t) + 1|^p \, dt \right)^{\frac{1}{p}} < \delta$$

for $\varepsilon > 0$ small enough. Thus, f cannot be an interior point of P. ◊

Example 3 would not work for $p = \infty$ and would also not for continuous functions with the supremum norm. The cone $P := \{f \in C([0,1];\mathbb{R}) \mid f(t) \geq 0 \text{ for all } t \in [0,1]\}$ contains interior points in $(C([0,1];\mathbb{R}), \|\cdot\|_\infty)$.

Necessary Conditions

Definition 6.2:

(1) A point $u \in V$ is called a regular point for an equality constraint with a continuously differentiable mapping $h : V \to W$ if $h'(u)$ maps surjectively from V to W.

(2) Assume that W has a positive cone P that contains an interior point. Then $u \in V$ is called a regular point of g, if $g(u) \leq_P 0$, and if there exists a $w \in V$ such that $g(u) + g'(u)(w) <_P 0$.

The following theorem states necessary conditions for u^* to be a solution to (6.1).

Theorem 6.3:

(1) If u^* is a solution of (6.1) with the equality constraint $h(u) = 0$ and u^* is a regular point of h, then there exists a Lagrangian multiplier functional $z^* \in W^*$ such that

$$c'(u^*) + z^* \circ h'(u^*) = 0$$

and $z^*(h(u^*)) = \langle z^*, h(u^*)\rangle_{W^* \times W} = 0$.

(2) If u^* is a solution of (6.1) with the inequality constraint $g(u) \leq_P 0$ and u^* is a regular point of g, then there exists $0 \leq_{P^\oplus} z^* \in W^*$ such that

$$\varphi'(u^*) + z^* \circ g'(u^*) = 0$$

and $z^*(g(u^*)) = \langle z^*, g(u^*)\rangle_{W^* \times W} = 0$.

Proof. Theorem 6.3 and a proof can be found in any of the references mentioned in the introduction of this section or any other source on Lagrangian multipliers in Banach spaces. Specifically we refer to [Lue69, p. 243] for the equality constraints and to [Lue69, p. 249] for inequality constraints. □

Sufficient Conditions

In [FKS20] the objective is linear, the constraint is given by a quadratic form, and the problem is considered in a Hilbert space setting. It turns out that with these additional properties the necessary conditions are already sufficient, Theorem 6.9. However, this is in general not the case.

In contrast to finite-dimensional problems, finding sufficient conditions infinite-dimensional problems can become highly challenging. Furthermore, sufficient conditions are rare in the literature. We make some additional assumptions and work with inequality constraints and cones to continue with [Lue69, Sec. 8.4]. Alternatively, [Zei85, Thm. 48A] cites a result going back to [DM65] that contains necessary and sufficient conditions dealing with equalities and inequalities simultaneously.

Theorem 6.4:
Assume that the positive cone P of W has non-empty interior and is closed. Suppose there exists $u^* \in V$ and $0 \leq_{P^\oplus} z^* \in W^*$ such that the Lagrangian $L(u, z) := c(u) + \langle z, g(u)\rangle_{W^* \times W}$ has a saddle point at (u^*, z^*):

$$L(u^*, z) \leq L(u^*, z^*) \leq L(u, z^*)$$

for all $u \in V$ and $z \geq_{P^\oplus} 0$. Then u^* solves (6.1) *with the inequality constraint.*

Proof. This result for inequality constraints is contained in [Lue69, pp. 220-221, Thm. 1 & 2]. □

Application to Strongly Continuous Semigroups

Let us now consider a C_0 semigroup of linear and bounded operators $(S_t(v))_{t\in[0,T]}$ on a Banach space $(X, \|\cdot\|_X)$ and its corresponding infinitesimal generator $G(v)$ that depends on some possibly infinite-dimensional parameter $v \in V$. We assume that $S_t(v)$ is continuously Fréchet differentiable with respect to v for all $t \in [0, T]$. In general, the dependence of the eigen- and singular spectrum of an operator can be complicated and highly non-linear, even if the operator itself is linear in v. The differentiability of $S_t(v)$ justifies using a local linear approximation of this dependence

$$S_t(v + u) = S_t(v) + S_t'(v)u + r_t(v, u) \quad \text{ with } \lim_{u\to 0} \frac{r_t(v, u)}{\|u\|_V} = 0 \ .$$

Now we use the implicit function argument from Theorem 5.12 to deduce the continuous Fréchet differentiability with respect to v of any simple and isolated eigenvalue $\lambda_k(v)$ and the corresponding eigenfunction $f_k(v)$ of $S_t(v)$ for some arbitrary but fixed $t \in (0, T]$.

The same argument can be applied to $S_t(v)^*S_t(v)$ to get the continuous Fréchet differentiability of simple and isolated singular pairs of $S_t(v)$. The spectral mapping property (3.3) extends the differentiability to the point spectrum of the infinitesimal generator $G(v)$ via

$$\sigma_p(G(v)) = \frac{1}{t} \log(\sigma_p(S_t(v)\backslash\{0\}) \ . \tag{6.2}$$

Also see [KLP19, Sec. 5] and [FKS20, Sec. 6] for the previous arguments.

Let c_v be the linear functional constructed by linearization of the change of a simple and isolated eigenvalue $\mu(v)$ of $G(v)$ with respect to a change u in the parameter v.

$$c_v(u) = \mu'(v)(u) \ .$$

Alternatively, we can choose c_v to be constructed by linearization of the change of a simple and isolated eigenvalue $\lambda(v)$ or singular value $\sigma(v)$ of $S_t(v)$. We look at the following optimization problem

$$\begin{aligned} \min_{u\in V} \ & c_v(u) \\ \text{s.t. } \ & g(u) \leq 0 \end{aligned} \tag{6.3}$$

with $g : V \to \mathbb{R}^k$ continuously differentiable. The image space $\mathbb{R}^k$ of g guarantees that the canonical positive convex cone $\mathbb{R}^k_{\geq 0}$ in $\mathbb{R}^k$ has a non-empty interior.

Assumption 5:
For the optimization problem (6.3) *there exists a unique solution* u^* *that is a regular point of* g *fulfilling the condition*

$$g(u^*) + g'(u^*)(w) < 0$$

for some $w \in V$.

Assumption 5 can be difficult to prove in applications depending on g. For the case of equality constraints $h(u) = 0$ the regular point property is usually easier to verify.

Now we can apply the theory introduced above considering necessary and sufficient conditions. The solution u^* for (6.3) is only locally the best direction of change for $\lambda(v)$. Linearizing around the new position $\lambda(v + u^*)$ and iterating the optimization process leads to a gradient type method; see Algorithm 2 in Section 6.4.

The conditions and assumptions of this section can be verified in the setting of [FKS20]. Thus, the results above, especially Theorem 6.3 and Theorem 6.4, are an alternative way to arrive at necessary and sufficient conditions for a unique optimum besides [FKS20, Prop. 6.5]. The approach from [FKS20] is reproduced in Section 6.2. In particular, Section 6.1 gives a slightly more general approach than [FKS20, Sec. 6] to necessary and sufficient conditions for (6.3). We would like to point out that Section 6.1 and Section 6.2 show that our optimization approach is independent of and also compatible with the augmentation and the reflection introduced in Chapter 3 and Section 2.5.

6.2 Optimal Perturbation of the Spectrum of the Augmented Reflected Generator

This section uses similar ideas as the previous section but in a more specific setting. We consider Hilbert spaces and a real-valued constraint describing an ellipsoid. Furthermore, we formulate the optimization problem with the goal of increasing or decreasing the coherence of a coherent family $(A_t^{\pm})_{t\in[0,T]}$ induced by the k-th eigenpair of the augmented reflected generator $\hat{\boldsymbol{G}}$ (Thm. 3.21) by optimizing over small time-dependent perturbations $u(t,x)$ of the velocity field $v(t,x)$. Recalling the notation from Chapter 2 and Chapter 3, we denote objects in the reflected setting with a ˆ and augmented objects with bold letters. We consider a set $\mathbb{X} \subset \mathbb{R}^d$ that satisfies (A0); page 13.

The space $H^m((0,T)\times\mathbb{X};\mathbb{R}^d)$ is the Sobolev space of vector fields mapping from on $(0,T)\times\mathbb{X}$ to $\mathbb{R}^d$ whose weak derivatives of order up to $m \in \mathbb{N}\cup\{0\}$ are L^2-functions. To apply the embedding theorem [AF03, Thm. 4.12] ($H^m \hookrightarrow C^{1+\alpha}$) we require $m \geq 1+\alpha+\frac{d}{2}$ for $\alpha \in (0,1]$. We use $u, v \in C^{(\alpha,1+\alpha)}$ to satisfy the assumptions of Chapter 2, Chapter 3, and Chapter 5. The restriction $\mathrm{div}_x v = 0$ on the velocity field should hold for $v + u^*$ after applying the optimal perturbation u^*. This enables iterative applications of the local optimization and Theorem 3.21. Therefore, we consider the subspace U of $H^m((0,T)\times\mathbb{X};\mathbb{R}^d)$ consisting of spatially divergence-free vector fields u that satisfy homogeneous Neumann boundary conditions $\frac{\partial u}{\partial n} = 0$ on $\partial\mathbb{X}$. We consider small perturbations u lying in a bounded, closed, and strictly convex subset $\mathcal{C} \subset U$.

Remark 42:
Similar to the approach here from [FKS20], the authors in [FS17] are looking for a perturbation u to maximize the local change of the real part of the second eigenvalue μ_2 or a group of leading eigenvalues of the generator with respect to the change in the velocity field. In [FS17] the Ulam-discretized generator (Sec. 4.1.1) corresponding to the vector field v is perturbed and optimized using linear programming. Then, a new perturbed velocity field $v + u$ can be inferred from the optimized discretized generator [FS17, Sec. 5]. As in [FK17] the results in [FS17] assume that the velocity field is time-periodic. The reflection trick (Sec. 2.5) can be applied to aperiodic velocity fields to enable the application of the approach from [FS17] to aperiodic v. The reflection can be incorporated by additional constraints into the linear program for the Ulam-discretized generator [FS17, Sec. 4.4]. In [FKS20] and in this thesis, the authors consider aperiodic velocity fields and in contrast to [FS17] the velocity field is perturbed directly in the infinite-dimensional velocity field space. The resulting optimization problem is solved in the infinite-dimensional setting using Lagrange multipliers in Hilbert spaces. △

To apply the theory of Lagrangian multipliers in the infinite-dimensional case, we need sufficient regularity of the Perron–Frobenius operator $\mathcal{P}_{0,T}$, Theorem 2.6, with respect to the velocity v which has been proven in [KLP19] and has been covered in Chapter 5.

Equation (6.2) shows that this continuous differentiability extends to the spectrum of $\hat{\boldsymbol{G}}$. The first variation of the k-th eigenvalues of the augmented reflected generator μ_k with respect to u is detailed in (6.5).

In the following, we derive the objective functional, specify the constraints, and obtain necessary and sufficient conditions for the solution to the linear optimization problem with quadratic constraints (6.9).

6.2.1 Derivation of the Problem

The Objective Functional

For a chosen eigenvalue μ_k of $\hat{\boldsymbol{G}}$ we manipulate the real part of μ_k by optimally perturbing the original velocity field v by some u within the chosen constraints. Following Theorem 3.21 the real part of μ_k quantifies the coherence of the family $(A_t)_{t\in[0,T]}$ induced by the corresponding eigenfunction. The dependence of an eigenpair or a singular pair with respect to a perturbation u can in general be quite complicated. Therefore, we choose to locally approximate the change by computing a first variation or first-order Taylor expansion. Without loss of generality, we assume in the following that μ_k is real. In the complex case we would simply consider the real parts with small appropriate modifications. With the assumptions on the spatial domain $\mathbb{X}$, on the velocity field v, on the perturbation u, and with $m \geq 1 + \alpha + \frac{d}{2}$, it follows that the continuous embedding $H^m((0,T)\times\mathbb{X};\mathbb{R}^d) \hookrightarrow C^{(\alpha,1+\alpha)}([0,T]\times\overline{\mathbb{X}};\mathbb{R}^d)$ holds [AF03, Thm. 4.12]. The diffusivity $\sigma(t,x) = \varepsilon I_{d\times d}$ is constant and therefore smooth enough to apply the results of Chapter 5 to $\mathcal{P}_{0,T}$. Assuming that σ_k, the k-th singular value of $\mathcal{P}_{0,T}$, is simple and isolated, Section 5.4 guarantees the Fréchet differentiability of the singular pair (σ_k, f_k) with respect to u. The equation (2.28) and the expression $\hat{\mathcal{P}}_{0,2T} = \mathcal{P}_{0,T}^*\mathcal{P}_{0,T}$ relate the $[0,T]$ dynamics represented the singular values and singular functions of $\mathcal{P}_{0,T}$ to the $[0,2T]$ dynamics after reflection represented by the eigenvalues and eigenfunctions of $\hat{\mathcal{P}}_{0,2T}$.

The spectral mapping property of Theorem 3.19, also (3.23),

$$\exp(2T\sigma(\hat{\boldsymbol{G}})) = \sigma(\hat{\mathcal{P}}_{0,2T})\backslash\{0\} = \sigma(\mathcal{P}_{0,T}^{*}\mathcal{P}_{0,T})\backslash\{0\}\,,$$

implies that the eigenvalue $\mu_k(\hat{\boldsymbol{G}}) \neq 0$ of $\hat{\boldsymbol{G}}$, the eigenvalue $\lambda_k(\hat{\mathcal{P}}_{0,2T})$ of $\hat{\mathcal{P}}_{0,2T}$ and the singular value $\sigma_k(\mathcal{P}_{0,T})$ of $\mathcal{P}_{0,T}$ satisfy

$$\exp(2T\mu_k(\hat{\boldsymbol{G}})) = \lambda_k\big(\hat{\mathcal{P}}_{0,2T}\big) = (\sigma_k(\mathcal{P}_{0,T}))^2,$$

which extends the continuous Fréchet differentiability with respect to v to the spectrum of $\hat{\boldsymbol{G}}$. In particular, for μ_k it follows that

$$\mu_k = \frac{1}{2T}\log\lambda_k = \frac{1}{T}\log\sigma_k\ .$$

The Fréchet differentiability of μ_k allows us to calculate the first variation of μ_k in v with respect to the change u. We wish to obtain an explicit expression of our objective functional in terms of objects we can compute. Therefore, we use that the Gateaux derivative of μ_k at v in the direction u exists and coincides with the Fréchet derivative of μ_k at $\hat{v}$ applied to the direction $\hat{u}$ induced by u. We can consider $\hat{\boldsymbol{G}}$, μ_k and similar augmented reflected objects to depend equivalently on v, u or on $\hat{v}, \hat{u}$, because the mapping $v \mapsto \hat{v}$ is linear, bounded and bijective; see (2.26).

For a small $\delta > 0$ and some $u \in U$ we insert the reflected perturbed velocity field $\hat{v} + \delta\hat{u}$ into (3.21) to obtain:

$$\hat{\boldsymbol{G}}(v+\delta u)\hat{\boldsymbol{f}} = (\hat{\boldsymbol{G}}+\delta\hat{\boldsymbol{E}}(u))(\hat{\boldsymbol{f}}) = -\mathrm{div}_{(\theta,x)}\left(\begin{pmatrix}1\\ \hat{v}\end{pmatrix}\hat{\boldsymbol{f}}\right) + \frac{1}{2}\Delta_{(\theta,x)}\boldsymbol{\varepsilon}^2\hat{\boldsymbol{f}}\,\underbrace{-\delta\mathrm{div}_{(\theta,x)}\left(\begin{pmatrix}0\\ \hat{u}\end{pmatrix}\hat{\boldsymbol{f}}\right)}_{=\delta\hat{\boldsymbol{E}}(u)\hat{\boldsymbol{f}}}\,. \tag{6.4}$$

Here we used the notations: $\hat{\boldsymbol{G}} = \hat{\boldsymbol{G}}(v)$, $\hat{\boldsymbol{v}} = (1, \hat{v})$, $\hat{\boldsymbol{u}} = (0, \hat{u})$, and $\hat{\boldsymbol{E}}(u)$ the perturbation of the generator given by

$$\hat{\boldsymbol{E}}(u)\hat{\boldsymbol{f}} = -\mathrm{div}_{(\theta,x)}(\hat{\boldsymbol{u}})\hat{\boldsymbol{f}} - \hat{\boldsymbol{u}}\nabla_{(\theta,x)}\hat{\boldsymbol{f}}\,.$$

For the left and right eigenfunctions, $\hat{\boldsymbol{g}}^k(\delta)$ and $\hat{\boldsymbol{f}}^k(\delta)$ respectively, of $\hat{\boldsymbol{G}} + \delta\hat{\boldsymbol{E}}(u)$ corresponding to $\mu_k(\delta)$, we have

$$\begin{aligned}(\hat{\boldsymbol{G}} + \delta\hat{\boldsymbol{E}}(u))\ \ \hat{\boldsymbol{f}}^k(\delta) &= \mu_k(\delta)\hat{\boldsymbol{f}}^k(\delta),\\ (\hat{\boldsymbol{G}} + \delta\hat{\boldsymbol{E}}(u))^*\hat{\boldsymbol{g}}^k(\delta) &= \mu_k(\delta)\hat{\boldsymbol{g}}^k(\delta),\end{aligned}$$

where we assume the normalization $\langle\hat{\boldsymbol{f}}^k(\delta), \hat{\boldsymbol{f}}^k(\delta)\rangle_{L^2} = \langle\hat{\boldsymbol{g}}^k(\delta), \hat{\boldsymbol{f}}^k(\delta)\rangle_{L^2} = 1$. For $\delta = 0$, we use the shorthand $\hat{\boldsymbol{f}}^k = \hat{\boldsymbol{f}}^k(0)$ and $\hat{\boldsymbol{g}}^k = \hat{\boldsymbol{g}}^k(0)$. To estimate the effect of the perturbation u on μ_k we linearize $\mu_k(\delta)$ at $\delta = 0$. This gives

$$\frac{d}{d\delta}\mu_k(\delta)|_{\delta=0} = \frac{d}{d\delta}\langle\hat{\boldsymbol{g}}^k(\delta), (\hat{\boldsymbol{G}} + \delta\hat{\boldsymbol{E}}(u))\hat{\boldsymbol{f}}^k(\delta)\rangle_{L^2}|_{\delta=0} = \langle\hat{\boldsymbol{g}}^k, \hat{\boldsymbol{E}}(u)\hat{\boldsymbol{f}}^k\rangle_{L^2}, \tag{6.5}$$

using the properties of $\hat{\boldsymbol{f}}^k$ and $\hat{\boldsymbol{g}}^k$, and the normalizations above. This argument is also used in [FS17, Sec. 4.3] in the finite-dimensional setting.

The approximation of the local change of the eigenvalue is explicitly given by

$$\langle \hat{\boldsymbol{g}}^k, \hat{\boldsymbol{E}}(u)\hat{\boldsymbol{f}}^k\rangle_{L^2} = \int_{[0,2T]\times\mathbb{X}} \hat{\boldsymbol{g}}^k(\boldsymbol{x}) \left(-\mathrm{div}_{(\theta,x)} \left(\begin{pmatrix} 0 \\ \hat{u} \end{pmatrix} \hat{\boldsymbol{f}}^k \right)(\boldsymbol{x}) \right) d\boldsymbol{x} =: c(u), \tag{6.6}$$

where $c : \mathcal{C} \to \mathbb{R}$ is the linear objective functional depending on the change u. If μ_k is complex, then one considers the real part of the functional c. Lemma 6.5 and its proof due to the author have been published in [FKS20, Lem. 6.1].

Lemma 6.5:
The objective functional $c : H^m((0,T) \times \mathbb{X}) \to \mathbb{R}$, with $m \geq 1$, is continuous and Fréchet differentiable. The Fréchet derivative is Lipschitz continuous.

Proof. Using (6.6), the following estimate shows that c is Lipschitz continuous.

$$\begin{aligned} |c(u)| &\leq \int_{[0,2T]\times\mathbb{X}} \left| \hat{\boldsymbol{g}}^k \hat{\boldsymbol{f}}^k \mathrm{div}_{\boldsymbol{x}} \begin{pmatrix} 0 \\ \hat{u} \end{pmatrix} \right| + \left| \hat{\boldsymbol{g}}^k \left\langle \begin{pmatrix} 0 \\ \hat{u} \end{pmatrix}, \nabla_{\boldsymbol{x}} \hat{\boldsymbol{f}}^k \right\rangle_{\mathbb{R}^{d+1}} \right| d\boldsymbol{x} \\ &\leq K_1 \|\hat{\boldsymbol{g}}^k\|_\infty \left(\|\hat{\boldsymbol{f}}^k\|_\infty \int_{[0,2T]\times\mathbb{X}} \left| \mathrm{div}_{\boldsymbol{x}} \begin{pmatrix} 0 \\ \hat{u} \end{pmatrix} \right| d\boldsymbol{x} + \int_{[0,2T]\times\mathbb{X}} \|\nabla_{\boldsymbol{x}} \hat{\boldsymbol{f}}^k\|_\infty \|\hat{u}\|_2 \, d\boldsymbol{x} \right) \\ &\leq K_2 \|\hat{\boldsymbol{g}}^k\|_\infty \|\nabla_{\boldsymbol{x}} \hat{\boldsymbol{f}}^k\|_\infty \|u\|_{H^1} \end{aligned}$$

Here $\|\cdot\|_\infty$ denotes the canonical $L^\infty((0,2T)\times\mathbb{X})$ norm. The Fréchet differentiability of c is straightforward, because c is linear and bounded. Furthermore, $c'(u) = c$ holds and implies the Lipschitz continuity of the derivative. □

More properties of c are discussed in Section 6.2.2.

Quadratic Constraints

As mentioned above, we consider perturbations $u \in \mathcal{C}$, a bounded, closed, and strictly convex subset of $U \subset H^m((0,T) \times \mathbb{X}; \mathbb{R}^d)$. For the linear objective functional c to be a good estimate for the change of μ_k, we require the perturbation u to be small using a bound $R > 0$ on the norm of u. Consider the ball or ellipsoid given by the following energy constraint (6.7). For multi-indices α and a weight vector $\omega = (\omega_\alpha)_{|\alpha|\leq m}$ with $0 < \omega_\alpha \in \mathbb{R}$ for all $|\alpha| \leq m$ let

$$\begin{aligned} 0 \overset{!}{\geq} h(u) := B_\omega(u,u) - R^2 &:= \sum_{|\alpha|\leq m} \omega_\alpha \|D^\alpha u\|_{L^2}^2 - R^2 \\ &= \sum_{|\alpha|\leq m} \omega_\alpha \langle D^\alpha u, D^\alpha u\rangle_{L^2} - R^2, \end{aligned} \tag{6.7}$$

with $D^\alpha = (\partial_1^{\alpha_1} \cdots \partial_d^{\alpha_d})$. The constraint functional h is a continuously Fréchet differentiable mapping from H^m to $\mathbb{R}$, because B_ω is a positive definite, bounded bilinear form if $0 < \omega_\alpha \in \mathbb{R}$ for all $|\alpha| \leq m$. We use h instead of g for the inequality constraint, because we use g for eigenfunctions and singular functions. Furthermore, the inequality constraint will turn into an equality constraint, when we prove that the optimum has to be on the boundary of the feasible set, see Lemma 6.7. For generality, we consider $\mathcal{C} = U \cap \{h \leq 0\}$, where U is a subspace of $H^m((0,T) \times \mathbb{X}; \mathbb{R}^d)$ containing admissible perturbations that might only have a relative interior. For a definition of *relative interior* and related concepts see [Roc70, II.6].

The constraint (6.7) implies that there are constants $\gamma > 0$ (B_ω is bounded) and $\beta > 0$ (B_ω is positive definite) such that

$$\beta\|u\|^2_{H^m} \leq B_\omega(u,u) \leq \gamma\|u\|^2_{H^m} \ .$$

The following theorem, mentioned and partially proven in [McI68, Appendix], is important for this thesis and the results in [FKS20, Sec. 6 & 7].

Theorem 6.6:
For a bounded bilinear form B acting on a Hilbert space $(H, \langle\cdot,\cdot\rangle_H, \|\cdot\|_H)$,

$$B \,:\, H \times H \to \mathbb{R} \qquad \exists\gamma > 0 \,:\, B(u,v) \leq \gamma\|u\|_H\|v\|_H \qquad \forall u,v \in H\,,$$

there exists a linear, bounded operator $T \,:\, H \to H$ such that

$$B(u,v) = \langle u, Tv\rangle_H \qquad \forall u,v \in H \ .$$

If B is symmetric, then T is self-adjoint. If in addition B is positive definite

$$\exists\beta > 0 \,:\, \beta\|u\|^2_H \leq B(u,u) \quad \forall u \in H\,,$$

then T is also injective and has a continuous inverse.

Note that there are probably multiple proofs throughout the literature for this statement that share the core strategy. However, the following proof has been done independently by the author and has been published in [FKS20, App. C].

Proof. For an arbitrary but fixed $v \in H$ consider the linear functional $\ell_v \,:\, u \mapsto B(u,v) = \ell_v(u)$. The Riesz representation theorem implies that there exists $z_v \in H$ such that $\ell_v(u) = \langle u, z_v\rangle_H$ for all $u \in H$. It remains to show that the mapping $T \,:\, v \mapsto z_v = T(v)$ is linear and bounded.

Consider $v + \lambda w \in H$ for $\lambda \in \mathbb{R}$ and $v, w \in H$, then

$$\langle u, T(v+\lambda w)\rangle_H = B(u, v+\lambda w) = B(u,v) + \lambda B(v,w) = \langle u, T(v)\rangle_H + \lambda\langle u, T(w)\rangle_H$$

holds for all $u \in H$. Thus, T is linear. The boundedness follows from

$$\|Tv\|_H = \sup_{\|u\|_H=1} |\langle u, Tv\rangle_H| = \sup_{\|u\|_H=1} |B(u,v)| \leq \gamma\|v\|_H \ .$$

Let us assume that B is symmetric, then

$$\langle u, Tv\rangle_H = B(u,v) = B(v,u) = \langle v, Tu\rangle_H$$

shows that T is self-adjoint.

Now assume that B is additionally positive definite. The estimate

$$\|v-w\|_H\,\|Tv-Tw\|_H \geq \langle v-w, T(v-w)\rangle_H \geq \beta\|v-w\|^2_H > 0 \qquad \text{for } v \neq w \in H \qquad (6.8)$$

implies injectivity. Thus, T^{-1} is defined on $\mathrm{ran}(T)$, the range of T, and it is continuous.

Let $x, y \in H$ be such that $u = Tx$ and $v = Ty$. Then

$$\begin{aligned}\|T^{-1}u - T^{-1}v\|_H &= \|T^{-1}Tx - T^{-1}Ty\|_H = \|x-y\|_H \\ &\overset{(6.8)}{\leq} \frac{1}{\beta}\|Tx - Ty\|_H = \frac{1}{\beta}\|u-v\|_H\end{aligned}$$

holds for all $u, v \in \operatorname{ran}(T)$. □

Theorem 6.6 guarantees the existence of a linear, bounded, injective, and self-adjoint operator $J_B(\omega)$ with

$$\langle J_B(\omega)u, v\rangle_{H^m} = B_\omega(u,v) \quad \text{for all } u, v \in H^m\ .$$

The operator $J_B(\omega)$ is used to derive an explicit formula (6.14) for the optimal solution u^* of the optimization problem (6.9).

6.2.2 Optimality Conditions

The optimization problem

$$\begin{aligned}&\min\ c(u) \\ &\text{s.t. } u \in \mathcal{C} \Leftrightarrow h(u) \leq 0 \ \text{ and } u \in U\end{aligned} \tag{6.9}$$

has a continuously differentiable linear objective functional c and a quadratic constraint h that induces a closed, bounded, strictly convex feasible set $\mathcal{C} = \{u \in U \mid h(u) \leq 0\}$ on a subspace U. The situation considered here and in [FKS20, Sec. 6] is like a flipped quadratic programming problem, having a linear objective and a quadratic constraint. Applying the theory of Lagrange multipliers introduced in Section 6.1 leads to an explicit solution formula to this problem. Lemma 6.7 establishes a general existence and uniqueness result that corresponds to the existence part of Assumption 5 in Section 6.1. The main idea of Section 6.2.2 is visualized in Figure 6.1 for $\dim(U) = 2$.

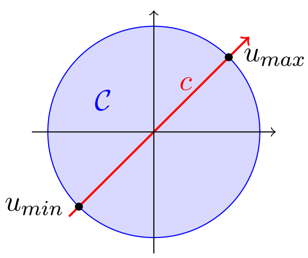

Figure 6.1: Illustration of the optimization problem of a linear objective functional c (red) and a quadratic constraint $\mathcal{C}$ (ball) (blue) in two dimensions.

Lemma 6.7:
Let $\mathcal{C}$ be a closed, bounded, and strictly convex subset of $H^m((0,T) \times \mathbb{X}; \mathbb{R}^d)$ containing the zero element in its (relative) interior and $c : \mathcal{C} \to \mathbb{R}$ be a bounded linear functional that does not uniformly vanish on $\mathcal{C}$. Then the optimization problem $\min_{u \in \mathcal{C}} c(u)$ has a unique solution $u^* \in \mathcal{C}$.

Lemma 6.7 and its proof due to the author have been published in [FKS20, Lem. 6.2].

Proof.

Existence: Continuity of c and boundedness of $\mathcal{C}$ imply the existence of $\alpha := \inf_{u\in\mathcal{C}} c(u) > -\infty$. Let $u_k \in \mathcal{C}$ be a sequence such that $\lim_{k\to\infty} c(u_k) = \alpha$. This sequence is bounded. By the Eberlein–Šmulian theorem [Cia13, Sec. 5.14] there exists a weakly convergent subsequence $u_{n_k} \rightharpoonup u^*$. The set $\mathcal{C}$ is closed and convex and therefore $\mathcal{C}$ is also weakly closed, which implies $u^* \in \mathcal{C}$. By the definition of weak convergence $c(u^*) = \lim_{k\to\infty} c(u_{n_k}) = \alpha$ follows. Therefore, u^* is a solution to the optimization problem.

Uniqueness: Assume that there are two solutions $u_1 \neq u_2$ with $c(u_1) = c(u_2) = \alpha$. The strict convexity of $\mathcal{C}$ implies that $u_3 := u_1/2 + u_2/2$ is in $\operatorname{relint}(\mathcal{C})$, the relative interior of $\mathcal{C}$. Now $c(u_3) = \alpha$ follows, because c is linear. Choose $r > 0$ small enough such that $(U \cap B(u_3, r)) \subset \operatorname{relint}(\mathcal{C})$. Since c does not vanish everywhere on $\mathcal{C}$ and the zero vector is in $\operatorname{relint}(\mathcal{C})$, there exists some direction $w \in \mathcal{C}$ such that $c(w) < 0$ and $\|w\|_{H^m} \leq 1$. By linearity of c we have $c(u_3 + (r/2)w) < \alpha$, contradicting the optimality of $u_1 \neq u_2$ and establishing uniqueness of the optimum.

□

The uniqueness argument in the proof of Lemma 6.7 shows that we may replace our constraint $h(u) \leq 0$ with $h(u) = 0$, because the optimum in our setting will always be on the boundary $\partial\mathcal{C} = \{u \in U \mid h(u) = 0\}$.

Necessary and Sufficient Conditions

Lemma 6.8 guarantees that the unique solution u^* from Lemma 6.7 is a regular point for the equality constraint $h(u) = 0$ according to Definition 6.2.

Lemma 6.8:
The unique optimal solution u^* of (6.9) is a regular point for $h : U \to \mathbb{R}$.

To distinguish between the point at which the derivative is taken and the input of the resulting mapping, square brackets indicate the reference point of the derivative, and parentheses indicate the input of the resulting mapping. Thus, $h'[u](v)$ denotes the derivative of h at u, which again is a linear mapping, applied to v. Lemma 6.8 and its proof due to the author have been published in [FKS20, Lem. 6.3].

Proof. Following Definition 6.2, the point u^* is a regular point for $h : U \to \mathbb{R}$ if the derivative of h at u^*, denoted by $h'[u^*] : U \to \mathbb{R}$, is surjective. Since $h(u) = B_\omega(u, u) - R^2$, and because the functional $h'[u]$ acts as $v \mapsto h'[u](v) = \langle J_B(\omega)v, u\rangle_{H^m} + \langle J_B(\omega)u, v\rangle_{H^m}$, follows that $h'[u]$ is surjective onto $\mathbb{R}$ for all $u \neq 0$. □

Now we can apply Theorem 6.3. For the continuously Fréchet differentiable functional c having a local extremum under the constraint $h(u) = 0$ at the regular point u^*, Theorem 6.3 implies there exists an element $z_{u^*} \in \mathbb{R}$ such that the Lagrangian functional $L(u) = c(u) + z_u h(u)$ is stationary at u^*. This gives the two necessary conditions:

$$c'[u^*] + z_{u^*} h'[u^*] = 0, \tag{6.10}$$

$$h(u^*) = 0. \tag{6.11}$$

Exploiting the Hilbert space structure, the linearity of c and the specific structure of the constraint h, we prove that the necessary conditions (6.10) and (6.11) are already sufficient. The direct approach in Theorem 6.9 establishes sufficient conditions without relying on cones like Theorem 6.4.

Theorem 6.9:
For the quadratic constraint $u \in \mathcal{C} = U \cap \{h \leq 0\}$ and a linear objective functional c that does not vanish on $\mathcal{C}$ there are exactly two elements $u, w \in \mathcal{C}$ that satisfy (6.10) *and* (6.11). *The property $z_u > 0$ makes u the unique minimizer and $z_w < 0$ makes w the unique maximizer.*

Theorem 6.9 and its proof due to the author have been published in [FKS20, Prop. 6.5].

Proof. Lemma 6.7 guarantees the existence of two extrema, namely, one minimum and one maximum, and therefore two distinct elements $u, w \in \mathcal{C}$ satisfying (6.10) and (6.11). We show that these are the only such elements. There exist $z_u, z_w \in \mathbb{R}\backslash\{0\}$ such that

$$\underbrace{c'[u]}_{=c\neq 0} + z_u h'[u] = 0 \text{ and } c'[w] + z_w h'[w] = 0.$$

Comparing these two equations and using $c'[u](\cdot) = c'[w](\cdot) = c(\cdot)$, we obtain the functional equation $h'[w] = (z_u/z_w)h'[u]$. Thus, the linear functional $h'[w]$ is a scalar multiple of $h'[u]$. By the Riesz representation theorem, we have $w = (z_u/z_w)u$, because $h'[u](\cdot) = 2\langle \cdot, J_B(\omega)u\rangle_{H^m}$ holds. The necessary condition $h(u) = h(w) = 0$ implies that $h'[u](u) = 2B_\omega(u, u) = 2R^2$ and similarly that $h'[w](w) = 2B_\omega(w, w) = 2R^2$. Thus, either $z_u = z_w$ or $z_u = -z_w$. If $z_u = z_w$, then we have $u = w$, while if $z_u = -z_w$, then $u = -w$. Thus, the only possibility for distinct u and w is that $u = -w$, and therefore there are at most two functions satisfying the necessary conditions.

Without loss of generality, we assume that u is a minimum. The assumption that c does not vanish on $\mathcal{C}$ and the result $c(u) = -c(w)$ imply $c(u) < 0$ and $c(w) > 0$. The equation

$$c'[u](u) + z_u h'[u](u) = c(u) + z_u 2R^2 = 0$$

and $c(u) < 0$ give $z_u > 0$. Thus, $z_w < 0$ holds and w is a maximum with $c(w) > 0$. □

The injective operator $J_B(\omega)$ enables us to solve the necessary and sufficient conditions (6.10) and (6.11) with regard to the optimal solution u^*, leading to the explicit solution formula (6.14) below. First, we transform (6.10) into an equation in H^m using the Riesz representation theorem. The optimum u^* exists and satisfies the equation

$$c_R + 2zJ_B(\omega)u^* = 0 \text{ in } H^m \qquad \text{with } z = z_{u^*} \in \mathbb{R}\,. \tag{6.12}$$

The Riesz representation of the functional c on H^m is denoted by $c_R \in H^m$. Equation (6.12) is important, because J_B is in general only injective and not surjective. Following equation (6.12) the element c_R is in the range of $J_B(\omega)$ and we can apply $J_B(\omega)^{-1}$ to c_R. Note that an expression for c_R can be derived from (6.6). Now we can solve (6.12) for $J_B(\omega)u^*$ and for u^*, because Theorem 6.9 guarantees $z \neq 0$. This leads to

$$J_B(\omega)u^* = -\frac{1}{2z}c_R, \quad \text{and} \quad u^* = -\frac{1}{2z}J_B(\omega)^{-1}c_R.$$

The condition (6.11) implies

$$R^2 = \frac{\langle J_B(\omega)^{-1} c_R, c_R \rangle_{H^m}}{4z^2}. \tag{6.13}$$

Solving (6.13) for $z > 0$, using this Lagrange multiplier z to solve for u^* leads to the following explicit expressions

$$0 < z = \frac{\langle J_B(\omega)^{-1} c_R, c_R \rangle_{H^m}^{\frac{1}{2}}}{2R}, \qquad u^* = -\frac{J_B(\omega)^{-1} c_R}{2z} . \tag{6.14}$$

6.3 Discretization

To apply the results from the previous sections to examples, we start by considering the discretization of the relevant objects and the discrete problem. Then, we introduce the set of feasible perturbations, the subspace $U \subset H^m$, and consider two standard mathematical models of idealized atmospheric dynamics. Before discretizing the objective functional, we construct a finite-dimensional version $\mathcal{C}_N$ of the constraint set $\mathcal{C}$. For $N \in \mathbb{N}$, let $(\varphi_\ell)_{\ell=1}^N$ be linearly independent elements of H^m with $\operatorname{div}_x(\varphi_\ell) = 0$ and let $U_N := \operatorname{span}(\varphi_\ell)_{\ell=1}^N$. Representing the elements of the intersection $U_N \cap \mathcal{C}$ by their coefficient vectors in $\mathbb{R}^N$ with respect to the chosen basis we define $\mathcal{C}_N$ via

$$\mathbb{R}^N \supset \mathcal{C}_N \simeq \mathcal{C} \cap U_N \subset H^m .$$

Coefficient vectors in $\mathbb{R}^N$ and matrices in $\mathbb{R}^{N \times N}$ are denoted with a bar $\bar{}$. The $\hat{}$ for objects of the reflected setting is omitted in the following calculations for easier readability, but note that the calculations are performed for the objects in the reflected setting. Using the chosen basis to discretize the energy neighborhood constraint (6.7) leads to a quadratic constraint in the coefficient vector $\bar{u} \in \mathbb{R}^N$,

$$(\bar{B}_\omega)_{ij} := \sum_{|\alpha| \le m} \omega_\alpha \langle D^\alpha \varphi_i, D^\alpha \varphi_j \rangle_{L^2}, \qquad \bar{u}^\top \bar{B}_\omega \bar{u} \le R^2 \Leftrightarrow \bar{u} \in \mathcal{C}_N \simeq \mathcal{C} \cap U_N \ni u = \sum_{\ell=1}^N \bar{u}_\ell \varphi_\ell ,$$

which describes a strictly convex set, specifically, a ball or an ellipsoid, in $\mathbb{R}^N$. According to equation (6.6), the objective functional involves left and right eigenfunctions

$$c(u) = \langle \boldsymbol{g}^k, \boldsymbol{E}(u) \boldsymbol{f}^k \rangle_{L^2} .$$

Therefore, we have to account for possibly different bases for discretization.

(i) The perturbation library $(\varphi_\ell)_{\ell=1}^N$ for the discretization of the perturbation u.

(ii) A test basis and an ansatz basis for the discretization of $\boldsymbol{G}$, the augmented reflected generator.

The linearity of $\boldsymbol{E}$ in u, see (6.4), allows us to decompose in ℓ

$$c(u) = c\left(\sum_{\ell=1}^N \bar{u}_\ell \varphi_\ell\right) = \langle \boldsymbol{g}^k, \boldsymbol{E}(u) \boldsymbol{f}^k \rangle_{L^2} = \sum_{\ell=1}^N \bar{u}_\ell \langle \boldsymbol{g}^k, \boldsymbol{E}_\ell \boldsymbol{f}^k \rangle_{L^2}$$

and compute the discretization $\bar{\boldsymbol{E}}_\ell$ of each $\boldsymbol{E}_\ell := \boldsymbol{E}(\varphi_\ell)$ separately. The matrix representation of $\boldsymbol{E}_\ell$, more precisely of $\hat{\boldsymbol{E}}_\ell$, can be computed similarly to the discretization of $\hat{\boldsymbol{G}}$, detailed in Section 4.1.

Let $(\chi_j)_{j=1}^{n_1}$ be the basis for the discretization of $\boldsymbol{f}^k$ and let $(\xi_i)_{i=1}^{n_2}$ be the basis for $\boldsymbol{g}^k$. Inserting $\boldsymbol{f}^k = \sum_{j=1}^{n_1} \bar{f}_j^k \chi_j$ and $\boldsymbol{g}^k = \sum_{i=1}^{n_2} \bar{g}_i^k \xi_i$ into (6.6) leads to

$$\begin{aligned} c(u) = \langle \boldsymbol{g}^k, \boldsymbol{E}(u)\boldsymbol{f}^k \rangle_{L^2} &= \Big\langle \sum_{i=1}^{n_2} \bar{g}_i^k \xi_i, \boldsymbol{E}(u)\big(\sum_{j=1}^{n_1} \bar{f}_j^k \chi_j\big) \Big\rangle_{L^2} \\ &= \sum_{\ell=1}^{N} \sum_{i=1}^{n_2} \sum_{j=1}^{n_1} \bar{g}_i^k \bar{f}_j^k \left\langle \chi_j, -\mathrm{div}_{(\theta,x)} \left(\begin{pmatrix} 0 \\ \varphi_\ell \end{pmatrix} \xi_i \right) + \begin{pmatrix} 0 \\ \varphi_\ell \end{pmatrix}^\top \nabla_{(\theta,x)} \xi_i \right\rangle_{L^2} \bar{u}_\ell . \end{aligned}$$

This calculation gives a finite-dimensional representation of $\boldsymbol{E}(u)$ as a map from $\mathrm{span}(\xi_j)_j$ times $\mathrm{span}(\chi_i)_i$ to $\mathbb{R}$. We use Ulam's method for the generator to discretize $\boldsymbol{G}$ and $\boldsymbol{E}_\ell$, taking $n_1 = n_2$ and $\xi_i = \chi_i$ to be (normalized) indicator functions of space-time boxes. The cost vector can be assembled as follows

$$\bar{c}_\ell := c(\varphi_\ell) = \bar{g}^k \bar{\boldsymbol{E}}_\ell \bar{f}^k = \sum_{j=1}^{n_1} \sum_{i=1}^{n_1} \bar{g}_j^k \bar{f}_i^k \left\langle \chi_j, -\mathrm{div}_{(\theta,x)} \left(\begin{pmatrix} 0 \\ \varphi_\ell \end{pmatrix} \chi_i \right) \right\rangle_{L^2}, \quad \ell = 1, \ldots, N.$$

The discretized optimization problems

$$\begin{aligned} \min \quad & \bar{c}^\top \bar{u} \\ \text{s.t.} \quad & \bar{u}^\top \bar{B}_\omega \bar{u} - R^2 \le 0 \end{aligned} \qquad\qquad \begin{aligned} \max \quad & \bar{c}^\top \bar{u} \\ \text{s.t.} \quad & \bar{u}^\top \bar{B}_\omega \bar{u} - R^2 \le 0 \end{aligned}$$

have a linear objective and a single quadratic constraint. The energy constraint is induced by a scalar product, therefore the matrix $\bar{B}_\omega$ is invertible by typical arguments for Galerkin discretization, specifically, B_ω is symmetric and positive definite. The optimal perturbation can be obtained with the theory of Lagrangian multipliers. Analogously to the analysis leading to (6.14) we can derive an explicit formula for the optimal solution to the minimization problem

$$0 < z_{\min} = \frac{\left(\langle \bar{B}_\omega^{-1} \bar{c}, \bar{c} \rangle\right)^{\frac{1}{2}}}{2R}, \qquad \bar{u}_{\min} = -\frac{1}{2 z_{\min}} \bar{B}_\omega^{-1} \bar{c} \,. \tag{6.15}$$

The maximization problem $\max \bar{c}^\top \bar{u}$ is equivalent to the minimization problem $\min -\bar{c}^\top \bar{u}$. The maximizer $\bar{u}_{\max}$ can be obtained by using $z_{\max} = -z_{\min}$, Theorem 6.9.

The *admissible energy budget* R should be chosen sufficiently small to ensure that the linearization of the eigenvalue is a good approximation. The optimization process can be iterated as a gradient ascent or descent method to invest more energy in the perturbation. One iteration consists of constructing $\bar{c}$ and solving the equations (6.15). The assembly of $\bar{c}$ requires the computation of $\bar{\boldsymbol{G}}$, the discretization the augmented reflected generator, and its left and right eigenvectors $\bar{g}^k$, $\bar{f}^k$, and the perturbations $\bar{\boldsymbol{E}}_\ell$. Note that the $(\bar{\boldsymbol{E}}_\ell)_\ell$ and $\bar{B}_\omega$ are fixed through all optimization steps and do not need to be updated. Algorithm 2 summarizes the steps to obtain the optimal perturbation $\bar{u}_{\min,M}$ for minimizing the eigenvalue after M iterations using a budget R per iteration targeting the k-th eigenvalue with the perturbation library $(\varphi_\ell)_{\ell=1}^N$. This iteration scheme is applied to the examples in Section 6.4.

Algorithm 2 Optimal Spectral Perturbation for the Augmented Reflected Generator —Minimizing Version

function OptSpecPerturbMin($(\varphi_\ell)_{\ell=1}^N, k, R, M$)
  Compute the perturbations $\bar{\boldsymbol{E}}_\ell$ and the constraint matrix $\bar{B}_\omega$.
  Initialize $\bar{u}_{\min,0} = 0 \in \mathbb{R}^N$.
  for $i = 0, \ldots, M-1$ **do**
    Assemble $\bar{\boldsymbol{G}}(v + u_{\min,i})$ and compute the eigendata $\mu_{k,i}$, $\bar{\boldsymbol{f}}_i^k$, $\bar{\boldsymbol{g}}_i^k$.
    Construct the objective functional $\bar{c}_{\ell,i} = \bar{g}_i^k \bar{\boldsymbol{E}}_\ell \boldsymbol{f}_i^k$ for $\ell = 1, \ldots, N$.
    Compute the Lagrange multiplier $z_{\min,i+1} > 0$ and $\bar{u}_{\min,i+1}$ according to (6.15).
  return $\bar{u}_{\min,M}$.

Remark 43:

- Algorithm 2 is a slightly idealized version. In reality the targeted eigenvalue μ_k can change its position. This may require more attention. See Section 6.4.1 for more details.
- The maximizing version of Algorithm 2 only differs in choosing the negative Lagrange multiplier $z_{\max,i+1} = -\frac{1}{2R}(\langle \bar{B}_\omega^{-1}\bar{c}_i, \bar{c}_i\rangle)^{\frac{1}{2}} < 0$, which leads to $\bar{u}_{\max,i}$, in each iteration. Note that in general $\bar{u}_{\max,i} \neq -\bar{u}_{\min,i}$ for $i > 1$.
- All of our finitely many perturbation ansatz functions $(\varphi_\ell)_{\ell=1}^N$, introduced in the next paragraph, are C^m-regular. Thus, $\|\cdot\|_{H^m}$ and $\|\cdot\|_{L^2}$ are equivalent on $U_N = \operatorname{span}(\varphi_\ell)_\ell$. Therefore, for convenience, we use $m = 0$ in (6.7) to calculate $\bar{B}_\omega$ in the numerical examples, although strictly the functional c is only well defined for $u \in H^m$ with $m \geq 1$.
- The object $\boldsymbol{E}_\ell$ or $\boldsymbol{E}$ should be considered a perturbation of the generator $\boldsymbol{G}$ but not a generator of the perturbation, because it does not have the same properties as $\boldsymbol{G}$. The perturbation $\boldsymbol{E}_\ell$ or $\boldsymbol{E}$ does not have the spatial diffusion Δ_x and is missing the constant drift in θ; (6.4).
- The derivations, the arguments and Algorithm 2 derived above for $\hat{\boldsymbol{G}}$ hold for the generator in the autonomous case, the augmented generator in the non-autonomous periodic case and the augmented reflected generator in the non-autonomous case equally. They only require minor straightforward modifications for the specific cases not covered here.

△

Perturbations

The possible choices for the admissible perturbations depend of course on the application, the example or the model under consideration. The perturbation fields should have sufficient regularity. Furthermore, they should be compatible with the spatial domain $\mathbb{X}$ and the boundary conditions as well as other specific assumptions, such as zero divergence in our setting.

In the examples below the spatial domain $\mathbb{X}$ is always a rectangle. To ensure that the homogeneous Neumann boundary condition and zero divergence condition are satisfied, the spatial components of the basis vectors $(\varphi_\ell)_{\ell=1}^N$ are constructed from suitable smooth stream functions Ψ_{kl}. The φ_ℓ are then multiplied by time-dependent scalar (amplitude) functions ϕ_r.

For a rectangular domain $[a_x, b_x] \times [a_y, b_y]$, $a_x, a_y, b_x, b_y \in \mathbb{R}$, the stream functions are given by

$$\Psi_{kl}(t,x,y) = \sin\left(\frac{k\pi(x-a_x-c_x t)}{b_x-a_x}\right)\sin\left(\frac{l\pi(y-a_y-c_y t)}{b_y-a_y}\right),$$

$k = 1,\ldots,K$, $l = 1,\ldots,L$. The Ψ_{kl} are slightly modified Fourier modes that induce a velocity field $\psi_{kl} := (-\frac{\partial\Psi_{kl}}{\partial y}, \frac{\partial\Psi_{kl}}{\partial x})$ with k horizontal gyres and l vertical gyres; see Figure 6.6. By construction, these velocity fields satisfy the homogeneous Neumann boundary conditions in space (depending on c_x and c_y) and are divergence free in space. These fields may move in the x direction with constant speed c_x or in the y direction with constant speed c_y.

We use the time-dependent modulations of the amplitude

$$\phi_{-1}(t) := \frac{t}{T}, \qquad \phi_r(t) := \sin^r\left(\frac{t}{T}2\pi\right), \quad r = 0,2$$

and multiply them with $\tilde{\psi}_{kl}$ the $L^2((0,T)\times\mathbb{X})$-normalized versions of the functions ψ_{kl} to obtain

$$\varphi_{kl,r}(t,x,y) := \phi_r(t)\tilde{\psi}_{kl}(t,x,y)\,. \tag{6.16}$$

Remark 44:
We omit using $r = 1$ for the sine modulation, since this would cause it to have both positive and negative values, which in turn would cause the perturbing velocity field to change sign during the evolution on $[0,T]$. Such perturbing fields proved to be less efficient in early numerical experiments. The increasing time-linear modulation is assigned $r = -1$ to avoid confusion. △

In summary, amplitude-modulation of the perturbing fields is described by $\phi_r(t)$, $r \in \{-1,0,2\}$, and we have $3KL = N$ basis functions $(\varphi_\ell)_{\ell=1}^N$ in total.

6.4 Numerical Examples

The results of this section were obtained by the author in the publication [FKS20, Sec. 7].

6.4.1 The Forced Double Gyre Flow

The forced double gyre flow has been used as an example in Section 4.2. There, the focus was to extract coherent families. Now, we want to optimally manipulate these families.

Increasing Coherence

Continuing the investigation from Section 4.2, we now want to increase the coherence of the left-right separation represented by the 2nd eigenpair $(\mu_2, \boldsymbol{f}_2)$ of $\hat{\boldsymbol{G}}$, shown in Figure 4.2 (a).

Remark 45:
Before we describe our procedure, we want to point out the following consideration regarding the total energy of the system before and after the manipulation. Measuring the total energy with the space-time L^2 norm of the original velocity field v, see (4.6), gives $\|v\|_{L^2} \approx 1.6$. In the optimization procedure described in Section 6.3, the bound R in the quadratic constraint is related to the local validity of the objective functional. Remembering that $\|\cdot\|_{L^2}$ and $\|\cdot\|_{H^m}$ are equivalent on U_N, the value R can also be seen as an *energy budget* in the Hilbert space H^m.

Thus, with each iteration of the optimization procedure, the amount of energy that we may introduce into the system is R. Therefore, after (too) many iterations the original dynamics may become irrelevant. $\triangle$

The optimization budget for this example is $R = 0.05$ per iteration. We iterate our optimization procedure 8 times to invest a total energy of 0.4, which is 25% of the original energy.

A quarter of the original energy may seem like a moderate injection of energy. While in general almost any perturbation decreases coherence, to increase it, the dynamics and the perturbation need to work together, which makes it harder to increase coherence. We consider the maximization problem to increase the targeted eigenvalue and bring the corresponding singular value closer to one. Recall that $\bar{u}_{\max}$ is obtained from the formula (6.15) using $z_{\max}$. We use the maximization version of Algorithm 2 to obtain $\bar{u}_{\max,8}$ to improve coherence and minimize mixing. The other eigenvalues μ_k of the generator $\hat{\boldsymbol{G}}$ also change when we perturb the velocity field v. In each iteration we check *a posteriori* that the selected eigenvalue μ_2 did indeed increase. This can also be considered an *a posteriori* indicator for the validity of the objective functional. The linearization of μ_2 around v might be a bad estimate for the change of μ_2 if the perturbation u is too large.

We choose the basis functions from (6.16) for $k = 1, \ldots, 5$, $l = 1, 2, 3$ with the time modulations $r = -1, 0, 2$ and $c_x = 0 = c_y$, $a_x = 0 = a_y$, $b_x = 2$, $b_y = 1$, hence $N = 45 = 5 \cdot 3 \cdot 3$, to span our space of admissible perturbations U_N. The optimal perturbation to increase coherence after 8 iterations is denoted by $\bar{u}_{\max,8} \in \mathcal{C}_N \subset \mathbb{R}^N$ or $u_{\max,8} = \sum_{\ell=1}^{N} (\bar{u}_{\max,8})_\ell \varphi_\ell \in \mathcal{C} \cap U_N$. The resulting absolute and relative effective change of μ_2 is:

$$\mu_2(u_{\max,8}) - \mu_2(0) = 0.0233, \quad \frac{\mu_2(u_{\max,8}) - \mu_2(0)}{|\mu_2(0)|} = 0.2575, \quad \frac{\sigma_2(u_{\max,8}) - \sigma_2(0)}{|\sigma_2(0)|} = 0.0975.$$

In the numerical experiments, each iteration increases the eigenvalue roughly by 0.003. The effect of perturbing v by $u_{\max,8}$ is illustrated in Figure 6.2. For for a similar simulation as shown in Figure 6.2, 200,000 particles were seeded on the right side of the vertical line $x = 1$ and evolved forward in time with the noisy flow using Runge–Kutta–Maruyama with time step size $h = \frac{1}{100}$ for $T = 4$ time units and noise strength $\varepsilon = 0.1$. This was done for the original v and the optimized velocitiy field $v + u_{\max,8}$. For the original velocity field v roughly 15% of the seeded particles end up on the left side of the domain, whereas for the optimally perturbed velocity field only about 10% of the particles end up on the left side (results not shown). Repeating the experiment with a noisy evolution with $\varepsilon = 0.01$ using Runge–Kutta–Maruyama with step size $h = \frac{1}{100}$ leads to 9% of the particles changing sides for v. This is reduced to 5% for the coherence-improved velocity field $v + u_{\max,8}$. The results are illustrated in Figure 6.2 (b)–(d), where the seeded particles are shown at initial time $t = 0$ and colored again according to their position left or right of the line $x = 1$ after the noisy evolution, at time $t = T$ shown in Figure 6.2 (a). Note that the time direction is not important. We could have colored at the initial time $t = 0$ and evolved forward. This would lead to qualitatively identical pictures.

The optimal manipulation to increase the left-right coherence in the periodically forced double gyre has also been considered in the aforementioned work [FS17, Sec. 6.3].

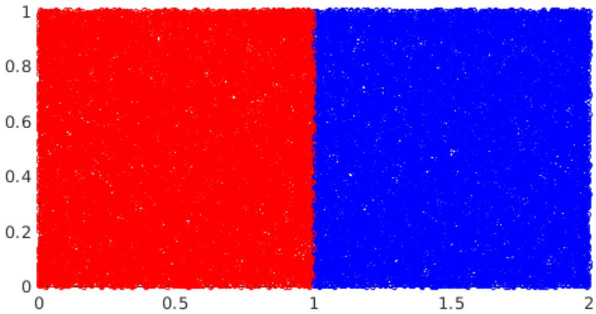

(a) Imposed coloring at final time.

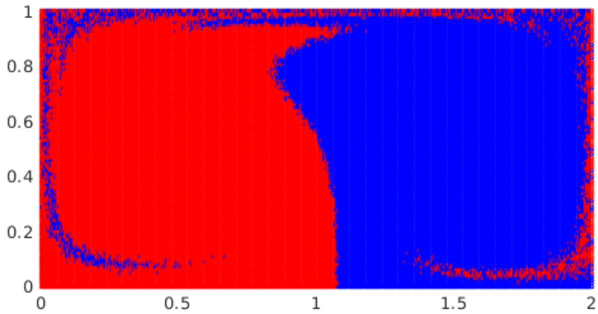

(b) Coloring at initial time corresponding to (a) using the original unperturbed velocity field v.

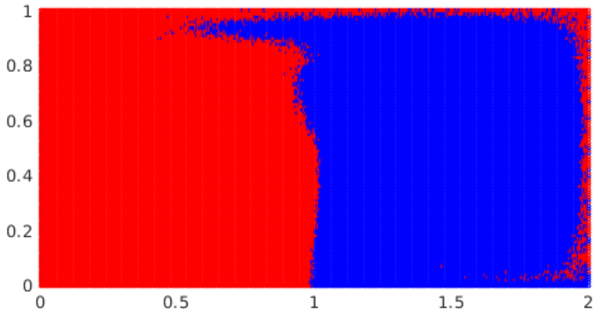

(c) Coloring at initial time corresponding to (a) using the velocity field $v + u_{\max,8}$ optimized for increasing coherence.

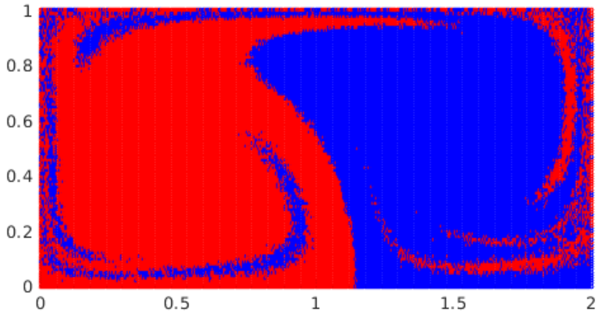

(d) Coloring at initial time corresponding to (a) using the velocity field $v + u_{\min,8}$ optimized for decreasing coherence.

Figure 6.2: (a) The left-right (red-blue) coloring imposed at final time $t = T$ on particles evolved with noise $\varepsilon = 0.01$; (b) The particles shown at time $t = 0$ for the original flow; (c) The particles shown at time $t = 0$ for the coherence-increasing optimized velocity field; (d) The particles shown at time $t = 0$ for the coherence-decreasing velocity field. This figure has been published in [FKS20, Fig. 6].

Decreasing Coherence

The goal of this paragraph is to illustrate the capabilities of our approach to decrease the coherence of the two gyres related to μ_5, see Section 4.2 Figure 4.2. In the previous paragraph the left-right separation was the targeted feature.

Remark 46:
Following the approach above, but using the minimization version of Algorithm 2 we obtain $u_{\min,8}$ to increase mixing across the left-right separatrix. The resulting flow is visualized in Figure 6.2 (d). These results are consistent with the results of [FS17], where the *lobes* of stable and unstable manifold intersections increased [FS17, Fig. 11 & 14]. △

The two central vortices are encoded in the 5th eigenpair $(\mu_5, \boldsymbol{f}_5)$. Due to the decrease of the eigenvalue, the vortices correspond to the 6th eigenpair after the first iteration. For this experiment we use the same perturbation library, energy constraint and budget $R = 0.05$ as above for again 8 iterations. After the first iteration of the minimization, the gyre feature corresponding to the 5th eigenpair is pushed to the 6th eigenpair spot. This shows that the rankings of features with respect to their coherence can change between iterations. Thus, we have to keep track of the position of the eigenvalues during the whole optimization. For the results shown here, this tracking was done manually between each step. The tracking could be done in an automated fashion by computing correlations between eigenvectors of successive iterates, similar to the identification of companion eigenvectors in Section 4.3.

Algorithm 2 together with the tracking described above gives $\bar{u}_{\min,8}$ and $u_{\min,8}$ and the following changes after 8 iterations:

$$\mu_5(0) - \mu_6(u_{\min,8}) = 0.16\,, \qquad \frac{\mu_5(0) - \mu_6(u_{\min,8})}{|\mu_5(0)|} = 0.36\,, \qquad \frac{\sigma_5(0) - \sigma_6(u_{\min,8})}{|\sigma_5(0)|} = 0.48\,.$$

Again we seed particles in the vortices induced by the level sets of the fifth eigenvector shown in Figure 4.2 and propagate them with and without perturbation. Figure 6.3 depicts the results of these computations. Increasing mixing for the double gyre flow has also been considered

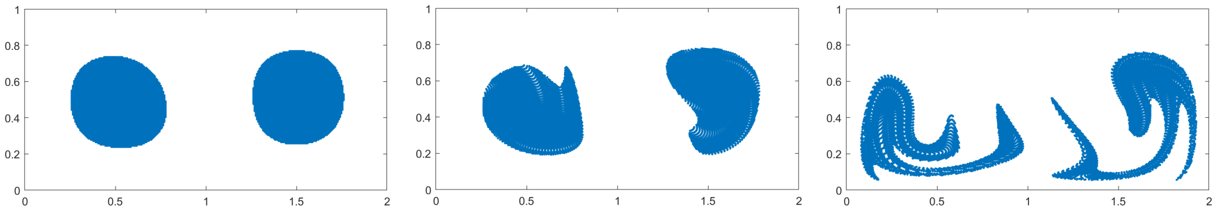

(a) Initial sets seeded according to fifth eigenvector for the evolution.

(b) Particles after original evolution for $T = 4$ time units.

(c) Particles after optimally perturbed evolution for $T = 4$ time units.

Figure 6.3: Test particles and their forward-time evolution. This figure has been published in [FKS20, Fig. 7].

in [FS17, Sec. 6.2]. In particular, the Figure 6.3 could be compared with the figures [FS17, Fig. 13, 16 & 17].

6.4.2 Manipulation of Non-Eigenfeatures

According to the theory in Chapter 3, the previous example targeted eigenvalues of $\hat{\boldsymbol{G}}$ which are used to quantify coherence. Sometimes it may be of interest to target specific features that are not encoded in the eigenfunctions. These features may be obtained by further processing eigenvectors, with for example the sparse eigenbasis approximation (SEBA) introduced in [FRS19], or motivated by the phase space geometry. The SEBA approach has been combined with the augmented reflected generator approach in Section 4.3. In the following we describe a heuristic to target these non-eigenfeatures.

Theorems 3.19 and Theorem 3.21 give

$$\begin{aligned} &\mathcal{P}_{0,T}^{*}\mathcal{P}_{0,T}\boldsymbol{f}(0,\cdot) = e^{2T\mu}\boldsymbol{f}(0,\cdot) \\ &\qquad\qquad \Updownarrow \\ &\qquad\qquad \hat{\boldsymbol{G}}\boldsymbol{f} = \mu\boldsymbol{f}, \text{ where } (\hat{\boldsymbol{G}}\boldsymbol{f})(\theta,\cdot) = -\partial_\theta \boldsymbol{f}(\theta,\cdot) + \hat{G}(\theta)\boldsymbol{f}(\theta,\cdot)\,. \end{aligned}$$

Recall that any non-constant eigenfunction $\boldsymbol{f}$ of the augmented reflected generator has zero mean. The positive and negative support of $\boldsymbol{f}$ induce finite-time coherent families $(A_t^+)_t$,$(A_t^-)_t$. Furthermore, the coherence ratio of the family is bounded according to Theorem 3.21 by an expression involving the corresponding eigenvalue μ. For normalized eigenfunctions $\boldsymbol{f}$ such that $\|\boldsymbol{f}\|_{L^2} = 1$, we see that a smaller $\|\hat{\boldsymbol{G}}\boldsymbol{f}\|_{L^2} = |\mu|\|\boldsymbol{f}\|_{L^2}$ suggests more coherence for the feature encoded in $\boldsymbol{f}$. We choose $\|\hat{\boldsymbol{G}}\boldsymbol{f}\|_{L^2}$ as a heuristic quantifier for coherent features encoded in non-eigenfunctions $\boldsymbol{f}$.

Let $\boldsymbol{\varphi}$ be a general normalized zero-mean non-eigenfunction corresponding to a *space-time feature* with $\boldsymbol{\varphi} \in \mathcal{D}(\hat{\boldsymbol{G}})$, the domain of the augmented reflected generator. For example, $\boldsymbol{\varphi}$ could be a mean-removed SEBA vector or a mean-removed mollified version of the indicator function $\mathbb{1}_{\boldsymbol{C}}$ such that $\varphi \in \mathcal{D}(\hat{\boldsymbol{G}})$. Here, $\boldsymbol{C}$ is a possibly coherent family $\boldsymbol{C} \subset \boldsymbol{X}$ of sets in augmented-space representation, and the augmented-space Lebesgue measure of $\boldsymbol{C}$ is denoted by $\Lambda^{d+1}(\boldsymbol{C})$. The removal of the mean from $\boldsymbol{\varphi}$ does not qualitatively influence the optimization approach in (6.17) below, since $\hat{\boldsymbol{G}}\mathbb{1}_{\boldsymbol{X}} = 0$. We keep the centering for the intuitive connection with eigenfeatures and Theorem 3.21. In general, we would like $\boldsymbol{\varphi}$ to represent a finite-time coherent set. Therefore we consider features satisfying $\boldsymbol{\varphi}(\theta, \cdot) \approx \boldsymbol{\varphi}(2T - \theta, \cdot)$.

Analogously to the case of an eigenfunction $\boldsymbol{f}$, we quantify the *coherence of a feature* $\boldsymbol{\varphi}$ that is not necessarily an eigenfunction, by measuring $\|\hat{\boldsymbol{G}}\boldsymbol{\varphi}\|_{L^2}$. This approach is motivated by the following considerations. If a family of sets encoded by the eigenvector $\boldsymbol{f}$ is perfectly coherent (in the absence of diffusion), then the temporal change $\partial_\theta \boldsymbol{f}(\theta)$ of the sets at any time θ, should be identical to the mass transport within in the set described by the Fokker–Planck equation (2.27) $\partial_\theta \boldsymbol{f}(\theta, \cdot) = \hat{G}(\theta)\boldsymbol{f}(\theta, \cdot)$. Thus, for strongly coherent features $\boldsymbol{\varphi}$ it holds that $\partial_\theta \boldsymbol{\varphi}(\theta, \cdot) - \hat{G}(\theta)\boldsymbol{\varphi}(\theta, \cdot) \approx 0$ for all θ, leading to $\|\hat{\boldsymbol{G}}\boldsymbol{\varphi}\|_{L^2} \approx 0$.

Remark 47:
The discussion in [FKS20, Sec. 3] considers a geometric view on the very same situation: In the equations [FKS20, (3.3),(3.6)], if the boundary of a time-dependent set moves with a velocity $b(t, x)$ that is approximately equal to the velocity field $v(t, x)$ driving the dynamics, then the outflow from this family of sets will be small—and this can analogously be quantified by the space-time flux [FKS20, (3.7)]. △

To target a coherent feature encoded in $\boldsymbol{\varphi}$ and increase its coherence we can minimize $\|\hat{\boldsymbol{G}}\boldsymbol{\varphi}\|_{L^2}^2$ with respect to the perturbations. This is in general a non-linear problem. Again, we use the regularity of $\hat{\boldsymbol{G}}$ to linearize locally. This leads to the linear objective functional given by:

$$\begin{aligned} c_{\boldsymbol{\varphi}}(u) &= \frac{d}{d\delta} \left(\left\| \hat{\boldsymbol{G}}(v + \delta u)\boldsymbol{\varphi} \right\|_{L^2}^2 \right) \Big|_{\delta=0} = \frac{d}{d\delta} \left(\left\| \left(\hat{\boldsymbol{G}}(v) + \delta \hat{\boldsymbol{E}}(u) \right)\boldsymbol{\varphi} \right\|_{L^2}^2 \right) \Big|_{\delta=0} \\ &= 2 \left\langle \hat{\boldsymbol{G}}(v)\boldsymbol{\varphi}, \hat{\boldsymbol{E}}(u)\boldsymbol{\varphi} \right\rangle_{L^2} . \end{aligned} \tag{6.17}$$

We aim to optimize c_φ subject to the energy constraints on the perturbation u introduced in (6.7). To destroy a coherent feature $\boldsymbol{\varphi}$ we can maximize c_φ. We can target different features simultaneously. For example, if we want to increase coherence of a feature $\boldsymbol{\varphi}_1$ and decrease the coherence of another feature $\boldsymbol{\varphi}_2$, then we can minimize the objective

$$c_{\boldsymbol{\varphi}_1, \boldsymbol{\varphi}_2}(u) = \alpha_1 c_{\boldsymbol{\varphi}_1}(u) - \alpha_2 c_{\boldsymbol{\varphi}_2}(u),$$

with weights $\alpha_1, \alpha_2 > 0$.

6.4.3 Traveling Wave

Let us consider a traveling wave example that has also been investigated in [Pie91, SW06, FLS10] given by

$$x'(t) = c_{\text{drift}} - c_A \sin(x - \nu t)\cos(y) \qquad y'(t) = c_A \cos(x - \nu t)\sin(y)$$

with $c_A = 0.15$ on the space-time domain $[0, 8] \times (2\pi S^1 \times [0, \pi])$. In this system, two rotating gyres move in the x direction with speed $\nu = 0.25$ and are superimposed with a constant drift $c_{\text{drift}} = 1$.

Due to the constant movement and the periodicity in the x direction, we choose a different perturbation library than in Section 6.4.1 given by Ψ_{kl} with $k = 2, 4, \dots, 20$, $l = 1, \dots, 5$ and $c_x = \nu$; see (6.16) and Section 6.3. We choose $a_x = 0, a_y = 0, b_x = 2\pi, b_y = \pi, c_y = 0$ to adjust (6.16) to this example.

Remark 48:
The paper [Bal15] has investigated a similar dynamical system and considered single perturbations drawn one at a time from a family similar to ours. We consider general linear combinations in $\mathcal{C} \cap U_N$. In [Bal15], mixing is measured by the flux out of a small *gate* connecting a stable and unstable manifold. $\triangle$

As described above, we measure mixing with the decay of the L^2-norm of an initial concentration field and compute the unique perturbation in a bounded, closed and strictly convex subset of a 150-dimensional, $N = 3 \cdot 10 \cdot 5$, subspace that optimizes the change in the desired direction. The resolution for the discretization of $\hat{\boldsymbol{G}}$ is $80 \times (80 \times 40)$ and we choose $\varepsilon = 0.1$. The feature is the mean-centered version of the time-constant and horizontally constant profile

$$\boldsymbol{\varphi}(t, x, y) = 1 - \cos(2y), \tag{6.18}$$

visualized in Figure 6.4 (a). We need to update the perturbation by computing (6.17) in each iteration. We iterate 35 times with an energy budget of $R = 0.1$ to increase the coherence. This corresponds to $\approx 1\%$ of the original energy of v per iteration. Figure 6.4 (b) shows the final time-slice of the original (deterministic) evolution of the particles in Figure 6.4 (a), while Figure 6.4 (c) shows the final time-slice of the optimized evolution. The optimal perturbation u

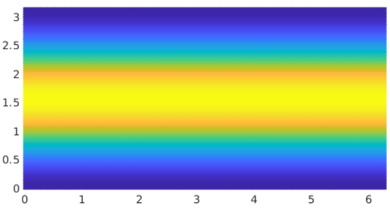

(a) Initial particles colored according to the feature (6.18).

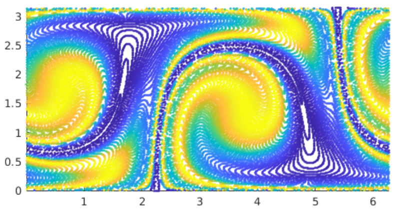

(b) Particles after original evolution for $T = 4$ time units.

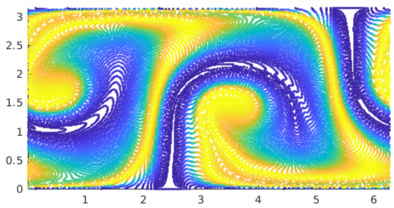

(c) Particles after optimally perturbed evolution for $T = 4$ time units.

Figure 6.4: Forward evolution of particles colored by the chosen feature. Yellow (respectively, blue) regions correspond to high-density (respectively, low-density) regions. This figure has been published in [FKS20, Fig. 8].

can be a linear combination of elements of our chosen library. It is of interest to know which perturbing basis functions receive the most energy from the budget. The basis function induced by $\varphi_{0,2,1}$ is equal to the original velocity field up to the constant horizontal drift c_{drift}. Thus, it is expected that this basis function is favored by the optimization because it is effective in countering the original velocity field's rotation and steering the flow towards the laminar feature. The contributions of each basis function in the optimal solution are shown in Figure 6.5, ordered according to magnitude and grouped according to the spatial mode. The first to fourth spatial modes with the largest contribution are visualized with level sets in Figure 6.6.

The combined effect of these modes is to steer the traveling double gyre optimally towards a laminar horizontal flow; Figure 6.7 (c). As expected, the biggest contribution comes from the basis function $\varphi_{0,2,1}$.

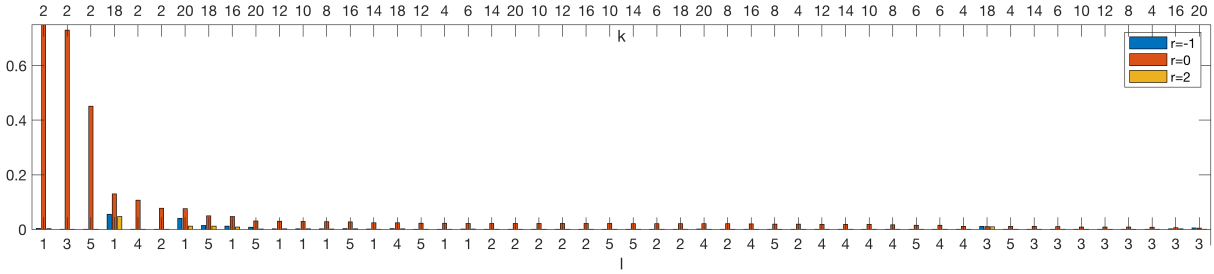

Figure 6.5: Plot of optimal perturbation coefficients $\bar{u}_\ell$ ordered in decreasing magnitude and grouped by spatial mode ψ_{kl} , see (6.16). The corresponding k and l are labels on upper and lower horizontal x axes, respectively. The plot is cut off at $y = 0.75$ for visualization purposes. The first red bar has height 7.6. This figure has been published in [FKS20, Fig. 9].

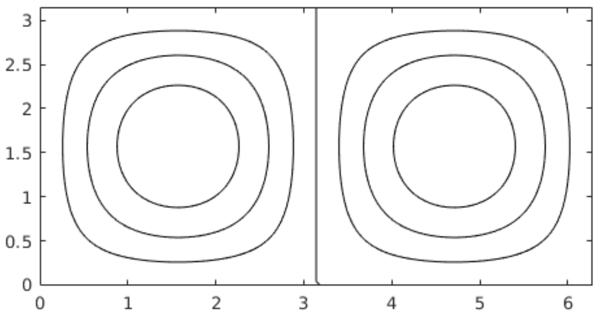

(a) Stream function for $k = 2$, $l = 1$.

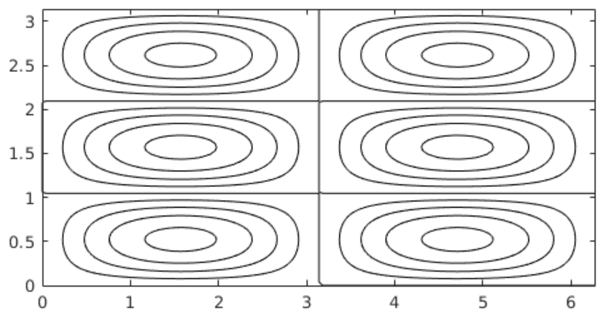

(b) Stream function for $k = 2$, $l = 3$.

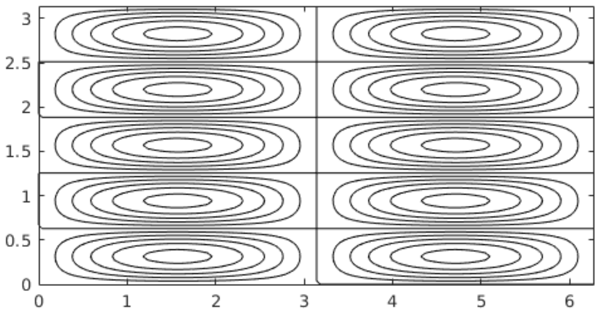

(c) Stream function for $k = 2$, $l = 5$.

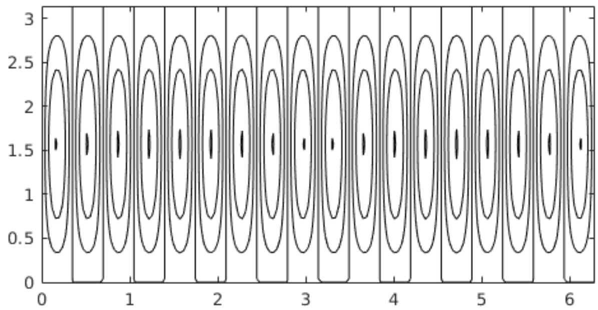

(d) Stream function for $k = 18$, $l = 1$.

Figure 6.6: Stream functions of basis functions with highest amplitudes after the optimization. This figure has been published in [FKS20, Fig. 10].

The above computations were performed for 100 iterations to investigate the asymptotic behavior under large perturbations. After 95 iterations the increase in coherence diminishes rapidly, as the value of the objective function $\|\hat{\boldsymbol{G}}(v+u)\boldsymbol{\varphi}\|_{L^2}^2$ approaches a plateau. The corresponding velocity field approaches a laminar flow (results not shown), because the optimal perturbation cancels the rotational part of the original velocity field.

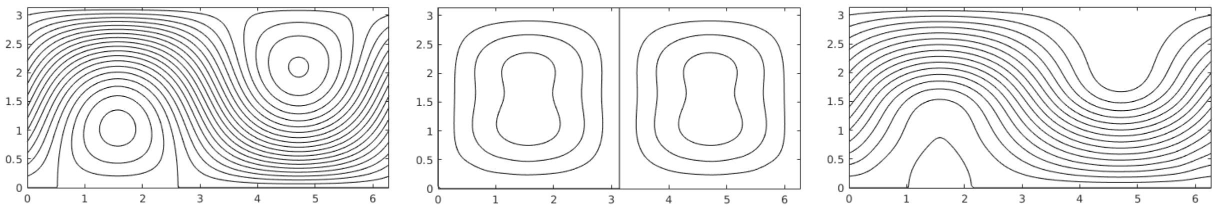

(a) Stream function of the original traveling double gyre.

(b) Stream function of optimal perturbation $u_{(35)}$.

(c) Stream function of final velocity field $v + u_{(35)}$.

Figure 6.7: Stream functions of the original velocity field, the optimal perturbation, and the perturbed velocity field at $t = 0$. This figure has been published in [FKS20, Fig. 11].

7 Outlook

In this thesis the physically relevant idea of coherent sets is analyzed from a functional analytic perspective. In Chapter 3 we utilized abstract results on evolution families, and we connected the augmented reflected generator $\hat{\boldsymbol{G}}$ to finite-time coherent sets. This offers an alternative approach to computing finite-time coherence families from velocity field data without expensive trajectory computation. This approach has been demonstrated numerically in Chapter 4 using standard examples. In general, the unbounded linear operator $\hat{\boldsymbol{G}}$ is not easy to analyze, but it is affine-linear in the velocity field v. The Fréchet differentiability of the transfer operators with respect to the velocity field v, shown in Chapter 5, extends to simple and isolated eigenpair of $\hat{\boldsymbol{G}}$. This enabled the optimal manipulation method presented in Chapter 6.

7.1 Birth and Death of Coherent Sets

The time span $[0, T]$ under consideration influences the results of the coherent set analysis. If the time span is too long, we cannot expect significant coherent sets, because the material may be well mixed. If the time span is too short, we may not find significant coherent sets, because the dynamics might be insufficiently developed and hence the coherent sets cannot be distinguished from their mixing surroundings yet. Sometimes the underlying physical systems give some intuition for important time scales, such as the average turnover time in Rayleigh–Bénard convection; see [SSP$^+$19]. Some physical systems are less accessible and may have coherent sets with highly varying life span, for example ocean eddies.

The work [FK21] is one of the first to systematically analyze the birth and death of coherent sets. It uses a similar idea to the augmentation approach introduced in Chapter 3. In [FK21] the authors use a pure diffusion process, a one-dimensional Wiener process $(w_t)_t$, in the augmented variable

$$d\theta_t = a\, dw_t$$

to explore a space-time manifold and a co-evolved space-time manifold for the birth and death of coherent sets and thereby need to relax the *materialness* of the extracted sets. The parameter a controls the *materialness*. For $a \to \infty$ the extracted sets become purely material and the diffusive time evolution corresponds to averaging in time, this links the approach to previously established approaches for coherent set analysis [FK21, Sec. 3]. The eigendata of the corresponding evolution operator is separated into temporal and spatial components. The birth and death of coherent sets is then detected by a change in the spatial norms across time-fibers of a spatial eigenfunction.

Remark 49:
The work [BGTHD21] explores another transfer operator-based approach to investigate the birth and death as well as the life span of coherent sets. The method in [BGTHD21] uses ideas from numerical ergodic theory and does not use augmentation. $\triangle$

7.2 Generalizations

Boundary Conditions

In this thesis and in the field of coherence one often assumes reflecting boundary conditions for the SDE, which induce homogeneous Neumann boundary conditions for the parabolic PDE, the Fokker–Planck equation. This corresponds well with the conservation of mass or probability. However, sometimes a closed system is not feasible. Therefore, the important question arises: How can we adapt the approach to coherence as well as the associated methods introduced here to open system or systems with sources or sinks or other dynamics on the boundaries of $\mathbb{X}$? There exists a vast literature on possibly non-homogeneous Dirichlet, Neumann and Robin (mixed) boundary conditions for parabolic evolution equations. For many cases the conditions and thus the results from [Tan97] used here immediately apply. There are some works investigating the evolution of densities and mixing in open systems, for example [FJ18] and [KPGT22].

The Non-Volume Preserving Setting

The transfer operator approach to coherent sets has been extended to the non-volume preserving setting in, for example, [Fro13] and [Den17] by introducing normalized transfer operators. How this generalization can be carried over to the generator approach, and how the Fréchet differentiability and the optimal perturbation approach can be extended to the non-volume preserving setting, remains an open but important question. The following remark from [KLP19, Rem. 5.2] addresses this question for the Fréchet differentiability with respect to the velocity field v from Chapter 5.

Remark 50:

We can consider the transfer operator $\mathcal{P}_{0,t}(u) : L^p(\mu_0^u) \to L^p(\mu_t^u)$ for non-stationary dynamics, see [Fro13, Den17]. Here μ_0^u is some given initial distribution and μ_t^u is its push-forward. The reason for this is that the transfer operator is well-defined non-expansive between these spaces for any $p \in [1, \infty]$, even for purely deterministic systems; see [Den17, Thm. 5, p. 21]. The dependence of μ_t^u on the perturbation u of the velocity field v poses additional difficulties. It is a non-trivial problem to compare $\mathcal{P}_{0,t}(u)f \in L^p(\mu_t^u)$ for different u with one another. One approach could be to work with a *common space* $L^p(\Lambda)$. Some results on perturbed operators mapping to different spaces are given in [Kol06, MNP13, ZP07]. $\triangle$

Furthermore, [FK20] and [HKK20] investigate transport, coherent sets and mixing in the non-volume preserving setting.

The following possibility for generalization is concerned with a different dependence of v on time.

7.2.1 Skew-Product Systems

In Chapter 3 we naturally arrived at the constant advancement in the augmented time coordinate

$$d\theta_t = 1\, dt\,.$$

There are several possibilities to expand this. We could look at the case when the velocity field v does not directly depend on time but depends on θ_t which is given by an evolution

$$d\theta_t = c(\theta_t)dt + \gamma(\theta_t)dw_t \quad \theta(0) = \theta_0\,.$$

Choosing the dynamics for θ to be independent of the spatial variable ensures a skew-product structure. A generalization, that seems natural, is a continuous flow φ_t

$$\theta_t = \varphi_t(\theta_0)$$

of homeomorphisms on a complete, separable, and compact metric space (Θ, d) without boundaries. Together with an ODE or an SDE for the spatial component $x(t)$ or X_t in $\mathbb{X}$, this leads to a (random) dynamical system and a skew-product flow [Arn03]. Considering again the evolution of densities in the stochastic case, we get the two-parameter family of solution operators $\mathcal{P}_{\theta,t}$, with $\mathcal{P}_{\theta_0,t} f_0 = f_t$ for the Fokker–Planck equation

$$\partial_t f(t,x) = -\mathrm{div}_x \left(v(\varphi_t(\theta_0), x) f(t,x) \right) + \frac{\varepsilon^2}{2} \Delta_x f(t,x) = G(\varphi_t \theta_0) f(t,x)$$

with initial value $f(0,\cdot) = f_0$ and homogeneous Neumann boundary conditions. The two-parameter family $(\mathcal{P}_{\theta,t})_{(\theta,t)}$ naturally induces a cocycle $(\mathcal{P}_{\cdot,t})_t$ over the flow $(\varphi_t)_t$ and a linear skew-product flow

$$\Psi \,:\, (\theta, f_0) \mapsto (\varphi_t \theta, \mathcal{P}_{\theta,t} f_0)\,.$$

Mather Semigroups

The theory of Mather semigroups [CL99, Chap. 6] can be seen as the analogue to evolution semigroups but for ergodically driven systems. We consider abstract Cauchy problems of the form

$$\begin{cases} \theta_t = \varphi_t \theta_0 \\ \dfrac{df(t)}{dt} = G(\theta_t) f(t) = G(\varphi_t \theta_0) f(t) \end{cases}$$

with θ living in the compact driving space Θ and the family $(G(\theta))_{\theta \in \Theta}$ of unbounded operators on a Banach space V. This gives a two-parameter solution family $(U(\theta,t))_{(\theta,t)}$. The first parameter is the initial configuration θ, and the second parameter is the time span of the evolution. Furthermore, $(U(\theta,t))_{(\theta,t)}$ induces a cocycle $(U(\cdot,t))_t$ over $(\varphi_t)_t$ and a skew-product flow [CL99, Def. 6.1 & (6.1)]. We can define the Mather semigroup in analogy to the evolution semigroup. Let μ be a σ-finite regular Borel measure on Θ, that is positive on open sets. We assume that the Radon–Nikodym derivative $\frac{d\mu \circ \varphi_{-t}}{d\mu}$ belongs to $L^\infty(\Theta)$ and is uniformly bounded in t.

Definition 7.1:
Let $(\varphi_t)_t$ be a continuous flow on a compact metric space (Θ, d), then the corresponding Mather semigroup $(M_t)_t$ is given on $C(\Theta; V)$ by

$$(M_t f)(\theta_s) = U(\varphi_{-t}\theta_s, t) f(\varphi_{-t}\theta_s)$$

and on $L^p(\Theta, \mu; V)$, $p \in [1, \infty)$, by

$$(M_t f)(\theta_s) = \left(\frac{d\mu \circ \varphi_{-t}}{d\mu} \right)^{\frac{1}{p}} U(\varphi_{-t}\theta_s, t) f(\varphi_{-t}\theta_s)\,.$$

The next theorem from [CL99, Thm. 6.20, Thm. 6.33, Prop. 6.23] ensures that $(M_t)_t$ is indeed a C_0 semigroup and that $(M_t)_t$ has an infinitesimal generator, which can be characterized as follows under some conditions on $(G(\theta))_{\theta \in \Theta}$.

Theorem 7.2:
The family $(M_t)_t$ is a C_0 semigroup on $C(\Theta; V)$ (respectively, $L^p(\Theta, \mu; V)$) if and only if (respectively, if) φ_t induces an exponentially bounded strongly continuous cocycle $U(\cdot, t)$. The Mather semigroup $(M_t)_t$ has the infinitesimal generator

$$(\boldsymbol{G}f)(\theta) = -\frac{d}{dt} (f \circ \varphi_t)(\theta)|_{t=0} + G(\theta) f(\theta)$$

on $C(\Theta; V)$.

The following theorem from [CL99, Thm. 6.30] gives a spectral mapping property for the Mather generator.

Theorem 7.3:
Let $\boldsymbol{G}$ be the generator of the Mather semigroup $(M_t)_t$ on $C(\Theta; V)$, and let φ_t induce a strongly continuous, exponentially bounded cocycle $(U(\cdot, t))_t$. If the flow φ_t is aperiodic, then

$$\sigma(M_t) \backslash \{0\} = e^{t\sigma(\boldsymbol{G})} .$$

Furthermore, the spectrum $\sigma(\boldsymbol{G})$ is translation invariant along the imaginary axis, and the spectrum $\sigma(M_t)$, for $t > 0$ is invariant with respect to rotations centered at the origin.

A spectral mapping property for the $L^p(\Theta, \mu; V)$ setting can be found in [CL99, Thm. 6.37]. For a non-aperiodic case see [CL99, Thm. 7.25].

Stochastically Persistent Coherent Sets

The question arises: How can we connect the Mather generator to an appropriate notion of coherence? Additionally, the question arises: What we can expect in the finite-time or the infinite-time setting? We propose the following notion of *escape rate* as a first step for the infinite-time perspective towards *stochastically persistent coherent sets*.

$$E\left((A_\theta)_{\theta \in \Theta}, \theta_0\right) := -\limsup_{t \to \infty} \frac{1}{t} \log \mathbb{P}\left(X_r \in A_{\varphi_r \theta_0}, \forall r \in [0, t]\right)$$

The hope is that ergodicity of the flow φ_t can be used in the spirit of [FS13, Prop. 2.4] to obtain independence of the initial configuration θ_0, and that similar arguments to Chapter 3 and [FLQ10] give a connection for eigendata of the Mather generator and coherent sets.

Remark 51:

- The publication [GD20] investigates the extraction and prediction of coherent patterns in incompressible flows for skew-product systems on an augmented manifold with ergodic driving. The work [GD20] considers the deterministic setting and adds some artificial noise on the operator level to regularize the spectrum.
- The work [BGT20] utilizes new advancements in multiplicative ergodic theory to investigate the material transport and transfer operators in non-autonomous dynamical systems.
- The work [Gia19] offers data-driven tools based on diffusion maps to deal with the case where the ergodic driving is not explicitly given.

△

From this starting point, we can try to join the results from [FLQ13], [FGTQ15], [GTQ15] and [GT18] and follow the strategy used for the generalization from [FS10] over [FJK13, FK17] to [FKS20] by also using Oseledets theory.

7.3 Numerics

The generator approach to coherence together with an Ulam-type method for discretization was successfully introduced in [Kol11]. This approach was then extended to time-dependent problems using augmentation and reflection, requiring some extensions of the numerical methods.

Spectral and Higher-Order Methods

The works [FJK13], [FK17], and [Thi20] introduced higher-order, hybrid, and purely spectral approaches for the generator and the augmented generator. A transfer of those approaches to the augmented reflected generator has yet to be done. As mentioned in Section 4.1.2, the authors of [FKS20] started experimenting with a Chebyshev hybrid (spectral in time) approach for the augmented reflected generator. This turned out to be not straightforward, because, as expected, the irregularity of $\hat{v}$ at $t = T$ does not behave well with the spectral approach in time.

Eigenvalue Problems

When computing coherent families with Ulam's approach for the augmented reflected generator, we noticed that the assembly of the matrix representation of the augmented reflected generator is rather fast. This was one of the goals of the generator approach. The most time-consuming part is the computation of the eigenvalues. As mentioned in Section 4.1 the Ulam representation of the generator, the augmented generator and the augmented reflected generator is sparse, but it is not symmetric. Therefore, we have to compute the eigenvalues of smallest magnitude including complex ones. As we have seen in (3.31), in the reflected setting any non-real eigenvalue has to be a companion eigenvalue (4.4). Therefore, it would be preferable to have an algorithm that *quotients out* these companion eigenvalues and only computes the $k = 0$ representatives of the classes $[\lambda_i + k\frac{2\pi i}{\tau}]$, because the companion eigenmodes do not contain any additional information.

7.4 Optimization

Physically Relevant Perturbations

The perturbation library chosen in Section 6.3 contains rather idealized versions and maybe physically questionable perturbations. However, the optimization method derived in Chapter 6 is well-suited for a data-driven approach. Assume that a set of realizable and thus experimentally measurable perturbation velocity fields $(\Psi_k)_k$ is given on a uniform grid or even on a different grid for each k. Then, each Ψ_k can be treated analogously to the analytically given perturbations by the theory of Chapter 6 using sufficient interpolation between grid points. Within the DFG SPP 1881 'Turbulent Superstructures' the authors of [FKS20] consulted with physicists and engineers about real or at least physically relevant perturbations. As it turned out, this question is not easy to answer, and in the end the Fourier modes chosen in Section 6.3 are a reasonable starting point. These velocity fields may be approximately realized in a laboratory using Lorentz forces induced by magnets and an electric current through a conductive fluid; see [RHG99], [KO11] and the references therein. Further starting points for relevant perturbations would be boundary shapes and boundary conditions, because those can be modified in experiments. However, these do not fit in a straightforward way into the optimal spectral manipulation methodology presented here.

Analytical Example

From a mathematical perspective a non-trivial analytical example would be desirable. This includes a velocity field v with explicitly computable eigenfunctions of $\hat{\boldsymbol{G}}(v)$ and an explicit perturbation library such that the optimal perturbation u can be calculated explicitly by hand. Furthermore, with an explicit eigenfunction of $\hat{\boldsymbol{G}}(v+u)$, we could compare exactly the change in the eigenvalue and the change in the coherent family.

Alternative Constraints

Due to the affine-linearity of the generator, the augmented generator, and the augmented reflected generator in the velocity field v and the Fréchet differentiability shown in Chapter 5, we were able to utilize powerful tools from the field of optimization in Chapter 6. To arrive at an exact formula (6.14) for the optimal perturbation, we assumed a very specific but reasonable structure for the constraints, namely, a quadratic form (6.7), a kind of smooth energy bound. We have seen in Figure 6.1 and Lemma 6.7 that some kind of boundedness constraint is necessary for the existence of an optimum, and that the strict convexity is useful for the uniqueness. However, the theory of Lagrangian optimization offers a lot more tools; see [Ste18]. For example, we could ask for the optimal perturbation to be contained in an intersection of affine half-spaces. For a sequence $(\alpha_i)_{i\in\mathbb{N}} \subset V^*$ of linear and bounded functionals on a Banach space V and some shift vectors $(\beta_i)_{i\in\mathbb{N}} \subset V$ the set

$$U = \{u \in V \mid \alpha_i(u) + \alpha_i(\beta_i) \le 0 \text{ for all } i \in \mathbb{N}\} = \bigcap_{i\in\mathbb{N}} \{u \in V \mid \alpha_i(u+\beta_i) \le 0\}$$

is possibly unbounded but convex and useful, assuming that it is non-empty. Although this set cannot be defined by a single smooth function, every single face of this polyhedron can. Similar to the arguments in Chapter 6 one may be able to derive a set of optimal perturbations. Even a cube centered at 0 with side length 2ε gives an unbounded convex set in an infinite-dimensional Hilbert space $(H, \langle\cdot,\cdot\rangle_H)$.

Example 4: Unbounded Cube

The closed cube in a Hilbert space $(H, \langle\cdot,\cdot\rangle_H)$ centered at 0 with side length 2ε can be constructed as the intersection of affine half-spaces. For an orthonormal basis (ONB) $(e_i)_{i\in\mathbb{N}} \subset H$ the functionals and shifts

$$\alpha_{i,1}(v) := \langle e_i, v\rangle_H = v_i\,, \quad \alpha_{i,2}(v) := -\alpha_{i,1}\,, \quad \beta_{i,2} := \varepsilon e_i\,, \quad \beta_{i,1} := -\beta_{i,2}\,, \qquad \varepsilon > 0$$

give the cube $U_C = \{v = \sum_{i\in\mathbb{N}} v_i e_i \in H \mid -\varepsilon \le v_i \le \varepsilon \text{ for all } i \in \mathbb{N}\}$. On the one hand, due to the properties of the ONB (or any Schauder basis), any $v = \sum_{i\in\mathbb{N}} v_i e_i \in H$ can only violate the cube constraints for finitely many i, because $v_i \to 0$ for $i \to \infty$. On the other hand, the cube U_C is unbounded, because v, with $v_i = \varepsilon$ for $i = 1, \ldots, n \in \mathbb{N}$, belongs to U_C and satisfies $\|v\|_H = \varepsilon\sqrt{n}$. This shows that already a cube is a non-trivial structure in infinite dimensions. $\diamondsuit$

The situation is different for the simplex-type set $U_S = \{v = \sum_{i\in\mathbb{N}} v_i e_i \in H \mid \sum_{i\in\mathbb{N}} |v_i| \leq \varepsilon\}$ which can also be constructed as a countable intersection of affine half-spaces. However, U_S is convex and bounded. For $v \in U_S \subset U_C$ holds

$$\|v\|_H^2 = \sum_{i\in\mathbb{N}} |v_i|^2 \leq \varepsilon \sum_{i\in\mathbb{N}} |v_i| \leq \varepsilon^2 .$$

Any linear objective functional $c \in H^*$ has a Riesz representation $c_R = \sum_{i\in\mathbb{N}} c_i e_i \in H$. We can define the directions of strongest impact

$$\overline{c} := \max_{i\in\mathbb{N}} |c_i| < \infty \quad \text{and} \quad I := \{i \in \mathbb{N} \mid |c_i| = \overline{c}\} ,$$

where $\bar{c}$ exists and I is a finite set, because $(e_i)_{i\in\mathbb{N}}$ is an ONB. Then, the set of minima of c on U_S is given by

$$\left\{ u = \sum_{i\in I} -\operatorname{sgn}(c_i) u_i e_i \in H \;\middle|\; \sum_{i\in I} u_i = \varepsilon \,,\, u_i \geq 0 \text{ for all } i \in I \right\} .$$

The idea is that u_i is an investment for the directions of best yield given by I. As a starting point for an introduction to polyhedra in infinite dimensions we refer to [FV04] and [D'A11].

Remark 52:

- Of course other smooth equality constraints h and inequality constraints g that are not quadratic forms but give (strictly) convex and bounded sets

  $$U = \{u \in V \mid g(u) \leq 0 \text{ and } h(u) = 0\}$$

  can be treated with the methods presented in Chapter 6 and the references therein.

- Assuming that the Fréchet differentiability from Chapter 5 or similar results hold in Banach spaces, we can use Section 6.1 and many results from the theory of Lagrangian multipliers [Ste18] that have been derived in the Banach space setting. However, deriving explicit formulas in the Banach and not Hilbert space setting is an interesting but difficult extension especially regarding the importance of the L^1 setting.

$\triangle$

Bibliography

[AF03] R. A. Adams and J. J. F. Fournier. *Sobolev Spaces*. Elsevier, 2003.

[AFJ21] F. Antown, G. Froyland, and O. Junge. Linear response for the dynamic Laplacian and finite-time coherent sets. *Nonlinearity*, 34(5):3337, 2021.

[AGG+86] W. Arendt, A. Grabosch, G. Greiner, U. Moustakas, R. Nagel, U. Schlotterbeck, U. Groh, H. P. Lotz, and F. Neubrander. *One-parameter semigroups of positive operators*, volume 1184. Springer, 1986.

[AJKW17] A. Andersson, A. Jentzen, R. Kurniawan, and T. Welti. On the differentiability of solutions of stochastic evolution equations with respect to their initial values. *Nonlinear Analysis*, 162:128–161, 2017.

[Alt16] H. W. Alt. *Linear functional analysis*. Springer, 2016.

[AM17] H. Arbabi and I. Mezić. Study of dynamics in post-transient flows using Koopman mode decomposition. *Physical Review Fluids*, 2(12):124402, 2017.

[And09] S. Andres. *Diffusion Processes with Reflection*. Doctoral thesis, Technische Universität Berlin, Fakultät II - Mathematik und Naturwissenschaften, Berlin, 2009.

[Arn92] V. I. Arnold. *Ordinary differential equations*. Springer Science & Business Media, 1992.

[Arn03] L. Arnold. *Random Dynamical Systems*. Springer Monographs in Mathematics. Springer-Verlag, 2003.

[AT86] P. Acquistapace and B. Terreni. On fundamental solutions for abstract parabolic equations. In *Differential equations in Banach spaces*, pages 1–11. Springer, 1986.

[AT87] P. Acquistapace and B. Terreni. A unified approach to abstract linear nonautonomous parabolic equations. *Rendiconti del seminario matematico della Università di Padova*, 78:47–107, 1987.

[Bal14] V. Baladi. Linear response, or else. *arXiv preprint arXiv:1408.2937*, 2014.

[Bal15] S. Balasuriya. Dynamical systems techniques for enhancing microfluidic mixing. *Journal of Micromechanics and Microengineering*, 25(9):094005, 2015.

[Bal18] V. Baladi. Dynamical zeta functions and dynamical determinants for hyperbolic maps: A functional approach. In *Ergebnisse der Mathematik und ihrer Grenzgebiete. 3. Folge / A Series of Modern Surveys in Mathematics*, volume 48. Springer International Publishing, 2018.

[BAS00] P. L. Boyland, H. Aref, and M. A. Stremler. Topological fluid mechanics of stirring. *Journal of Fluid Mechanics*, 403:277–304, 2000.

[BGT20] C. Blachut and C. González-Tokman. A tale of two vortices: How numerical ergodic theory and transfer operators reveal fundamental changes to coherent structures in non-autonomous dynamical systems. *Journal of Computational Dynamics*, 7(2):369, 2020.

[BGTHD21] C. Blachut, C. González-Tokman, and G. Hernandez-Duenas. A patch in time saves nine: Methods for the identification of localised dynamical behaviour and lifespans of coherent structures. *arXiv preprint arXiv:2109.09970*, 2021.

[BK17] R. Banisch and P. Koltai. Understanding the geometry of transport: diffusion maps for Lagrangian trajectory data unravel coherent sets. *Chaos: An Interdisciplinary Journal of Nonlinear Science*, 27(3):035804, 2017.

[BKK$^+$17] A. Bittracher, P. Koltai, S. Klus, R. Banisch, M. Dellnitz, and C. Schütte. Transition manifolds of complex metastable systems. *Journal of Nonlinear Science*, 28(2):471–512, 2017.

[BL07] O. Butterley and C. Liverani. Smooth Anosov flows: correlation spectra and stability. *J. Mod. Dyn.*, 1(2):301–322, 2007.

[Bog98] V. I. Bogachev. *Gaussian measures.* Number 62 in Mathematical Surveys and Monographs. American Mathematical Soc., 1998.

[Bot13] F. Botelho. On the Lagrange multiplier theorem in Banach spaces. *Computational and Applied Mathematics*, 32(1):135–144, 2013.

[Boy01] J. P. Boyd. *Chebyshev and Fourier spectral methods.* Courier Corporation, 2001.

[BPN13] G. R. Bowman, V. S. Pande, and F. Noé, editors. *An Introduction to Markov State Models and Their Application to Long Timescale Molecular Simulation*, volume 797 of *Advances in Experimental Medicine and Biology.* Springer, 2013.

[BRS20] W. Bahsoun, M. Ruziboev, and B. Saussol. Linear response for random dynamical systems. *Advances in Mathematics*, 364:107011, 2020.

[CAG08] L. Cortelezzi, A. Adrover, and M. Giona. Feasibility, efficiency and transportability of short-horizon optimal mixing protocols. *Journal of Fluid Mechanics*, 597:199–231, 2008.

[Cia13] P. G. Ciarlet. *Linear and nonlinear functional analysis with applications*, volume 130. Siam, 2013.

[CKRZ08] P. Constantin, A. Kiselev, L. Ryzhik, and A. Zlatoš. Diffusion and mixing in fluid flow. *Annals of Mathematics*, pages 643–674, 2008.

[CL71] M. G. Crandall and T. M. Liggett. Generation of semi-groups of nonlinear transformations on general Banach spaces. *American Journal of Mathematics*, 93(2):265–298, 1971.

[CL99] C. Chicone and Y. Latushkin. *Evolution semigroups in dynamical systems and differential equations*. Number 70 in Mathematical Surveys and Monographs. American Mathematical Soc., 1999.

[D'A11] P. D'Allessandro. Generalizing polyhedra to infinite dimension. *Australian Journal of Mathematical Analysis and Applications*, 7(2, Art. 24):1–22, 2011.

[Dav07] E. B. Davies. *Linear operators and their spectra*, volume 106. Cambridge University Press, 2007.

[DDJS99] P. Deuflhard, M. Dellnitz, O. Junge, and C. Schütte. Computation of essential molecular dynamics by subdivision techniques I: Basic concept. In *Computational Molecular Dynamics: Challenges, Methods, Ideas*, Lecture Notes in Computational Science and Engineering 4, pages 98–115. Springer-Verlag, 1999.

[Den17] A. Denner. *Coherent structures and transfer operators*. PhD thesis, Technische Universität München, 2017.

[DFH$^+$09] M. Dellnitz, G. Froyland, C. Horenkamp, K. Padberg-Gehle, and A. S. Gupta. Seasonal variability of the subpolar gyres in the Southern Ocean: a numerical investigation based on transfer operators. *Nonlinear Processes in Geophysics*, 16(8):655–664, 2009.

[DFK22] M. C. Denes, G. Froyland, and S. R. Keating. Persistence and material coherence of a mesoscale ocean eddy. *Physical Review Fluids*, 7(3):034501, 2022.

[DG10] L. Demkowicz and J. Gopalakrishnan. A class of discontinuous Petrov–Galerkin methods. part i: The transport equation. *Computer Methods in Applied Mechanics and Engineering*, 199(23-24):1558–1572, 2010.

[DG11] L. Demkowicz and J. Gopalakrishnan. A class of discontinuous Petrov–Galerkin methods. part ii: Optimal test functions. *Numerical Methods for Partial Differential Equations*, 27(1):70–105, 2011.

[DG14] A. B. Dieker and X. Gao. Sensitivity analysis for diffusion processes constrained to an orthant. *Ann. Appl. Probab.*, 24(5):1918–1945, 2014.

[DGN12] L. Demkowicz, J. Gopalakrishnan, and A. H. Niemi. A class of discontinuous Petrov–Galerkin methods. part iii: Adaptivity. *Applied numerical mathematics*, 62(4):396–427, 2012.

[DJ99] M. Dellnitz and O. Junge. On the approximation of complicated dynamical behavior. *SIAM Journal on Numerical Analysis*, 36(2):491–515, 1999.

[DJM16] A. Denner, O. Junge, and D. Matthes. Computing coherent sets using the Fokker–Planck equation. *Journal of Computational Dynamics*, 3(2):163–177, 2016.

[DL91] J. Ding and T. Y. Li. Markov finite approximation of Frobenius–Perron operator. *Nonlinear Analysis: Theory, Methods & Applications*, 17(8):759–772, 1991.

[DM65] A. Y. Dubovitskii and A. A. Milyutin. Extremum problems in the presence of restrictions. *Zhurnal Vychislitel'noi Matematiki i Matematicheskoi Fiziki*, 5(3):395–453, 1965.

[Don11] M. B. Donato. The infinite dimensional Lagrange multiplier rule for convex optimization problems. *Journal of Functional Analysis*, 261(8):2083–2093, 2011.

[DS88] N. Dunford and J. T. Schwartz. *Linear operators, part 1: general theory*, volume 10. John Wiley & Sons, 1988.

[Emm13] E. Emmrich. *Gewöhnliche und Operator-Differentialgleichungen: Eine integrierte Einführung in Randwertprobleme und Evolutionsgleichungen für Studierende.* Springer-Verlag, 2013.

[EN00] K.-J. Engel and R. Nagel. *One-parameter semigroups for linear evolution equations*, volume 194. Springer Science & Business Media, 2000.

[FGP10] F. Flandoli, M. Gubinelli, and E. Priola. Flow of diffeomorphisms for SDEs with unbounded Hölder continuous drift. *Bull. Sci. Math.*, 134(4):405–422, 2010.

[FGTQ14] G. Froyland, C. González-Tokman, and A. Quas. Detecting isolated spectrum of transfer and Koopman operators with Fourier analytic tools. *Journal of Computational Dynamics*, 1(2):249, 2014.

[FGTQ15] G. Froyland, C. González-Tokman, and A. Quas. Stochastic stability of Lyapunov exponents and Oseledets splittings for semi-invertible matrix cocycles. *Communications on Pure and Applied Mathematics*, 68(11):2052–2081, 2015.

[FGTW16] G. Froyland, C. González-Tokman, and T. M. Watson. Optimal mixing enhancement by local perturbation. *SIAM Review*, 58(3):494–513, 2016.

[FHRvS15] G. Froyland, C. Horenkamp, V. Rossi, and E. van Sebille. Studying an Agulhas ring's long-term pathway and decay with finite-time coherent sets. *Chaos: An Interdisciplinary Journal of Nonlinear Science*, 25(8):083119, 2015.

[Fis11] G. Fischer. *Lernbuch Lineare Algebra und Analytische Geometrie.* Springer, 2011.

[FJ18] G. Froyland and O. Junge. Robust FEM-based extraction of finite-time coherent sets using scattered, sparse, and incomplete trajectories. *SIAM Journal on Applied Dynamical Systems*, 17(2):1891–1924, 2018.

[FJK13] G. Froyland, O. Junge, and P. Koltai. Estimating long-term behavior of flows without trajectory integration: The infinitesimal generator approach. *SIAM Journal on Numerical Analysis*, 51(1):223–247, 2013.

[FK17] G. Froyland and P. Koltai. Estimating long-term behavior of periodically driven flows without trajectory integration. *Nonlinearity*, 30(5):1948, 2017.

[FK20] G. Froyland and E. Kwok. A dynamic Laplacian for identifying Lagrangian coherent structures on weighted Riemannian manifolds. *Journal of Nonlinear Science*, 30(5):1889–1971, 2020.

[FK21] G. Froyland and P. Koltai. Detecting the birth and death of finite-time coherent sets. *arXiv preprint arXiv:2103.16286 ; to appear in Communications on Pure and Applied Mathematics*, 2021.

[FKS20] G. Froyland, P. Koltai, and M. Stahn. Computation and optimal perturbation of finite-time coherent sets for aperiodic flows without trajectory integration. *SIAM Journal on Applied Dynamical Systems*, 19(3):1659–1700, 2020.

[FLL+99] E. Fournie, J.-M. Lasry, J. Lebuchoux, P.-L. Lions, and N. Touzi. Applications of Malliavin calculus to Monte Carlo methods in finance. *Finance and Stochastics*, 3:391–412, 1999.

[FLQ10] G. Froyland, S. Lloyd, and A. Quas. Coherent structures and isolated spectrum for Perron–Frobenius cocycles. *Ergodic Theory and Dynamical Systems*, 30(3):729–756, 2010.

[FLQ13] G. Froyland, S. Lloyd, and A. Quas. A semi-invertible Oseledets theorem with applications to transfer operator cocycles. *Discrete & Continuous Dynamical Systems*, 33(9):3835–3860, 2013.

[FLS10] G. Froyland, S. Lloyd, and N. Santitissadeekorn. Coherent sets for nonautonomous dynamical systems. *Physica D: Nonlinear Phenomena*, 239(10):1527–1541, 2010.

[FP09] G. Froyland and K. Padberg. Almost-invariant sets and invariant manifolds—connecting probabilistic and geometric descriptions of coherent structures in flows. *Physica D: Nonlinear Phenomena*, 238(16):1507–1523, 2009.

[FPET07] G. Froyland, K. Padberg, M. H. England, and A. M. Treguier. Detection of Coherent Oceanic Structures via Transfer Operators. *Physical Review Letters*, 98(22):224503, 2007.

[FPG14] G. Froyland and K. Padberg-Gehle. Almost-invariant and finite-time coherent sets: directionality, duration, and diffusion. In *Ergodic theory, open dynamics, and coherent structures*, pages 171–216. Springer, 2014.

[Fri75] A. Friedman. *Stochastic differential equations and applications. Vol. 1.* Academic Press, 1975.

[Fri08] A. Friedman. *Partial differential equations of parabolic type.* Courier Dover Publications, 2008.

[Fro13] G. Froyland. An analytic framework for identifying finite-time coherent sets in time-dependent dynamical systems. *Physica D: Nonlinear Phenomena*, 250:1–19, 2013.

[Fro15] G. Froyland. Dynamic isoperimetry and the geometry of Lagrangian coherent structures. *Nonlinearity*, 28(10):3587, 2015.

[FRS19] G. Froyland, C. P. Rock, and K. Sakellariou. Sparse eigenbasis approximation: Multiple feature extraction across spatiotemporal scales with application to coherent set identification. *Communications in Nonlinear Science and Numerical Simulation*, 77:81–107, 2019.

[FS10] G. Froyland and O. Stancevic. Escape rates and Perron–Frobenius operators: Open and closed dynamical systems. *Discrete & Continuous Dynamical Systems-B*, 14(2):457, 2010.

[FS13] G. Froyland and O. Stancevic. Metastability, Lyapunov exponents, escape rates, and topological entropy in random dynamical systems. *Stochastics and Dynamics*, 13(04):1350004, 2013.

[FS17] G. Froyland and N. Santitissadeekorn. Optimal mixing enhancement. *SIAM Journal on Applied Mathematics*, 77(4):1444–1470, 2017.

[FSM10] G. Froyland, N. Santitissadeekorn, and A. Monahan. Transport in time-dependent dynamical systems: Finite-time coherent sets. *Chaos: An Interdisciplinary Journal of Nonlinear Science*, 20(4):043116, 2010.

[FV04] V. P. Fonf and L. Veselỳ. Infinite-dimensional polyhedrality. *Canadian Journal of Mathematics*, 56(3):472–494, 2004.

[GD20] D. Giannakis and S. Das. Extraction and prediction of coherent patterns in incompressible flows through space–time Koopman analysis. *Physica D: Nonlinear Phenomena*, 402:132211, 2020.

[GG19] S. Galatolo and P. Giulietti. A linear response for dynamical systems with additive noise. *Nonlinearity*, 32(6):2269, 2019.

[GGZ74] H. Gajewski, K. Gröger, and K. Zacharias. *Nichtlineare Operatorgleichungen und Operatordifferentialgleichungen*. Akademie-Verlag Berlin, 1974.

[Gia19] D. Giannakis. Data-driven spectral decomposition and forecasting of ergodic dynamical systems. *Applied and Computational Harmonic Analysis*, 47(2):338–396, 2019.

[GL06] S. Gouëzel and C. Liverani. Banach spaces adapted to Anosov systems. *Ergodic Theory and dynamical systems*, 26(1):189–217, 2006.

[GM05] E. Gobet and R. Munos. Sensitivity analysis using Itô-Malliavin calculus and martingales, and application to stochastic optimal control. *SIAM J. Control Optim.*, 43(5):1676–1713, 2005.

[GT18] C. González-Tokman. Multiplicative ergodic theorems for transfer operators: Towards the identification and analysis of coherent structures in non-autonomous dynamical systems. *Contemp. Math*, 709:31–52, 2018.

[GTQ15] C. González-Tokman and A. Quas. A concise proof of the multiplicative ergodic theorem on Banach spaces. *Journal of Modern Dynamics*, 9(01):237–255, 2015.

[Hal80] J. K. Hale. *Ordinary differential equations.* Robert E. Krieer, New York, 1980.

[Hel19] F. Hellwig. *Adaptive Discontinuous Petrov–Galerkin Finite-Element-Methods.* PhD thesis, Humboldt-Universität zu Berlin, 2019.

[HKK18] G. Haller, D. Karrasch, and F. Kogelbauer. Material barriers to diffusive and stochastic transport. *Proceedings of the National Academy of Sciences*, 115(37):9074–9079, 2018.

[HKK20] G. Haller, D. Karrasch, and F. Kogelbauer. Barriers to the transport of diffusive scalars in compressible flows. *SIAM Journal on Applied Dynamical Systems*, 19(1):85–123, 2020.

[HM10] M. Hairer and A. J. Majda. A simple framework to justify linear response theory. *Nonlinearity*, 23(4):909, 2010.

[Hör15] L. Hörmander. *The analysis of linear partial differential operators I: Distribution theory and Fourier analysis.* Springer, 2015.

[HP86] U. G. Haussmann and E. Pardoux. Time reversal of diffusions. *The Annals of Probability*, pages 1188–1205, 1986.

[HP98] G. Haller and A. Poje. Finite time transport in aperiodic flows. *Physica D: Nonlinear Phenomena*, 119(3-4):352–380, 1998.

[HS11] G. Haller and T. Sapsis. Lagrangian coherent structures and the smallest finite-time Lyapunov exponent. *Chaos: An Interdisciplinary Journal of Nonlinear Science*, 21(2):023115, 2011.

[IK08] K. Ito and K. Kunisch. *Lagrange multiplier approach to variational problems and applications.* SIAM, 2008.

[Itô57] S. Itô. Fundamental solutions of parabolic differential equations and boundary value problems. *Japanese journal of mathematics: transactions and abstracts*, 27:55–102, 1957.

[Kat13] T. Kato. *Perturbation theory for linear operators*, volume 132. Springer Science & Business Media, 2013.

[KCS16] P. Koltai, G. Ciccotti, and C. Schütte. On metastability and Markov state models for non-stationary molecular dynamics. *The Journal of chemical physics*, 145(17):174103, 2016.

[KK20] D. Karrasch and J. Keller. A geometric heat-flow theory of Lagrangian coherent structures. *Journal of Nonlinear Science*, 30(4):1849–1888, 2020.

[KKS16] S. Klus, P. Koltai, and C. Schütte. On the numerical approximation of the Perron–Frobenius and Koopman operator. *Journal of Computational Dynamics*, 3(1):51–77, 2016.

[KL99] G. Keller and C. Liverani. Stability of the spectrum for transfer operators. *Annali della Scuola Normale Superiore di Pisa-Classe di Scienze*, 28(1):141–152, 1999.

[Klo19] B. Kloeckner. Effective perturbation theory for linear operators. *Journal of Operator Theory*, 2019.

[KLP19] P. Koltai, H. C. Lie, and M. Plonka. Fréchet differentiable drift dependence of Perron–Frobenius and Koopman operators for non-deterministic dynamics. *Nonlinearity*, 32(11):4232, 2019.

[KO11] D. H. Kelley and N. T. Ouellette. Separating stretching from folding in fluid mixing. *Nature Physics*, 7(6):477–480, 2011.

[Kol06] A. V. Kolesnikov. Mosco convergence of Dirichlet forms in infinite dimensions with changing reference measures. *Journal of Functional Analysis*, 230(2):382–418, 2006.

[Kol11] P. Koltai. *Efficient approximation methods for the global long-term behavior of dynamical systems: theory, algorithms and examples.* Logos Verlag Berlin GmbH, 2011.

[KPGT22] A. Klünker, K. Padberg-Gehle, and J.-L. Thiffeault. Open-flow mixing and transfer operators. *Philosophical Transactions of the Royal Society A*, 380(2225):20210028, 2022.

[KR18] P. Koltai and D. Renger. From large deviations to semidistances of transport and mixing: Coherence analysis for finite Lagrangian data. *Journal of nonlinear science*, 28(5):1915–1957, 2018.

[Kre85] U. Krengel. *Ergodic Theorems*, volume 6 of *de Gruyter Series in Mathematics*. Walter de Gruyter, 1985.

[KS91] I. Karatzas and S. Shreve. *Brownian motion and stochastic calculus*, volume 113, 2nd edition. Springer Science & Business Media, 1991.

[Kun97] H. Kunita. *Stochastic flows and stochastic differential equations*, volume 24. Cambridge university press, 1997.

[Kun19] H. Kunita. *Stochastic flows and jump-diffusions.* Springer, 2019.

[Kur76] S. Kurcyusz. On the existence and nonexistence of Lagrange multipliers in Banach spaces. *Journal of Optimization Theory and Applications*, 20(1):81–110, 1976.

[L$^+$02] R. J. LeVeque et al. *Finite volume methods for hyperbolic problems*, volume 31. Cambridge University press, 2002.

[LH04] W. Liu and G. Haller. Strange eigenmodes and decay of variance in the mixing of diffusive tracers. *Physica D: Nonlinear Phenomena*, 188(1-2):1–39, 2004.

[Lie21] H. C. Lie. Fréchet derivatives of expected functionals of solutions to stochastic differential equations. *arXiv preprint arXiv:2106.09149*, 2021.

[LM94] A. Lasota and M. C. Mackey. *Chaos, Fractals, and Noise.* Springer-Verlag, 2. edition, 1994.

[LR15] W. Liu and M. Röckner. *Stochastic partial differential equations: an introduction.* Springer Cham, 2015.

[LS01] R. S. Liptser and A. N. Shiryaev. *Statistics of random processes. I*, volume 5 of *Applications of Mathematics (New York).* Springer-Verlag, Berlin, expanded edition, 2001. General theory, Translated from the 1974 Russian original by A. B. Aries, Stochastic Modelling and Applied Probability.

[LSS22] H. C. Lie, M. Stahn, and T. J. Sullivan. Randomised one-step time integration methods for deterministic operator differential equations. *Calcolo*, 59(1):1–33, 2022.

[LTD11] Z. Lin, J.-L. Thiffeault, and C. R. Doering. Optimal stirring strategies for passive scalar mixing. *Journal of Fluid Mechanics*, 675:465–476, 2011.

[Lue69] D. G. Luenberger. *Optimization by vector space methods.* John Wiley & Sons, 1969.

[Lun95] A. Lunardi. *Analytic semigroups and optimal regularity in parabolic problems.* Springer Science & Business Media, 1995.

[McI68] A. McIntosh. Representation of bilinear forms in Hilbert space by linear operators. *Transactions of the American Mathematical Society*, 131(2):365–377, 1968.

[Mei07] J. D. Meiss. *Differential dynamical systems.* SIAM, 2007.

[MMG$^+$07] G. Mathew, I. Mezić, S. Grivopoulos, U. Vaidya, and L. Petzold. Optimal control of mixing in Stokes fluid flows. *Journal of Fluid Mechanics*, 580:261–281, 2007.

[MMP84] R. MacKay, J. Meiss, and I. Percival. Transport in Hamiltonian systems. *Physica D: Nonlinear Phenomena*, 13(1-2):55–81, 1984.

[MMP05] G. Mathew, I. Mezić, and L. Petzold. A multiscale measure for mixing. *Physica D: Nonlinear Phenomena*, 211(1-2):23–46, 2005.

[MNP13] D. Mugnolo, R. Nittka, and O. Post. Norm convergence of sectorial operators on varying Hilbert spaces. *Operators and Matrices*, 7(4):955–995, 2013.

[Mon13] M. Monoyios. Malliavin calculus method for asymptotic expansion of dual control problems. *SIAM J. Financial Math.*, 4(1):884–915, 2013.

[OBPG15] S. Ober-Blöbaum and K. Padberg-Gehle. Multiobjective optimal control of fluid mixing. *PAMM*, 15(1):639–640, 2015.

[Oks13] B. Oksendal. *Stochastic differential equations: an introduction with applications.* Springer Science & Business Media, 2013.

[Pav14] G. A. Pavliotis. *Stochastic processes and applications: diffusion processes, the Fokker–Planck and Langevin equations*, volume 60. Springer, 2014.

[Paz83] A. Pazy. *Semigroups of linear operators and applications to partial differential equations*, volume 44. Springer Science & Business Media, 1983.

[Pie91] R. T. Pierrehumbert. Chaotic mixing of tracer and vorticity by modulated travelling Rossby waves. *Geophysical & Astrophysical Fluid Dynamics*, 58(1-4):285–319, 1991.

[Pie94] R. T. Pierrehumbert. Tracer microstructure in the large-eddy dominated regime. *Chaos, Solitons & Fractals*, 4(6):1091–1110, 1994.

[Pil14] A. Pilipenko. *An introduction to stochastic differential equations with reflection*, volume 1. Universitätsverlag Potsdam, 2014.

[PR14] E. Pardoux and A. Râşcanu. *Stochastic differential equations, Backward SDEs, Partial differential equations*, volume 69. Springer, 2014.

[Pro99] A. Provenzale. Transport by coherent barotropic vortices. *Annual review of fluid mechanics*, 31(1):55–93, 1999.

[PWS+11] J. Prinz, H. Wu, M. Sarich, B. Keller, M. Senne, M. Held, J. Chodera, C. Schütte, and F. Noé. Markov models of molecular kinetics: Generation and validation. *J. Chem. Phys.*, 134(17):174105, 2011.

[RBBV+07] I. Rypina, M. Brown, F. Beron-Vera, H. Kocak, M. Olascoaga, and I. Udovydchenkov. On the Lagrangian dynamics of atmospheric zonal jets and the permeability of the stratospheric polar vortex. *Journal of the Atmospheric Sciences*, 64(10):3595–3610, 2007.

[RHG99] D. Rothstein, E. Henry, and J. P. Gollub. Persistent patterns in transient chaotic fluid mixing. *Nature*, 401(6755):770–772, 1999.

[RKLW90] V. Rom-Kedar, A. Leonard, and S. Wiggins. An analytical study of transport, mixing and chaos in an unsteady vortical flow. *Journal of Fluid Mechanics*, 214:347–394, 1990.

[Roc70] R. Rockafellar. *Convex Analysis.* Princeton University Press, 1970.

[Ros55] P. Rosenbloom. Perturbation of linear operators in Banach spaces. *Arch. Math (Basel)*, 6(2):89–101, 1955.

[RS80] M. Reed and B. Simon. *Methods of Modern Mathematical Physics: Volume 1: Functional Analysis.* Academic Press, 1980.

[Rud91] W. Rudin. *Functional analysis.* MacGraw-Hill Book Co, 1991.

[RY99] D. Revuz and M. Yor. *Continuous martingales and Brownian motion*, volume 293 of *Grundlehren der Mathematischen Wissenschaften [Fundamental Principles of Mathematical Sciences].* Springer-Verlag, Berlin, third edition, 1999.

[Sch99] R. Schnaubelt. Sufficient conditions for exponential stability and dichotomy of evolution equations. *Forum Mathematicum*, pages 543–566, 1999.

[SFHD99] C. Schütte, A. Fischer, W. Huisinga, and P. Deuflhard. A direct approach to conformational dynamics based on hybrid Monte Carlo. *Journal of Computational Physics*, 151(1):146–168, 1999.

[SLM05] S. C. Shadden, F. Lekien, and J. E. Marsden. Definition and properties of Lagrangian coherent structures from finite-time Lyapunov exponents in two-dimensional aperiodic flows. *Physica D: Nonlinear Phenomena*, 212(3):271–304, 2005.

[SS13] C. Schütte and M. Sarich. *Metastability and Markov state models in molecular dynamics*, volume 24. American Mathematical Soc., 2013.

[SSA09] M. K. Singh, M. F. Speetjens, and P. D. Anderson. Eigenmode analysis of scalar transport in distributive mixing. *Physics of Fluids*, 21(9):093601, 2009.

[SSP$^+$19] C. Schneide, M. Stahn, A. Pandey, O. Junge, P. Koltai, K. Padberg-Gehle, and J. Schumacher. Lagrangian coherent sets in turbulent Rayleigh–Bénard convection. *Physical Review E*, 100(5):053103, 2019.

[Ste18] D. Steck. *Lagrange multiplier methods for constrained optimization and variational problems in Banach spaces.* PhD thesis, Universität Würzburg, 2018.

[Sul15] T. J. Sullivan. *Introduction to uncertainty quantification*, volume 63. Springer, 2015.

[SW06] R. M. Samelson and S. Wiggins. *Lagrangian transport in geophysical jets and waves: The dynamical systems approach.* Springer Science & Business Media, 2006.

[Tan97] H. Tanabe. *Functional analytic methods for partial differential equations.* Marcel Dekker Inc., 1997.

[TDG04] J.-L. Thiffeault, C. R. Doering, and J. D. Gibbon. A bound on mixing efficiency for the advection–diffusion equation. *Journal of Fluid Mechanics*, 521:105–114, 2004.

[Thi08] J.-L. Thiffeault. Scalar decay in chaotic mixing. In *Transport and Mixing in Geophysical Flows*, pages 3–36. Springer, 2008.

[Thi12] J.-L. Thiffeault. Using multiscale norms to quantify mixing and transport. *Nonlinearity*, 25(2):R1, 2012.

[Thi20] A. Thies. Markov-Approximation des Erzeugers des Frobenius–Perron Operators. Master's thesis, Freie Universität Berlin, 2020.

[TP08] J.-L. Thiffeault and G. A. Pavliotis. Optimizing the source distribution in fluid mixing. *Physica D: Nonlinear Phenomena*, 237(7):918–929, 2008.

[Tre00] L. N. Trefethen. *Spectral methods in MATLAB.* SIAM, 2000.

[Tro58] H. F. Trotter. Approximation of semi-groups of operators. *Pacific Journal of Mathematics*, 8(4):887–919, 1958.

[Ula60] S. M. Ulam. *A Collection of Mathematical Problems.* Number 8 in Interscience tracts in pure and applied mathematics. Interscience Publishers, 1960.

[VSPGS21] P. P. Vieweg, C. Schneide, K. Padberg-Gehle, and J. Schumacher. Lagrangian heat transport in turbulent three-dimensional convection. *Physical Review Fluids*, 6(4):L041501, 2021.

[Wal00] P. Walters. *An introduction to ergodic theory*, volume 79. Springer Science & Business Media, 2000.

[Wig05] S. Wiggins. The dynamical systems approach to Lagrangian transport in oceanic flows. *Annu. Rev. Fluid Mech.*, 37:295–328, 2005.

[Zei85] E. Zeidler. *Nonlinear Functional Analysis and its Applications: III: Variational Methods and Optimization.* Springer Science & Business Media, 1985.

[Zei90a] E. Zeidler. *Nonlinear Functional Analysis and Its Applications: II/A: Linear Monotone Operators.* Springer Science & Business Media, 1990.

[Zei90b] E. Zeidler. *Nonlinear Functional Analysis and Its Applications: II/B: Nonlinear Monotone Operators.* Springer Science & Business Media, 1990.

[ZP07] V. V. Zhikov and S. E. Pastukhova. On the Trotter–Kato theorem in a variable space. *Functional Analysis and Its Applications*, 41(4):264–270, 2007.